Mendelova univerzita v Brně
Agronomická fakulta
Ústav chemie a biochemie

Senzory pro ptačí chřipku

Disertační práce

Vedoucí práce:
prof. Ing. René Kizek, Ph.D.

Školitel specialista:
Ing. et Ing. David Hynek, Ph.D.

Vypracovala:
MVDr. Ludmila Krejčová

Brno 2014

PROHLÁŠENÍ

Prohlašuji, že disertační práce na téma „Senzory pro ptačí chřipku“ je samostatným autorským dílem podle Autorského zákona. Nositelem majetkového autorského práva je pracoviště a univerzita.

Výsledky práce shrnuté v této závěrečné práci byly financovány z veřejných prostředků z Evropských fondů a státního rozpočtu České republiky.

Disertační práce a výsledky v ní prezentované jsou dílem vypracovaným v Laboratoři metalomiky a nanotechnologií působící na půdě Agronomické fakultě Mendelovy univerzity v Brně a mohou být použity k dalšímu prezentování případně ke komerčním účelům jen se souhlasem vedoucího disertační práce a děkana. V opačném případě se jedná o porušení zákona.

V Brně dne 15.9. 2014

Ludmila Krejčová
podpis

Zpracovaná disertační práce byla finančně podpořena z prostředků specifického vysokoškolského výzkumu prostřednictvím projektu IGA AF č. IP 16/2013.

Tato práce vznikla v rámci CEITEC - Středoevropského technologického institutu s pomocí výzkumné infrastruktury financované projektem CZ.1.05/1.1.00/02.0068 z Evropského fondu regionálního rozvoje.

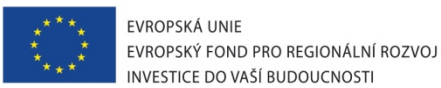

Poděkování

Největší díky bych ráda věnovala Renému Kizekovi za ochotu, se kterou se mi věnoval a za jeho čas a rady.

Velký dík patří Davidu Hynkovi za pomoc při tvorbě publikací, čas, podporu a nápady, kterými mě dokázal posunout vpřed. Dále bych chtěla poděkovat Vojtěchu Adamovi za konzultace, pomoc při interpretaci výsledků a tvorbě publikací.

Pavlu Kopelovi bych ráda poděkovala za spolupráci při přípravě kvantových teček a jejich konjugaci s biomolekulami.

Děkuji také všem spoluautorům publikací, které tvoří páteř mojí disertační práce za jejich podněty, připomínky a rady.

Dále děkuji všem kolegům z Laboratoře metalomiky a nanotechnologií na Mendelově univerzitě v Brně, za všestrannou pomoc a vytvoření perfektní pracovní atmosféry.

Za trpělivost, pochopení, duševní podporu, zázemí a lásku bych ráda poděkovala především rodičům a také dalším členům mé rodiny a přátelům.

Anotace

Rychlost mutací chřipkových virů je až stonásobně vyšší v porovnání s ostatními viry a právě díky rychlosti mutačních změn je chřipka považována za nejsilnějšího člena skupiny potencionálních původců pandemie. Abychom byli schopni předcházet vzniku a šíření pandemie, která by mohla ohrozit život sedmi miliard lidí, je nezbytné mít k dispozici metody pro rychlou a citlivou detekci jakéhokoliv subtypu chřipkového viru. Jedním z progresivních směrů detekce biomolekul jsou elektrochemické senzory a biosenzory. Cílem dizertační práce bylo navržení senzoru pro detekci chřipkových virů, především ptačí chřipky subtypu H5N1, založeného na izolaci částí virionu pomocí paramagnetických částic a následné elektrochemické detekci cílové molekuly. Byly navrženy a optimalizovány metody pro izolaci a detekci chřipkového antigenu (hemaglutininu) a nukleové kyseliny (DNA oligonukleotidu odvozeného od chřipkového genomu). V obou případech bylo použito kvantových teček (QDs) pro označení cílové molekuly. QDs, respektive jejich elektro-aktivní kovová část, byly využity k nepřímé elektrochemické detekci cílové molekuly.

Cílem práce bylo vyvinout rychlé, citlivé a levné metody pro izolaci a následnou elektrochemickou detekci chřipkových virů s možným využitím square-wave voltametrie, cyklické voltametrie a diferenční pulzní voltametrie.

Klíčová slova: chřipka, hemaglutinin, paramagnetické částice, elektrochemie, kvantové tečky

Annotation

Mutation rate of influenza viruses is up to a hundred times higher, when compared to other viruses. Thanks to the speed of mutational changes, influenza is considered as the strongest member of the group of potential pandemics agents. In order to prevent the occurrence and spread of pandemic, which could have impact on worldwide population, we need methods for rapid detection of each subtype of influenza viruses. One of the most progressive way of detection of biomolecules are electrochemical sensors and biosensors. The aim of the thesis was to design sensors and biosensors for influenza virus detection, especially avian influenza H5N1, that are based on the isolation of two different parts of influenza virion using paramagnetic particles, coupled with subsequent electrochemical detection of isolated target molecules. We designed and optimized methods for isolation and detection of influenza antigen (hemagglutinin) and influenza nucleic acid (DNA oligonucleotide derived from genomic RNA of influenza). In both cases, quantum dots (QDs) were used as the label of target molecules for electrochemical detection. Two fast, sensitive and low-cost methods for isolation and electrochemical detection, square-wave voltammetry and differential pulse voltammetry were applied.

Keywords: influenza, hemagglutinin, paramagnetic particles, electrochemistry, quantum dots

Obsah

1 ÚVOD

Před třiceti lety se řada vědců začínala domnívat, že jsou infekční onemocnění na ústupu. Celá řada onemocnění, která dříve znamenala ohrožení života (tuberkulóza, neštovice, černý kašel), pozbyla svého významu díky vakcinaci, preventivní péči a rozšiřujícímu se spektru léků. U některých onemocnění (malárie), se očekávalo, že jednoho dne sama vymizí. Část vědců se domnívala, že jednoho dne bude možné kapitolu s názvem „infekční choroby" navždy uzavřít. Následující roky ukázaly, že tyto domněnky byly jen pouhým snem.

V roce 1981 bylo v USA rozpoznáno nové onemocnění AIDS *(Curran, a kol., 1985)* (nyní 42 miliónů nakažených virem HIV) a o několik let později další v podobě viru hepatitidy C (ročně diagnostikováno 25 000 infikovaných a až 10 tisíc úmrtí) *(Hill a Cooke, 2014)*. V letech 2002-2003 vypukla epidemie SARS a z počtu 8 273 případů bylo 775 smrtelných (9,6%) *(Yasui, a kol., 2014)*. A co současnost a rok 2014? Největší hrozbou je epidemie eboly v Africe. V březnu 2014 byl v Africe diagnostikován první smrtelný případ, související s touto epidemií, během třech měsíců zemřelo 599 lidí, což je nejvíce od objevu této nemoci v roce 1976 *(Ansumana, a kol., 2014)*. V návaznosti na HIV, hepatitidu C, SARS a Ebolu může být zničující pandemie chřipky další příčinou globálního ohrožení zdraví a života sedmi miliard lidí.

V současnosti představuje chřipka jednu z největších hrozeb celosvětové populace *(Stohr, 2014)*. Není divu, že Světová zdravotnická organizace (WHO) iniciovala Globální chřipkový program (GIP), který poskytuje členským státům strategické vedení, technickou podporu a koordinaci činností nezbytných pro zlepšení připravenosti zdravotnických systémů pro boj s následky sezónní (případně pandemické chřipky), která může představovat riziko ohrožení zdraví a života jednotlivců nebo celosvětové populace (http://www.who.int/influenza/en/) *(Perdue a Nguyen, 2012, Shindo a Briand, 2012)*. Podle WHO je sezónní chřipka ročně zodpovědná za několik milionů případů akutních onemocnění a téměř půl miliónů úmrtí *(Jones, 2012)*.

Sociální, ekonomické a ekologické dopady každoročních sezónních epidemií jsou značné a je velmi těžké odhadnout, jaké by byly v případě pandemie. Ekonomické ztráty spojené s pandemií Vysoce patogenní ptačí chřipky (HPAI) byly v USA

vyčísleny na desítky nebo stovky miliónů dolarů *(McLeod a Guerne-Bleich, 2006)*. V Evropě nebyla situace o nic lepší, v Nizozemí trvala epidemie HPAI dva měsíce, postihla 255 farem a muselo být zabito více než 30 milionů kusů drůbeže *(Stegeman, a kol., 2004)*.

Důsledky chřipkových pandemií jsou známy z historie 20. století, které bylo poznamenáno celkem třemi chřipkovými pandemiemi: Španělská chřipka (1918), Asijská chřipka (1957) a Hong-Kongská chřipka (1968) *(Ryan, 2009)*. Španělská chřipka je považována za nehorší v historii, počet obětí byl vyčíslen na téměř 50 miliónů *(Lina, 2008)*. V 21. století byly zaznamenány dvě epidemie s pandemickým potenciálem (ptačí a prasečí chřipka), ani jedna však zatím neměla tak závažné dopady, jak se očekávalo *(Freidl, a kol., 2014, Noisumdaeng, a kol., 2014)*. Nedávno však byly popsány další, původně ptačí subtypy H7N7 a H7N2 *(Belser, a kol., 2008)*, H9N2 *(Pushko, a kol., 2009)*, H7N9 *(Rebmann a Zelicoff, 2012)*, které jsou schopny vyvolat onemocnění u lidí, a tak diskuze nad hrozbou v podobě vzniku pandemie stále neutichla. Mnoho vědců, zabývajících se výzkumem v oblasti chřipkových virů, se shoduje na riziku výskytu další chřipkové pandemie. Otázkou tak zůstává, kdy a kde se objeví a jak moc bude závažná *(Chan, a kol., 2010, Kobasa, a kol., 2004, Komadina, a kol., 2014)*.

V současnosti jsme lépe připraveni na boj proti vzniku a šíření epidemií, zejména co se týká prevence, diagnostiky a terapie *(Rao a Nyquist, 2014, Tarbet, a kol., 2014, Zhang a Wang, 2014)*. Na druhou stranu díky letecké přepravě lidí, zvířat, potravin a surovin roste riziko extrémně rychlého rozšíření pandemie. Ve spojení s dalšími rizikovými faktory, jako jsou růst počtu obyvatel a globalizace, se zdá být situace spíš horší *(Muscatello, a kol., 2014)*. A proto je nutné hledat nové možnosti v oblasti prevence, léčby a diagnostiky.

2 CÍLE PRÁCE

- Sumarizovat dostupné informace týkající se využití senzorů a biosenzorů pro detekci ptačí chřipky.
- Elektrochemicky charakterizovat chřipkový antigen hemaglutinin a označit ho kvantovými tečkami. Izolovat a elektrochemicky detekovat vzniklý komplex.
- Elektrochemicky charakterizovat chřipkovou nukleovou kyselinu a označit ji kvantovými tečkami. Izolovat a elektrochemicky detekovat vzniklý komplex.
- Současně detekovat tři různé subtypy chřipky v jednom vzorku pomocí nepřímé detekce třech různých kvantových teček a použít je jako elektro-aktivní značky.

3 LITERÁRNÍ PŘEHLED

3.1 Chřipkové viry

Viry způsobující chřipku patří do čeledi *Orhomyxoviridae*, a jsou klasifikovány na základě rozdílů v antigenní výbavě, struktuře a hostitelské specifitě na tři rody: chřipka typu A, chřipka typu B a chřipka typu C *(Fauquet a Pringle, 1997, Salez, a kol., 2014)*. Pro označování chřipkových izolátů je používána standardní nomenklatura, specifikující typ viru, druh hostitele (vynechává se, pokud je hostitelem člověk), geografickou polohu prvního výskytu viru, pořadové číslo izolace, rok izolace a u virů chřipky typu A i subtypy HA a NA antigenů: A /horse/ Prague/1/ 56 (H3N8).

3.1.1 Chřipka typu A

Chřipkové viry typu A jsou nejvíce virulentní, způsobují onemocnění savců a ptáků. Viry typu A mohou být dále klasifikovány na subtypy na základě sérologických a genetických rozdílů v povrchových glykoproteinech hemaglutininu (HA) a neuraminidázy (NA) *(Gilbert, 2013)*. Do roku 2009 bylo identifikováno 16 subtypů HA (H 1-16) a 9 subtypů NA (N 1-9). Všech 16 HA a 9 NA subtypů bylo prokázáno u vodních ptáků, kteří jsou považováni za přírodní rezervoár chřipkových virů *(Bahl, a kol., 2009, Gilbert, 2013)*. Během posledních let byly popsány tři nové endemicky se vyskytující subtypy (H17, H18 a N10), jejichž přirozenými hostiteli jsou létaví savci. N10 byl objeven v roce 2009 u guatemalských netopýrů *(Zhu a Wilson, 2012)*. V roce 2012 byl objeven H17 u kaloňů *(Sun, a kol., 2013, Zhu, a kol., 2013)* a o rok později byl objeven u netopýrů v Peru H18 *(Tong, a kol., 2013)*. Chřipka typu A je nejčastějším původcem sezónních chřipkových epidemií a jediným původcem pandemií. Důvodem jejich úspěšnosti je intenzita mutačních změn a fakt, že viry typu A podléhají oběma mechanismům evolučních změn (antigenní drift, antigenní shift) *(Li, a kol., 2011, Martcheva, 2012)*. Viry typu A způsobují středně těžká až těžká onemocnění u lidí všech věkových kategorií a u širokého spektra zvířat (koně, psi, fretky, mořští savci) *(Bi, a kol., 2010, Volz, a kol., 2013)*. V přírodě jsou viry typu A udržovány díky volně žijícímu vodnímu ptactvu, které má funkci přírodního rezervoáru *(Li, a kol., 2011)*. Většina „ptačích“ subtypů nejsou pro své přirozené hostitele patogenní a dokonce se ani u svých přirozených hostitelů nemění *(Freidl, a kol., 2014)*. Genetické i antigenní

variace chřipky typu A jsou popsány napříč celou řadou hostitelských druhů *(Volz, a kol., 2013)*.

3.1.2 Chřipka typu B

Chřipkové viry typu B způsobují méně závažná onemocnění a vyskytují se téměř výhradně v lidské populaci (jediným dalším známým hostitelem jsou tuleni) *(Bodewes, a kol., 2013, Kim, a kol., 2014)*. V porovnání s chřipkou typu A je typ B méně častým původcem epidemií a jeho mutační rychlost je 2-3x menší. U virů typu B dochází k mutačním změnám jen prostřednictvím antigennímu driftu. Všechny výše popsané aspekty (úzké hostitelské spektrum, nižší mutační rychlost a nižší genetická rozmanitost) znemožňují virům typu B způsobit pandemii *(Kim, a kol., 2014)*.

3.1.3 Chřipka typu C

Chřipka typu C je jen výjimečně detekována jako příčina onemocnění, ve většině případů probíhá onemocnění subklinicky. Typ C je schopen infikovat pouze lidi (nejčastěji děti) *(Principi, a kol., 2013)* a prasata *(Sheng, a kol., 2014)*, je typický endemickým výskytem, který nebývá spojován s epidemiemi. V případě chřipky typu A byly jako rezervoárová zvířata popsáni vodní páci, pro chřipku typu B a C jsou jediným známým rezervoárem lidé.

3.2 Replikace, životní cyklus viru chřipky

Pro viry je charakteristická biotropie - viry nemají schopnost metabolizmu ani tvorby energie (ATP) a nejsou schopné tvořit aminokyseliny pro stavbu virových proteinů, tudíž se mohou rozmnožovat a růst pouze v metabolizující hostitelské buňce.

Virus chřipky se přenáší kapénkovou infekcí u savců u ptáků oro-fekální cestou, k přenosu může dojít i prostřednictvím tělních tekutin (krev, sliny) *(Imai, a kol., 2013, Oh a Hurt, 2014)*. Viry chřipky jsou schopné přežít týden při teplotě lidského těla, více jak měsíc při teplotě kolem 0 °C a neurčitou dobu při teplotách hluboko pod bodem mrazu (jezera na severní Sibiři). Mohou být lehce zničeny desinfekcí, detergenty, poklesem pH prostředí (< 2), nebo účinkem teploty (56 °C, > 1h).

Chřipkové viry se replikují v sloupcových epiteliálních buňkách dýchacích cest *(Bouvier a Lowen, 2010)*. Odtud se šíří pomocí respiračního sekretu v malých částicích aerosolu, vznikajícího při kýchání, kašlání, a mluvení *(Imai, a kol., 2013)*. Délka inkubační doby chřipky je krátká (1-4 dnů) a spolu s výbušnou povahou nástupu chřipkových epidemií a pandemií, potvrzuje, že jeden nakažený může přenést virus na velký počet vnímavých jedinců během několika dní. H1N1 a H3N2 subtypy chřipky A a chřipka typu B jsou v současné době v oběhu společně *(Jones, 2012)*. Prevalence těchto tří skupin virů se může lišit časově a geograficky v rámci jedné země, ale i mezi zeměmi a kontinenty během jednoho chřipkového období *(Bouvier a Lowen, 2010)*.

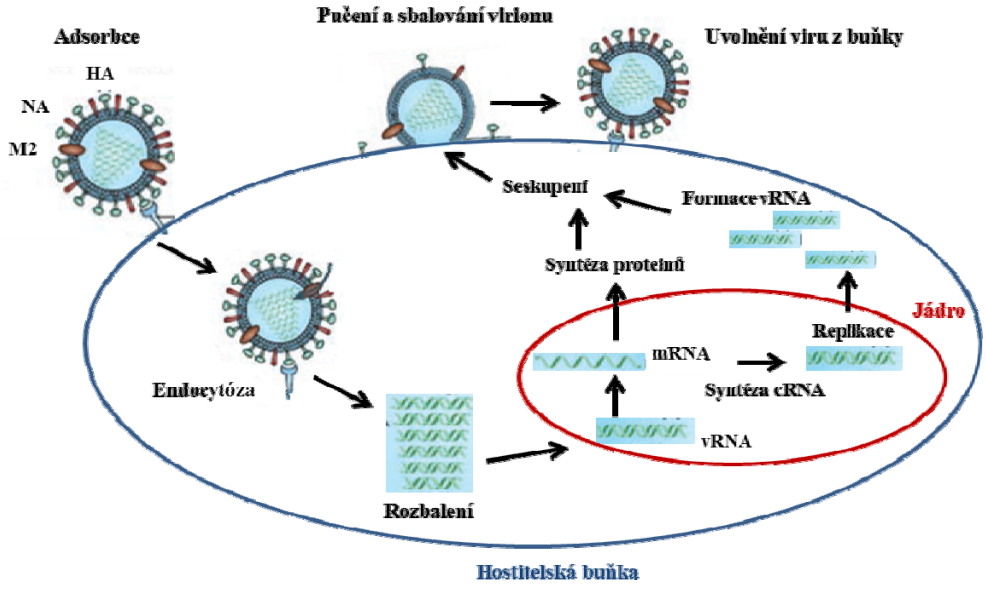

Obrázek č. 1: Schématické znázornění životního cyklu viru chřipky v hostitelské buňce.

Počátečním krokem infekce je vazba chřipkového virionu na povrch hostitelské buňky. Tento děj se odehrává interakcí HA na straně viru a receptoru tvořeného sialovou kyselinou na straně hostitel. Po úspěšném přichycení viru na receptor, dojde ke splynutí membrán (hostitelské buňky a viru) a je vytvořen nový obal kolem pohlceného viru *(Hyland, a kol., 2006)*. Nově vzniklý kompartment se označuje endozom. Hostitelská buňka se následně pokusí natrávit pohlcený virus okyselením endozomu a transformací do lysozomu za účelem zničení pohlcené částice. Pokles pH na hodnotu 6,0 nevede ke zničení endocytovaného viru, ale k aktivaci HA *(Glodowski, a kol., 2007, Isin, a kol., 2002, Watanabe, a kol., 2010)*. Původní složený trimer HA se stává nestabilní a doje k jeho částečnému rozvinutí a uvolnění hydrofilní části

polypeptidového řetězce, který byl dříve ukryt uvnitř proteinu *(Edinger, a kol., 2014, Garten a Klenk, 1999)*. Tento fúzní polypeptidový řetězec funguje jako háček, který se zasekne do endozomální membrány a táhne ji do blízkosti vlastní virové membrány, dokud obě membrány nesplynou *(Edinger, a kol., 2014)*. Vzápětí dojde k uvolnění virové RNA (v RNA), proteinů komplexu polymerázy a RNA dependentní polymerázy do cytoplazmy hostitelské buňky *(Hooper a Bloom, 2013, Watanabe, a kol., 2010)*. Následně se z příslušných molekul vytvoří polymerázový komplex, který je transportován do jádra hostitelské buňky, kde RNA dependentní polymeráza vytvoří komplementární pozitivní cRNA, která je buď exportována do cytoplazmy a následně translatována nebo zůstává v jádře. Chřipkové viry nejsou schopné kódovat aparát k vytvoření 5´ čepičky na vlastní mRNA. 5´ čepička je odštěpena z hostitelské mRNA a následně navázána na vlastní mRNA *(Watanabe, a kol., 2010)*. Nově syntetizované virové proteiny jsou transportovány díky Golgiho aparátu na povrch buňky, nebo jsou přeneseny do jádra, kde se váží na vRNA a podílí se na vytvoření nové virové částice. Ostatní virové proteiny mají celou řadu funkcí jako je štěpení buněčné mRNA, aby vir získal nukleotidy pro syntézu vRNA, nebo inhibují translaci hostitelské mRNA.

vRNA budoucích virů, nasyntetizované proteiny polymerázy a ostatní virové proteiny se seskupí uvnitř hostitelské buňky do budoucích virionů. Na povrchu hostitelské buňky se utvoří pučící útvar (budoucí virus), pokrytý HA a NA antigeny, do kterého se vloží jádro viru *(Cheng, a kol., 2012)*. Aby mohl nový virus opustit hostitelskou buňku, musí NA enzymaticky rozštěpit skupiny kyseliny sialové z hostitelských glykoproteinů, které tvoří receptory původní hostitelské buňky (stejné receptory využívali HA k vazbě viru na počátku infekce) *(Garcia a Aris-Brosou, 2014, Chen, a kol., 2001)*. Po uvolnění nově replikovaných virionů dochází ke smrti hostitelské buňky.

V nově syntetizované RNA se díky absenci opravných mechanizmů RNA dependentní RNA polymerázy, nalézá dost neopravených chyb (jeden nukleotid na každých 10kbp), což vede k tomu, že téměř každý virus obsahuje mutaci *(Rossman a Lamb, 2011)*.

3.3 Struktura chřipkového virionu

Chřipkové viriony jsou částice obalené lipoproteinovou membránou. Kapsida viru může mít sférický nebo vláknitý tvar. Genom chřipkových virů je lineární, tvořený segmentovanou ssRNA s negativní polaritou a je zmapován a popsán od roku 1976 *(Palese a Schulman, 1976, Ritchey, a kol., 1976)*. Do roku 2001 bylo u chřipky typu A a B popsáno 8 genomových segmentů a předpokládalo se, že kódují 10 proteinů: nukleoprotein (NP), hemaglutinin (HA), neuraminidázu (NA), proteiny polymerázového komplexu (PB1 PB2 a PA), matrixové proteiny (M1 a M2) a nestrukturální proteiny 1 (NS1 a NS2) *(Noda a Kawaoka, 2006)*. V roce 2001 byl ale objeven mitochondriální protein PB1-F2 *(Chen, a kol., 2001)* a do roku 2012 bylo objeveno dalších šest proteinů: PB1-N40 *(Wise, a kol., 2009)*, PA-X *(Jagger, a kol., 2012)* a NS3 *(Forbes, a kol., 2013)*, M42 *(Wise, a kol., 2012)*, PA-N155 *(Muramoto, a kol., 2013)* a PA-N182 *(Muramoto, a kol., 2013)*.

Celková velikost genomu chřipky typu A je 13,5 kbp, velikost segmentů se pohybuje od 890 do 2341 bp *(Vasin, a kol., 2014)*. U chřipky typu A a B je většina proteinů uzavřena do dvouvrstevného lipidového obalu, výjimku tvoří tři povrchové proteiny - dva z nich mají antigenní povahu: trimer HA a tetramer NA a jsou na povrchu viru zastoupeny v poměru 4-5:1 ve prospěch HA. Třetí protein M2 je integrovaný v membráně viru a plní funkci iontového kanálu *(Denis, a kol., 2008)*.

Segmenty vRNA jsou asociovány s komplexem polymerázy a nukleoproteinem (NP) a dohromady tvoří ribonukleoproteiny (RNP), které jsou odpovědné za transkripci a replikaci viru *(Edinger, a kol., 2014, Reguera, a kol., 2014)*. Strukturu nativních RNP popsal Arranz a kol. *(Arranz, a kol., 2012)*.

Chřipkové proteiny a genomové segmenty, které je kódují

- PA, PB1, PB2, PB1-F2 transkripty se nachází na 1., 2., a 3. segmentu, jedná se o polymerázový komplex, PB1-F2 vzniká translací alternativního otevřeného čtecího rámce
- HA (Hemaglutinin) transkript se nachází na 4. segmentu
- NP (Nukleoprotein) transkript se nachází na 5. segmentu
- NA (Neuraminidása) transkript se nachází na 6. segmentu

- M1 (Matrix) transkript se nachází na 7. segmentu
- M2 (M2 iontový kanál) transkript se nachází na 7. segmentu, vzniká sestřihem M1 transkriptu, slouží jako kanál pro protony přenášené z buňky do viru, což je nezbytný krok pro replikaci viru.
- NS1 transkript se nachází na 8. segmentu
- NS2 (NEP Nuclear export protein) transkript se nachází na 8. segmentu, vzniká sestřihem transkriptu NS1, slouží k exportu segmentů z jádra při zvýšené koncentraci M1

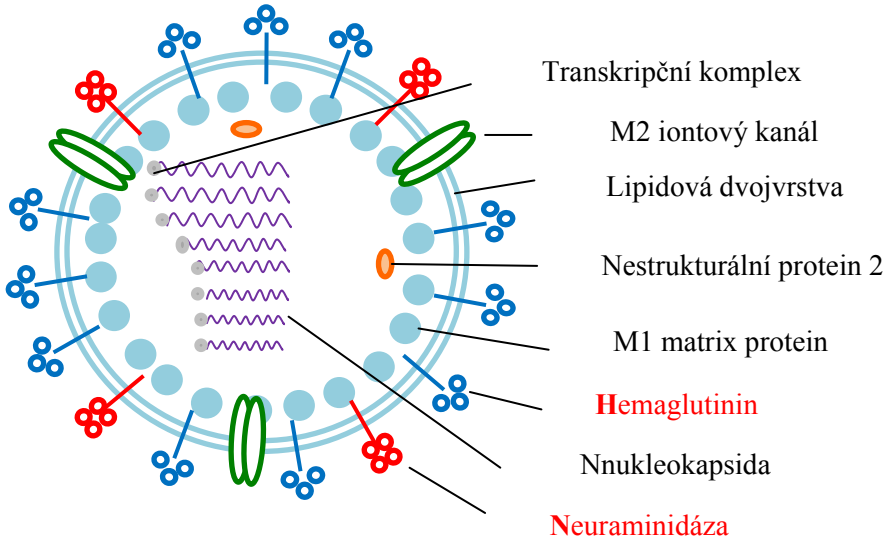

Obrázek č. 2: Struktura chřipkového virionu, červeně jsou zvýrazněny antigeny.

3.3.1 Virová polymeráza (komplex PB1, PB2 a PA)

Všechny segmenty chřipkového genomu jsou sbalené do komplexů, obsahující RNA polymerázu a nukleoprotein. Komplexy se označují jako ribonukleoproteiny (RNPs) a představují minimální transkripční a replikační aparát chřipkového viru. Během transkripce virová polymeráza syntetizuje polyadenylovanou mRNA s čepičkou *(Reguera, a kol., 2014, Vasin, a kol., 2014)*, což je struktura na 5' konci eukaryotických a virových mRNA, která chrání mRNA před rozkladem buněčnými enzymy a usnadňuje transport mRNA a spuštění translace na ribozomu. Během replikace virová RNA polymeráza tvoří komplementární RNA (c RNA), která slouží jako templát pro syntézu nových kopií vRNA *(Moeller, a kol., 2012, Rossman a Lamb, 2011)*. Molekulární podstata transkripce a replikace není doposud zcela

objasněna, ale nedávné výzkumy naznačují, že by transkripce mohla být prováděna cis-působící RNA polymerázou, zatímco replikace trans-působící RNA polymerázou *(Fodor, 2013)*. Virová polymeráza obsahuje dva základní polymerázové proteiny PB1, a PB2 a dále kyselý protein PA, sestavené do struktury trimeru, kde se C konec PA váže na N konec PB1 a C konec PB1 na N konec PB2 *(Arranz, a kol., 2012, Moeller, a kol., 2012)*. PB1 představuje aktivní místo pro vazbu k 5´a 3´ terminálním koncům vRNA a cRNA *(Cobbin, a kol., 2014)*. PA a PB2 hrají roli při iniciaci transkripce, vazby a štěpení hostitelské pre-mRNA *(Fodor, 2013)*. Řada kmenů chřipkových virů, exprimuje protein PB1-F2, který je transkribována z alternativního otevřeného čtecího rámce (+1 ORF) PB1. PB1-F2 protein se podílí na indukci apoptózy buněk hostitele, reaguje s PB1, ovlivňuje aktivitu polymerázy a přispívá k virové patogenezi některých kmenů chřipkových virů *(Conenello, a kol., 2011)*.

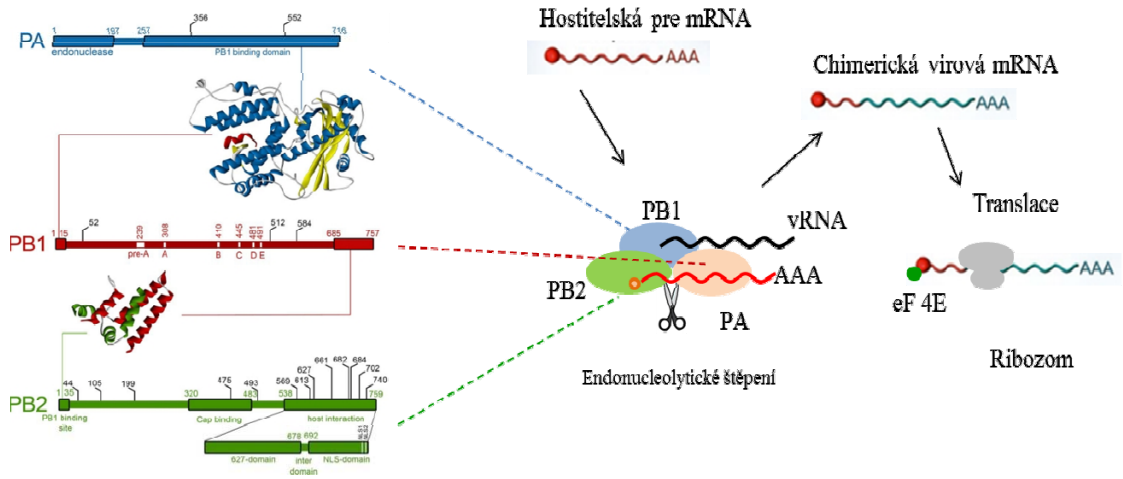

Obrázek č. 3: Seskupení BP1, PB2 a PA podjednotek do virové polymerázy a schématické znázornění funkce komplexu virové polymerázy. Levá část převzata: Boivin, 2010, J. Bio. Chem..

3.3.2 Hemaglutinin

Hemaglutinin (HA) je trans-membránový glykoprotein, jehož velikost je 13,5 nm a molekulová hmotnost asi 76 kDa. HA je cílovou molekulou pro neutralizační protilátky a z toho důvodu je považován za hlavní povrchový antigen. Primární funkcí HA je iniciace infekce, podílí se na rozpoznání hostitelské buňky a vazbě viru na její receptor, který je tvořený sialovou kyselinou *(Edinger, a kol., 2014, Cheng, a kol., 2012)*. Po vazbě viru na receptor dochází ke vstupu viru do hostitelské buňky a uvolnění virové RNA z virionu, což umožní následnou replikaci. V současnosti jsou nejrozšířenější HA

subtypy chřipky typu A v lidské populaci H1 (H1N1) a H3(H3N2). Výjimečně mohou způsobit onemocnění u lidí i subtypy, které jsou jinak typické pro vodní ptáky H5 *(Nasreen, a kol., 2013, Van Kerkhove, 2013)* a H7 *(Guo, a kol., 2014)* a H9 *(Bi, a kol., 2010)*.

HA monomery jsou syntetizovány samostatně jako prekurzory HA0, které jsou proteolyticky štěpeny na dvě menší podjednotky (HA1 a HA2) *(Skehel a Wiley, 2000, Stevens, a kol., 2006)*. Štěpeny jsou disulfidické můstky spojující HA1 a HA2, které byly vtvořeny při replikaci viru v procesu skládání HA0). Štěpení HA0 může probíhat v Golgiho aparátu, nebo extracelulárně (pomocí enzymů produkovaných buňkami respiračního systému), proces štěpení HA0 je zásadní pro infekčnost virové částice *(Garten a Klenk, 1999, Leikina, a kol., 2002)*. Po rozštěpení HA0 prekurzorů se trojice HA struktur spojí za vzniku trimeru, který má tvar houby *(Xu, a kol., 2010)*. Klobouk houby je tvořen z antiparalelních ß-listů HA1 podjednotek a oblast kmene je tvořena ze tří spirálovitě stočených α-šroubovic (HA2) *(Gamblin a Skehel, 2010)*. Podjednotka HA1, neboli receptor vázající oblast umožňuje vazbu viru na receptory hostitelské buňky, tvořenými kyselinou sialovou vázanou galaktózou *(Xu, a kol., 2010)*. Lidské HA receptory přednostně rozpoznávají α-2,6 glykosidickou vazbou, zatímco ptačí viry upřednostňují vazbu α-2,3 *(Edinger, a kol., 2014, Xu, a kol., 2010)*. Preference jednoho z typů receptorů, je dána počtem aminokyselin v HA. Kmen HA trimeru (tvořený HA2 subjednotkami) obsahuje fúzní doménu nezbytnou pro fúzi membrán při iniciaci infekce *(Edinger, a kol., 2014)*.

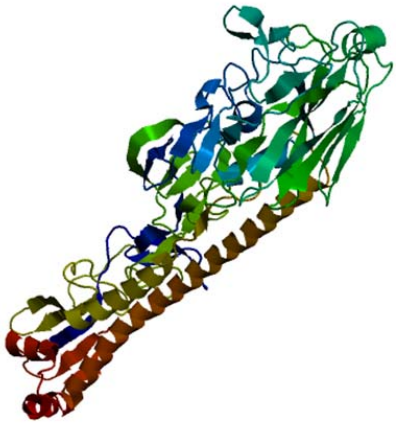

Obrázek č. 4: Hemaglutinin (Influenza A virus (A/Hong Kong/483/1997(H5N1)), ilustrační obrázek, sequence identity 44%, residue range: 16 to 519, zdroj: http://www.proteinmodelportal.org/.

3.3.3 Nukleoprotein

Nukleoprotein je také základní složkou virového transkripčního aparátu a je spojen s virovým obalem pomocí M1 proteinu *(Fodor, 2013)*. NP je RNA vázající protein, který váže virovou RNA a tvoří s ní NP-RNA komplex. Ten představuje šablonu pro transkripci a replikaci účinkem virové polymerázy *(Chenavas, a kol., 2013)*.

Obrázek č. 5: Nukleoprotein (Influenza A virus (Influenza A virus (A/Hong Kong/213-DkPass/2003(H5N1)), ilustrační obrázek, sequence identity 96%, residue range: 22 to 496, zdroj: http://www.proteinmodelportal.org/.

Pomocí SPR (surface plasmon resonance) s vysokým rozlišením byla odhalena struktura NP jako trimerní komplex skládající se z hlavy, těla a ocasu *(Ng, a kol., 2008)*. NP má schopnost polymerizovat a vytvářet trimerní struktury z NP monomerů, vzájemně spojenými pomocí smyčky a kapsy sousedících NP *(Hosaka, 1997, Reguera, a kol., 2014)*. Ačkoliv je NP považován za fylogeneticky konzervativní strukturu, má NP chřipky typu B, na rozdíl od typu A, strukturu tetrameru *(Ng, a kol., 2012)*. Jednou z primárních funkcí NP je pokrývání vRNA, což usnadňuje její skládání do dsRNP struktury *(Zheng a Tao, 2013)*. NP též interaguje s PB1 a PB2 subjednotkami virové polymerázy *(Edinger, a kol., 2014, Fodor, 2013)*.

3.3.4 Neuraminidáza

Neuraminidáza (NA) představuje další povrchový antigen chřipkových virů, jehož hlavní funkcí je uvolňování nově replikovaných virionů z hostitelské buňky. Aby mohl virus opustit hostitelskou buňku, musí neuraminidáza enzymaticky rozštěpit sialovou

kyselinu z glykoproteinů na povrchu hostitelské buňky *(Cheng, a kol., 2012)*. NA je enzym s hydrolytickou aktivitou, štěpící glykosidickou vazbu mezi kyselinou sialovou (N-acetylneuraminovou) a D-galaktózaminem nebo D-galaktózou, které tvoří receptor pro HA na povrchu hostitelské buňky *(Hooper a Bloom, 2013, Samson, a kol., 2013)*. Zbytky sialové kyseliny u savců vázány na terminálních pozicích v komplexu s glykany a tak NA, která má exo-glykosidázovou aktivitu, využívá tyto terminální zbytky jako substrátu *(Kim, a kol., 2013)*. NA se uplatňuje též při průniku viru přes vrstvu mucinu na sliznici, pučení viru a následné eluci viru z buněk *(Air, 2012)*. Některé nedávné studie poukazují i na to, že NA může přebrat i funkci vazby receptoru na hostitelských buňkách *(Lin, a kol., 2010)*.

V roce 2012 byla izolátu A/Tanzania/205/2010 popsána mutace D151G, která umožňuje NA přebrání funkce HA a zprostředkovává vazbu receptoru hostitelské buňky *(Zhu, a kol., 2012)*. V roce 2013 vytvořili Hooper a spolupracovníci mutaci G147R, díky které převezme NA zcela funkci HA. I když byla tato mutace vytvořena za laboratorních podmínek, k podobné mutaci může dojít téměř kdykoli i přirozenou cestou *(Hooper a Bloom, 2013)*. Virus s touto mutací kompletně přebírá funkci HA, což bylo potvrzeno na kmenech chřipkových virů s mnohonásobnými mutacemi a delecemi v konzervativní (receptor vázající) části HA *(Hooper a Bloom, 2013)*.

Protilátky proti neuraminidáze brání šíření infekce mezi buňkami, ale nemají neutralizační aktivitu *(Matrosovich, a kol., 2004)*. NA, stejně jako HA, podléhá změnám typu antigenní drift a mimo jiné obsahuje několik důležitých aminokyselin, které mohou podléhat mutacím s následným vznikem rezistence k inhibitorům neuraminidázy (NAIs) *(Yen, a kol., 2013)*, pokud je aminokyselina arginin (R) nahrazena v pozici 292 lysinem (K) dojde ke vzniku mutace R292K a rezistence k Oseltamiviru a Zanamiviru *(Chachra a Rizzo, 2008, Yen, a kol., 2013)*.

Další významnou mutací, která s sebou přináší rezistenci k Oseltamiviru, je H274Y. Tato mutace má za následek zmenšení počtu NA na povrchu buňky (což sníží anitivirální efekt NA). Defekt, který vznikl úbytkem NA, může vyvolat sekundární mutaci, která obnoví původní vlastnosti viru *(Bloom, a kol., 2010)*.

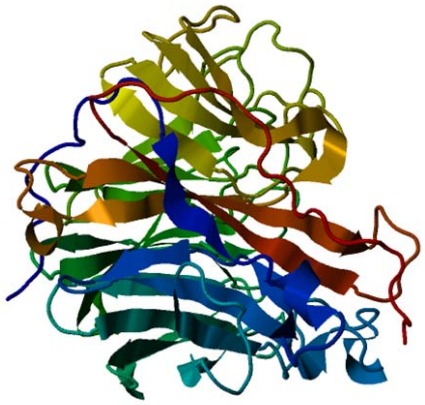

Obrázek č. 6: Neuraminidáza (Influenza A virus (A/Hong Kong/483/1997(H5N1)), ilustrační obrázek, sequence identity 94%, residue range: 64 to 448, zdroj: http://www.proteinmodelportal.org/.

3.3.5 Matrixové proteiny (M1 a M2)

Sedmý segment v RNA kóduje matrixový protein (M1) a iontový kanál (M2). M1 protein tvoří strukturovanou vrstvu pod virovou membránou, reaguje s povrchovými glykoproteiny a tvoří most mezi obalem viru a jádrem (vRNP). M1 protein může být vizualizován pomocí elektronové mikroskopie *(Fontana a Steven, 2013)*. M2 je multifunkční membránový protein tvořící protonový kanál, který hraje roli při uvolňování genomu z virového obalu *(Schnell a Chou, 2008)*. Proces vstupu viru do buňky a uvolnění RNP z obalu vyžaduje koordinovanou činnost M2 a M1 proteinů *(Rossman a Lamb, 2011, Schnell a Chou, 2008)*. Po vstupu do hostitelské buňky a uvolnění z endozomu se začne zvyšovat aktivita M2 iontového kanálu, a tím se zvýší tok kladně nabitých částic, které vyvolávají pokles pH uvnitř virionu. Výsledkem okyselení vnitřního prostředí viru, je narušení vazby HA a M1 a otevření virové částice, následně se HA přemístí a splyne s vnitřní membránou endozomu, RNP je transportován k jádru, kde začíná syntéza virové RNA *(Vasin, a kol., 2014)*.

3.3.6 Nestrukturální proteiny (NS1 a NS2)

Osmý segment chřipkových virů typu A kóduje dva proteiny označované od prvotních studií jako nestrukturální proteiny (NS1a NS2) *(Lamb a Choppin, 1983)*. Tyto proteiny jsou získávány alternativním sestřihem mRNA *(de Chassey, a kol., 2013)*. Oba proteiny mají důležité funkce při replikaci a proto jsou považovány za cíl pro vývoj

nových léků. NS1 je multifunkční protein s významnou úlohou při úniku před působením účinků imunitního systému hostitele *(Hale, a kol., 2008)*. Podstatou účinku NS1 je blokování syntézy interferonů interferonů α/β *(Jiao, a kol., 2008, Kim, a kol., 2002)*. NS1 je RNA vázající protein, který se v počáteční fázi infekce podílí na regulaci mnoha buněčných procesů, jako je inhibice hostitelské mRNA polyadenylace, inhibice jaderného exportu polyadenylované hostitelské mRNA, inhibice sestřihu mRNA a inhibice interferonem-zprostředkované anti-virové odpovědi *(Fortes, a kol., 1994, Garcia-Sastre, a kol., 1998, Hatada, a kol., 1999)*. NS1 redukuje syntetické i plicní prozánětlivé cytokiny *(Hyland, a kol., 2006)*. NS2 také označovaný jako NEP, hraje klíčovou roli při transportu RNA a polymerázových proteinů v průběhu replikace a v porovnání s NS1 je podstatně méně popsaný *(Akarsu, a kol., 2011)*. Byl nalezen jako součást purifikovaných virových částic nebo v jádru infikovaných eukaryotických buněk *(Kim, a kol., 2002, Smith, a kol., 1987)*. Řada studií dokazuje, že se podílí na regulaci replikace virové RNA *(Perez, a kol., 2010, Varble, a kol., 2010)*.

3.4 Mutační změny

Příčinou vzniku epidemií a pandemií jsou konstantně probíhající mutace, rychlost mutačních změn chřipky je v porovnání s některými dalšími viry (ebola) až 100 krát vyšší. Chřipkové antigeny (HA a NA) se mění zřejmě v důsledku postupného vývoje imunity (případně částečné imunity) populace *(Hall, a kol., 2013, Ito, a kol., 1998)*. Antigenní mutace se objeví a následně může být vybrána jako převládající kmen viru, pokud se liší od předcházejícího viru, který byl potlačen specifickou protilátkou, vzniklou v populaci jako důsledek infekce. Proces vzniku mutace viru a následné vytvoření post-infekčních protilátek u hostitele se opakuje kontinuálně a představuje evoluční mechanismus chřipkových virů, který umožňuje virům způsobovat opakované infekce a příležitostné pandemie s vysokou morbiditou a mortalitou *(Ito, a kol., 1998, Martcheva, 2012)*. Úspěšnost šíření chřipkových virů je založena na dvou typech antigenních změn.

3.4.1 Antigenní drift

Antigenní posun (drift) představuje menší a postupnou změnu antigenních vlastností viru, které způsobují opakování epidemie v jedno- až tří-letých intervalech a umožňují

reinfekci osob, které již nákazu daným typem prodělaly. Antigenní drift je menší změna ve struktuře povrchových antigenů a je výsledkem bodových mutací v konkrétním genovém segmentu *(Ferguson, a kol., 2003, Martcheva, 2012)*. Antigenní drift je často příčinou epidemií, protože imunita, která byla vytvořena po expozici předchozími subtypy, v případě nově zmutovaného subtypu nechrání jedince kompletně. Drift se vyskytuje u všech tří chřipkových rodů a je považován za pokračující evoluce chřipkových virů.

3.4.2 Antigenní shift

Antigenní zlom (shift) je závažnějším typem antigenní změny (větší změna ve struktuře povrchových antigenů) a vyskytuje se pouze u virů chřipky typu A. Antigenní shift je definován jako výskyt nového viru, imunologicky naprosto odlišného od chřipkových virů cirkulující v posledních letech *(Katz, a kol., 1999)*. Antigenní posun nastane, když je nový subtyp chřipky, který se běžně vyskytuje pouze u ptáků a prasat, přenesen na člověka *(Bahl, a kol., 2009)*. Ke vzniku nových pandemických kmenů může docházet po genetickém přeskupení mezi lidským a zvířecím chřipkovým virem, nebo prostřednictvím přímého přenosu zvířecího kmene chřipky na člověka *(Kim, a kol., 2014)*. Nový subtyp se objevuje náhle a jeho šíření má obvykle pandemický charakter. Tato změna nastává jedenou za 10 - 40 let. Antigenní shift představuje velkou změnu v genomu chřipky, což vede k infekci velké části populace, většinou napříč všemi věkovými skupinami a je spojen se zvýšeným procentem těžkých onemocnění a úmrtností *(Ferguson, a kol., 2003)*. Příčinou však není jen zvýšená závažnost onemocnění, ale hlavně zvýšený počet nakažených osob *(Ferguson, a kol., 2003, Mills, a kol., 2006)*. Antigenním shiftem vznikají pandemie, vyskytující se pouze u jednoho rodu a to influenzy typu A. Příčinou je virus, který běžně vyvolává onemocnění u jednoho druhu zvířat a který díky mutaci (v důsledku rekombinace) získá schopnost nakazit celou řadu dalších druhů včetně člověka *(Enserink, 2005, Gething, a kol., 1980)*. Obecně rozdíly v povrchových proteinech brání „v přeskoku“ přes mezidruhovou bariéru a infekci člověka, tato bariéra může být obejita mutací, jako v případě HPAI *(Kuiken, a kol., 2006, Mills, a kol., 2006)*.

3.5 Epidemie a pandemie

Pandemie chřipky a přírodní katastrofy mají něco společného. Víme, že se budou opakovat, ale naznáme místo, datum ani rozsah. Nemáme tušení, o jaký subtyp se bude jednat, jak rychle a v kolika vlnách se bude šířit. Nevíme, jestli zabije 1, 10 nebo 100 miliónů lidí.

Chřipka představuje vážné respirační onemocnění, které může být vysilující i pro zdravý organismus a může s sebou přinést řadu komplikací vedoucích k hospitalizaci nebo ke smrti, a to hlavně u pacientů patřících do rizikové skupiny. Každoroční chřipková epidemie má za následek 3-5 miliónů případů vážných onemocnění a 300-500 tisíc úmrtí *(Volz, a kol., 2013)*.

Nové epidemie chřipky typu A vznikají bodovou mutací (antigenní drift) dvou povrchových glykoproteinů: hemaglutiniu (HA) a neuraminidázy (NA). K těmto mutacím dochází v ročních nebo dvouletých intervalech. Nové varianty HA a NA antigenů jsou schopny se vyhnout imunitní reakci a tak nedochází k vytvoření trvalé imunity ani po vakcinaci ani po přirozené infekci *(Tsang, a kol., 2014)*, tyto konstantně probíhající, malé bodové mutace způsobující změny v antigenní výbavě viru chřipky. Nahromadění bodových mutací HA (nebo HA a NA) jsou příčinou výskytu pravidelných sezónních epidemií.

Na rozdíl od epidemií jsou pandemie vzácnější, ale interval mezi jednotlivými pandemiemi je postupně snižován. První záznamy o chřipkové pandemii se datují k 16. století a za posledních 4 století bylo zaznamenáno celkem 31 pandemií *(Yoshikura, 2014)*. V průběhu 20. století byly popsány tři pandemie. Tou nejhorší byla Španělská chřipka v roce 1918 *(Ito, a kol., 1998, Lina, 2008)*. Tato pandemie si vyžádala 50 miliónů obětí během 25 týdnů, což je více, než si AIDS vyžádala v průběhu 25 let. Dalšími dvěma pandemiemi byla Asijská chřipka (1957) a Hong-Kongská chřipka (1968), obě pandemie následující po Španělské chřipce byly mnohem mírnější *(Ito, a kol., 1998, Lina, 2008, Yoshikura, 2014)*. Španělské chřipka byla pravděpodobně ptačího původu (H1N1) *(Tumpey, a kol., 2005)*, vzhledem k tomu, že i další pandemické kmeny H2N2 v roce 1957 a H3N2 v roce 1968 obsahovali geny z ptačích virů, není pochyb, že všechny tři pandemie vznikly přeskupením genů (reasortment).

Co se týká klinických příznaků při onemocnění chřipkou, jsou velmi variabilní, ať už jde o epidemii nebo pandemii. Je možné, že polovina nakažených nemá vůbec žádné klinické příznaky. Klinický obraz může být od mírně závažných onemocnění až po těžké, které mohou ve svém důsledku ovlivnit kromě respiračního ústrojí i další orgány: srdce, mozek, játra, ledviny a svaly a nervovou soustavu *(Baguelin, a kol., 2012, Martcheva, 2012)*. Klinický průběh chřipky je ovlivněn na jednu stranu vlastnostmi viru na druhé straně stavem pacienta, v případě pacienta hraje roli věk, stav imunitního systému, kouření, komorbidita a také těhotenství *(Laskowski, a kol., 2014, Nicholson, a kol., 2003)*. V závažných případech může dojít i ke smrti, která nastává v důsledku primární virové nebo sekundární bakteriální pneumonie. Většinou dochází ke smrti převážně lidí v rizikové skupině (chronický nemocní pacienti, kojenci a staří lidé). Jen v případě pandemií 1918 a 1968 docházelo k úmrtí převážně u mladých jedinců *(Baguelin, a kol., 2012, Kobasa, a kol., 2004)*. Co se týká replikace viru v lidském organizmu je virus omezen na cylindrické epiteliální buňky respiračního systému. V momentě, kdy virus vstoupí do buňky je zahájena replikace, dochází ke kaskádě cytopatických efektů, hlavně tím, že poklesne syntéza proteinů hostitelské buňky. Ztráta kriticky důležitých proteinů hostitelské buňky vede k smrti nekrózou.

3.6 Vysoce patogenní ptačí chřipka

Pandemie v průběhu posledních několik století pravidelně opakovaly každých 10-40 let, podle tohoto scénáře bychom měli očekávat další pandemii v nejbližší době. Jedním z horkých kandidátů je ptačí chřipka, subtyp H5N1, vyznačující se endemickým výskytem u divokých vodních ptáků a domácí drůbeže v Asii. Vodní ptáci jsou hlavním přírodním rezervoárem ptačí chřipky typu A a onemocnění u nich probíhá často asymptomaticky. Většina ptačích chřipkových virů je hostitelsky specifická a jen některé mají zoonotický potenciál, což je činí schopnými vyvolat onemocnění u člověka. V roce 1997 bylo v Hongkongu laboratorně potvrzeno 18 případů ptačí chřipky u lidí, z čehož 6 bylo smrtelných *(Dankar, a kol., 2013)*. Dle údajů WHO bylo do roku 2014 nakaženo 650 lidí, z čehož 386 zemřelo *(http://www.who.int/influenza/en/, 2014)*. Pandemický potenciál subtypu H5N1 je už nyní alarmující a v budoucnu může ještě růst. Kromě subtypu H5N1 *(Van Kerkhove, 2013)*, bylo v posledních letech detekováno i několik dalších subtypů, běžně nalézaných ptáků, které dokázali překonat bariéru mezidruhového přenosu a infikovat člověka H9N2 *(Tretyakova, a kol., 2013)*,

H7N7 *(Stegeman, a kol., 2004)*, H7N2 *(Eames, a kol., 2010)*, H7N3 *(Rudenko, a kol., 2014)*, H7N9 *(Qiu, 2014)* a H10N7 *(Arzey, a kol., 2012)*. Klinická zpráva pacientů, kteří onemocněli ptačí chřipkou, popisuje horečnaté onemocnění a postižení horních nebo dolních cest dýchacích *(Conenello, a kol., 2011, de Jong, a kol., 2005)*. Kromě vysoké úmrtnosti bylo onemocnění subtypem H5N1 doprovázené dalšími netypickými rysy, jako příznaky postižení gastrointestinálního traktu u dospělých a vyšší míra dalších komplikací, jako je syndrom akutní respirační tísně, jaterní dysfunkce a selhání ledvin *(de Jong, a kol., 2005, Yuen, a kol., 1998)*. Viry ptačí chřipky subtypů H5, H7 a H9 jsou na vrcholu seznamu subtypů s největším pandemickým potenciálem, výše zmíněné subtypy získaly poměrně rychle schopnost přenosu z ptáka na člověka a je jen otázkou času, než získají i schopnost přenosu z člověka na člověka.

3.7 Chřipka

3.7.1 Klinické příznaky

Chřipka je nejčastější příčinou akutního respiračního onemocnění všech věkových skupin. Spektrum onemocnění se pohybuje od asymptomatických až po smrtelné, ale většina onemocnění probíhá jako akutní horečnaté onemocnění, které odezní bez komplikací. Po krátké inkubační době (obvykle 2 dny) se chřipka prezentuje náhlým nástupem horečky a zimnice, doprovázené bolestí v krku, dále bolestí hlavy a svalů, malátností, nechutenstvím a suchým kašlem. Horečka dosahuje vrcholu během 24 hodin od počátku nakažení a trvá 1-5 dny. Klinické příznaky zahrnují pocit nevolnosti, horečku, nastříknuté cévky v očích, hyperemické sliznice, a výtok z nosu.

3.7.2 Komplikace

Nejčastější komplikací je zápal plic jako důsledek sekundární bakteriální infekce, jejichž původcem jsou nejčastěji *Streptococcus pneumoniae, Staphylococcus aureus* a *Haemophilus influenzae*, tato komplikace se vyskytuje zejména u starších pacientů *(Joseph, a kol., 2013)*. Reye syndrom je komplikace, která se vyskytuje výhradně u dětí užívajících Aspirin hlavně ve spojení s chřipkou typu a je prezentováno zvracením a zmateností, které může progredovat do kómatu a otoku mozku, často s fatálním koncem *(Yuen, a kol., 1998)*. Další komplikací může být myokarditida a chronické bronchitidy. Komplikace s následkem smrti se vyskytují v počtu 0,5-1 na 1000 případů *(Muscatello, a kol., 2014)*.

3.7.3 Vakcinace

V současnosti jsou k dispozici dva druhy vakcín. V prvním případě se jedná o trivalentní inaktivovanou vakcínu (Trivalent inacitvated influenza vaccine - TIV), která je na trhu od roku 1940 *(Van Buynder, a kol., 2013)*. TIV je podávána intramuskulárně nebo intradermálně a obsahuje tři inaktivované viry chřipky: typ A (H1N1), typ A (H3N2) and type B, TIV vakcína obsahuje buď rozštěpené viriony nebo jejich subjednotky *(Barker a Snape, 2014, Palese a Garcia-Sastre, 2002)*. Dalším typem vakcíny proti chřipce je živá oslabená vakcína (Live attenuated influenza vaccine - LAIV), která obsahuje stejné viry jako TIV *(Cao, a kol., 2014)*. Každý virus se kultivuje odděleně, inaktivuje se a kombinuje se se zbývajícími dvěma viry *(Tretyakova, a kol., 2013)*. Vakcína se aplikuje vstřikem do nosních dírek (polovina dávky do každé nosní dírky). Tretyakova a spolupracovníci popsali rekombinantní viru podobnou částici (virus like particles – VLP), obsahující HA proteiny odvozené z virů subtypů H5N1, H7N2 a H9N2 jako experimentální vakcínu proti chřipce, ke koexpresi byl použit bakulovirový vektor *(Tretyakova, a kol., 2013)*. Rekombinantní VLP se jeví jako velmi slibné přístup pro výrobu vakcíny proti chřipce *(Perrone, a kol., 2009)*. Další možností jsou DNA vakcíny obsahující plazmidy, kódující jeden nebo více proteinů chřipkových virů, výsledky z testování DNA vakcín byly zatím hlášeny jen experimentů provedených na zvířecích modelech *(Bragstad, a kol., 2013, Liu, a kol., 2014, Wei, a kol., 2012)*.

3.7.4 Terapie

Pro léčbu a profylaxi chřipky jsou schváleny dvě skupiny antivirotik: blokátory M2 proteinu a inhibitory neuraminidázy (NAI). M2 blokátory jsou starší skupinou antivirotik, jejich účinek spočívá v blokování M2 proteinu, který plní funkci iontového kanálu a podílí se na iniciaci infekce hostitelské buňky *(Tisdale, 2009)*. Do skupiny blokátorů M2 proteinu patří amantadin a rimantidin. Pokud jsou M2 blokátory podávány v počátečním období infekce (do 48h od prvních příznaků), mohou redukovat dobu vylučování viru, zkracovat délku onemocnění a zmírňovat závažnost symptomů *(Pielak, a kol., 2009)*. Jejich podávání za účelem profylaxe je nutné zvážit, neboť u nich byly prokázány nežádoucí účinky na CNS *(Garcia a Aris-Brosou, 2014)*. Léčba pomocí M2 blokátorů má další dvě úskalí, jednak nejsou účinné v terapii chřipky typu B a v případě chřipky typu A byl prokázán častý výskyt rezistentních kmenů. Pielak a kol.

zaznamenali, že léčba M2 blokátory může vyvolat vznik rezistentních variant chřipky typu A u 30 - 80% osob *(Pielak, a kol., 2009)*. Druhou, novější skupinou jsou léky, které se řadí do skupiny zvané inhibitory neuraminidázy, do této skupiny patří dva léky Zanamivir a Oseltamivir *(van der Vries, a kol., 2013)*. NAI jsou v současné době předepisovány k léčbě chřipky častěji než M2 blokátory, důvody jsou dva jednak je to rostoucí rezistence chřipky typu A k M2 blokátorům a dále jejich neúčinnost v případě léčby chřipky typu B *(Hai, a kol., 2013, van der Vries, a kol., 2013)*. Zanamivir je distribuován v podobě prášku, který je aplikován vdechováním a je určen pro nekomplikované akutní případy chřipky u osob starších 7 let, u kterých symptom neprobíhají delší dobu než 48 hodin. Oseltamivir je podáván ve formě kapslí a je určen pro léčbu osob starších 1 roku se symptom trvajících maximálně 48 hodin, i v případě aplikace Oseltamiviru byla prokázána rezistence *(McGettigan, a kol., 2014)*. V případě Oseltamiviru je rezistence způsobena mutací H275Y, v případě Zanamiviru mutace Q136K *(Okomo-Adhiambo, a kol., 2014)*. Rezistence je v současnosti jedním z největších problémů antivirotické léčby a to v případě obou skupin léčiv.

3.8 Laboratorní diagnostika

Od roku 1933, kdy byl poprvé charakterizován lidský chřipkový virus, byla vyvinuta celá řada diagnostických postupů a testů. Během chřipkové sezóny se diagnostika často spoléhá na predikci na základě kašle a vysoké horečky. V takovém případě diagnostické testy nejsou vyžadovány a jsou prováděny jen v případech, pokud nejsou klinické příznaky jednoznačné, nebo kdy je nutné rozhodnout o další antivirotické nebo antibiotické léčbě. Nejpoužívanějšími metodami jsou: detekce antigenu, izolace viru a reverzní transkripční polymerázová reakce (RT-PCR), přičemž další skupinu tvoří sérologické testy *(Comin, a kol., 2013, Dong, a kol., 2014, Schutten, a kol., 2013)*. Neméně důležitou roli v diagnostice hraje správné načasování odběru vzorků a jejich kvalita *(Singh, a kol., 2014)*. Pro detekci antigenu, izolaci viru a RT-PCR jsou vzorky odebírány z respiračního traktu (stěry, výtěry a laváže), pro sérologické testy je nezbytný odběr krve.

Virus může být izolován z krku nebo nosohltanu pomocí stěrů získaných během prvních tří dní od nástupu onemocnění. Transport vzorků by měl probíhat co nejkratší

dobu a vzorky by měly být uchovávány při teplotě 2-8°C, v transportním médiu *(Ferdinands, a kol., 2014)*.

Krev (plná krev nebo sérum) se odebírá pro účely sérologického vyšetření (protilátky proti chřipce). Párové vzorky by měly být odebrány s 14-21 denním rozestupem a pro signifikantní zvýšení by měl být vzestup titru protilátek čtyřnásobný.

Kultivace viru se provádí naočkováním do amniového nebo alantoického vaku kuřecích embryí, případně na buněčných kulturách, které podporují replikaci virů. Průkaz virů chřipky zabere 2 dny a další 1-2 dny jsou nezbytné k dodatečné identifikaci typu/subtypu viru *(Li, a kol., 2014)*. Kultivace virů má důležitou úlohu při definování etologie lokální epidemie. Serologický průkaz vyžaduje signifikantní vzestup titru protilátek IgG. Vzorek z akutní fáze onemocnění by měl být odebrán nejpozději 5. den od počátku onemocnění a párový vzorek (rekonvalescentní) ideálně 21. den od počátku onemocnění. Mezi nejvíce používané sérologické testy se řadí inhibice hemaglutininu a fixace komplementu. Klíčovým testem pro průkaz chřipky je HI, který závisí na schopnosti viru hemaglutinovat lidské nebo kuřecí erytrocyty a inhibici této schopnosti pomocí specifické protilátky *(Comin, a kol., 2013)*. Diagnostika se opírá o minimálně čtyřnásobný vzestup titru protilátek. Rychlé diagnostické testy jsou potřebné pro posouzení nutnosti použít antivirotika a jejich včasné podání *(Comin, a kol., 2013, Schnell a Chou, 2008)*. Rychlá diagnostika hraje roli také při kontrole infekce v nemocničním prostředí a snižování přenosu infekce z pacienta na pacienta.

3.8.1 Přímé metody

Pro přímou detekci (detekuje se virová částice nebo antigen) je možno použít celou řadu metod, jako jsou enzyme-linked immunoassay, imunofluorescence a RT-PCR *(Kim a Poudel, 2013)*.

3.8.1.1 Imunofluorescence

Pro přímou imunofluorescenci, je nutné fixovat potencionálně infikované buňky respiračního epitelu, obsahující chřipkové viry a jejich antigeny, které jsou detekovány pomocí specifických protilátek konjugovaných s fluorescenčním barvivem (přímá imunofluorescence) *(Del Pozo, a kol., 2014)*, případně mohou být detekovány anti-protilátkou konjugovanou s fluorescenčním barvivem (nepřímá immunofluerescence)

(Noisumdaeng, a kol., 2014). Běžně používanými fluorescenčními barvivy jsou fluorescein a rhodamin. V obou případech se k vizualizaci reakce používá fluorescenční mikroskop, kde pozitivní buňky (infikované) jsou rozlišené intenzivním zbarvením a změnou morfologie. Přímá imunofluorescence je sice rychlejší, ale většinou méně senzitivní. Imunoflurescenceční metody umožňují rychlý průkaz viru, ale vyžadují správný odběr vzorků respiračního epitelu pacienta *(Del Pozo, a kol., 2014)*. Nevýhodou stanovení jsou individuální rozdíly ve vzorcích, interpretace je často subjektivní a správnost závisí na schopnosti a zkušenosti pracovníka.

3.8.1.2 Enzyme-linked immuno sorbent assay (ELISA)

ELISA, někdy také označována jako EIA (Enzyme immunoassay), funguje na bázi imunoenzymatické reakce a lze s ní rovněž detekovat jak antigen (přímá ELISA) *(Glikmann, a kol., 1995)*, tak i protilátku (nepřímá ELISA) *(Schutten, a kol., 2013)*. Podstatou metody je specifická interakce antigenu a protilátky. V případě přímé detekce (detekce antigenu - HA) je na povrch reakční nádoby nejprve pevně ukotvena protilátka (adsorpce nebo kovalentní vazba), v dalším kroku následuje vazba antigenu ze vzorku. Následuje vazba další protilátky konjugované s enzymem, katalyzujícím chemickou přeměnu chromogenního substrátu, který je do směsi přidán po dokončení vazby mezi antigenem a oběma protilátkami (v mezikrocích je vždy odstraněn přebytek reaktantu a následuje promytí). Enzym katalyzuje chemickou přeměnu substrátu na produkt, což se projeví změnou barvy. Změna barvy je detekována spektrofotometricky (v případě použití chromogenního substrátu) nebo fluorimetricky. Koncentrace produktu je přímo úměrná koncentraci detekovaného antigenu (nebo protilátky) *(Glikmann, a kol., 1995)*. ELISA a imunochromatografie jsou velmi rychlé (10-30 minut), ale jsou dražší než imunofluorescence nebo kultivace.

3.8.1.3 Imunochromatografie

Principem imunochromatografických metod je reakce antigenu přítomného ve vzorku s konjugátem za vzniku komplexu antigen-konjugát, který migruje směrem ke specifické protilátce imobilizované na porézní membráně (nitrocelulóza). Je-li ve vzorku přítomen antigen, vznikne v místě vazby antigenu a imobilizované protilátky band (pozitivní průkaz viru) *(Mitamura, a kol., 2013)*. Nadbytek konjugátu přítomného v testu, migruje dále membránou a váže se na další imobilizovaný protein, vzniká druhý

band, což je signálem pro ukončení testu. Hodnocení testu je prováděno vizuálně pomocí konjugovaných částic, kterými jsou nejčastěji zlato nebo uhlík *(Li, a kol., 2011, Park)*.

3.8.1.4 Polymerázová řetězová reakce spojená s reverzní transkripcí (RT-PCR)

RT-PCR zahrnuje kromě běžné amplifikace DNA (klasická PCR) ještě proces, při kterém je izolovaná chřipková vRNA přepsána na DNA (cDNA) pomocí reverzní transkriptázy *(Schnell a Chou, 2008)*. Následuje amplifikace pomocí primerů, komplementárních ke specifickému chřipkovému úseku vRNA přepsané na cDNA.. Výhodou této metody je vysoká senzitivita, možnost detekce subtypu, případně fylogenetická analýza *(Kim a Poudel, 2013)*. Nevýhodou je rychlá RNA degradace pomocí ribonukleáz (které jsou navíc termostabilní), což vyžaduje rychlé zpracování vzorků a použití inhibitorů RNas.

3.8.1.5 Izolace virů z infekčního materiálu

Při izolaci (kultivaci) viru je nutné naočkovat odebraný vzorek na vnímavé buňky a následně detekovat přítomnost viru díky zmožení viru na buňkách. Izolace vyžaduje rychlý transport vzorku do laboratoře, aby nedošlo k inaktivaci viru. V současné době je kultivace stále více vytlačována metodou PCR, nicméně stále poskytuje cenné informace o kvantitě a infekční povaze virů *(Li, a kol., 2011, Schutten, a kol., 2013)*.

K izolaci a množení virů se požívají:

- Buněčné kultury
- Kuřecí embrya
- Vnímavá zvířata

Izolace viru na buněčných kulturách

Pro kultivaci chřipkových virů je možné použít celou řadu buněčných linií, těmi nejpoužívanějšími jsou Madin-Darby canine kidney cells (MDCK) *(Danilenko, a kol., 2014)*. Kultivace tkáňových linií se provádí ve skleněných nebo plastových láhvích. Důležitým kritériem pro úspěšnou kultivaci je volba správného kultivačního média, teploty a složení atmosféry. Pro zvýšení úspěšnosti infekce se buňky ošetřují trypsinem.

Výhodou kultivace je vysoká citlivost, nevýhodou doba trvání (běžně zabere kultivace více než dva týdny) *(Danilenko, a kol., 2014)*.

Izolace viru na kuřecích embryích

Odebraný vzorek (stěr nebo výplach z dýchacích cest pacienta) je inokulován do amniové dutiny u 10-12ti denních kuřecích embryí *(Li, a kol., 2011)*. Zvýšení výtěžku viru je možno dosáhnout po 2-4 denní kultivaci. Poté se odebírá amniová tekutina, ve které se zjišťuje virus. Je stále používaná, ale nikoliv pro rutinní diagnostiku, ale spíše jako referenční metoda a to díky vysoké citlivosti *(Kandeil, a kol., 2014, Li, a kol., 2011)*.

Izolace viru na laboratorních zvířatech

I když lze adaptovat virus chřipky na laboratorní zvířata a všechny kmeny viru chřipky aglutinují ptačí erytrocyty (i některé savčí), pro rutinní diagnostiku chřipky se laboratorní zvířata nepoužívají. K biologickým pokusům se nejčastěji používají kuřata a kachňata *(Kalthoff, a kol., 2014)*. Fretky jsou používané jako model pro humánní infekci *(Belser, a kol., 2014, Kalthoff, a kol., 2014)*.

3.8.2 Nepřímé metody - sérologické testy

Sérologické testy detekují přítomnost chřipky stanovením přítomných protilátek. Sérologické testy nám mohou poskytnout informaci o přítomnosti specifických protilátek proti konkrétnímu antigenu, o množství celkových protilátek, nebo o množství konkrétní třídy protilátek (IgG, IgA, IgM). Mezi nejpoužívanější testy patří: inhibice hemaglutininu (HI), fixace komplement (CF), nepřímá immunofluorescence a ELISA (která je vhodná jak pro přímou, tak i nepřímou detekci) *(Comin, a kol., 2013, Dong, a kol., 2014)*. Sérologické testy nejsou vhodné pro diagnostiku akutních případů chřipky, ale jsou vhodné pro rozlišení akutní (nárůst IgM) a prodělané infekce (nárůst IgG). Pro sérologickou diagnostiku jsou nutné párové vzorky (první vzorek na začátku infekce, další po 14 dnech) a je nutný alespoň čtyřnásobný nárůst titrů protilátek. Sérologie může být použita pro testování účinnosti imunizace vakcinací.

3.8.2.1 Hemaglutinačně inhibiční test (HIT)

Tento typ testů je poměrně pracný a časově náročný a vyžaduje standardizaci postupu *(Schutten, a kol., 2013)*. Přítomnost protilátek je indikována inhibicí hemaglutinace (tvorba sraženiny, shlukování erytrocytů) a sedimentací erytrocytů. Jejich výhodou je vysoká citlivost (umožňují detekci protilátek řádově v pg) *(Comin, a kol., 2013)*. Reagencie pro test jsou levné a dostupné, je možné použít morčecí nebo slepičí červené krvinky, které se ředí na 0,4 - 0,5%. Sérum musí být nejprve zbaveno nespecifických hemaglutininů a inhibitorů hemaglutinace *(Lin, a kol., 2012)*. Nejnižší ředění séra, které inhibuje hemaglutinační reakci je HI titr. HIT je citlivější než fixace komplementu a má tu výhodu, že umožňuje přesnější rozlišení mezi HA subtypy.

3.8.2.2 Komplement fixační reakce (CFT)

CFT metody jsou založeny na schopnosti tvorby komplexu antigen-protilátka, komplement se naváže na komplex antigen protilátka, což má za následek, že není dostatek komplementu, který by byl schopný lyzovat senzitivní ovčí erytrocyty, které tvoří detekční složku testu. Tato metoda je náročná, vyžaduje kontrolu každého kroku a je méně citlivá než HIT, ale její výhodou je nízká cena *(Doller, a kol., 1987)*.

3.8.2.3 Enzyme linked immuno sorbent assay (ELISA)

I když je HIT stále považován za zlatý standard pro subtypizaci HA, je ELISA dobrou alternativou k HIT testu a může být snadněji automatizována *(Comin, a kol., 2013, Mookkan, a kol., 2013)*. ELISA je mnohem citlivější než HI a CF *(Dong, a kol., 2014)*. Dostupná je celá řada komerčních EIA testů, které jsou schopny detekovat IgG, IgA či IgM. Test není vhodný pro detekci akutní infekce.

3.9 Senzory a biosenzory

3.9.1 Senzory pro detekci ptačí chřipky

Senzor je nedílnou součástí měřícího zařízení, které převádí vstupní signál na signál vhodný pro měření a vyhodnocení. Elektrochemické senzory mohou být děleny na senzory s kapalným nebo pevným elektrolytem *(Palecek a Bartosik, 2012)* a dále na potenciometrické nebo ampérometrické *(Willander, a kol., 2014)*. Citlivou vrstvu tvoří rozhraní mezi elektrodou a analyzovaným prostředím, přičemž samotným senzorem

(převodníkem) je pracovní elektroda. Ideální senzor je vysoce specifický a senzitivní pouze k detekované složce. Přítomnost ostatních složek by neměla nijak ovlivnit signál detekované veličiny.

3.9.2 Biosenzory pro detekci ptačí chřipky

Biosenzor je analytický přístroj obsahující citlivý prvek biologického původu, který je buď součástí, nebo v těsném kontaktu s fyzikálně-chemickým převodníkem a poskytuje průběžný elektronický signál, který je přímo úměrný koncentraci jedné nebo několika (skupin) chemických látek ve vzorku *(Rechnitz, 1991)*. Biosenzor se tedy od senzoru liší přítomností biologické (biorekogniční) složky, která má bio-afinitní nebo bio-katalytickou úlohu. Bio-katalytickou úlohu mají v biosensorech nejčastěji buňky, tkáně, orgány, organely nebo enzymy. Principem je přeměna analytu v průběhu chemické reakce (sledovaný analyt je nejčastěji substrátem enzymové reakce). Do skupiny bio-afinitních senzorů patří nukleové kyseliny, lektiny a protilátky, v tomto případě je analyt specificky vázán. Typický biosenzor se skládá ze tří částí, biologický prvek (enzym, protilátka, DNA, atd), čidlo pro snímání signálu (elektrické, optické nebo tepelné), a prvek pro zesílení / zpracování signálu *(Velasco-Garcia a Mottram, 2003)*. Způsob převodu signálu závisí na typu fyzikálně chemické změny vyplývající z počátečního a konečného signálu *(Singh, a kol., 2014)*. V mnoha případech je důležitou součástí biosenzoru membrána, která pokrývá bio-rekogniční část senzoru a jejíž hlavními funkcemi jsou selektivní propustnost, řízení difúze analytu, ochrana proti mechanickému poškození a podpora biologické složky *(Merkoci, a kol., 2005, Sadik, a kol., 2009)*. Mezi nejčastěji používané biologické části senzorů patří enzymy *(Cosnier a Mailley, 2008, Dey a Raj, 2014, Qureshi, a kol., 2009)*, protilátky a *(Cosnier a Mailley, 2008, Nidzworski, a kol., 2014)*, oligonukleotidy *(Aydinlik, a kol., 2011, Grabowska, a kol., 2014, Muti, a kol., 2010)*. Běžně používané elektrochemické převodníky jsou potenciometrické *(Liu, a kol., 2011, Souza, a kol., 2011)*, ampérometrické *(Komarova, a kol., 2005)* a vodivostní *(Gooding, 2002)*. Dalším příkladem převodníků jsou piezoelektrické měniče *(Cai, a kol., Tam, a kol., 2009)*.

4 MATERIÁL A METODIKA

4.1 Chemikálie

Tris (2-karboxyetyl) fosfin byl zakoupen od Molecular Probes (USA). Všechny dále uvedené chemikálie byly zakoupeny od firmy Sigma-Aldrich (USA) v ACS kvalitě (pokud není uvedeno jinak). Pro syntézu kvantových teček (QDs) byly použity tyto chemikálie: dusičnan kademnatý $Cd(NO_3)_2 \cdot 4H_2O$, 3-merkaptopropionová kyselina, hydroxid amonný, sulfid sodný monohydrate $Na_2S \cdot 9H_2O$, dusičnan zinečnatý $Zn(NO_3)_2 \cdot 6H_2O$, octan olovnatý $Pb(OAc)_2 \cdot 3H_2O$. Pro přípravu pufrů byly použity: Acetátový pufr (CH_3COONa, CH_3COOH), Amoniakální pufr ($Co(NH_3)_6Cl_3$, $NH_3(aq)$, NH_4Cl), Tris-glycinový pufr (Trizma-báze, glycin a SDS). Fosfátový pufr (PB) (NaH_2PO_4, Na_2HPO_4). Fosfátový pufru I (pH = 6.5, NaCl, Na_2HPO_4, NaH_2PO_4). Hybridizační pufr (fosfátový pufr, guanidin thiocynate, Tris, pH = 7.5). Eluční roztok (fosfátový pufr II NaCl, Na_2HPO_4, NaH_2PO_4). Jako matrix pro detekci pomocí MALDI byla použita 3-hydroxyskořicová kyselina(Sigma-Aldrich, USA).

Zásobní roztoky QDs, standardů a všech potřebných pufrů byly připraveny v ACS vodě (Sigma-Aldrich, USA) a uchovány v temnu, při 4 °C. Hodnoty pH byly měřeny s použitím WTW inoLab Level 3 (Weilheim, Německo). pH-elektroda (SenTix-H) byla pravidelně kalibrována souborem WTW pufrů. Příprava deionisované vody byla provedena demineralizací pomocí reverzní osmózy na přístrojích Aqua Osmotic 02 (Aqua Osmotic, Česká republika) a následně purifikací pomocí Millipore RG (Millipore Corp., USA). Deionisovaná voda byla použita pro promývání, oplach a přípravu pufrů.

Pro účely izolace cílových biomolekul byly použity dva typy paramagnetických částic (MPs): Streptavidin Dynabeads M-270 (Life Technologies, USA) a Dynabeads Oligo $(dT)_{25}$ (Invitrogen, Norsko). Biotinylovaný multivalentní glykan (01-078 [Neu5Acα2-3Galβ1-3GlcNAcβ1-PAA-biotin]) byl zakoupený od firmy GlycoTech (USA). HA odvozené od virů chřipky typu A (H5N1, a H1N1) exprimované v Baculoviru, byly objednány od Prospec-Tany TechnoGene Ltd (Izrael). Jako standard HA byla použita vakcína proti chřipce Vaxigrip ® (Sanofi Pasteur, Francie), která obsahovala rozštěpené viriony následujících kmenů: A/California/7/2009 (H1N1),

A/Victoria/361/2011 (H3N2) a B/Wisconsin/1/2010. Vzorek inaktivovaného viru H5N1 byl darován Veterinární a farmaceutickou univerzitou v Brně.

PNA oligonucleotid (cystein-CCTCAAGGAG) byl syntetizován firmou Biosynthesis (Biosynthesis, USA). K PNA komplementární a od chřipky odvozená DNA sekvence (5´ AAAAACTCCTTGAGG 3´) byla objednaná od Sigma Aldrich (Sigma-Aldrich, USA).

4.2 Metody a instrumentace

4.2.1 Izolace cílových molekul pomocí MPs, ep Motion 5075

Automatická pipetovací stanice epMotion 5075 byla použita pro izolaci cílových biomolekul, kterými byly ODN a HA, označeny kvantovými tečkami (QDs). V obou případech byly jako platforma pro izolaci použity MPs. V případě izolace komplexu HA-QDs byly použity Streptavidin Dynabeads M-270. Pro izolace komplexu ODN-QDs Dynabeads Oligo $(dT)_{25}$. Důležitou částí pipetovací stanice je pohyblivé rameno s optickým senzorem, uzpůsobené pro uchycení pipetovacích nástavců a nástavce pro přenášení mikrotitrační destičky. Další nedílnou součástí zařízení je počítač s řídícím softwarem a dále pracovní plocha vybavená špičkami (objem 50µl, 300µl, 100µl), magnetickou a termostatovanou podložkou a zásobníky na vzorky a pufry.

Izolace komplexu ODN-QDs

Nejprve bylo pipetováno 10 µl Dynabeads Oligo $(dT)_{25}$ (Invitrogen, Norsko) do jednotlivých jamek v mikrotitrační destičce a destička byla přenesena na magnet a nakonec byl odpipetován uchovávací roztok z MPs. Potom byly MPs třikrát promyty 20 µl fosfátového pufru I (PBI). Následně byl přidán hybridizační pufr (10 µl) 10 µl polyA-modifikované próby (komplementární řetězec ODN k cílové molekule) a směs byla následně inkubována (15 min, 25°C). Dalším krokem bylo trojnásobné promytí obsahu jamek 20 µl PBI. Následoval druhý hybridizační krok, kdy do jamek bylo napipetováno 10 µl komplexu cílového ODN značeného QDs a 10 µl hybridizačního pufru a opět proběhla ikubace (15 min, 25°C). Procedura byla zakončena trojnásobným promytím pomocí 20 µl PBI. V posledním kroku bylo přidáno 30 µl elučního roztoku a mikrotitrační jamka byla inkubována (5 min, 85°C). Destička byla přenesena na magnet a supernatant byl odpipetován do nových jamek.

Izolace komplexu HA-QDs

Prvním krokem automatické izolace bylo pipetování 10 µl of Dynabeads® M-270 Streptavidin, do jamek mikrotitrační destičky (Eppendorf, Německo). Po té byla destička přenesena na magnet a byl odpipetován uchovávací roztok z MPs. Následně byly MPs promyty 100 µl fosfátovým pufrem (PB). Poté bylo pipetováno 20 µl biotinylovaného multivalentního glykanu. Následovala inkubace (30 min, 25 °C, 400 rpm). V dalším kroku byly jamky třikrát promyty 100 µl PB a bylo přidáno 20 µl vzorku (komplex HA s Cd QDs). Směs byla opět inkubována a následně třikrát promyta 100 µl PB. V posledním kroku bylo přidáno 35 µl of PB a komplex MPs-glykan-HA CdQDs byl rozbit ultrazvukem (2 min). Mikrotitrační destička byla přenesena na magnet a supernatant byl odpipetován z MPs do nových jamek.

Obrázek č. 7: Automatická pipetovací stanice ep Motion, a) řídící počítač, b) rameno pohyblivé v osách x, y a z pro uchopení pipetovacích nástavců a drapáku pro přenos mikrotitračních destiček, c) optické čidlo, d) vybavení pracovní plochy (magnetické a termoregulační podložky, zásobníky pufrů a vzorků).

4.2.2 Elektrochemická detekce izolovaných cílových molekul

Izolované komplexy cílových molekul (HA, ODN) s QDs byly detekovány elektrochemicky pomocí analyzátoru 663 VA Stand v elektrochemické cele s klasickým tříelektrodovým zapojením. Visící rtuťová kapková elektroda (HMDE) s plochou kapky 0,4 mm^2 byla použita jako pracovní elektroda. Ag/AgCl/3M KCl elektroda jako referentní a platinová elektroda jako pomocná. Analyzované vzorky byly před vlastním stanovením deoxygenovány probubláváním argonu (99,999 %). Jako pracovní elektrolyt byl vybrán acetátový pufr (CH_3COONa, CH_3COOH, pH 5).

Detekce signálu ODN a PNA (CA pík)

Pro detekci CA píku byla zvolena přenosová adsorptivní technika spojená se square wave voltametrií (AdT SWV) s následujícími parametry: počáteční potenciál 0 V; koncový potenciál -1.85 V; frekvence 10 Hz; potenciálový krok 0.005 V; amplituda 0.025 V.

Pro detekci PNA ODN byly použity metody AdT SWV, DPV a cyklická voltametrie (CV), parametry metod jsou uvedené ve vědeckém článku IX (výsledky).

Detekce signálu kovové části QDs (pík kovu)

Pro detekci signálu kovové části QDs (pík kovu) byla zvolena metoda diferenční pulzní voltametrie, parametry metody byly následující: Cd (počáteční potenciál -0.9 V; konečný potenciál -0.45 V); Zn (počáteční potenciál -1.2 V; konečný potenciál -0.85 V); Pb (počáteční potenciál -0.6 V; konečný potenciál -0.25 V); ostatní parametry byly shodné: depoziční potenciál -0.9 V; depozice 240 s; čas equilibrace 5 s; modulační čas 0.06; interval 0.2 s; potenciálový krok 0.002 V; amplituda 0.025V.

Detekce katalytického signálu HA

HA byl detekován pomocí Brdičkovi reakce *(Skalickova, a kol., 2013)*, adsorptivní přenosovou technikou ve spojení s diferenční pulzní voltametrií (AdT DPV). Veškerá měření probíhala též na přístroji 663 VA Stand (Metrohm, Switzerland) s chlazenou elektrochemickou celou a klasickým tříelektrodovým zapojením (viz výše). Teplota elektrochemické cely, ve které probíhala měření, byla 4 °C. Stálá teplota byla udržována

zařízením Julabo F25 instrument (JulaboDE, Německo). Před měřením byl vzorek deoxygenován argonem (99,999 %, 120 s). Měření HA probíhala v prostředí Brdičkova elektrolytu: 1mM $Co(NH_3)_6Cl_3$ a 1M amoniakální pufr (NH_3(aq) + NH_4Cl, pH = 9.6). Parametry AdT DPV byly následující: počáteční potenciál -0.7 V; konečný potenciál -1.75 V; modulační čas 0.057 s; časový interval 0.2 s; potenciálový krok 0.002 V; modulační amplituda 0.025V. Pro zpracování a vyhodnocení všech výsledků byl použit software GPES 4.9.

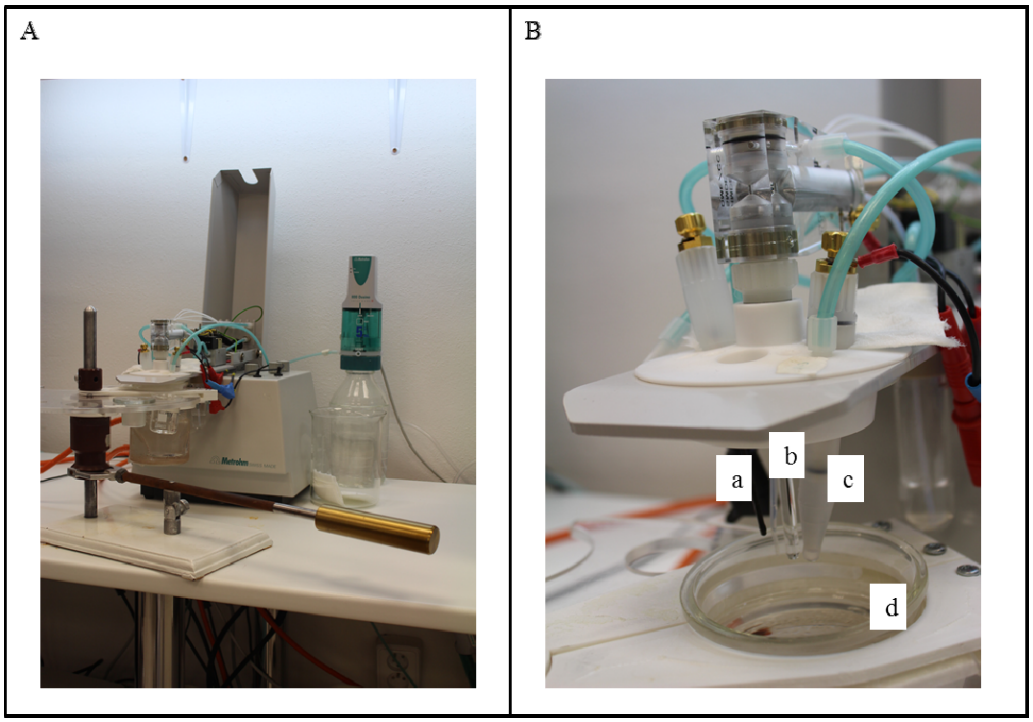

Obrázek č. 8: Automatická pipetovací stanice ep Motion, a) řídící počítač, b) rameno pohyblivé v osách x, y a z pro uchopení pipetovacích nástavců a drapáku pro přenos mikrotitračních destiček, c) optické čidlo, d) vybavení pracovní plochy (magnetické a termoregulační podložky, zásobníky pufrů a vzorků).

4.2.3 Hmotnostní spektrometrie, MALDI-TOF

K charakterizaci HA byl použit MALDI-TOF hmotnostní spektrometr Bruker ultrafleXtreme (Bruker Daltonik GmbH, Německo) s 355 nm Nd:YAG laserem s maximální frekvencí 2000 Hz, s nastaveným urychlujícím napětím 25 kV a zpožděnou extrakcí 100 ns. Měření probíhalo v lineárním, pozitivním iontovém módu. Pro sběr a zpracování dat byly použity programy flexControl verze 3.4 a flexAnalysis verze 2.2. Roztok matrice byl složen z nasyceného roztoku kyseliny α-kyan-4-hydroxyskořicové

(Sigma-Aldrich) v 30% acetonitrilu a 0.1% kyselině trifluoroctové. Pracovní roztoky byly připravovány každý den ze zásobních roztoků. Vzorek vakcíny byl před nanášením smíchán v objemovém poměru 1:1 s nasyceným roztokem matrice, a poté byl nanášen vždy 1 μl směsi na jeden spot destičky MTP Anchorchip 384 BC (Bruker Daltonik). Kalibrační roztoky standardů proteinů (Bruker Daltonik) byly použity pro externí kalibraci. Hmotnostní spektra byla typicky získávána zprůměrováním 20 subspekter z celkových 500 laserových pulsů.

4.2.4 Skenovací elektrochemický mikroskop (SECM)

Charakterizace MPs a MPs-glykan-HACdS byla provedena pomocí SECM CHI 920C v amperometrickém módu. Pro pracovní a substrátovou elektrodu byly zvoleny následující parametry: WE (pracovní elektroda, Pt): 0,25 V, čas k ustálení proudové odezvy 2 s; sensitivita 1,0 E^{-9} A/V; rychlost skenování: 10 μm/0,02 s SA (substrátová elektroda, Au): 0,1 V; sensitivita 1.0 E^{-6} A/V. Ferrocenmethanol byl použit jako elektrochemický mediátor. Všechna měření byla provedena se stejnou vzdáleností mezi hrotem elektrody a substrátem (d=30 μm).

Elektrochemická cela byla čištěna ultrazvukem (ve směsi acetonu a etanolu, poměr 1:1) a následně čištěna peroxidem a kyselinou sýrovou (1:3). Čištění elektrody trvalo 5 minut a z povrchu elektrody byly odstraněny veškeré nečistoty. Hrot byl čištěn ultrazvukem pouze v etanolu. Po chemickém čištění, byla spuštěna cyklická voltametrie (CV) v 30% (*v/v*) kyselině sírové. Nakonec byly všechny výše zmíněné části opláchnuty miliQ vodou a osušeny dusíkem. Tato procedura byla opakována po každém dalším měření.

4.2.5 Gelová elektroforéza, charakterizace a separace HA a HA-QDs

Pro gelovou elektroforézu bylo použito zařízení Mini Protean Tetra apparatus s rozměrem gelu 8.3 × 7.3 cm (Bio-Rad, USA). Nejdříve byl nalit 15 % nebo 12.5 % (*m*/*V*) separační gel, který byl převrstven 5 % (*m*/*V*) koncentračním gelem. Gel byl připravený z 30 % (*m*/*V*) akrylamidového zásobního roztoku s 1 % (*m*/*V*) bis-akrylamidem. Polymerizace separačního a koncentračního gelu probíhala při pokojové teplotě po dobu 45 min nebo 30 min. Před vlastní analýzou byly vzorky smíchány s neredukujícím pufrem v poměru 2:1. Vzorky byly inkubovány při teplotě 93°C po dobu 3 min a nanášeny na gel. Pro stanovení molekulové hmotnosti byl použit proteinový

žebříček “Precision plus protein standards” od firmy Biorad (USA). Parametry elektroforézy byly nastaveny následovně: napětí 150 V, délka trvání 1 h a teplota 23 °C. Separace probíhala v prostředí Tris-glycinového pufru (0.025 M Trizma-base, 0.19 M glycin a 3.5 mM SDS, pH = 8.3). Následně byl gel obarven Coomassie-blue. Procedura barvení pomocí Coomassie-blue staining byla převzata od *Wong et al. (Wong, a kol., 2000)*.

4.2.6 Výroba čipu, 3D tiskárna

Pro výrobu mikrofluidního 3D čipu byl použit modelovací program Blender 2.65 (http://www.blender.org/community/get-involved). Model z tohoto programu byl exportován do STL formátu and a následně editován programem netFabb (Parsberg, Německo). Takto opravený model v STL formátu byl otevřen v programu G3DMAKER (DO-IT, Česká republika) 3D a vytištěn pomocí 3D tiskárny EASY 3D MAKER (DO-IT, Česká republika). Jako materiál byl použit polylaktid (PLA) (DO-IT, Česká Republika), který byl aplikován extrusí (tavící hlava) při teplotě 210 °C na zahřívanou podložku (40 ° C). Každý čip byl nejprve zbaven drobných nepřesností, a následně osazen třemi elektrodami (pracovní skleněná uhlíková mikroelektroda (GCm), referenční uhlíková elektroda s průměrem 0.5 mm, a pomocná elektroda z platinového drátku). Posledním krokem při výrobě čipu bylo přiložení plastového víka.

5 VÝSLEDKY A DISKUSE

Výsledková část předkládané dizertační práce je přiložena ve formě publikací v odborných časopisech a dále doplněna o komentáře autorky. U každé práce je vyznačen i podíl autorky na vytvoření publikace, se kterým souhlasí všichni uvedení spoluautoři.

5.1 Senzory a biosenzory pro detekci chřipky

5.1.1 Vědecký článek I

KREJCOVA, L.; HYNEK, D.; ADAM, V.; HUBALEK, J.; KIZEK, R.
Electrochemical Sensors and Biosensors for Influenza Detection.
International Journal of Electrochemical Science, 2012, roč. 7. č. 11, s. 10779-10801.
ISS 1452-3981. IF: 1.956
Podíl autorky Krejčová L.: 60 % textové části práce

Vznik pandemie, která by mohla ohrozit 7 miliard lidí je jednou z největších hrozeb lidstva. Na základě znalostí historie a epidemiologických dat je chřipka považována za potencionálního původce číslo jedna *(Lazzari a Stohr, 2004, Lina, 2008)*. Klíčovým nástrojem pro boj proti vzniku a šíření pandemie je včasná a přesná diagnóza. Současně používané metody detekce jsou často náročné na vybavení, personál a čas. Z toho důvodu je předmětem zájmu hledání rychlé, citlivé a selektivní metody pro detekci chřipky. Slibnou oblast představuje využití nanočástic ve spojení s elektrochemickou detekcí. Cílem našeho článku bylo popsat a diskutovat strategie pro detekci chřipkových virionů, proteinů a nukleových kyselin a prezentovat souhrn poznatků publikovaných do roku 2012.

Základní členění vědeckého článku I tvoří dvě kapitoly, senzory a biosenzory. První definuje senzory a blíže popisuje čtyři typy pracovních elektrod (rtuťové, amalgámové, uhlíkové a tištěné) a jejich využití pro elektrochemickou detekci biomolekul. Podkapitola rtuťové elektrody pojednává o historii tohoto typu senzorů a obsahuje popis současně používaných technik, především pro detekci nukleových kyselin (DNA, RNA), jako jsou cyklická voltametrie (CV), diferenční pulzní voltametrie (DPV), square wave voltametrie (SWV), eliminační voltametrie (EVLS) a

chronopotenciometrie. Diskutováno je i spojení adsorptivní přenosové techniky (AdTS) s výše uvedenými metodami pro zvýšení citlivosti detekce nukleových kyselin *(Palecek a Bartosik, 2012)*.

Další podkapitolou senzorů jsou amalgámové elektrody, které jsou netoxické a v řadě případů mohou úspěšně nahradit rtuťové elektrody *(Yosypchuk a Barek, 2009, Yosypchuk, a kol., 2002, Yosypchuk a Novotny, 2002)*. I zde je diskutováno využití techniky AdTS pro anlýzu DNA se snadnou detekcí pikogramových množství modifikované DNA nebo ODN *(Fadrna, a kol., 2005, Yosypchuk, a kol., 2006)* a dále využití amalgámové elektrody k detekci DNA bez nutnosti použití elektrochemicky aktivní značky *(Fojta, a kol., 2010)*.

V případě uhlíkových elektrod jsou popsány různé typy senzorů obsahující jako vodivý materiál uhlík, který je umístěn v pojivu, která mohou být tekutá (uhlíkové pastové elektrody) nebo pevná (tištěné uhlíkové elektrody). Velkou výhodou uhlíkových elektrod je možnost modifikace pojiva chemickými nebo biologickými látkami a čímž je možné zvýšit citlivost a specifitu stanovení *(Jacobs, a kol., 2010)*. V kapitole jsou popsány i uhlíkové nanotrubice a jejich využití pro hybridizační DNA senzory *(Qureshi, a kol., 2009)*.

Poslední podkapitolou senzorů jsou tištěné elektrody (Screen printed electrode – SPE). Pro detekci virové nukleové kyseliny se často používá hybridizační reakce na povrchu elektrody *(Adam, a kol., 2010, Martinez-Paredes, a kol., 2009)*. Druhou možností je využití modifikovaných povrchů SPE. K modifikaci povrchu SPE se používají různé typy nanočástic (chitosan/Fe_3O_4 a zlaté) *(Lam Dai, a kol., 2011, Qureshi, a kol., 2009)*.

Druhá část článku je věnována biosenzorům, jejichž nedílnou součástí je biologická složka spojená s detektorem. Biologickou částí biosenzorů bývají enzymy, protilátky a nukleové kyseliny. S hybridizačním typem biosenzorů (kde biologickou část tvoří komplementární řetězec k cílové sekvenci), se setkáváme poměrně často. Pro tyto účely byly testovány různé typy pracovních elektrod, ale nejčastěji zlaté, uhlíkové *(Malecka, a kol., 2012)* a rtuťové *(Palecek a Bartosik, 2012)*. Dalším směrem ve vývoji biosenzorů jsou microarray (DNA nebo genové čipy), použitelné pro současné stanovení více specifických sekvencí. Microarray jsou tvořeny pevnou podložkou, na jejímž povrchu

jsou zakotvené próby (komplementární sekvence k cílovým molekulám). Microarray se používají k detekci *(Li, a kol., 2009)*, subtypizaci *(Kongchanagul, a kol., 2011)* nebo identifikaci *(Liu, a kol., 2006)* chřipkových kmenů. Další podkapitola biosenzorů je věnována křemenným mikrovážkám (quartz crystal microbalance, QCM). Principem je měření změny frekvence křemenného rezonátoru. Změna frekvence je dána přidáním nebo odebráním hmoty, například v důsledku oxidace nebo depozice filmu na povrchu krystalu *(Liu, a kol., 2008)*. QCM systém může být použit ve vakuu, v plynné fázi nebo v kapalině *(Owen, a kol., 2007)*. Měření v kapalném prostředí je vhodné pro sledování afinitních reakcí. QCM se používá i ke zkoumání interakce biomolekul. Další možností využití QCM je konstrukce imunosenzoru, kde se využívá afinity mezi cílovou molekulou (HA) a protilátky *(Hewa, a kol., 2009, Liu, a kol., 2008, Owen, a kol., 2007)*. Další velká skupina biosenzorů je založena na použití nanočástic. Pro účely izolace a detekce chřipky jsou hojně využívané QDs *(Krejcova, a kol., 2012, Li, a kol., 2012)*, MPs *(Krejcova, a kol., 2012)*, zlaté nanočástice *(Mu, a kol., 2010)* nebo modifikované uhlíkové nanočástice *(Muti, a kol., 2012)*.

Pro detekci chřipky se často používají i biosenzory na bázi aptamerů, což jsou molekuly složené z několika nukleotidů (méně než 100). Výběr vhodné sekvence, která umožňuje vysoce selektivní vazbu cílové biomolekuly (proteinu, sacharidu, nukleové kyseliny) je klíčovým prvkem. V případě detekce chřipky jsou nejčastěji využívány sekvence vázající HA *(Misono a Kumar, 2005)*.

Dalším možným přístupem k detekci chřipky pomocí biosenzorů je měření impedance. Tato stanovení jsou založena na dvou možných přístupech: impedanční spektroskopii *(Hassen, a kol., 2011)* a konstrukci elektrochemických impedančních imunosenzorů *(Wang, a kol., 2009)*.

Zájem o senzory a biosenzory se neustále stupňuje a to jak v oblasti výzkumu, tak v oblasti komerčního využití. Spojení nanotechnologií a různých typů elektrod představuje řadu možností detekce specifických markerů nebo specifických DNA sekvencí, charakteristických pro konkrétní onemocnění. A právě detekční systémy spojené s nanotechnologiemi bývají nejčastěji zaměřeny na konstrukci senzorů a biosenzorů pro identifikaci zájmových molekul.

Int. J. Electrochem. Sci., 7 **(2012)** 10779 - 10801

International Journal of
ELECTROCHEMICAL
SCIENCE
www.electrochemsci.org

Review Paper

Electrochemical Sensors and Biosensors for Influenza Detection

Ludmila Krejcova[1], *David Hynek*[1,2], *Vojtech Adam*[1,2], *Jaromir Hubalek*[1,2] *and Rene Kizek*[1,2,*]

[1] Department of Chemistry and Biochemistry, Faculty of Agronomy, Mendel University in Brno, Zemedelska 1, CZ-613 00 Brno, Czech Republic, European Union
[2] Central European Institute of Technology, Brno University of Technology, Technicka 3058/10, CZ-616 00 Brno, Czech Republic, European Union
[*]E-mail: kizek@sci.muni.cz

Received: 3 September 2012 / *Accepted:* 28 September 2012 / *Published:* 1 November 2012

World Health Organization, United Nations and national governments are doing detailed monitoring of influenza viruses due to the fact that there is considerable concern about the emergence of new global pandemics with significant socio-economic impact. These concerns are based on known epidemiological data and knowledge, because antigens (hemagglutinin and neuraminidase) of influenza viruses can easily and quickly changed. Result of mutational changes is the emergence of a new subtype of the virus, which can cause a worldwide pandemic with a high fatality rate due to its virulence properties (Spanish Flu 1918, Asian Flu 1957, Hong Kong Flu 1968). Assessment of pathogenicity and virulence is the key to taking appropriate health actions in the outbreak of several tens of hours. Methods used for detection of viruses demand on equipment and personnel, and, moreover, confirmation (diagnosis) of infection lasts hours to days. Given the above, finding methods for rapid, sensitive and selective detection of the virus in the environment, body fluids and tissues is still challenging. A promising area of nanotechnology seems to using nanoparticles in combination with electrochemical detection. The aim of this review is to describe and discuss the previously known facts in the detection of influenza viruses and to outline the challenges and trends in the field of electrochemical detection. In this paper, there are described and discussed appropriate strategies for detection viral nucleic acid, specific viral proteins and virions. The strategies are divided into two main parts as sensors and biosensors.

Keywords: influenza virus; electrochemical detection; biosensor; sensor; nucleic acid; viral protein; viral genome; magnetic nanoparticle; quantum dots; voltammetry

1. INTRODUCTION

Influenza viruses belong to the family *Orthomyxoviridae*, which is the member of the group ssRNA viruses with negative polarity. This family contains three genera: Influenza A, Influenza B and Influenza C [1-3]. These genera differ from each other by the presence species-specific nucleo-protein

antigens, the number of gene segments, host specificity and clinical manifestations. Size of influenza virion is 80-120 nm and its schematic structure, which is similar for all genera, is shown in Fig. 1.

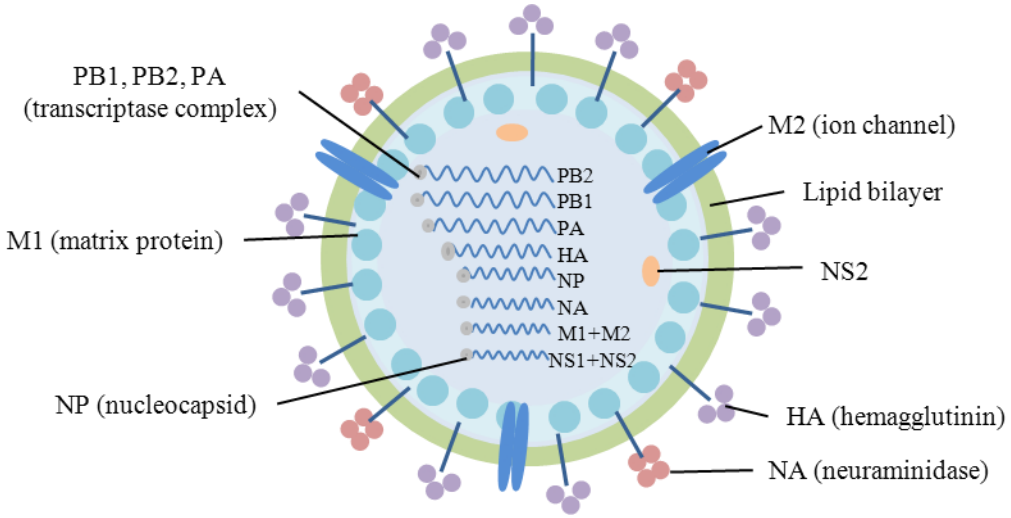

Figure 1. Structure of influenza virion. The influenza virion (as the infectious particle is called) is roughly spherical. It is an enveloped virus – that is, the outer layer is a lipid membrane, which is taken from the host cell, in which the virus multiplies. Inserted into the lipid membrane are 'spikes', which are proteins – actually glycoproteins, because they consist of protein linked to sugars – known as HA (hemagglutinin) and NA (neuraminidase). These are the proteins that determine the subtype of influenza virus (A/H1N1, for example). The HA and NA are important in the immune response against the virus; antibodies against these spikes may protect against infection. M2 protein is anchored in the lipid membrane. Beneath the lipid membrane is a viral protein called M1, or matrix protein. This protein, which forms a shell, gives strength and rigidity to the lipid envelope. Within the interior of the virion are the viral RNAs – 8 of them for influenza A viruses. These are the genetic material of the virus; they code one or two proteins. Each RNA segment, as they are called, consists of RNA joined with several proteins shown in the diagram: B1, PB2, PA, NP. These RNA segments are the genes of influenza virus. The interior of the virion also contains another protein called NS2.

The enveloped influenza A virions have three membrane proteins: hemagglutinin (HA), neuraminidase (NA) and ion channel (M2). There is a matrix protein (M1) just below the lipid bilayer, a ribonucleoprotein core (consisting of 8 viral RNA segments and three proteins: PA, PB1, PB2), and the NEP/NS2 protein [2]. Influenza B virions have four proteins in the envelope: HA, NA, NB, and BM2. Like the M2 protein of influenza A virus, the BM2 protein is a proton channel that is essential for the uncoating process. The NB protein is believed to be an ion channel, but it is not required for viral replication in cells [3]. The enveloped virions of influenza C viruses have hexagonal structures on the surface and form long (500 μm) cordlike structures as they bud from the cell. Like the influenza A and B viruses, the core of influenza C viruses consists of a ribonucleoprotein made up of viral RNA

and four proteins. The M1 protein lies just below the membrane, as in influenza A and B virions. A minor viral envelope protein is CM2, which functions as an ion channel. The major influenza C virus envelope glycoprotein is called HEF (hemagglutinin-esterase-fusion) because it has the functions of both the HA and the NA. Therefore the influenza C virion contains 7 RNA segments, not 8 RNAs like influenza A and B viruses [4,5].

Wild aquatic birds are the natural hosts for a large variety of influenza A. Occasionally, viruses are transmitted to other species and may then cause devastating outbreaks in domestic poultry or give rise to human influenza pandemics. It is not surprising that the type A viruses are the most virulent human pathogens among the three influenza types and cause the most severe disease. The influenza A virus can be subdivided into different serotypes based on the antibody response to these viruses. The serotypes that have been confirmed in humans, ordered by the number of known human pandemic deaths, are [6]:

- H1N1, which caused Spanish Flu in 1918, and Swine Flu in 2009
- H2N2, which caused Asian Flu in 1957
- H3N2, which caused Hong Kong Flu in 1968
- H5N1, which caused Bird Flu in 2004
- H7N7, which has unusual zoonotic potential
- H1N2, endemic in humans, pigs and birds
- H9N2
- H7N2
- H7N3
- H10N7

The type B virus only circulates among human beings, and it can make people ill in a geographically limited area, often, when the type A influenza is subsiding. Type B influenza breaks out less frequently than influenza A, so when people fall ill with influenza B, it is often more serious because only a few will have developed antibodies. Influenza C is less common than the other types and usually only causes mild disease (in children and old and altered immunity people) [6]. Nearly all adults have been infected with influenza C virus, which causes mild upper respiratory tract illness. Lower respiratory tract complications are rare. There is no vaccine against influenza C virus.

Antigenic equipment of influenza viruses can be easily and quickly changed. These changes are probably responsible for the degree of virulence. Influenza viruses have on their surface two types of glycoprotein antigens: *hemagglutinin* (responsible for the ability of the virus entering into the host cell and replication) and *neuraminidase* (which is used by the release of newly formed virus particles from host cells) [7]. HA is a trimeric glycoprotein expressed on the influenza virus membrane [8]. HA of influenza viruses binds to host cell surface complex glycans via a terminal sialic acid (Sia) with α2-3

and α2-6 linkages, and this is the first key step in the process of infection [9-13]. NA acts as the receptor destroying enzyme in virus release [14]. The process is shown in Fig. 2.

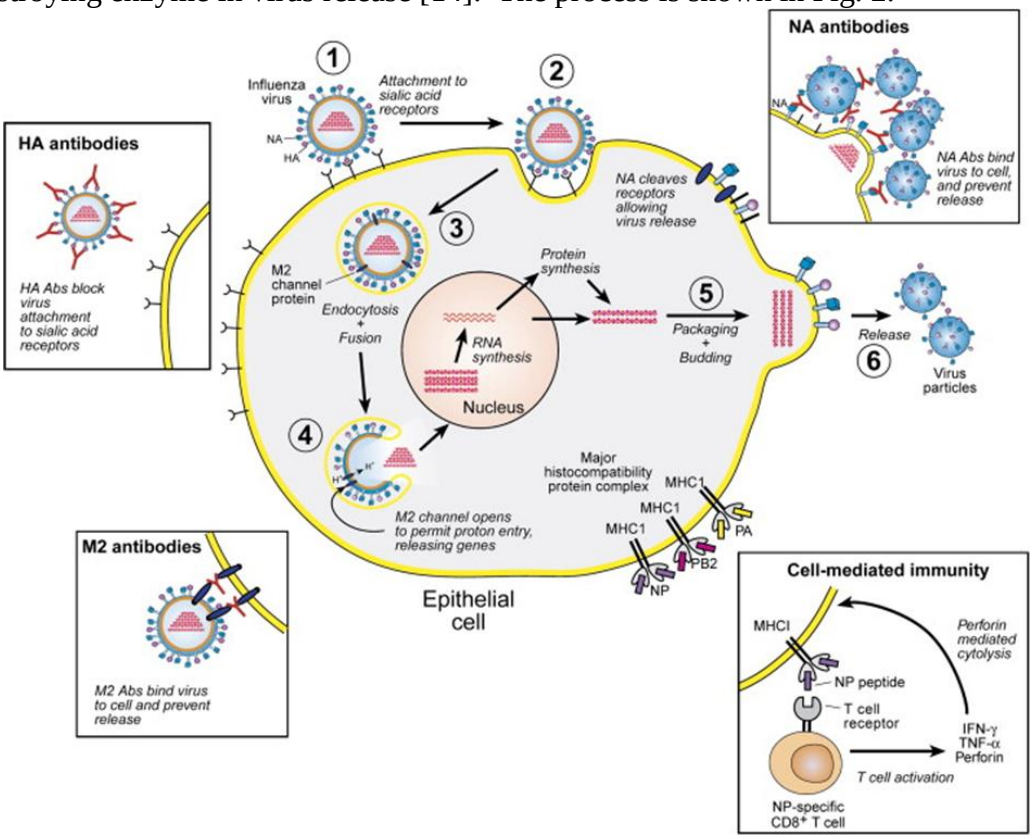

Figure 2. Life Cycle of Influenza Virus and Role of the Adaptive Immune Response during Infection (adopted from [15]. Influenza virus attaches to the epithelial cell surface through binding of the viral hemagglutinin (HA) protein to cell surface sialic acid receptors (1, 2). The virion is internalized through endocytosis and fusion (3). Opening of the M2 channel allows proton flow across the viral membrane (4), triggering fusion of viral and endosomal membranes and release of viral genes into the cytoplasm, from where they travel to the nucleus. Viral proteins produced in cytoplasm assemble with viral genes and bud from the cell membrane as progeny virions (5). Release of new virus particles (6) requires the viral neuraminidase (NA) protein, which cleaves sialic acid receptors from the cell membrane. Antibodies (Abs) to the HA protein block virus attachment (inset, upper left), thereby decreasing the number of cells infected. They can also function to prevent fusion (4). Abs to the NA protein (inset, upper right) bind virus to the cell, preventing release of new virions. Abs to theM2 protein bind virus to the cell and prevent release of viral particles into the extracellular fluid (inset, lower left). Cell-mediated immunity contributes to resistance when CD8+ T cells specific for viral proteins such as nucleoprotein (NP) or polymerase proteins (PB2 and PA recognize viral peptides presented by MHC class I proteins, resulting in the release of cytokines with antiviral activity (IFN-g and TNF-a) and perforins that mediate cytolysis of the infected cell (inset, lower right). Lysis of the infected cell decreases the amount of virus released by the cell. The latter three mechanisms, NA Abs, M2 Abs, and CD8+ T cells, operate after a cell becomes infected. Only HA Abs prevent infection; this is likely to be why they are the most effective *in vivo*. Reprinted with the permission.

Subtypes of influenza viruses are classified just according to NA and HA forms. 16 subtypes of HAs with differences in their primary sequences have been identified [16]. Among these 16-subtypes, only three HA-subtypes H1N1, H2N2, and H3N2, have successfully adapted to humans [17]. 9 subtypes of NA surface antigens were described. Only 103 of all 144 possible HA × NA combinations have been found yet [18].

Possible rapid spread of potential new pandemic subtype of influenza viruses is the great threat. Global civilization, the whole world airplane transport and other ways of global transport create the suitable conditions for extremely rapid spreading of potential pandemic. Simple instrumentation, quick and low cost detection of influenza viruses is of great interest in this case, because such method could reveal the threat before its spreading. However, most frequently used methods for the detection of viruses are laborious, time consuming, expensive, need specialized facility and trained staff. Cultivation of viruses in cell culture, immunofluorescence, polymerase chain reaction (PCR), enzyme-linked immunosorbent assay (ELISA) and serological methods belong to these methods [19-21].

Cultivation of viruses in cell culture is considered as the gold standard for virus detection. Conventional classic laboratory diagnosis of influenza is based on virus isolation and serologic testing. Primary rhesus monkey (PMK) or Madin-Darby canine kidney (MDCK) cells are mostly used for the isolation of viruses. Cell cultures are examined for cytopathic effect and screened by hemadsorption with confirmation by immunofluorescent monoclonal antibody against influenza A or B. This method is laborious and slow, usually takes 5-7 days [22,23]. Some laboratories replace conventional culture with shell-vial culture. Shell-vial assays that use R-mix cells, a combination of mink lung cells and human adenocarcinoma cells (strains Mv1Lu and A549, respectively), coupled with immunofluorescent staining demonstrates faster results and sensitivity that approaches based on conventional virus culture. Turn around time for shell-vial assay using R-mix cells is 1.4 days, compared to a turn around time of 5.2 days for conventional virus culture [24]. For some viruses, which have not cytopathic effect, this method is not appropriate. Some viruses are difficult to cultivate or uncultivable in cell culture. In these cases, cultivation in chick embryos or in experimental animals is used.

Besides cultivation assay, immunofluorescence of clinical specimens using monoclonal antibodies against influenza virus antigen is a reliable and relatively rapid technique for the detection of influenza [25]. Influenza A virus may also be detected rapidly in nasal secretions by ELISA [26]. The rapid detection of both types of influenza infections would allow appropriate antiviral therapy and is particularly important, since agents active against both influenza A and B are now available [27]. At present, six rapid diagnostic tests for influenza are used [24]. All tests, besides one, are based on directed influenza virus antigens determination. ZstatFlu test (Zyme Tx, Inc., Oklahoma City, OK, USA) detects influenza virus due to NA enzyme activity. In contrast to cell culture, rapid diagnostic tests do not detect influenza B as efficiently as influenza A virus [24]. *Boon et al.* applied mouse monoclonal antibody or anti-influenza nucleoprotein MoAb for detection of the virus [28]. In another

work *Chen et al.* detected avian H5N1 influenza virus using five monoclonal antibodies 8H5, 8G9, 13D4, 2F2, and 3G4 raised against H5N1 virus strains Chicken/HK/YU22/2002 [29].

PCR, as another method used for virus detection, is very sensitive to target molecule, but it is also very sensitive to contamination of the template nucleic acid and give sometimes false positive result. The most commonly used is reverse transcription-polymerase chain reaction (RT-PCR) [30,31], RT-PCR with detection by ELISA [32], real-time reverse transcription-polymerase chain reaction (RRT-PCR) [33,34], and nucleic acid sequence-based amplification (NASBA) [35,36]. RT-PCR, ELISA RT-PCR, and RRT-PCR are very similar to each other. Difference lies in PCR product detection. RT-PCR detects the PCR product by using electrophoresis in an agarose gel to separate the PCR product by size, which allows a presumptive identification. As a more specific alternative, ELISA can be used instead of agarose gel electrophoresis. RRT-PCR test uses a fluorescently labelled probe to detect the increase in PCR product while the test is being performed: i.e., the results are reported in real time [37]. The other test used for avian influenza is NASBA, which directly amplifies and detects RNA [35,36]. All these methods can provide fast and sensitive diagnostic results, and many published tests using different primers and probes have been reported [38-40]. *Pipper et al.* reported new model of microfluidic platform that can detect highly pathogenic avian influenza virus H5N1 in a throat swab sample by using magnetic forces to manipulate a free droplet containing superparamagnetic particles. In a sequential process, the viral RNA was isolated, purified, preconcentrated by 50,000% and subjected to ultrafast real-time RT-PCR [41]. Compared to commercially available tests, the bioassay is equally sensitive and is 440 % faster. Serological methods of influenza infection is based on demonstration of a four-fold or greater rise in specific antibody titre between acute and convalescent serum samples, measured by hemagglutination inhibition, complement fixation or neutralization tests [24,42]. Serological methods require seroconversion and therefore are not able to detect acute infection.

The most important prerequisite in the fight against influenza virus and possible pandemic is early isolation and detection of the viral nucleic acid presence. Broadening of the range of applicable methods for influenza detection has a great importance. It is necessary to change the conditions and properties of detection (requirements of easy-to-use and well portable instrumentation, rapidity of test and low cost). In our review we focus on sensors and biosensors for influenza virus detection, which can be meet the above mentioned criteria. Sensors and biosensors connected with electrochemical detection seem to be the best way for influenza virus detection. Therefore, these are mainly discussed.

2. SENSORS

The sensor is an essential part of the measuring device that converts the input signal to the quantity suitable for the measurement and interpretation. Electrochemical sensors can be divided into sensors with liquid electrolyte or solid electrolyte [43]. Electrochemical sensors can operate in

potentiometric or amperometric way. The interface between the electrode and the analysed environment here serves as a sensitive layer. The working electrode is actual physical transducer. A good sensor obeys the following rules: good specifity and sensitivity, insensitivity to any other property likely to be encountered in its application, and does not influence the measured quantity [44,45].

2.1 Mercury electrodes

The most common applied sensors for influenza virus detection are different types of electrodes. Electrochemical determination of different characteristic oligonucleotides (ODNs) is most common way of detection [46-49]. First electrochemical method called oscillographic polarography used for detection of DNA was suggested by Jaroslav Heyrovsky in 1941, but commercially available instruments became available in the first half of the 1950's [50,51]. Usually derivative curves were recorded, such as dE/dt against E. Both redox and adsorption/desorption phenomena were reflected by this method. The method was simple and fast, possessing advantages of its cyclic mode, later appreciated in cyclic voltammetry. In spite of the fact that Berg claimed DNA is not electroactive [52], Palecek showed that it was wrong presumption caused by using inappropriate electrochemical method [51], because these compounds are electroactive as it was shown by oscillographic polarography of DNA measured by Palecek [53,54]. Since than, there have been done great progress and development in electrochemistry of nucleic acids at various electrodes [55]. In the case of using of mercury electrode as a working one, the attention has been aiming at various electrochemical methods including linear sweep and cyclic polarography/voltammetry [56] (elimination polarography/voltammetry [57,58]), differential pulse polarography/voltammetry [59], square wave polarography/voltammetry [60,61], AC polarography/voltammetry [62] and chronopotentiometry [63,64] for analysis of DNA. Coupling of adsorptive transfer stripping technique (AdTS) to the above-mentioned methods is very promising for nucleic acid studying and is discussed [43]. In addition, coupling of separation (paramagnetic micro and nano particles) and detection tools (mercury electrode) brings numerous advantages including simplicity, easy-to-use and sensitivity [55,65-72].

2.2 Amalgam electrodes

It was reviewed few times that amalgam electrodes (AE) can successfully substitute mercury electrodes [73-75]. Amalgam electrodes coupled with AdTS were successfully used for investigation of DNA, various DNA bases, and oligonucleotides (ODNs), making an easy detection of picogram amounts of the modified DNA or ODN [76-78]. DNA possesses intrinsic electrochemical activity due to the presence of electrochemically reducible or oxidizable nucleobases and exhibits characteristic, structure-sensitive adsorption/desorption behaviour at amalgam electrodes. Thus, label-free electrochemical DNA sensing is in principle possible [66].

2.3 Carbon electrodes

Heterogeneous carbon electrodes are electrochemical sensors containing carbon as an electrically conductive material, which is placed in the matrix (binder). Binders can be liquid (carbon paste electrodes) or fixed (printed carbon electrode). The advantage of these electrodes is the possibility of modifying by chemical or biological agents to a mixture of carbon and a binder to enhance the selectivity and specificity of the assay [79]. Other advantages of carbon electrodes are wide range of working potentials (depending on the type of carbon from the environment and - 1.7 V to + 1.2 V), low background current and low cost [80,81].

Concerning carbon paste electrodes (CPE), they are composed from carbon powder and liquid binder in an appropriate ratio. Paste is filled into the suitable electrode housing. Pastes mixtures contain highly conductive graphite and electrically non-conductive, chemically inert and water insoluble liquid (paraffin, mineral and silicone oils). Stability of these electrodes is several weeks [81-83].

Carbon nanotubes (CNT) that become one of the most extensively studied nanostructures because of their unique properties belong to another popular materials used for electrodes fabrication. There are exist two variants – singlewalled (SWCNT) and multiwalled (MWCNT) carbon nanotubes. Both types offered a porous structure with a large effective surface area, highly electrocatalytic activities and conductivity. CNT can enhance the electrochemical reactivity of important biomolecules. The remarkable sensitivity of CNT enables us to use them as highly sensitive nanoscale sensors. These properties make CNT extremely attractive for a wide range of electrochemical sensors ranging from amperometric enzyme electrodes to DNA hybridization biosensors, because these electrodes have been successfully modified by nucleic acids and other types of biomolecules [84]. Noncovalent interaction along the CNTs sidewalls via physical adsorption or entrapment and covalent binding via carboxylate chemistry or nonselective attack of nanotube sidewalls by highly reactive species give an overview of the functionalized CNTs methodologies for DNA, antigen-antibody, cells, and other molecules sensing [85]. For DNA determination various ways are possible to be used. One of them is determination of DNA due to oxidation of guanine or adenine residues of ssDNA [86].

2.4 Screen printed electrodes

This type of electrodes is prepared by screen printing technique (Screen Printed Electrodes). If the used material is carbon, then this is Screen Printed Carbon Electrodes (SPCE). However, name Thick-Film Electrodes (TFE) better characterizes the dimensions of the electrodes as tens micrometers film. The polymer paste containing carbon nanoparticles is printed through the patterned screen on the ceramic or plastic carrier (substrate). After curing binder (solvent evaporation at room temperature or higher, typically 60-120 °C, or using UV-radiation), the electrode is ready for use. The whole process

can be repeated several times. In the next phase more electrodes including reference and auxiliary can be applied [87,88].

In general, detection of viral ODNs on screen printed electrode (SPE) is connected with hybridization reaction [65,89-91]. Two ways of influenza virus detection using SPE is applied as i) direct using of SPE and ii) using of SPE with modified surface. First way is connected with the usage of SPCE. In this case, various carbon structures as nanowires and nanotubes (singlewalled, multiwalled) with different dimensions are employed. Comparison of determination of viral nucleic acid by SPCE to carbon paste and mercury electrodes was discussed [65].

The second way as utilization of modified surfaces of SPE for viral nucleic acid detection is more frequent. Mostly use surfaces are based on carbon, which is modified with various particles as chitosan/Fe_3O_4 nanoparticles and gold nanoparticles. The most attractive feature of chitosan/Fe_3O_4 nanoparticles modified electrodes is a suitable microenvironment (Fe_3O_4 nanoparticles), which could contribute to electron transfer and thus sensitivity enhancement when using methylene blue (MB) as an external mediator and square wave voltammetry (SWV) as determination method [89]. Such modified SPE had a low detection limit (as low as 50 pM), acceptable stability and good reproducibility. On the other hand, gold nanoparticles, which are formed *in situ* by applying a constant current intensity during a fixed time, acts as an immobilization and transduction surface. Immobilization takes place through thiol-gold interaction in a relatively fast way, and the genosensor response is found to be linearly to the biotinylated viral nucleic acid concentration between 2.5 and 50 pM. Detection limit of 2.5 pM was estimated [90].

3. BIOSENSORS

A typical biosensor is constructed from three main parts (Fig. 3) as a recognition element (enzyme, antibody, DNA, etc.), a signal transducing structure (electrical, optical, or thermal), and an amplification/processing element [92].

The method of transduction depends on the type of physicochemical change resulting from the sensing event. Often, an important part of a biosensor is a membrane that covers the biological sensing element and has the main functions of selective permeation and diffusion control of analyte, protection against mechanical stresses, and support for the biological element [93,94]. The most commonly used sensing elements are enzymes [84,95,96], antibodies [85,97] and oligonucleotides [85,98,99]. Common used electrochemical transducers are potentiometric [100,101], amperometric [102] and conductometric [103,104]. In some applications piezoelectric transducers are used [105-108]. Short overview of biological elements and transducers commonly used in the fabrication of biosensors are shown in Table 1.

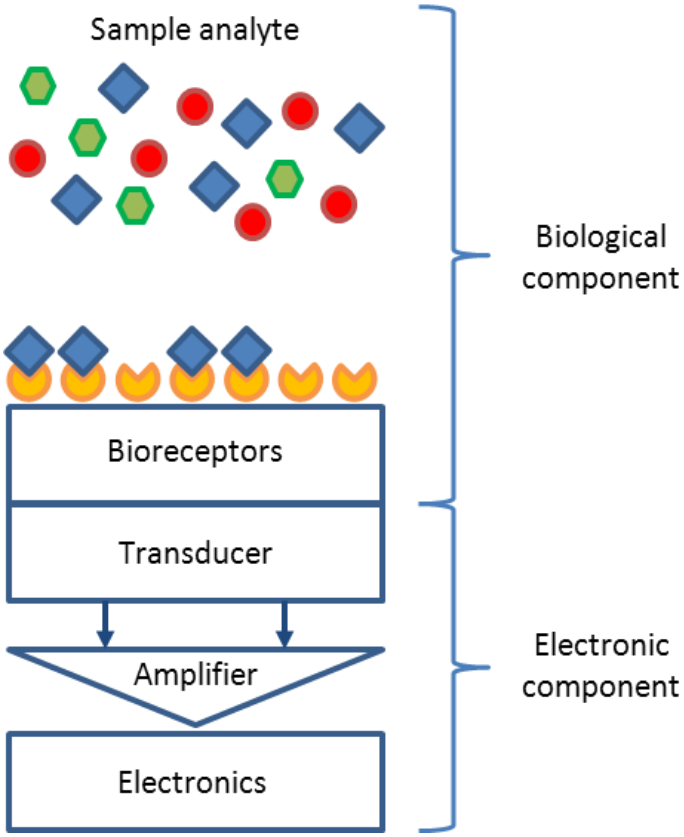

Figure 3. General structure of biosensor. Transducers are made as an electrochemical (potentiometry, amperometry) or optical (adsorption, fluorescence) parts. There are immobilised enzymes, microorganisms, DNA, antibodies and so one as bioreceptors applied.

Table 1. Biological elements and transducers. Adapted from [109].

Biological elements	Transducers
Enzymes	Electrochemical
Antibodies	Amperometric
Receptors	Potentiometric
Cells	Conductometric
Membranes	Optical
Tissues	Fibre optic
Organisms	Surface plasmon resonance
Organelles	Calorimetric
Nucleic acids	Heat conduction
Organic molecules	Isothermal
	Acoustic
	Surface acoustic wave
	Piezocrystal microbalance

3.1 Hybridization of Nucleic Acids on Working Electrodes

The surface-immobilization of ssODN probe on the electrode is a key step to fabricate the electrochemical oligonucleotide biosensor. It is not surprising that various electrodes have been modified and tested for DNA biosensing. SWCNTs array electrode was fabricated as a DNA hybridization biosensor based on the direct current response of guanine [110]. This biosensor gave, under optimum conditions, the response proportional to the concentration of target DNA within the range from 40 to 110 nM with a detection limit of 20 nM. Application of enzyme labels is another way of DNA detection. Heller's group applied this way and demonstrated that a highly sensitive amperometric monitoring of DNA hybridization (down to 5 zmol) could be achieved in connection with an horseradish peroxidase (HRP)-labelled target [111]. The enzyme labels to generate electrical signals are also extremely useful for ultrasensitive electrochemical bioaffinity assay of DNA as it is shown by Wang's group, which used CNTs for amplifying alkaline phosphatase (ALP) enzyme-based bioaffinity electrical sensing of DNA with a low detection limit of app. 1 fg/ml [112].

Avidin-biotin conjugation was also employed for influenza virus (type A) detection [113]. An electrochemical DNA biosensor was fabricated by avidin-biotin conjugation of a biotinylated probe DNA (5′-biotin-ATG AGT CTT CTA ACC GAG GTC GAA-3′) and an avidin-modified glassy carbon electrode (GCE) to detect the influenza virus (type A). An avidin-modified GCE was prepared by the reaction of avidin and a carboxylic acid-modified GCE, which was synthesized by the electrochemical reduction of 4-carboxyphenyl diazonium salt. The current value of the electrochemical DNA biosensor was evaluated after hybridization of the probe DNA (5′-biotin-ATG AGT CTT CTA ACC GAG GTC GAA-3′) and target DNA (5′-TTC GAC CTC GGT TAG AAG ACT CAT-3′) using cyclic voltammetry (Fig. 4). The current value decreased after the hybridization of the probe DNA and target DNA [113].

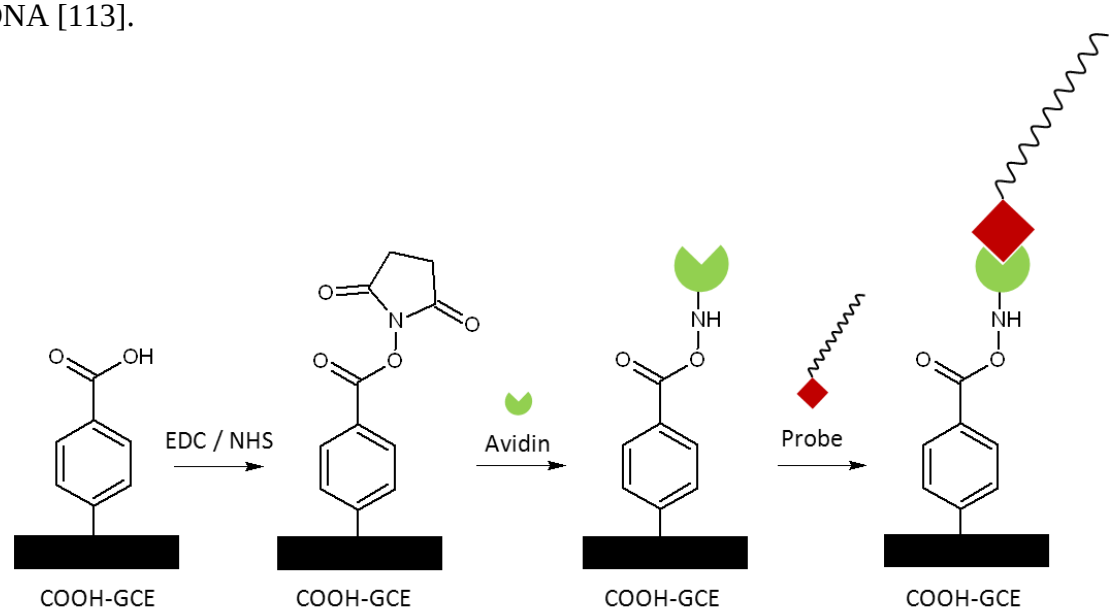

Figure 4. Scheme of immobilization of probe DNA on the surface of the COOH-modified GCE. (adopted from [113]).

In addition, biosensor that relies on the adsorption immobilization of the 18-mer single-stranded nucleic acid related to dengue virus gene 1 on activated pencil graphite was developed [100]. Hybridization between the probe and its complementary oligonucleotides (the target) was investigated by monitoring guanine oxidation by DPV. The electrochemical detection of annealing between the DNA probe immobilized on the modified electrode and the target was achieved. The target can be quantified in a range from 1 to 40 nM with good linearity and a detection limit app. 1 nM.

Determination of influenza viruses by electrochemical immunoassay also belongs to the possible ways of detection [114-116]. Usage of carbon nanotube electric immunoassay for the detection of swine influenza virus H1N1 was performed et al. [114]. The assay was based on the excellent electrical properties of SWCNTs. Antibody-virus complexes influenced the conductance of underlying SWCNT thin film, which has been constructed by facile layer-by-layer self-assembly. Pristine SWCNTs were functionalized to graft hydrophilic carboxylic groups for the stable dispersion to water. Polyelectrolytes used for layer-by-layer assembly as a polycation and polyanion were poly(diallyldimethyammonium chloride and poly(stylenesulfonate). Poly-L-lysine was used to immobilize the anti-virus antibody physically on the surface of SWCNTs. The antibody titre was determined by haemagglutinin inhibition assay [114]. This CNT-based immunoassay also has the potential to be used as a sensing platform for lab-on-chip system (Fig. 5).

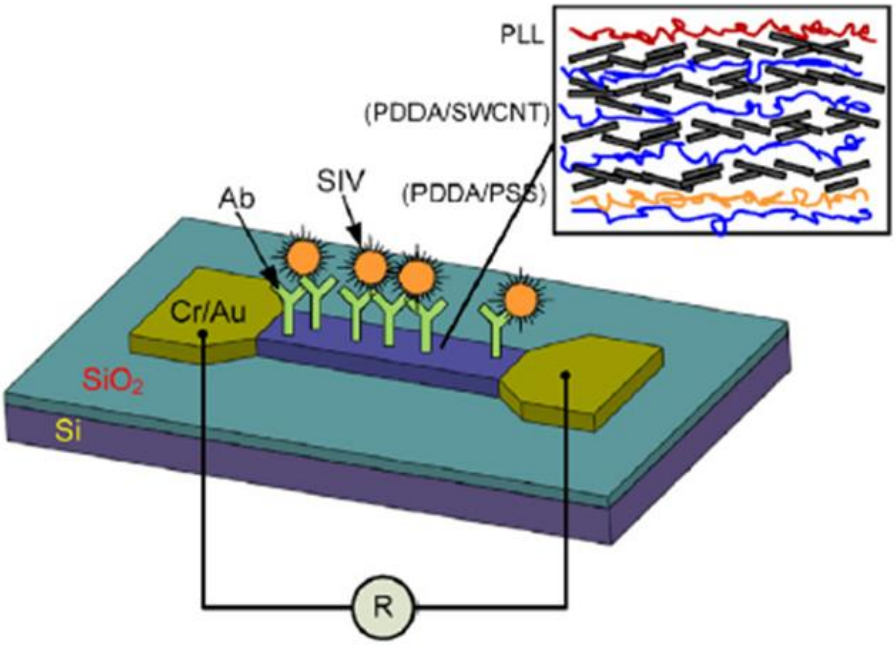

Figure 5. The fabricated carbon nanotube thin film immunochips: schematic of an individual immunochip with close-up hierarchy of SWCNT multilayer (adopted from [114]). Reprinted with the permission.

Gold electrodes provide an ideal material for labelling of ODNs due to their affinity with thiol groups. The Self Assembled Monolayer (SAM) is usually formed using mercaptopropionic acid. Thiolated ssODNs become the basis of wide range of biosensors, which are used for influenza detection too [117]. Immobilization of specific influenza antibodies onto bio-functionalized gold electrode is also possible [118]. Other way represent usage of gold nanowires [119] or planar nanogap electrodes [120]. Modifications of gold electrodes by carbon nanotubes [121], thiol groups [122,123] and enzymes [96] have been also published. The principle of biosensors is mostly putted up on hybridization reaction. Effectiveness of this reaction can be enhanced by usage of peptide nucleic acid (PNA). The enhanced of effectiveness is due to neutral character of PNA probe opposite negatively charged DNA probes [122,124].

Microarray

DNA microarray (DNA chip or gene chip) is based on parallel sample hybridization with specific probes (spots) on a solid surface (glass slide or silicon film). Custom probe specificity is determined by their sequences and by the sequences of anchored oligonucleotides. The basic division is according to the number of probes*:* low-density (the tenth hundreds specific probes) and high-density (thousands millions to specific probes). The low-density microarray is used for analysis of files of biomarkers and oligonucleotides. High-density is used for genomic analysis (sequencing DNA sections) or in RNA expression analysis. Most studies about influenza and microarray is based on detecting the presence [125] or typing and subtyping [7,126-130] or identification [131] of influenza, especially new strands of influenza virus. Procedures are almost based on virus-specific oligonucleotides determination [125,127-129]. The microarray utilizes mostly a panel of primers for multiplex PCR amplification of the HA, NA and MP genes of influenza viruses.

There have not been published numerous papers on the using of electrochemical microarrays for detection of influenza, but there is great potential. There was used the microarray silicon chip for the detection of influenza A virus [131]. The chip has 12 544 electrodes, each with a size of 44 μm in diameter, oligomers of 35-40 bases were synthesized at each electrode. After the *in situ* synthesis of microarray, the oligonucleotide probes on the chip were phosphorylated with T4 polynucleotide kinase for 30 min at 37 °C. The samples were first added to monolayers of Madin-Darby canine kidney cells and incubated for 1 h at 37°C to allow viral adsorption to the cells. The genotyping results showed that the device identified influenza A hemagglutinin and neuraminidase subtypes and sequenced portions of both genes, demonstrating the potential of integrated microfluidic and microarray technology for multiple virus detection. In addition, HRP as a biomarker for DNA hybridization detection was used in combination with the aforementioned electrochemical microarray [132]. The detection was based on electrochemical reduction of the enzymatic oxidization product of 3,3’,5,5’-tetramethylbenzidene (TMB). TMB oxidation was catalysed by HRP biomarker linked to a DNA target molecule (Fig. 6). Each target DNA oligomer was tagged with a biotin molecule and after hybridization the biotin is was with a streptavidin-HRP conjugate. Total RNA isolated from virus-containing material was reverse-

transcribed into cDNA, which was then PCR amplified to produce biotinylated single-strand DNA. Biotinylated-ssDNA was hybridized on 2 arrays containing probe specific sequences unique to Influenza A subtypes HA1 to 16 and NA subtypes 1 to 9 [132].

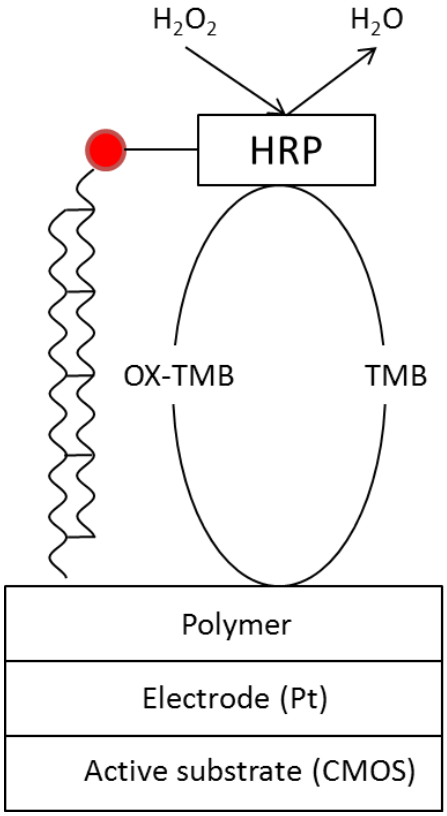

Figure 6. Diagram of the electrode surface after DNA probe hybridization and labelling of biotin with streptavidin-HRP conjugate. TMB is oxidized by HRP in the presence of H2O2 and subsequently reduced at the electrode surface during electrochemical detection (adopted from [132]).

3.2 Quartz Crystal Microbalance

Using quartz crystal microbalance (QCM) as an immuno biosensor for the detection of influenza virus has been carried out [105-108]. All of these procedures are used for detection of specific influenza antibodies and differ only in method of attachment of particles on the gold surface. The basic framework of the experiment is determination of influenza antibodies and then individual differences lie in the procedures for attaching the electrode surface. QCM influenza determination is possible without and/or with gold nanoparticles. The determination without gold nanoparticles was practised on influenza A virus (VR-544, H3N2) detection, which was based on the determination of H3N2 virus antigen and specific binding by polyclonal IgG antibodies against H3N2 on a crystal

surface [107]. On the other hand, determination with gold nanoparticles is carried out due to the increasing the sensitivity of the QCM immunosensor for the influenza viruses detection. This way of determination is applicable in connection with specific protein detection [106,108] and specific ODN-sequence detection [133]. These procedures have been applied on three types of influenza viruses H3N2 [107], H5N1 [105,108] and H1N1 [106].

3.3 Nanoparticles

Advanced materials represent a way how to enhance sensitivity and selectivity of electrochemical detection of nucleic acids. The materials can be divided into metal particles and quantum dots (QDs). Application of combination of MWCNTs and gold nanoparticles opened new possibility in nucleic acids detection by electrochemistry [115,116]. Various ways of determination are presented and differ from nanoparticle material and detected target. Two types of nanoparticles material are commonly used, gold [123,134-137] and iron [138]. Gold nanoparticles have been functionalized with virus specific antibodies or oligonucleotides. In each of these constructs, AuNPs act as both an easily conjugated scaffolding system for biological molecules and a powerful fluorescence quencher. Gold nanoparticles can be also immobilized and used as electrochemical transducers. Moreover, gold-coated magnetic beads were employed as the platforms for the immobilization and immunoreaction process, and horseradish peroxidase was chosen as an enzymatic tracer. The proteins (antibodies or immunocomplexes) attached on the surface of magnetic beads were found to induce a significant decline in their electric conductivity [115]. Modification of carbon electrodes with oxide nanoparticles (ZnO and SnO_2) was also tested for electrochemical monitoring of nucleic acid hybridization [139,140]. Kamikawa et al. dealt with the determination of influenza at gamma iron(III) oxide nanoparticles [138]. This way of determination was based on HA detection. Electrically active magnetic nanoparticles, consisting of aniline monomer polymerized around gamma iron(III) oxide (γ-Fe_2O_3) cores, served as the basis of a direct-charge transfer biosensor developed for detection of HA from the Influenza A virus. H5N1 preferentially bound alpha 2,3-linked host glycan receptors. Nanoparticles were immunofunctionalized with antibodies against target HA.

Usage of QDs for influenza detection in combination with electrochemical determination is rare. Determination of influenza virus made through combination of magnetic particles (MPs) and QDs with targeted DNA is presented by Krejcova et al. [141]. This way of detection was based on hybridisation reaction between anti-H5N1 and H5N1 ODNs chain, which was labelled with quantum dot. Differential pulse voltammetry was used for detection of cadmium(II) ions and square wave voltammetry for detection of cytosine-adenine peak in ODN-SH-CdS complex [141]. Similar approach was done in the study with influenza virus determination by using of paramagnetic particles modified with glycan, which can selectively bind to specific viral A/H5N1/Vietnam/1203/2004 protein labelled quantum dots [142]. Optimized detection of cadmium sulphide quantum dots (CdS QDs)-protein

complexes connected to paramagnetic microbeads was performed using differential pulse voltammetry on the surface of HMDE and/or GCE [142].

There was CdSe nanostructures applied for biosensor construction [143]. Based on these CdSe nanostructures, ssDNA/CdSe/GCE electrochemical DNA sensor was constructed. A novel method for detection the DNA sequences of avian influenza virus was presented (Probe DNA: 5′-GGA ATG GTA GAT GGA TGG TAT-3′; Target DNA: 5′-ATA CCA TCC ATC TAC CAT TCC-3′). This method was based on the change of electrochemical signal with the different combining ability of ssDNA and dsDNA with CdSe nanostructures. Methylene blue (MB) was used as the hybridization indicator and the response signal of MB was measured using differential pulse voltammetry after the working electrode was immersed in B–R buffer (pH 7.0). After DNA modification on the CdSe hollow spheres/GCE it was worth to note that the peak current of ssDNA/CdSe/GCE has dramatically decreased. This was due to the formation of the DNA layer on the surface of the CdSe nanostructures that hinds the electron-transfer process between MB molecules and CdSe/GCE surface, indicating that DNA has been successfully loaded on the CdSe/GCE and therefore the peak current was low correspondingly. After hybridization with complementary target DNA sequences, the signal increased obviously. This was because that hybridization would take place after target DNA sequences were immersed into complementary DNA sequences, which caused the target ssDNA sequences to form dsDNA. During the process, the structure of DNA changed dramatically. Before hybridization, the ssDNA can uncoil sufficiently to expose its bases. After hybridization, the dsDNA has a stable double-helix geometry, which makes the bases in the DNA lie inside the double-helix geometry of dsDNA, and negatively charged phosphate backbones be exposed outside. This special structure of dsDNA would greatly weaken the conjugated ability of dsDNA and CdSe. Therefore, after hybridization, the formed dsDNA would release from the CdSe/GCE surface. For the non-complementary DNA sequences, the signal almost unchanged because this DNA could not be hybridized with the probe DNA [143]. Other authors chose the following targets: human papillomavirus [96], mosaic virus [144] and Epstein-Barr virus [145].

3.4 Aptamers

The composition of aptamers is simple, generally has a few dozen nucleotides (less than 100), and thus the design of the aptamers is relatively simple. Due to the advantages of aptamers, their using for designing biosensors for identification and detection of pathogens is of extremely importance [146-148]. Application of aptamers for influenza detection is possible in several ways. First possible way is selection of aptamers against influenza virus hemagglutinin [149]. The best aptamer can be selected by surface plasmon resonance as an efficient methodology for selecting aptamer that has high affinity to HA of human influenza virus. This procedure allowed monitoring and selecting the target-bound aptamers specifically and simultaneously. Second possible way is detection of viral gene sequence using a DNA aptamer immobilized onto a hybrid nanomaterial-modified electrode [121]. The modified

electrode is assembled with MWNT, polypyrrole nanowires and gold nanoparticles (GNPs). This electrode offers a porous structure with a large effective surface area, highly electrocatalytic activities and electronic conductivity. The biosensor is based on the hybridization and preferred orientation of a DNA aptamer immobilized onto a modified electrode surface with its target (H5N1 specific sequence) present in solution [121]. Gopinath et al. reported another aptamer selection process of influenza A virus (H3N2). They used the whole-cell of H3N2 as targets to obtain the aptamers that specifically bound the HA protein on the surface of H3N2. The affinity between screening aptamers and HA proteins is 15-fold higher than the affinity between monoclonal antibodies and HA proteins [150]. Besides detection and determination of influenza virus, aptamers have other great feature, which is a position as a promising candidate for treatment and prophylaxis of influenza virus infections [151]. There were found DNA aptamers that specifically targeted the H5N1 influenza virus and their antiviral activity *in vitro* was also described. These aptamers would be expected to disrupt virus entry, and thus slow the infection process so the host immune system has time to respond. This is important in the absence of new vaccines to prevent the emergence of new viral infections.

3.5 Impedance

Impedance measurement is another way of electrochemical detection of influenza viruses. There are two basic methods: an impedance spectroscopy [152,153] and electrochemical impedance immunosensors [154-156] which are typically constructed using an mSAM base layer [157,158]. Upon hybridisation between the bioreceptor and the viral antigen, there is a measurable response in conductivity across the immunosensor surface, which is translated into a change in the resistance. Hassen et al. reports a quantitation of influenza A virus in samples containing large amounts of extraneous bovine serum albumin (BSA), foetal bovine serum (FBS) and hepatitis B virus (HBV) vaccine. Detection was carried out using electrochemical impedance spectroscopy with an antibody-neutravidin-thiol architecture immobilized on the surface of gold electrode [153]. Another method was based on an oligonucleotide DNA probe, complementary to the target H1N1 virus sequence, which was immobilized onto the electrode surface by covalent binding. Two different protocols (direct hybridization with the DNA target and a sandwich scheme) were employed and compared. In both cases the resulting hybrid was biotin-labelled to allow the additional conjugation with streptavidin gold nanoparticles (strept–AuNPs) [154].

Impedance imunnosensors were employed for the influenza detection due to HA [155] or DNA sequence [154] differentiation. Impedance immunosensor based on an interdigitated array microelectrode with antibodies against HA was developed. Polyclonal antibodies against AI virus H5N1 surface antigen HA were oriented on the gold microelectrode surface through protein A. Target H5N1viruses were then captured by the immobilized antibody, resulting in a change in the impedance of the IDA microelectrode surface [155].

4. CONCLUSION

Nanotechnologies together with various types of electrodes with many material-based advantages open many outstanding possibilities to be used in detection of markers of serious diseases, specific DNA sequences as markers for some viral infections and for suggesting and fabricating of biosensors. Main directions of this type of research can be as follows: a) DNA hybridization-based biosensors; b) drugs interaction; c) DNA protein interaction [159-162]. Sensors and biosensors have witnessed an escalating interest nowadays, both in the research and commercial fields. There are many fields, in which these instruments can be applied including those aimed at discrimination of different organism strains or the presence of viral nucleic acid [163].

Abbreviations:
A - adenine; AdS - adsorptive stripping technique; AC - alternating current voltammetry; AE - amalgam electrode; C - cytosine; CV – cyclic voltammetry; DME – dropping mercury electrode; dsDNA – doublestranded deoxyribonucleic acid; ssDNA – singlestranded deoxyribonucleic acid; DPV - differential pulse voltammetry; EVLS - elimination voltammetry with linear scan; G - guanine; HA – hemagglutinin; HMDE – hanging mercury drop electrode; LSV - linear sweep voltammetry; MNP - magnetic nanoparticle; MME - miniaturized mercury electrode; MWNT - multi-walled carbon nanotubes; NA – neuraminidase; ODN - oligonucleotide; mRNA – mediator ribonucleic acid; SPCPE - screen-printed carbon paste electrode; SWV - square wave voltammetry; T – thymine

ACKNOWLEDGEMENTS
Financial support from NanoBioTECell GA CR P102/11/1068, NANOSEMED GA AV KAN208130801 and CEITEC CZ.1.05/1.1.00/02.0068 is highly acknowledged.

References

1. Y. C. Hsieh, T. Z. Wu, D. P. Liu, P. L. Shao, L. Y. Chang, C. Y. Lu, C. Y. Lee, F. Y. Huang and L. M. Huang, *J. Formos. Med. Assoc.*, 105 (2006) 1.
2. A. W. Hampson and J. S. Mackenzie, *Med. J. Aust.*, 185 (2006) S39.
3. A. Beby-Defaux, G. Giraudeau, S. Bouguermouh and G. Agius, *Med. Mal. Infect.*, 33 (2003) 134.
4. M. R. Hillman, *Vaccine*, 20 (2002) 3068.
5. M. C. Zambon, *J. Antimicrob. Chemother.*, 44 (1999) 3.
6. E. Samorek-Salamonowicz, H. Czekaj and W. Kozdrun, *Med. Weter.*, 62 (2006) 488.
7. J. Q. Zhao, S. X. Tang, J. Storhoff, S. Marla, Y. P. Bao, X. Wang, E. Y. Wong, V. Ragupathy, Z. P. Ye and I. K. Hewlett, *BMC Biotechnol.*, 10 (2010) 1.
8. T. W. Lin, G. Y. Wang, A. Z. Li, Q. Zhang, C. M. Wu, R. F. Zhang, Q. X. Cai, W. J. Song and K. Y. Yuen, *Virology*, 392 (2009) 73.
9. J. J. Skehel and D. C. Wiley, *Ann. Rev. Biochem.*, 69 (2000) 531.
10. R. J. Russell, P. S. Kerry, D. J. Stevens, D. A. Steinhauer, S. R. Martin, S. J. Gamblin and J. J. Skehel, *Proc. Natl. Acad. Sci. U. S. A.*, 105 (2008) 17736.
11. H. Brody, *Nature*, 480 (2011) S1.
12. G. J. Nabel, C. J. Wei and J. E. Ledgerwood, *Nature*, 471 (2011) 157.

13. R. Konig, S. Stertz, Y. Zhou, A. Inoue, H. H. Hoffmann, S. Bhattacharyya, J. G. Alamares, D. M. Tscherne, M. B. Ortigoza, Y. H. Liang, Q. S. Gao, S. E. Andrews, S. Bandyopadhyay, P. De Jesus, B. P. Tu, L. Pache, C. Shih, A. Orth, G. Bonamy, L. Miraglia, T. Ideker, A. Garcia-Sastre, J. A. T. Young, P. Palese, M. L. Shaw and S. K. Chanda, *Nature*, 463 (2010) 813.
14. E. Suenaga, H. Mizuno and K. K. R. Penmetcha, *Biosens. Bioelectron.*, 32 (2012) 195.
15. K. Subbarao, B. R. Murphy and A. S. Fauci, *Immunity*, 24 (2006) 5.
16. R. A. M. Fouchier, V. Munster, A. Wallensten, T. M. Bestebroer, S. Herfst, D. Smith, G. F. Rimmelzwaan, B. Olsen and A. Osterhaus, *J. Virol.*, 79 (2005) 2814.
17. R. J. Garten, C. T. Davis, C. A. Russell, B. Shu, S. Lindstrom, A. Balish, W. M. Sessions, X. Y. Xu, E. Skepner, V. Deyde, M. Okomo-Adhiambo, L. Gubareva, J. Barnes, C. B. Smith, S. L. Emery, M. J. Hillman, P. Rivailler, J. Smagala, M. de Graaf, D. F. Burke, R. A. M. Fouchier, C. Pappas, C. M. Alpuche-Aranda, H. Lopez-Gatell, H. Olivera, I. Lopez, C. A. Myers, D. Faix, P. J. Blair, C. Yu, K. M. Keene, P. D. Dotson, D. Boxrud, A. R. Sambol, S. H. Abid, K. S. George, T. Bannerman, A. L. Moore, D. J. Stringer, P. Blevins, G. J. Demmler-Harrison, M. Ginsberg, P. Kriner, S. Waterman, S. Smole, H. F. Guevara, E. A. Belongia, P. A. Clark, S. T. Beatrice, R. Donis, J. Katz, L. Finelli, C. B. Bridges, M. Shaw, D. B. Jernigan, T. M. Uyeki, D. J. Smith, A. I. Klimov and N. J. Cox, *Science*, 325 (2009) 197.
18. E. F. Kaleta, G. Hergarten and A. Yilmaz, *Dtsch. Tierarztl. Wochenschr.*, 112 (2005) 448.
19. R. L. Caygill, G. E. Blair and P. A. Millner, *Anal. Chim. Acta*, 681 (2010) 8.
20. M. L. Landry, *Curr. Opin. Pediatr.*, 23 (2011) 91.
21. G. A. Storch, *Curr. Opin. Pediatr.*, 15 (2003) 77.
22. A. Z. Hu, M. Colella, J. S. Tam, R. Rappaport and S. M. Cheng, *J. Clin. Microbiol.*, 41 (2003) 149.
23. M. Gueudin, A. Vabret, J. Petitjean, S. Gouarin, J. Brouard and F. Freymuth, *J. Virol. Methods*, 109 (2003) 39.
24. J. P. Gavin and B. R. Thomson, *Clin. Appl. Immun. Rev.*, 4 (2003) 151.
25. C. G. Ray and L. L. Minnich, *J. Clin. Microbiol.*, 25 (1987) 355.
26. S. Davison, A. F. Ziegler and R. J. Eckroade, *Avian Dis.*, 42 (1998) 791.
27. D. E. Noyola, B. Clark, F. T. O'Donnell, R. L. Atmar, J. Greer and G. J. Demmler, *J. Clin. Microbiol.*, 38 (2000) 1161.
28. A. C. M. Boon, A. M. F. French, D. M. Fleming and M. C. Zambon, *J. Med. Virol.*, 65 (2001) 163.
29. Y. W. Chen, W. X. Luo, H. J. Song, B. Y. Yin, J. X. Tang, Y. X. Chen, M. H. Ng, A. E. T. Yeo, J. Zhang and N. S. Xia, *PLoS One*, 6 (2011) 1.
30. G. Cattoli, A. Drago, S. Maniero, A. Toffan, E. Bertoli, S. Fassina, C. Terregino, C. Robbi, G. Vicenzoni and I. Capua, *Avian Pathol.*, 33 (2004) 432.
31. E. Starick, A. Romer-Oberdorfer and O. Werner, *J. Vet. Med. Ser. B-Infect. Dis. Vet. Public Health*, 47 (2000) 295.
32. K. Dybkaer, M. Munch, K. J. Handberg and P. H. Jorgensen, *J. Vet. Diagn. Invest.*, 16 (2004) 51.
33. L. Di Trani, B. Bedini, I. Donatelli, L. Campitelli, B. Chiappini, M. A. De Marco, M. Delogu, C. Buonavoglia and G. Vaccari, *BMC Infect. Dis.*, 6 (2006) 1.
34. E. Spackman, D. A. Senne, T. J. Myers, L. L. Bulaga, L. P. Garber, M. L. Perdue, K. Lohman, L. T. Daum and D. L. Suarez, *J. Clin. Microbiol.*, 40 (2002) 3256.
35. R. A. Collins, L. S. Ko, K. Y. Fung, K. Y. Chan, J. Xing, L. T. Lau and A. C. H. Yu, *Biochem. Biophys. Res. Commun.*, 300 (2003) 507.
36. R. A. Collins, L. S. Ko, K. L. So, T. Ellis, L. T. Lau and A. C. H. Yu, *J. Virol. Methods*, 103 (2002) 213.
37. D. L. Suarez, A. Das and E. Ellis, *Avian Dis.*, 51 (2007) 201.
38. G. Vernet, *Expert Rev. Anti-Infect. Ther.*, 5 (2007) 89.

39. P. Neuzil, J. Pipper and T. M. Hsieh, *Mol. Biosyst.*, 2 (2006) 292.
40. P. Neuzil, C. Y. Zhang, J. Pipper, S. Oh and L. Zhuo, *Nucleic Acids Res.*, 34 (2006) 9.
41. J. Pipper, M. Inoue, L. F. P. Ng, P. Neuzil, Y. Zhang and L. Novak, *Nat. Med.*, 13 (2007) 1259.
42. N. J. Cox and K. Subbarao, *Lancet*, 354 (1999) 1277.
43. E. Palecek and M. Bartosik, *Chem. Rev.*, 112 (2012) 3427.
44. A. J. S. Ahammad, J. J. Lee and M. A. Rahman, *Sensors*, 9 (2009) 2289.
45. F. Wang and S. S. Hu, *Microchim. Acta*, 165 (2009) 1.
46. J. Wang, *Anal. Chim. Acta*, 469 (2002) 63.
47. M. Pumera, Nanoparticles and quantum dots as biomolecule labels for electrochemical biosensing, Nova Science Publishers, Inc, Hauppauge, 2009.
48. S. O. Kelley, E. M. Boon, J. K. Barton, N. M. Jackson and M. G. Hill, *Nucleic Acids Res.*, 27 (1999) 4830.
49. J. M. Gibbs, S. J. Park, D. R. Anderson, K. J. Watson, C. A. Mirkin and S. T. Nguyen, *J. Am. Chem. Soc.*, 127 (2005) 1170.
50. E. Palecek, *Electroanalysis*, 8 (1996) 7.
51. E. Palecek, *Talanta*, 56 (2002) 809.
52. H. Berg, *Biochem. Z.*, 329 (1957) 274.
53. E. Palecek, *Naturwissenschaften*, 45 (1958) 186.
54. E. Palecek, *Nature*, 188 (1960) 656.
55. D. Hynek, J. Prasek, P. Koudelka, J. Chomoucka, L. Trnkova, V. Adam, J. Hubalek and R. Kizek, *Curr. Phys. Chem.*, 1 (2011) 299.
56. A. Erdem and M. Ozsoz, *Electroanalysis*, 14 (2002) 965.
57. L. Trnkova, in V. Adam, R. Kizek (Editors), Utilizing of Electrochemical and Bioanalytical Methods in Biological Research, Research Signpost, Kerala, 2007, p. 51.
58. L. Trnkova, F. Jelen, J. Petrlova, V. Adam, D. Potesil and R. Kizek, *Sensors*, 5 (2005) 448.
59. M. Vorlickova and E. Palecek, *Int. J. Radiat. Biol.*, 26 (1974) 363.
60. D. Huska, J. Hubalek, V. Adam and R. Kizek, *Electrophoresis*, 29 (2008) 4964.
61. F. Jelen, M. Tomschik and E. Palecek, *J. Electroanal. Chem.*, 423 (1997) 141.
62. M. Fojta, L. Havran, J. Fulneckova and T. Kubicarova, *Electroanalysis*, 12 (2000) 926.
63. E. Palecek, M. Masarik, R. Kizek, D. Kuhlmeier, J. Hassmann and J. Schulein, *Anal. Chem.*, 76 (2004) 5930.
64. J. Wang, Analytical electrochemistry, Wiley-VCH, New York, 2000.
65. V. Adam, D. Huska, J. Hubalek and R. Kizek, *Microfluid. Nanofluid.*, 8 (2010) 329.
66. M. Fojta, L. Havran, P. Horakova, P. Kostecka, H. Pivonkova, E. Simkova, J. Spacek, Z. Vychodilova and P. Vidlakova, Electrochemical Analysis of DNA: When, How and Why to Use Electroactive Labels and Indicators, Lenka Srsenova-Best Servis, Usti Nad Labem, 2010.
67. L. Havran, P. Horakova, H. Pivonkova, M. Vrabel, H. Macickova-Cahova, J. Riedl, M. Hocek and M. Fojta, What is new in labeling and functionalization of DNA for electrochemical analysis, 2010.
68. J. Vacek, L. Havran and M. Fojta, *Chem. Listy*, 105 (2011) 15.
69. P. Vidlakova, P. Horakova, L. Tesnohlidkova, L. Havran, H. Pivonkova and M. Fojta, Monitoring DNA modification by platinum complexes at mercury electrodes, 2010.
70. F. Jelen, A. Kourilova, P. Pecinka and E. Palecek, *Bioelectrochemistry*, 63 (2004) 249.
71. E. Palecek, M. Fojta and F. Jelen, *Bioelectrochemistry*, 56 (2002) 85.
72. E. Palecek and M. Fojta, *Talanta*, 74 (2007) 276.
73. B. Yosypchuk and J. Barek, *Crit. Rev. Anal. Chem.*, 39 (2009) 189.
74. B. Yosypchuk and L. Novotny, *Electroanalysis*, 14 (2002) 1733.
75. B. Yosypchuk and L. Novotny, *Crit. Rev. Anal. Chem.*, 32 (2002) 141.

76. R. Fadrna, K. Cahova-Kucharikova, L. Havran, B. Yosypchuk and M. Fojta, *Electroanalysis*, 17 (2005) 452.
77. K. Kucharikova, L. Novotny, B. Yosypchuk and M. Fojta, *Electroanalysis*, 16 (2004) 410.
78. B. Yosypchuk, M. Fojta, L. Havran, M. Heyrovsky and E. Palecek, *Electroanalysis*, 18 (2006) 186.
79. C. B. Jacobs, M. J. Peairs and B. J. Venton, *Anal. Chim. Acta*, 662 (2010) 105.
80. I. Svancara, A. Walcarius, K. Kalcher and K. Vytras, *Cent. Eur. J. Chem*, 7 (2009) 598.
81. K. Kalcher, I. Svancara, M. Buzuk, K. Vytras and A. Walcarius, *Mon. Chem.*, 140 (2009) 861.
82. Svancara I., Kalcher K., Walcarius A. and K. Vytras, Electroanalysis with Carbon Paste Electrodes, CRC Press, Taylor &Francis Group, 2012.
83. I. Svancara, K. Vytras, K. Kalcher, A. Walcarius and J. Wang, *Electroanalysis*, 21 (2009) 7.
84. A. Qureshi, W. P. Kang, J. L. Davidson and Y. Gurbuz, *Diam. Relat. Mat.*, 18 (2009) 1401.
85. J. P. Lei and H. X. Ju, *Wiley Interdiscip. Rev.-Nanomed. Nanobiotechnol.*, 2 (2010) 496.
86. Y. K. Ye and H. X. Ju, *Biosens. Bioelectron.*, 21 (2005) 735.
87. M. A. Alonso-Lomillo, O. Dominguez-Renedo and M. J. Arcos-Martinez, *Talanta*, 82 (2010) 1629.
88. S. Centi, S. Laschi and M. Mascini, *Bioanalysis*, 1 (2009) 1271.
89. D. T. Lam, H. N. Binh, V. H. Nguyen, V. T. Hoang, L. N. Huy and X. N. Phuc, *Mater. Sci. Eng. C-Mater. Biol. Appl.*, 31 (2011) 477.
90. G. Martinez-Paredes, M. B. Gonzalez-Garcia and A. Costa-Garcia, *Electroanalysis*, 21 (2009) 379.
91. S. Girousi and V. Kinigopoulou, *Cent. Eur. J. Chem*, 8 (2010) 732.
92. M. N. Velasco-Garcia and T. Mottram, *Biosyst. Eng.*, 84 (2003) 1.
93. O. A. Sadik, A. O. Aluoch and A. L. Zhou, *Biosens. Bioelectron.*, 24 (2009) 2749.
94. A. Merkoci, M. Aldavert, S. Marin and S. Alegret, *TRAC-Trends Anal. Chem.*, 24 (2005) 341.
95. N. Djellouli, M. Rochelet-Dequaire, B. Limoges, M. Druet and P. Brossier, *Biosens. Bioelectron.*, 22 (2007) 2906.
96. H. Zhang, L. Liu, C. W. Li, H. Y. Fu, Y. Chen and M. S. Yang, *Biosens. Bioelectron.*, 29 (2011) 89.
97. T. Q. Huy, T. H. H. Nguyen, P. H. Chung, D. D. Anh, P. T. Nga and M. A. Tuan, *Appl. Surf. Sci.*, 257 (2011) 7090.
98. S. Cosnier and P. Mailley, *Analyst*, 133 (2008) 984.
99. A. Erdem, *Talanta*, 74 (2007) 318.
100. E. Souza, G. Nascimento, N. Santana, D. Ferreira, M. Lima, E. Natividade, D. Martins and J. Lima, *Sensors*, 11 (2011) 5616.
101. F. Liu, K. S. Choi, T. J. Park, S. Y. Lee and T. S. Seo, *BioChip J.*, 5 (2011) 123.
102. E. Komarova, M. Aldissi and A. Bogomolova, *Biosens. Bioelectron.*, 21 (2005) 182.
103. P. Kara, K. Kerman, D. Ozkan, B. Meric, A. Erdem, Z. Ozkan and M. Ozsoz, *Electrochem. Commun.*, 4 (2002) 705.
104. J. J. Gooding, *Electroanalysis*, 14 (2002) 1149.
105. S. P. Liu, G. M. Chen, Q. Zhou and Y. L. Wei, in M. Sasaki, G.C. Sang, Z. Li, R. Ikeura, H. Kim, F. Xue (Editors), ICMIT 2007: Mechatronics, Mems, and Smart Materials, Pts 1 and 2, Spie-Int Soc Optical Engineering, Bellingham, 2008, p. P7943.
106. T. M. P. Hewa, G. A. Tannock, D. E. Mainwaring, S. Harrison and J. V. Fecondo, *J. Virol. Methods*, 162 (2009) 14.
107. T. W. Owen, R. O. Al-Kaysi, C. J. Bardeen and Q. Cheng, *Sens. Actuator B-Chem.*, 126 (2007) 691.
108. S. A. Miller, L. A. Hiatt, R. G. Keil, D. W. Wright and D. E. Cliffel, *Anal. Bioanal. Chem.*, 399 (2011) 1021.

109. S. Subrahmanyam, S. A. Piletsky and A. P. F. Turner, *Anal. Chem.*, 74 (2002) 3942.
110. X. Z. Zhang, K. Jiao, S. F. Liu and Y. W. Hu, *Anal. Chem.*, 81 (2009) 6006.
111. Y. C. Zhang, H. H. Kim and A. Heller, *Anal. Chem.*, 75 (2003) 3267.
112. J. Wang, G. D. Liu and M. R. Jan, *J. Am. Chem. Soc.*, 126 (2004) 3010.
113. D. J. Chung, K. C. Kim and S. H. Choi, *Appl. Surf. Sci.*, 257 (2011) 9390.
114. D. J. Lee, Y. Chander, S. M. Goyal and T. H. Cui, *Biosens. Bioelectron.*, 26 (2011) 3482.
115. F. Li, L. Mei, Y. M. Li, K. H. Zhao, H. C. Chen, P. Wu, Y. G. Hu and S. B. Cao, *Biosens. Bioelectron.*, 26 (2011) 4253.
116. F. Li, R. Zhou, K. H. Zhao, H. C. Chen and Y. G. Hu, *Talanta*, 87 (2011) 302.
117. K. Malecka, I. Grabowska, J. Radecki, A. Stachyra, A. Gora-Sochacka, A. Sirko and H. Radecka, *Electroanalysis*, 24 (2012) 439.
118. M. F. Diouani, S. Helali, I. Hafaid, W. M. Hassen, M. A. Snoussi, A. Ghram, N. Jaffrezic-Renault and A. Abdelghani, *Mater. Sci. Eng. C-Biomimetic Supramol. Syst.*, 28 (2008) 580.
119. X. Z. Song, H. Yu, X. Chen, Y. Lasanajak, M. M. Tappert, G. M. Air, V. K. Tiwari, H. Z. Cao, H. A. Chokhawala, H. J. Zheng, R. D. Cummings and D. F. Smith, *J. Biol. Chem.*, 286 (2011) 31610.
120. H. Cho, S. K. Kim, Y. Jung, J. Jung and B. H. Chung, *Chem. Commun.*, 47 (2011) 5756.
121. X. G. Liu, Z. Q. Cheng, H. Fan, S. Y. Ai and R. X. Han, *Electrochimica Acta*, 56 (2011) 6266.
122. J. Zhang, B. P. Ting, N. R. Jana, Z. Q. Gao and J. Y. Ying, *Small*, 5 (2009) 1414.
123. K. Y. Zhang and Y. Z. Zhang, *Electroanalysis*, 22 (2010) 673.
124. J. B. Raoof, R. Ojani, S. M. Golabi, E. Hamidi-Asl and M. S. Hejazi, *Sens. Actuator B-Chem.*, 157 (2011) 195.
125. X. H. Li, X. Qi, L. Miao, Y. Wang, F. Z. Liu, H. W. Gu, S. W. Lu, Y. H. Yang and F. Y. Liu, *Diagn. Microbiol. Infect. Dis.*, 65 (2009) 261.
126. J. P. Li, S. Chen and D. H. Evans, *J. Clin. Microbiol.*, 39 (2001) 696.
127. X. P. Kang, Y. Q. Li, H. H. Sun, W. L. Wu, H. Liu, F. Lin, C. F. Qing, G. H. Chang, Q. Y. Zhu, W. J. Chen and Y. H. Yang, *Arch. Virol.*, 155 (2010) 55.
128. V. A. Ryabinin, E. V. Kostina, A. A. Neverov, G. A. Maksakova and A. N. Sinyakov, *Russ. J. Bioorg. Chem.*, 36 (2010) 634.
129. E. V. Kostina, V. A. Ryabinin, A. P. Agafonov, V. A. Ternovoi and A. N. Sinyakov, *Russ. J. Bioorg. Chem.*, 37 (2011) 644.
130. A. Kongchanagul, O. Suptawiwat, C. Boonarkart, R. Kitphati, P. Puthavathana, M. Uiprasertkul and P. Auewarakul, *J. Med. Virol.*, 83 (2011) 1410.
131. R. H. Liu, M. J. Lodes, T. Nguyen, T. Siuda, M. Slota, H. S. Fuji and A. McShea, *Anal. Chem.*, 78 (2006) 4184.
132. K. M. Roth, K. Peyvan, K. R. Schwarzkopf and A. Ghindilis, *Electroanalysis*, 18 (2006) 1982.
133. D. J. Li, J. P. Wang, R. H. Wang, Y. B. Li, D. Abi-Ghanem, L. Berghman, B. Hargis and H. G. Lu, *Biosens. Bioelectron.*, 26 (2011) 4146.
134. B. Mu, X. L. Huang, P. C. Bu, J. Zhuang, Z. X. Cheng, J. Feng, D. L. Yang, C. S. Dong, J. B. Zhang and X. Y. Yan, *J. Virol. Methods*, 169 (2010) 282.
135. K. C. Halfpenny and D. W. Wright, *Wiley Interdiscip. Rev.-Nanomed. Nanobiotechnol.*, 2 (2010) 277.
136. P. J. Jannetto, B. W. Buchan, K. A. Vaughan, J. S. Ledford, D. K. Anderson, D. C. Henley, N. B. Quigley and N. A. Ledeboer, *J. Clin. Microbiol.*, 48 (2010) 3997.
137. T. M. H. Lee, L. L. Li and I. M. Hsing, *Langmuir*, 19 (2003) 4338.
138. T. L. Kamikawa, M. G. Mikolajczyk, M. Kennedy, P. Zhang, W. Wang, D. E. Scott and E. C. Alocilja, *Biosens. Bioelectron.*, 26 (2010) 1346.

139.T. Yumak, F. Kuralay, M. Muti, A. Sinag, A. Erdem and S. Abaci, *Colloid Surf. B-Biointerfaces*, 86 (2011) 397.
140.M. Muti, F. Kuralay, A. Erdem, S. Abaci, T. Yumak and A. Sinag, *Talanta*, 82 (2010) 1680.
141.L. Krejcova, D. Hynek, P. Kopel, V. Adam, J. Hubalek, L. Trnkova and R. Kizek, *Electrophoresis*, In press. (2012).
142.L. Krejcova, D. Dospivova, M. Ryvolova, P. Kopel, D. Hynek, S. Krizkova, J. Hubalek, V. Adam and R. Kizek, *Electrophoresis*, In press. (2012).
143.H. Fan, P. Ju and S. Y. Ai, *Sens. Actuator B-Chem.*, 149 (2010) 98.
144.J. H. Chen, J. Zhang, H. H. Yang, F. F. Fu and G. N. Chen, *Biosens. Bioelectron.*, 26 (2010) 144.
145.L. Y. Chen, Z. J. Qi, R. J. Chen, Y. Li and S. Q. Liu, *Clin. Chim. Acta*, 411 (2010) 1969.
146.Y. X. Wang, Z. Z. Ye, C. Y. Si and Y. B. Ying, *Chin. J. Anal. Chem.*, 40 (2012) 634.
147.S. C. B. Gopinath, *Arch. Virol.*, 152 (2007) 2137.
148.S. P. Song, L. H. Wang, J. Li, J. L. Zhao and C. H. Fan, *TRAC-Trends Anal. Chem.*, 27 (2008) 108.
149.T. S. Misono and P. K. R. Kumar, *Anal. Biochem.*, 342 (2005) 312.
150.S. C. B. Gopinath, T. S. Misono, K. Kawasaki, T. Mizuno, M. Imai, T. Odagiri and P. K. R. Kumar, *J. Gen. Virol.*, 87 (2006) 479.
151.C. S. Cheng, J. Dong, L. H. Yao, A. J. Chen, R. Q. Jia, L. F. Huan, J. L. Guo, Y. L. Shu and Z. Q. Zhang, *Biochem. Biophys. Res. Commun.*, 366 (2008) 670.
152.K. Kiilerich-Pedersen, C. R. Poulsen, T. Jain and N. Rozlosnik, *Biosens. Bioelectron.*, 28 (2011) 386.
153.W. M. Hassen, V. Duplan, E. Frost and J. J. Dubowski, *Electrochimica Acta*, 56 (2011) 8325.
154.A. Bonanni, M. I. Pividori and M. del Valle, *Analyst*, 135 (2010) 1765.
155.R. H. Wang, Y. Wang, K. Lassiter, Y. B. Li, B. Hargis, S. Tung, L. Berghman and W. Bottje, *Talanta*, 79 (2009) 159.
156.J. H. Lin, J. Lum, R. H. Wang, S. Tung, B. Hargis, Y. B. Li, H. G. Lu, L. Berghman and Ieee, in 2010 IEEE Sensors, Ieee, New York, 2010, p. 1558.
157.M. Billah, H. C. W. Hays and P. A. Millner, *Microchim. Acta*, 160 (2008) 447.
158.N. K. Chaki and K. Vijayamohanan, *Biosens. Bioelectron.*, 17 (2002) 1.
159.P. Babula, J. Vanco, L. Krejcova, D. Hynek, J. Sochor, V. Adam, L. Trnkova, J. Hubalek and R. Kizek, *Int. J. Electrochem. Sci.*, 7 (2012) 7349.
160.D. Dospivova, K. Smerkova, M. Ryvolova, D. Hynek, V. Adam, P. Kopel, M. Stiborova, T. Eckschlager, J. Hubalek and R. Kizek, *Int. J. Electrochem. Sci.*, 7 (2012) 3072.
161.D. Hynek, L. Krejcova, O. Zitka, V. Adam, L. Trnkova, J. Sochor, M. Stiborova, T. Eckschlager, J. Hubalek and R. Kizek, *Int. J. Electrochem. Sci.*, 7 (2012) 34.
162.D. Hynek, L. Krejcova, O. Zitka, V. Adam, L. Trnkova, J. Sochor, M. Stiborova, T. Eckschlager, J. Hubalek and R. Kizek, *Int. J. Electrochem. Sci.*, 7 (2012) 13.
163.J. Wang and A. Erdem, An overview to magnetic beads used in electrochemical DNA biosensors, Springer, Dordrecht, 2003

5.1.2 Vědecký článek II

KREJCOVA, L.; HYNEK, D.; MICHALEK, P.; MILOSAVLJEVIC, V.; KOPEL, P.; ZITKA, O.; KONECNA, M.; KYNICKY, J.; ADAM, V.; HUBALEK, J.; KIZEK, R. Electrochemical Sensors and Biosensors for Influenza Detection - Literature Survey 2012-2013.

International Journal of Electrochemical Science, 2014, roč. 9. č. 7, s. 3440-3448. ISS 1452-3981. IF: 1.956

Podíl autorky Krejčová L.: 55 % textové části práce

Předmětem vědeckého článku II byla aktualizace poznatků z oblasti senzorů a biosenzorů pro detekci chřipky za časové období 2012-2014 a to z důvodu velmi rychlého vývoje v aplikaci nových metod a materiálů ve zmíněné oblasti. Předchozí přehledový článek byl rozdělen na dvě části: senzory a biosenzory, i v této publikaci jsme zachovali původní členění. Dále jsme shrnuli důvody posunu od senzorů k biosenzorům a detailněji popsali vývoj v oblasti biosenzorů, neboť vývoj v oblasti senzorů, hlavně pak v oblasti amalgámových a rtuťových elektrod je zanedbatelný. V případě zlatých a uhlíkových elektrod je tomu naopak. Zlaté elektrody jsou využívány nejčastěji a to díky snadno modifikovatelnému povrchu *(Zhou, a kol., 2013)*. Aplikace zlatých elektrod se ubírá dvěma směry a to jak pro účely detekce *(Wicklein, a kol., 2013)*, tak magnetoimunosensingu *(Zhou, a kol., 2013)*. Mnohem větší rozvoj byl pozorován v oblasti biosenzorů. Podkapitola hybridizace na elektrodách se zaměřila na detekci ODN a to buď ve spojení s PCR amplifikací *(Fialova, a kol., 2013)*, nebo detekcí specifických sekvencí pomocí QDs *(Krejcova, a kol., 2012)*, a nebo současnou detekcí dvou různých od chřipky odvozených sekvencí pomocí hybridizace na povrchu zlaté elektrody *(Grabowska, a kol., 2013, Malecka, a kol., 2013)*. Další podkapitolou biosenzorů je využití QCM a to jak pro detekci chřipkových virů *(Wang a Li, 2013)* tak pro studii vazebných vlastností chřipkových virů *(Gou, a kol., 2012)*. Další podkapitolou je využití nanočástic, kde se vývoj ubíral směrem k využití QDs *(Krejcova, a kol., 2012, Krejcova, a kol., 2013)*, protilátkami značené CuO NPs *(Gou, a kol., 2012)* a využití Au NPs konjugovanými protilátkami proti chřipce *(Grabowska, a kol., 2013)*. Značný rozvoj byl sledován i v oblasti využití aptamerů a impedance, ale největší rozmach na poli biosensingu byl pozorován právě v oblasti využití NPs.

Int. J. Electrochem. Sci., 9 **(2014)** 3440 - 3448

International Journal of ELECTROCHEMICAL SCIENCE
www.electrochemsci.org

Short Review

Electrochemical Sensors and Biosensors for Influenza Detection – Literature Survey 2012-2013

*Ludmila Krejcova[1,2], David Hynek[1,2], Petr Michalek[1,2], Vedran Milosavljevic[1,2], Pavel Kopel[1,2], Ondrej Zitka[1,2], Marie Konecna[1,2], Jindrich Kynicky[3], Vojtech Adam[1,2], Jaromir Hubalek[1,2], Rene Kizek[*1,2]*

[1]Department of Chemistry and Biochemistry, Faculty of Agronomy, Mendel University in Brno, Zemedelska 1, CZ-613 00 Brno, Czech Republic, European Union
[2]Central European Institute of Technology, Brno University of Technology, Technicka 3058/10, CZ-616 00 Brno, Czech Republic, European Union
[3]Karel Englis College, Sujanovo nam. 356/1, CZ-602 00, Brno, Czech Republic, European Union
[*]E-mail: kizek@sci.muni.cz

Received: 18 January 2014 / *Accepted:* 17 March 2014 / *Published:* 14 April 2014

This review summarized published information in the area of electrochemical detection of influenza virus in 2012 – 2013. The attention was mainly paid to summarize the news in the field of sensors and biosensors for influenza detection. Further, the impedance and quartz crystal microbalance sensing devices are also discussed.

Keywords: Influenza Virus; Electrochemical Detection; Biosensor; Sensor; Nucleic Acid; Viral Protein; Paramagnetic Nanoparticle; Voltammetry

1. INTRODUCTION

Because of new development in the assays for "pathogen determination and quantification", this review follows our previously published one focused on sensors and biosensors in the field of electrochemical detection of influenza virus [1]. Very fast development of this global research area leading to the application of new methods and materials in pathogen determination is obvious [2-4]. Therefore, the update of electrochemical detection approaches for influenza virus in the years 2012 and 2013 is summarized in this text.

Family of influenza viruses contains three genera: Influenza A, Influenza B and Influenza C. These three genera differ from each other in inside, species-specific nucleo-protein antigen, the number of gene segments, host specificity and clinical manifestations protein [5]. Because of the fact that the individual subtypes of influenza virus differ from each other by the variations in membrane virus constitution (membrane protein, ion channels, matrix proteins), various ways of detection based

on individual parts of virus are investigated. Utilization of individual differences could help in detection of individual subtypes of influenza virus.

2. SENSORS

Our last review, which is updated by this text, was divided on two basic parts according to the way of virus determination. These two basic ways were called as sensors and biosensors. The difference in both approaches lies in the presence of bio-recognition element in the sensor construction. Developmentally, the usage of electrochemical sensors is an older way. Reasons for the course change from sensors to biosensors in the area of virus determination have been summarized [6,7]. Nevertheless, development in this area is still going on.

While the development in the application of mercury and amalgam electrodes is negligible, the usage of carbon and gold electrodes is widespread. Gold electrode has well defined surface and thus, these are very suitable for the electrode surface modification. This is probably the main reason why the latest investigation is focused to this electrode material. Particularly, modification of gold electrode surface through the chemical reagents [8,9] or magnetoimmunosensing entity [10,11] was published. Chemical modification is in this case presented by two approaches, where the first one is based on the functional architecture introducing receptor molecules as a sensing entity that mimics those found in the membrane of target cells of influenza A virus [8]. The artificial receptors are built by sequential assembly of 1-octanethiol/octyl-galactoside hybrid bilayer, followed by an enzyme-mediated functionalization of the terminal galactoside groups with sialic acid molecules. The detection mechanism relies hence on the specific affinity between the sialic acid-galactose receptor moieties anchored on the modified electrode surface and the hemagglutinin (HA) viral surface protein. In contrast to immunosensors based on antibodies as bioreceptor, the sialylated modified gold electrode is also able to distinguish among influenza phenotypes. The second way of chemical modification is represented by the diazonium salt as modifier of electrode surface [9]. More precisely, 4-carboxy phenyl groups located on the electrode surface were prepared for the indium tin oxide, gold and glassy carbon electrode. Modified glassy carbon electrode was tested for the functionality as influenza ODN hybridisation biosensor [9]. In addition, modification of gold electrode surface using magnetoimmunosensing entities was based on the connection of gold electrode with magnet and next usage of magnetic particles as catchers and carriers of influenza virus [10,11]. The electrochemical response of suggested system was obtained from realized bienzymatic strategy. The first enzyme functional as tracer was tagged on immunomagnetic beads, which could be accumulated on the magneto controlled gold electrode and the second enzyme was immobilized on the electrode by layer-by-layer technique. This construction allowed obtaining the catalytically reduced electrochemical signal of H_2O_2 after the immunoreaction.

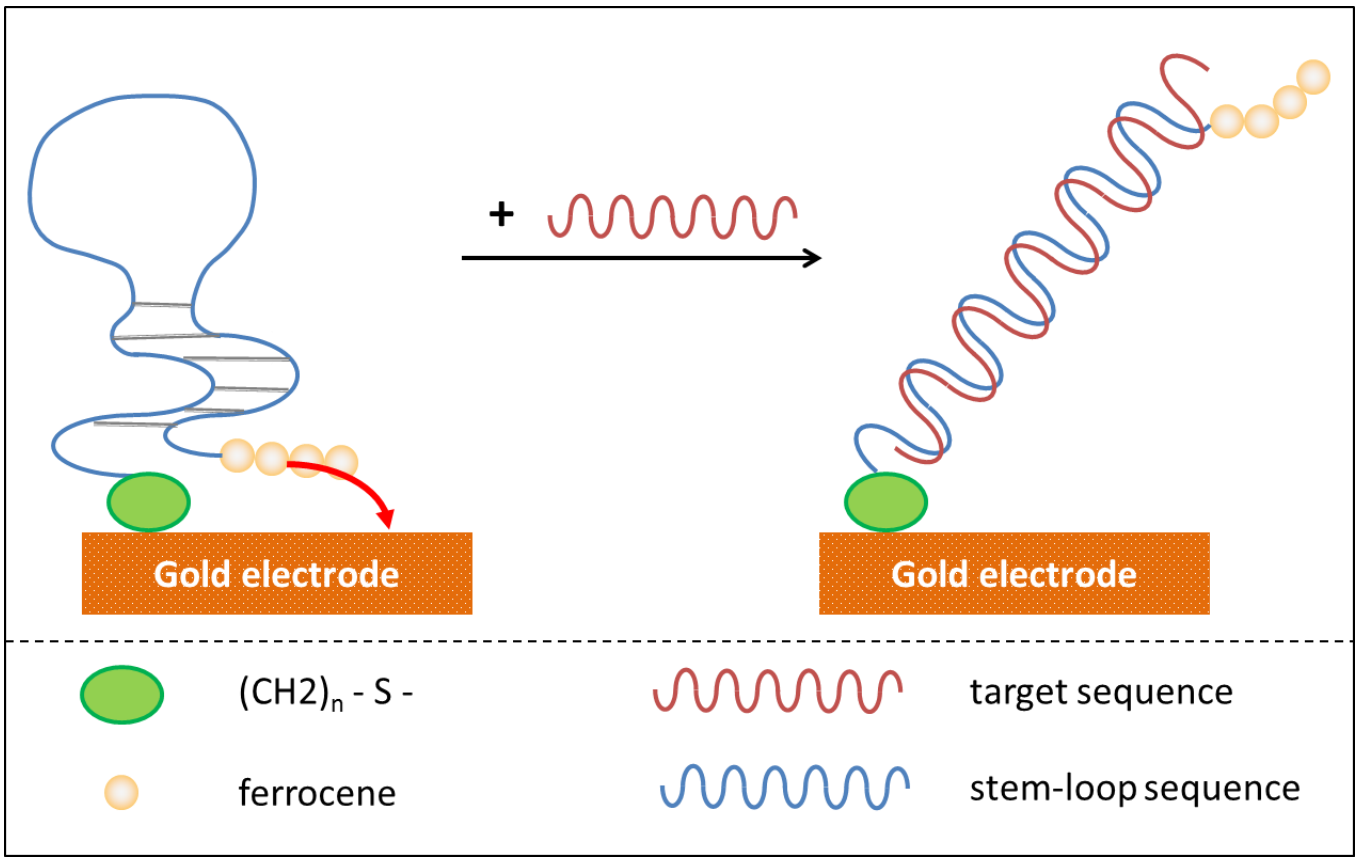

Figure 1. Schematic of the DNA detection system based on the stem-loop structured DNA probe. Probe was formed by the introduction of four ferrocene moieties at the 5′ end of a stem-loop oligonucleotide and a C6-thiol modifier group at the 3′ end. This 4Fc-DNA was immobilized on the surface of a gold electrode microsystem *via* standard thiol chemistry. Such architecture serves as sensor for DNA detection which is based on hybridization.

3. BIOSENSORS

3.1. Hybridisation on electrodes

ODNs belong to the first choice targets for formation of biosensing platform for pathogens. The simplest determined step is obviously hybridisation of target sequence. This procedure could be easily recorded by electrochemical methods. Well written overview of electrochemical real-time nucleic acid amplification was published by *Patterson et al.* [12]. This review is aimed on general pathogens quantification including influenza virus and divides presented information into four parts according the way of nucleic acid amplification as follows: solid polymerase chain reaction (PCR), solution-phase PCR using electrochemical reporters of product formation, solution-phase qPCR using sequence specific reporters, and isothermal amplification [12].

The newest ways of influenza determination based on hybridization reaction are connected with the application of electrochemical labels [13-19]. Usage of ferrocene as a modifier of specific ODN sequence was reported by *Chatelain et al.* [13]. They used four-ferrocene modified

oligonucleotide at the 5'-end and a C6-thiol modifier group at the 3'-end as a probe for DNA detection with a gold electrode microsystem (Fig. 1). The probe sequence had a stem-loop structure that fold efficiently on the electrode, and thus optimized electron transfer. Such architecture served as sensor for DNA detection based on hybridization.

Grabowska et al. constructed sensor consisting of two different oligonucleotide probes immobilized covalently on the surface of one gold electrode (via Au-S bond formation) [14]. This sensor was used for simultaneous determination of two different oligonucleotide targets. One of the probes, bound on its S'-end with ferrocene, was related to sequence encoding part of hemagglutinin from H5N1 virus. The second probe, bound on its S'-end with methylene blue, was related to the fragment of neuraminidase from the same virus. Such sensor is able to detect main markers of the influenza virus, hemagglutinin and neuraminidase.

Our group published magnetic electrochemical bar code array for detection of single point mutations (mismatches in up to four nucleotides) in H5N1 neuraminidase gene [17]. Paramagnetic particles covered with dT_{25} were used as a tool for isolation of complementary H5N1 chains (H5N1 Zhejin, China and Aichi). For detection of H5N1 chains, oligonucleotide chains of lengths of 12 (+5 adenine) or 28 (+5 adenine) bp labelled with quantum dots (CdS, ZnS and/or PbS) were used. The obtained signals identified mutations present in the neuraminidase gene sequence.

3.2. Quartz crystal microbalance

Quartz crystal microbalance (QCM) contributed to the influenza research in last two years by two various ways. The first way is represented by the detection of influenza virus [20,21] and the second by the study of influenza virus binding capabilities [22,23]. Application of QCM for influenza detection was done through two various parts of influenza virus. In the first case, the aptamer was used for the formation of switch on/off system based on the crosslinked polymeric hydrogel [21]. A selected aptamer with high affinity and specificity against H5N1 surface protein was used, and hybridization between the aptamer and ssDNA formed the crosslinker in the polymer hydrogel. The aptamer hydrogel was immobilized on the gold surface of QCM sensor using a self-assembled monolayer method. The hydrogel remained in the state of shrink if no H5N1 virus was present in the sample because of the crosslinking between the aptamer and ssDNA in the polymer network. When it exposed to the target virus, the binding reaction between the aptamer and H5N1 virus caused the dissolution of the linkage between the aptamer and ssDNA resulting in the abrupt swelling of the hydrogel. The second part of virus used for detection was hemagglutinin, its binding capabilities, respectively [20]. *Diltemiz et al.* used 4-aminophenyl boronic acid as a new ligand for binding of sialic acid (having an important role in binding of HA) via boronic acid sugar interaction. QCM sensor surface was modified with thiol groups and then 4-aminophenyl boronic acid and sialic acid were immobilized on sensor surfaces, respectively.

Further studies of influenza binding capabilities were focused on hemagglutinin and its interaction. The first example of such study was the work of *Takahashi et al.* [22]. They studied the association of a sulphated galactosyl ceramide (sulphatide) with the viral envelope glycoprotein

hemagglutinin. To determine whether the ectodomain of HA could bind to sulphatide, a secreted-type HA (sHA), in which the transmembrane region and cytoplasmic tail were deleted, was applied. sHA showed subtype-specific antigenicity and binding ability to both sulphatide and gangliosides. Kinetics of sHA binding to sulphatide was demonstrated by QCM analysis. The second example was the work of *Wangchareansak et al.* focused on behaviour of N-acetylglucosamine [23]. N-acetylglucosamine is a part of the oligosacharide ligand responsible for the first binding step of virus (ligand-virus interactions) to a host cell. For immobilization on the gold surface, N-acetylglucosamine was linked to p-nitrophenol, and the nitro group was reduced and then bound to cysteine via two-step synthesis.

3.3. Nanoparticles

The main benefits of nanoparticle application lie in the improvement of electrode surface in the view of electrochemical reaction or better way of isolation procedure. Papers published in last two years aimed to these two ways. *Yanxia et al.* labelled antibodies by CuO NPs [24]. After the immobilization of the antibodies (attached on the solid substrate via physical adsorption between hydrophobic groups of antibody molecules and polystyrene), the CuO NPs were dissolved by adding acid to produce copper ions, which were electrochemically detected with high sensitivity and specificity. Another way of electrode surface modification was presented by *Jang et al.* [25]. In their work usage of ZnO nanorod network for the immunosensor fabrication was described. The immunosensor was evaluated in the acetate buffer solution containing 3,3',5,5'-tetramethylbenzidine (TMB) via cyclic voltammetry.

The improvement of the isolation procedure was described by *Kamikawa et al.* using electrically active magnetic polyaniline-coated nanoparticles as the transducer in an electrochemical biosensor for rapidly identifying influenza strains based on receptor specificity [26]. Electrically active magnetic nanoparticles were prepared by synthesizing aniline monomer around gamma iron (III) oxide (gamma-Fe_2O_3) cores, yielding 25-100 nm diameter nanoparticles. The nanoparticles were coated with monoclonal antibodies specific to H5N1. In addition, *Krejcova et al.* used glycan modified magnetic particles for isolation of influenza hemaglutinin and reported a new three-dimensional (3D), bead-based microfluidic chip for rapid, sensitive and specific detection of influenza hemagglutinin [19].

Gopinath and co-workers described immuno-AuNP assay, where gold nanoparticles were conjugated to an antibody against A/Udorn/307/1972 (H3N2) influenza virus to detect viruses on a sensing plate designed for an evanescent field-coupled waveguide-mode sensor [27]. One year later *Gopinath and coworkers* applied sensor based on previous experiment for demonstration that the anti-A/Udorn/307/1972 polyclonal antibody has the ability to discriminate between old and recently emerged influenza A/H3N2 viruses [28]. The authors were successful in the reaching of their aims. Moreover, *Bamrungsap et al.* report on a lateral flow immunoassay (LFIA) for influenza A antigen using fluorescently-doped silica nanoparticles as reporters [29].

Application of quantum dots for the influenza detection was presented by our group only. Different ways using quantum dots as labels were published [15,17,18,30,31]. Two main parts of

influenza virus using for its detection was labelled by quantum dots, nucleic acids [16,18,31] and proteins (especially hemagglutinin) [15,30].

3.4 Aptamers

The utilization of aptamers for influenza electrochemical detection was published twice times in the defined time interval only [21,32]. The first experiment, published by *Wang et al.* [21], was described above in the section related to the QCM method. Another way of detection was based on the polymer microfluidic system with a functionalized conductive polymer microelectrode array [32]. *Kiilerich-Pedersen et al*. [32] show that DNA aptamer with affinity for influenza A virus (H1N1) were linked covalently to the conductive polymer microelectrodes in the microfluidic channel. The immobilization of aptamer on the electrodes provoked an increase in the impedance due to increased charge transfer resistance at the electrode/liquid interface. The binding of the virus to aptamers caused significant increase in the impedance already at very low concentrations. The washing the samples with PBS gave no significant change in the impedance signal, hence demonstrating that virus was bound to the aptamer.

3.5. Impedance

The utilization of impedance technique for the influenza determination had a great potential as it was shown in the last two years. Impedance determination was mainly connected with immunomagnetic separation [33-37]. Connection of immunomagnetic separation was studied mainly by the *Yan et al.* in four experiments differing in various technical designing of the experiments. They determined H5 subtype of avian influenza virus. In the first experiment [36], they used monoclonal antibodies against AIV H5N1 surface antigen hemagglutinin (HA), which were immobilized on the surface of gold microelectrodes through protein A for capturing influenza H5N1 in sample solutions. Electrochemical impedance spectroscopy was carried out in the presence of $[Fe(CN)_6]^{3-/4-}$ as a redox probe to describe the surface modification of microelectrodes and the binding of viruses. Other their experiments were connected with the application of immunomagnetic separation and differ in individual experiments design [33-35]. The first approach used streptavidin-coated magnetic nanobeads, where these particles were immobilized onto the biotin-labelled anti-H5 monoclonal antibodies to capture hemagglutinin (H5N1) from sample solutions by the specific immunoreaction. Then, these complexes were separated and concentrated by a magnetic field and the impedance magnitude was measured in a frequency range from 20 Hz to 1 MHz [35]. The second design was based on the modification of the surface of gold microelectrodes with protein A and then immobilization with monoclonal antibodies against an epitope in the hemagglutinin of H5 influenza subtype [34]. The binding of H5 subtype viruses onto the antibody-modified microelectrodes surface resulted in a change in the impedance, which was measured in the presence of $[Fe(CN)_6]^{3-/4-}$ as a redox probe. The third approach was based on the biotin labelled anti H5 monoclonal antibodies, which

were immobilized onto the streptavidin coated magnetic nanobeads to separate and concentrate avian influenza virus H5N1 [33].

Except *Yan et al.* one other group published impedance biosensor for influenza detection. *Lum et al.* improved the impedance detection by labelling attached influenza H5N1 entities by chicken red blood cells for the impedance signal amplification [37]. The main principle of their assay is described in Fig. 2.

The application of impedance technique for influenza detection may not be combined with immunomagnetic separation only. Another approach for influenza impedance detection was published by *Malecka et al.* [38]. They suggested a biosensor for detection of specific oligonucleotide sequences of H5N1 influenza virus. The NH2-ssDNA probe was deposited onto a gold electrode surface to form an amide bond between the carboxyl group of thioacid and the amino group from ssDNA probe. The signals generated as a result of hybridization were registered by impedance spectroscopy in the presence of $[Fe(CN)_6]^{3-/4-}$ as a redox mediator. This genosensor was capable to determine 180-bp (PCR products) oligonucleotides complementary sequences.

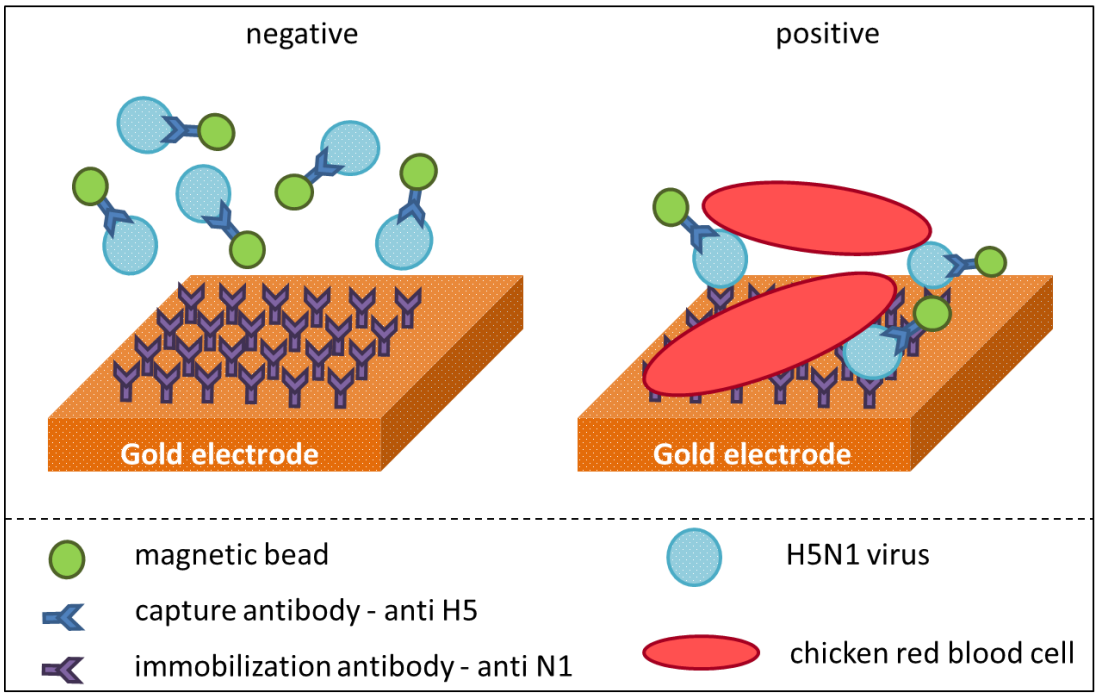

Figure 2. Design of non-Faradic impedance biosensor system using chicken red blood cells (RBCs) as bio-labels for improvement of impedance detection. A sample of influenza was isolated using immunomagnetic nanobeads coated with monoclonal antibody against H5. Second antibody against N1 subtype was interdigitated to microelectrode array. Target H5N1 virus was bound to the antibody on the electrode surface, causing a change in the impedance compared to a control sample. RBCs were used as biolabels to amplify the impedance change through their binding to the influenza virus on the electrode. RBCs were used as biolabels to amplify the antibody-virus binding due to their larger diameter (7-12 μm) compared to the virus (80-120 nm), and strong and specific binding by virus hemagglutinin to sialic acid linkages found on the cell surface. Both the virus and the RBC act as resistors in the system, and the RBC has a larger resistive value due to its larger size compared with the virus.

4. CONCLUSION

This review summarized published information in the area of electrochemical detection of influenza virus in the years 2012 – 2013. This text should be connection of our previous review focused on this area of research [1], where interesting and promising seems to be aiming the attention at the impedance and QCM ways of influenza virus detection.

ACKNOWLEDGEMENTS
Financial support from NanoBioMetalNet CZ.1.07/2.4.00/31.0023 is highly acknowledged.

CONFLICT OF INTEREST:
The authors have declared no conflict of interest.

References

1. L. Krejcova, D. Hynek, V. Adam, J. Hubalek and R. Kizek, *Int. J. Electrochem. Sci.*, 7 (2012) 10779.
2. C. I. L. Justino, T. A. P. Rocha-Santos and A. C. Duarte, *Trac-Trends Anal. Chem.*, 45 (2013) 24.
3. M. S. Cheng and C. S. Toh, *Analyst*, 138 (2013) 6219.
4. H. S. Moon, J. H. Lee, K. Kwon and H. I. Jung, *Anal. Lett.*, 45 (2012) 113.
5. A. Beby-Defaux, G. Giraudeau, S. Bouguermouh and G. Agius, *Med. Mal. Infect.*, 33 (2003) 134.
6. A. C. Chen and B. Shah, *Anal. Methods*, 5 (2013) 2158.
7. R. L. Caygill, G. E. Blair and P. A. Millner, *Anal. Chim. Acta*, 681 (2010) 8.
8. B. Wicklein, M. A. M. del Burgo, M. Yuste, E. Carregal-Romero, A. Llobera, M. Darder, P. Aranda, J. Ortin, G. del Real, C. Fernandez-Sanchez and E. Ruiz-Hitzky, *Adv. Funct. Mater.*, 23 (2013) 254.
9. D. J. Chung, S. H. Oh, S. Komathi, A. I. Gopalan, K. P. Lee and S. H. Choi, *Electrochim. Acta*, 76 (2012) 394.
10. C. H. Zhou, Y. M. Long, B. P. Qi, D. W. Pang and Z. L. Zhang, *Electrochem. Commun.*, 31 (2013) 129.
11. C. H. Zhou, Y. Shu, Z. Y. Hong, D. W. Pang and Z. L. Zhang, *Chem.-Asian J.*, 8 (2013) 2220.
12. A. S. Patterson, K. Hsieh, H. T. Soh and K. W. Plaxco, *Trends Biotechnol.*, 31 (2013) 704.
13. G. Chatelain, M. Ripert, C. Farre, S. Ansanay-Alex and C. Chaix, *Electrochim. Acta*, 59 (2012) 57.
14. I. Grabowska, K. Malecka, A. Stachyra, A. Gora-Sochacka, A. Sirko, W. Zagorski-Ostoja, H. Radecka and J. Radecki, *Anal. Chem.*, 85 (2013) 10167.
15. D. Fialova, L. Krejcova, L. Janu, I. Blazkova, O. Krystofova, D. Hynek, P. Kopel, J. Drbohlavova, M. Konecna, M. Vaculovicova, J. Kynicky, J. Hubalek, P. Babula, R. Kizek and V. Adam, *Int. J. Electrochem. Sci.*, 8 (2013) 10805.
16. L. Krejcova, D. Huska, D. Hynek, P. Kopel, V. Adam, J. Hubalek, L. Trnkova and R. Kizek, *Int. J. Electrochem. Sci.*, 8 (2013) 689.
17. L. Krejcova, D. Hynek, P. Kopel, M. A. M. Rodrigo, V. Adam, J. Hubalek, P. Babula, L. Trnkova and R. Kizek, *Viruses-Basel*, 5 (2013) 1719.
18. L. Krejcova, D. Hynek, P. Kopel, M. A. M. Rodrigo, K. Tmejova, L. Trnkova, V. Adam, J. Hubalek and R. Kizek, *Int. J. Electrochem. Sci.*, 8 (2013) 4457.
19. L. Krejcova, L. Nejdl, M. A. Merlos Rodrigo, M. Zurek, M. Matousek, D. Hynek, O. Zitka, P. Kopel, V. Adam and R. Kizek, *Biosens. Bioelectron.*, 54 (2014) 421.

20. S. E. Diltemiz, A. Ersoz, D. Hur, R. Kecili and R. Say, *Mater. Sci. Eng. C-Mater. Biol. Appl.*, 33 (2013) 824.
21. R. H. Wang and Y. B. Li, *Biosens. Bioelectron.*, 42 (2013) 148.
22. T. Takahashi, S. Kawagishi, M. Masuda and T. Suzuki, *Glycoconjugate J.*, 30 (2013) 709.
23. T. Wangchareansak, C. Sangma, P. Ngernmeesri, A. Thitithanyanont and P. A. Lieberzeit, *Anal. Bioanal. Chem.*, 405 (2013) 6471.
24. Y. X. Li, M. Hong, Y. Q. Lin, Q. Bin, Z. Y. Lin, Z. W. Cai and G. N. Chen, *Chem. Commun.*, 48 (2012) 6562.
25. Y. Jang, J. Park, Y. K. Pak and J. J. Pak, *J. Nanosci. Nanotechnol.*, 12 (2012) 5173.
26. T. L. Kamikawa, M. G. Mikolajczyk, M. Kennedy, L. L. Zhong, P. Zhang, E. B. Setterington, D. E. Scott and E. C. Alocilja, *IEEE Trans. Nanotechnol.*, 11 (2012) 88.
27. S. C. B. Gopinath, K. Awazu, M. Fujimaki, K. Shimizu and T. Shima, *PLoS One*, 8 (2013) 1.
28. S. C. B. Gopinath, K. Awazu, M. Fujimaki and K. Shimizu, *PLoS One*, 8 (2013) 1.
29. S. Bamrungsap, C. Apiwat, W. Chantima, T. Dharakul and N. Wiriyachaiporn, *Microchim. Acta*, 181 (2014) 223.
30. L. Krejcova, D. Dospivova, M. Ryvolova, P. Kopel, D. Hynek, S. Krizkova, J. Hubalek, V. Adam and R. Kizek, *Electrophoresis*, 33 (2012) 3195.
31. O. Zitka, S. Skalickova, M. A. M. Rodrigo, L. Krejcova, P. Kopel, V. Adam and R. Kizek, *Int. J. Electrochem. Sci.*, 8 (2013) 12628.
32. K. Kiilerich-Pedersen, J. Dapra, S. Cherre and N. Rozlosnik, *Biosens. Bioelectron.*, 49 (2013) 374.
33. X. F. Yan, M. H. Wang, X. H. Wen and D. An, *Chin. J. Anal. Chem.*, 41 (2013) 817.
34. X. F. Yan, M. H. Wang, X. H. Wen and D. An, in P. Yarlagadda, Y.H. Kim (Editors), Measurement Technology and Its Application, Pts 1 and 2, Trans Tech Publications Ltd, Stafa-Zurich, 2013, p. 367.
35. X. F. Yan, R. H. Wang, J. H. Lin, Y. T. Li, M. H. Wang, D. An, P. R. Jiao, M. Liao, Y. D. Yu and Y. B. Li, *Sens. Lett.*, 11 (2013) 1256.
36. X. F. Yan, Y. T. Li, R. H. Wang, J. H. Lin, X. H. Wen, M. H. Wang, D. An, W. J. Han, Y. D. Yu and Y. B. Li, *Chin. J. Anal. Chem.*, 40 (2012) 1507.
37. J. Lum, R. H. Wang, K. Lassiter, B. Srinivasan, D. Abi-Ghanem, L. Berghman, B. Hargis, S. Tung, H. G. Lu and Y. B. Li, *Biosens. Bioelectron.*, 38 (2012) 67.
38. K. Malecka, I. Grabowska, J. Radecki, A. Stachyra, A. Gora-Sochacka, A. Sirko and H. Radecka, *Electroanalysis*, 25 (2013) 1871.

5.2 Izolace a detekce chřipkové nukleové kyseliny

5.2.1 Vědecký článek III

KREJCOVA, L.; HYNEK, D.; KOPEL, P.; ADAM, V.; HUBALEK, J.; TRNKOVA, L.; KIZEK, R. Paramagnetic Particles Isolation of Influenza Oligonucleotide Labelled with CdS QDs.

Chromatographia, 2013, roč. 76. č. 7-8, s. 355-362. ISS 0009-5893. IF: 1.370

Podíl autorky Krejčová L.: 70 % textové části práce, 70 % experimentální části práce

Chřipkové viry jsou velmi náchylné ke změnám typu antigenní shift a drift *(Koel, a kol., 2013)*. Výskyt vysoce patogení HPAI je právě důsledkem jedné z nich *(Hall, a kol., 2013, Le a Nguyen, 2014)*. Vysoce nakažlivé a nebezpečné onemocnění, kterým HPAI bezesporu je, vyžaduje neustálé hledání rychlejších a citlivějších metod *(Iqbal, a kol., 2014)*. Hybridizace nukleové kyseliny na pevné základny je součastí řady biotechnologických postupů pro izolaci *(Miodek, a kol., 2014, Singh, a kol., 2014)*. Podstatou experimentu byl návrh senzoru pro detekci sekvence specifické pro subtyp H5N1. Autoři se zaměřili na popis MPs, QDs a jejich aplikaci pro detekci specifických chřipkových sekvencí na principu dvou, na sebe navazujících kroků: 1) izolace cílové sekvence (ODN) pomocí MPs modifikované anti-sense sekvencí a 2) detekci izolované, cílové sekvence pomocí QDs značky. Dílčím úkolem byla optimalizace teploty, doby hybridizace, koncentrace cílové chřipkové sekvence v komplexu s kademnatými QDs (ODN-SH-Cd) a automatizace celého postupu. Účinost hybridizace při různých podmínkách byla sledována elektrochemicky, a to jak přímo (detekce cílové sekvence - CA pík), tak nepřímo (detekce QDs - Cd pík). Optimální parametry byly vybrány následovně: hybridizační teplota 25°C, čas hybridizace 35 minut a koncentrace ODN v ODN-SH-Cd 20 μg/ml. Při těchto podmínkách byla elektrochemicky detekována největší výtěžnost izolace. Optimalizované podmínky izolace byly použity pro automatizaci celého procesu. Navržený detekční systém může být použit pro rychlou detekci jakékoliv specifické sekvence na základě komplementarity k anti-sense řetězci, kterým je modifikován povrch MPs.

Chromatographia (2013) 76:355–362
DOI 10.1007/s10337-012-2327-0

ORIGINAL

Paramagnetic Particles Isolation of Influenza Oligonucleotide Labelled with CdS QDs

Ludmila Krejcova · David Hynek · Pavel Kopel · Vojtech Adam · Jaromir Hubalek · Libuse Trnkova · Rene Kizek

Received: 22 June 2012 / Revised: 28 August 2012 / Accepted: 30 August 2012 / Published online: 4 October 2012

Abstract In this study, we describe hybridization design probes consisting of paramagnetic particles and quantum dots (QDs) with targeted DNA, and their application for detection of avian influenza virus (H5N1). Optical properties of QDs were beneficial, but the main attention was paid to the electroactivity of metal part of QDs and ODNs themselves. Differential pulse voltammetry was used for detection of cadmium(II) ions and square wave voltammetry for detection of cytosine–adenine peak in ODN-SH-Cd complex. It clearly follows from the obtained results that the optimized conditions were temperature of hybridization 25 °C, time of hybridization 35 min, and concentration of ODN-SH-Cd complex 20 μg mL^{-1}. The detection limit (3 signal/noise) was estimated as 15 ng mL^{-1} of ODN-SH-Cd.

Published in the special paper collection *Advances in Chromatography and Electrophoresis & Chiranal 2012* with guest editor Jan Petr.

L. Krejcova · D. Hynek · P. Kopel · V. Adam · L. Trnkova · R. Kizek (✉)
Department of Chemistry and Biochemistry, Faculty of Agronomy, Mendel University in Brno, Zemedelska 1, 613 00 Brno, Czech Republic
e-mail: kizek@sci.muni.cz

D. Hynek · P. Kopel · V. Adam · J. Hubalek · L. Trnkova · R. Kizek
Central European Institute of Technology, Brno University of Technology, Technicka 3058/10, 616 00 Brno, Czech Republic

J. Hubalek
Department of Microelectronics, Faculty of Electrical Engineering and Communication, Brno University of Technology, Technicka 3058/10, 616 00 Brno, Czech Republic

Keywords Biosensors · Voltammetry · Automated separation · Nanoparticles · Quantum dots · Hybridization · Virus

Introduction

Influenza is an infectious disease caused by RNA viruses of the family Orthomyxoviridae. Influenza viruses can be found in the aerosols formed by sneezing and coughing and may cause acute infection of upper respiratory tract [1, 2]. Vaccine against influenza exists; however, it is effective for one year against selected subtypes. This is due to mutational changes in the structure of the virus, thus the reuse of the same vaccine in the following year does not have a protected effect [3, 4]. It is clear that flu viruses are very susceptible to change antigenic equipment by drift and shift. These changes can easily create a new subtype, as in the case of highly pathogenic avian influenza. Owing to this, a great amount of research is being carried out in the search for rapid and more reliable detection methods [1, 5, 6].

Nucleic acid hybridization on solid bases is widely used in biotechnology for the isolation of targeted DNA. Among numerous methods used in this field, many probe–target DNA assays use oligo-conjugated paramagnetic particles (MPs) for the isolation of nucleic acids of interest [7, 8]. The advantage of magnetic separation is in the possibility of modifying the surface of MPs, and thus the elimination of interfering adsorption of non-target biomolecules [9–11], because MPs are able to respond to external magnetic field, which is used for efficient separation. Both magnetic separation and modification of MPs surfaces are beneficial for DNA isolation [12–14].

Isolated DNA is usually detected by hybridization process using different materials such as biotin–avidin, substrate

enzyme, antigen–antibody and fluorescent dyes or other optical active substances as quantum dots (QDs) [15, 16], because detection of hybridized DNA molecule is important for diagnosis of the presence of specific virus [17]. Application of optical detection methods based on fluorescently active labels is widespread [18–20]. Recent advantages in synthesis and surface modifications of QDs as a new type of fluorescently active labels have resulted in various applications of these particles [21–25]. Wang et al. described multi-target electrochemical DNA detection based on the use of different QDs. Multi-target electrical detection scheme developed by those authors incorporates the high sensitivity and selectivity advantages of nanoparticle-based electrical assays [17]. It is clear that besides optical properties of these nanoparticles, QDs can be also used as electroactive labels for determination of biologically active compounds [26]. Therefore, one of the main aims of this study was the electrochemical detection of the presence of Cd and cytosine–adenine (CA) in H5N1 influenza derived oligonucleotide labelled with CdS. This detection part was coupled to paramagnetic particle-based isolation protocol as the second main aim of our study. The suggested procedure is shown in Fig. 1.

Experimental Section

Preparation of CdS QDs

All chemicals were purchased from Sigma-Aldrich (St. Louis, USA) and used without further purification. CdS QDs were prepared with a slightly modified method published in [27]. Cadmium nitrate tetrahydrate $Cd(NO_3)_2{\cdot}4H_2O$ (0.03085 g, 0.1 mM) was dissolved in ACS water (25 mL). 3-Mercaptopropionic acid (35 µL, 0.4 mM) was slowly added to stirred solution. Afterwards, pH was adjusted to 9.11 with 1 M NH_3 (1.5 mL). Sodium sulphide nanohydrate $Na_2S{\cdot}9H_2O$ (0.02402 g, 0.1 mM) in 23 mL of ACS water was poured into the first solution with vigorous stirring. Obtained yellow solution was stirred for 1 h. CdS QDs were stored in dark at 4 °C. Fluorescence of the obtained QDs is shown in Fig. 2. We found that the synthesized objects were smaller than 10 nm.

Preparation of CdS Labelled H5N1 Influenza Oligonucleotide (ODN-SH-Cd)

ODN-SH H5N1 5′-SH-CTTCTTCTCTCTCCTTGAGG-3′ (100 µL, 100 µg mL^{-1}) was mixed with a solution of CdS QDs (100 µL). This mixture was shaken for 24 h at room temperature using Vortex Genie2 (Scientific Industries, New York, USA). Subsequently, solution was dialysed against 2,000 mL of mili Q water (24 h, 4 °C) on Millipore membrane filter 0.025 µm VSWP. During dialysis, the sample was diluted to 800 µL. Diluted sample was concentrated to 500 µL final volume on a centrifugal filter device Amicon Ultra 3k (Millipore, Billerica, USA). Centrifuge 5417R (Eppendorf, Hamburg, Germany) was utilized with following parameters 15 min, 4,500 rpm, 15 °C.

Robotic Pipetting Station

For automated samples handling before their electrochemical analysis, an automated pipetting station ep-Motion 5075 (Eppendorf) with computer controlling was used. Positions C1 and C4 were thermostated (Epthermoadapter PCR96). In B1 position, module reservoir for washing solutions and waste were placed. Tips were placed in positions A4 (epTips 50), A3 (epTips 300) and A2 (epTips 1000). Transfer was ensured by a robotic arm with pipetting adaptors (TS50, TS300, TS1000) numeric labelling refers to maximal pipetting volume in µL and a gripper for platforms transport (TG-T). The program sequence was edited and the station was controlled in pEditor 4.0. For sample preparation, two platforms were used: Thermorack for 24 × 1.5–2 mL microtubes (position C3), which was used for storage of working solutions, 96-well microplate with well volume of 200 µL (position C1), which was thermostated. After the separation, the MPs were forced using Promega magnetic pad (Promega, Madison, USA) (position B4) and the solutions were transferred to a new microplate.

Automatic Isolation of ODN-SH-Cd

Automatic pipetting station ep-Motion 5075 (Eppendorf) with original devices was used for fully automated influenza-derived oligonucleotide isolation process. The buffers used in isolation part of experiment were as follows: phosphate buffer I: 0.1 M NaCl + 0.05 M Na_2HPO_4 + 0.05 M NaH_2PO_4; phosphate buffer II: 0.2 M NaCl + 0.1 M Na_2HPO_4 + 0.1 M NaH_2PO_4; and hybridization solution: 100 mM Na_2HPO_4 + 100 mM NaH_2PO_4, 0.5 M NaCl, 0.6 M guanidium thiocyanate, 0.15 M Trizma base adjusted by HCl on pH of 7.5.

The protocol was as follows: 10 µL of Dynabeads Oligo $(dT)_{25}$ (1 µm diameter, Hämeenlinna, Finland) was dispensed in each well in the plate (PCR 96, Eppendorf. Plate was subsequently transferred to the magnet, stored solution from nanoparticles was aspirated to waste, and beads were further washed three times with 20 µL of phosphate buffer I. The next step was *first hybridization*. 10 µL of polyA-modified anti-sense H5N1 oligonucleotide and 10 µL of hybridization buffer (0.1 M phosphate buffer, 0.6 M guanidium thiocyanate, 0.15 M Tris) were added into each

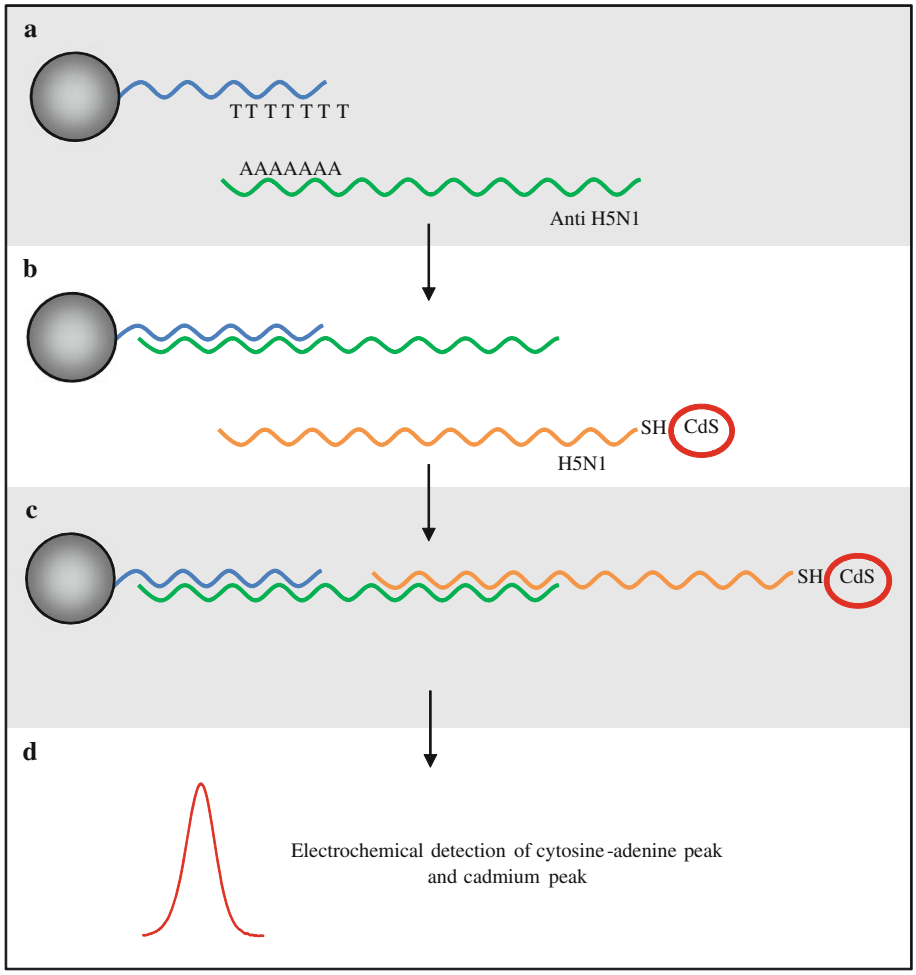

Fig. 1 Scheme of H5N1 (ODN-SH-Cd) isolation and electrochemical detection. **a** Anti-H5N1 binding to MP due to A-T complementarity, **b** addition of ODN-SH-Cd, **c** binding of ODN-SH-Cd to MP with anti-H5N1 and **d** electrochemical detection of ODN and Cd

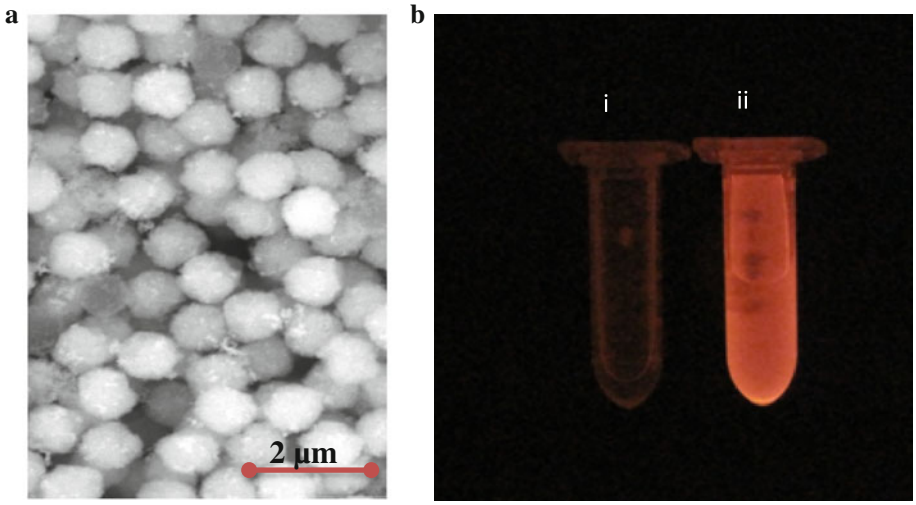

Fig. 2 **a** SEM micrograph of paramagnetic particles modified with dT25 (SEM HV 15.0 kV). **b** CdS QDs (*i*) without UV light, (*ii*) UV light 305 nm. The fluorescence was monitored by in vivo Xtreme system by Carestream, Woodbridge, USA. This instrument was equipped with 400 W xenon light source and 28 excitation filters (410–760 nm). The emitted light was captured by 4 MP CCD camera

well. Further, the plate was incubated (15 min, 25 °C, pipetting), followed by three times washing with 20 µL phosphate buffer I. The next step was *second hybridization*. 10 µL of Cd labelled H5N1 oligonucleotide and 10 µL of hybridization buffer (0.1 M phosphate buffer, 0.6 M guanidium thiocyanate, 0.15 M Tris) were added to each well, and the plate was incubated (15 min, 25 °C, pipetting), followed by three times washing with 20 µL of phosphate buffer I. Afterwards, 30 µL of elution solution (phosphate buffer II) was added into each well, and the plate was incubated (5 min, 85 °C, pipetting). After elution step, the plate was transferred to the magnet, and product from each

well was transferred to separate well. The whole procedure was optimized by other authors [28–30].

Methods for Detection of CA and Cd Peak (ODN-SH-Cd)

Measurements were performed at 663 VA Stand, 800 Dosino and 846 Dosing Interface (Metrohm, Zofingen, Switzerland) using a standard cell with three electrodes. A hanging mercury drop electrode with a drop area of 0.4 mm^2 was employed as the working electrode. An Ag/AgCl/3 M KCl electrode served as the reference electrode, while the auxiliary electrode was a glassy carbon electrode. All measurements were performed in the presence of 0.2 M acetate buffer (0.2 M CH_3COOH + 0.2 M CH_3COONa, pH 5.0) at 25 °C. Samples were deoxygenated by argon (99.99 %, 120 s). For smoothing and baseline correction, the software GPES 4.9 supplied by EcoChemie (Utrecht, Netherlands) was employed. For detection of DNA, CA peak measured by square wave voltammetry (SWV) was used. The parameters of electrochemical determination were as follows: initial potential 0 V; end potential −1.85 V; frequency 10 Hz; potential step 0.005 V; and amplitude 0.025 V. For electrochemical detection of cadmium (Cd peak), differential pulse voltammetry (DPV) was used. The parameters of electrochemical determination were as follows: initial potential −0.9 V; end potential −0.45 V; deposition potential −0.9 V; duration 240 s; equilibration time 5 s; modulation time 0.06; time interval 0.2 s; potential step 0.002 V; and modulation amplitude 0.025.

Scanning Electron Microscope

A modern scanning electron microscope (SEM) with motorized stage, full software control and image acquisition was recognized as a relatively easy way for automated high-resolution documentation of particles. For each experiment, three independent samples of particles on different tablet sections (glass, pure Si, and Millipore syringe filters) were documented. FEG-SEM TESCAN MIRA 3 XMU (Brno, Czech Republic) was used for documentation. This model is equipped with a high brightness Schottky field emitter for low noise imaging at fast scanning rates. The SEM was fitted with Everhart–Thronley type of SE detector, high speed YAG scintillator-based BSE detector and panchromatic CL Detector.

Descriptive Statistics

Data were processed using MICROSOFT EXCELs (USA) and STATISTICA.CZ Version 8.0 (Prague, Czech Republic). The results are expressed as mean ± SD unless noted otherwise. The detection limits (3 signal/noise, S/N) were calculated according to Long and Winefordner [31], whereas N was expressed as standard deviation of noise determined in the signal domain unless stated otherwise.

Results and Discussion

Rapid detection of the presence of virus represents a challenge for modern bioanalytical chemistry. For this purpose, MPs bring many advantages including possibility of miniaturization of the instrument as lab-on-chip [28]. Moreover, paramagnetic particles are suitable for sensing, therapeutic and diagnostic purposes [32]. In this study, particles modified with short thymine chain (dT25) were used (Fig. 2a). Next step was labelling of influenza derived thiolated oligonucleotide with CdS QDs. These QDs were prepared from cadmium nitrate tetrahydrate according to procedure mentioned in the "Experimental" section. The prepared CdS QDs had fluorescent properties as shown in Fig. 2b. The possibilities of labelling of nucleic acids and proteins with QDs are discussed by Joseph Wang and Cliphord Mirkin and showed many advantages for potential applications in nanomedicine [33–37]. The last part of preparation of sensing assay was full automation of the isolation with subsequent electrochemical detection of CdS labelled H5N1 influenza derived oligonucleotide (ODN-SH-Cd). Scheme of ODN-SH-Cd isolation and electrochemical detection is shown in Fig. 1.

Determination of Cadmium(II) Ions and ODNs

For the quantification of the interactions between CdS QDs and ODNs, determination of the presence of the formed complex via electrochemical detection of cadmium(II) ions is very advantageous, because electroanalysis of metal ions is well known, sensitive, and robust enough to be used routinely for analysis of various types of real samples [38, 39]. DPV was used for detection of cadmium(II) ions in CdS QDs. Peak of cadmium(II) ions enhanced with the increasing accumulation time up to 300 s, which was selected as the optimum for the following experiments (Fig. 3a). The obtained CdS QDs concentration dependence was linear within the range from 0.5 to 70 μg mL^{-1} as it follows $y = 0.6473x; R^2 = 0.9990, n = 5, \mathrm{RSD} = 2.1\ \%$ (Fig. 3b). If cadmium(II) ions (CdS) were detected in bounded forms with ODNs, then well-developed peaks of Cd(II) were measured at -0.58 ± 0.02 V ($n = 5$). Determined calibration dependence was following $y = 20.64x$; $R^2 = 0.9941$, $n = 5$, RSD = 3.8 % (Fig. 3c). The limit of detection (3 S/N) was determined as 1 ng mL^{-1} ODN-SH-Cd.

For the complete characterization of system, we needed electrochemical determination of ODNs. SWV was selected for this purpose. ODN-SH (full line) and ODN-

SH–Cd (dotted line) complex provided various SWV records (Fig. 4a). For ODN-SH characteristic, CA peak was detected at −1.348 ± 0.005 V). Oligonucleotide ODN-SH-Cd showed two peaks. The first one corresponded to cadmium(II) ions (Cd peak, −0.58 ± 0.005 V), and the second one to the nucleic acid (CA peak, −1.362 ± 0.002 V). There were also significant differences between CA peaks of Cd labelled and non-labelled oligonucleotides. Non-labelled ODN gave higher and thinner CA peak compared with ODN-SH-Cd. Slight difference in the CA peak position was determined (QDs labelled: −1.362 V and non-labelled: −1.348 V). The only difference between these oligonucleotides is the bound CdS to the 5′ SH end of influenza derived oligonucleotide. It follows that the change of the CA signal must be caused by QDs binding, but effect of CDs on the CA peak is not fully understood, but the changes can be associated with changes of electric properties of nucleic acids [40].

After characterization of labelled and non-labelled ODNs, the optimization of accumulation times for both ODNs was done. Binding of CdS to ODN-SH decreased CA peak in the whole tested interval, but in both cases, the value of 120 s was selected as optimal for further studies

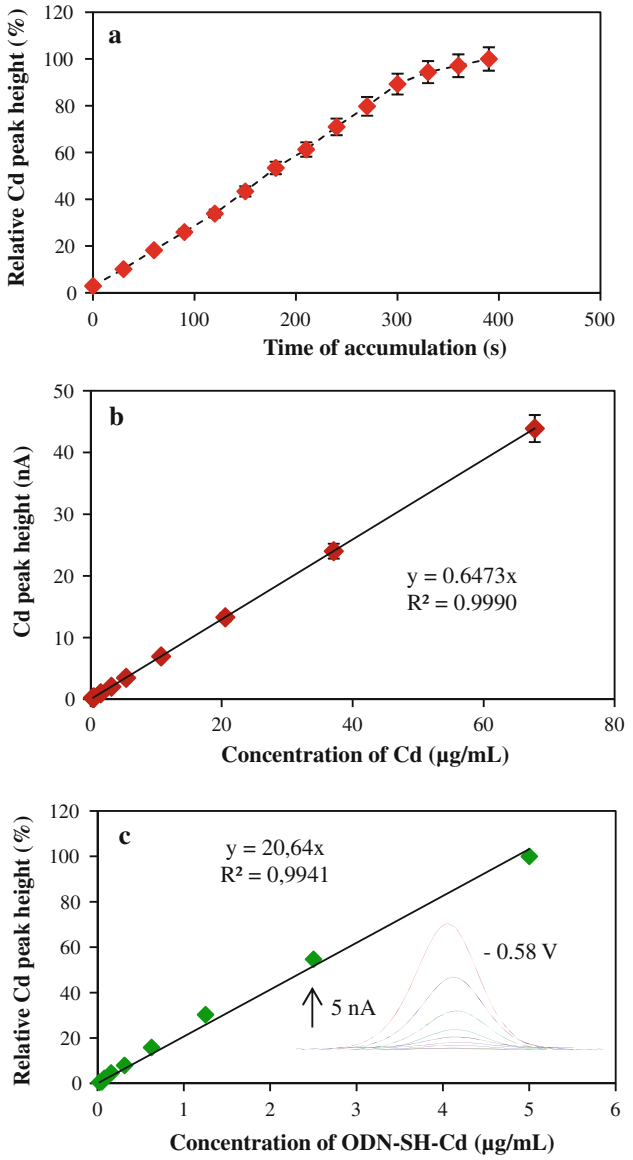

Fig. 3 **a** Optimization of time of accumulation for Cd(II) determination by DPV with parameters as follows: initial potential −0.9 V; end potential −0.45 V; deposition potential −0.9 V; duration 240 s; equilibration time 5 s; modulation time 0.06; time interval 0.2 s; potential step 0.002 V; and modulation amplitude 0.025. **b** Obtained calibration curve for Cd(II) ions. **c** Cadmium was determined in ODN-SH-Cd complex too. Dependence of cadmium signal (*peak height*) on concentration of complex is presented

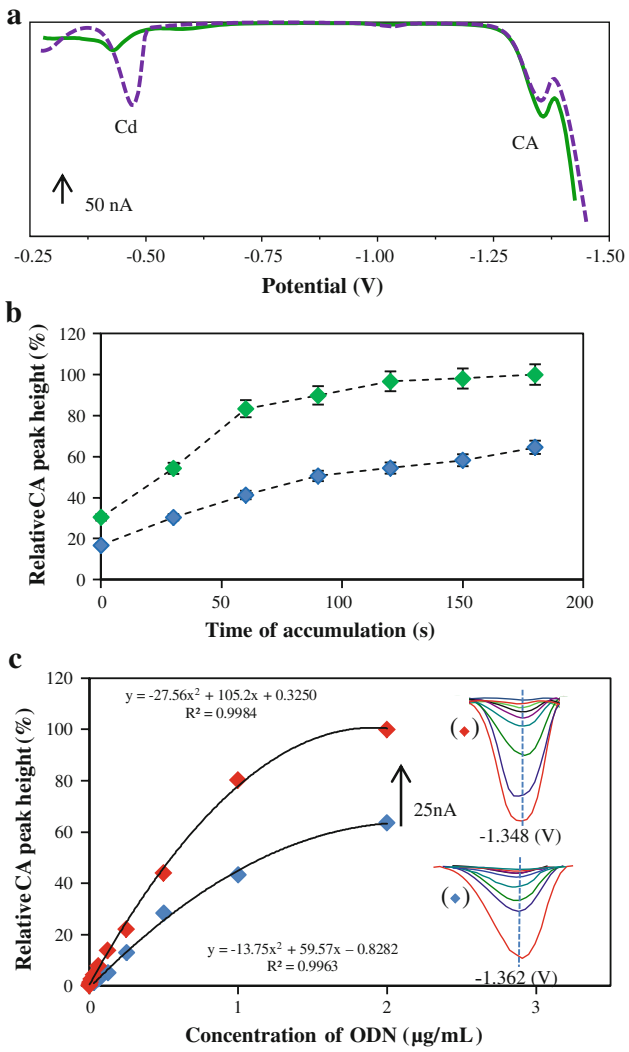

Fig. 4 **a** Comparison of typical SW voltammograms of ODN-SH (*full line*) and ODN-SH-Cd (*dotted line*). **b** Dependence of CA peaks of ODN-SH (*green diamonds*) and ODN-SH-Cd (*blue diamonds*) on accumulation time. **c** *Calibration curves* CA peaks of (*red diamonds*) ODN-SH and (*blue diamonds*) ODN-SH-Cd. Start concentration of both ODNs was 2 µg mL^{-1}. CA peak was measured by SWV

(Fig. 4b). Dependences of CA peak height on both labelled and non-labelled ODN concentrations are shown in Fig. 4c. It is shown that the both dependences have polynomial calibration equations. For ODN-SH, the equation was $y = -27.56x^2 + 105.2x + 0.3250$; $R^2 = 0.9984$, $n = 5$, RSD = 3.2 and for ODN-SH-Cd $y = -13.75x^2 + 59.57x - 0.8282$; $R^2 = 0.9963$, $n = 5$, RSD = 2.9. The detection limits (3 S/N) were estimated as 15 ng mL^{-1} of ODN-SH-Cd and 30 ng mL^{-1} of ODN-SH.

Optimization of Separation Process: Hybridizations

Paramagnetic particles (MPs) are able to respond to external magnetic field, which is used for efficient separation of different analytes from liquid samples. Isolation of biomolecules using MPs is usually followed by electrochemical detection. This way of isolation and detection is less time-consuming and it is highly sensitive to even small quantities of sample [28, 41]. In order to study using MPs as a tool for hybridization assays we designed a MP- and QD-based hybridization assay for the detection of avian influenza H5N1, respectively H5N1-derived oligonucleotide. Figure 1 shows a schematic view of the hybridization procedure for isolation and detection of target (ODN-SH-Cd). The separation procedure contains from four items arranged in the following order: (i) polyA-modified oligo probes (oligo anti-sense) bind on the surface of polyT MPs due to specific TA capturing, (ii) Cd QDs labelling target oligonucleotide, (iii) capturing of target QDs labelled oligonucleotide derived from an influenza sequence, and (iv) electrochemical detection of metal part of QDs marker by DPV. Electrochemical detection of influenza H5N1-derived oligonucleotide using SWV was connected too.

Based on the above mentioned results it can be concluded that CdS QDs can be used for detection of specific ODNs labelled with CdS QDs. Therefore, we were interested in the issue how we can affect the optimize isolation process. We aimed our attention to second hybridization, where the binding of target molecule on the modified MPs takes place. The hybridization process is influenced by wide range of hybridization conditions such as temperature, time, mixing, pH and composition of hybridization buffer. For the first step we aimed our attention to the temperature of hybridization process. The hybridization process was repeated four times under these temperatures of 15, 20, 25 and 30 °C. At the end of hybridization process, peaks of ODN (CA peak) and signals of Cd(II) ions (Cd peak) were determined. Measured peak height was recalculated with respect to the amount of ODN-SH-Cd molecules for both determined signals (Fig. 5a, b). It is evident that increasing temperature enhanced effectiveness of hybridization and thus CA and Cd peak heights. The most effective hybridization was carried out under 25 °C. This temperature is more effective than 30 °C, because T_m of influenza-derived oligonucleotide is 28 °C.

Second hybridization parameter, which was optimized, was time of hybridization. The obtained results show that peak heights of ODN and Cd(II) enhanced with the increasing time of hybridization (Fig. 6a). Response of Cd signal increased linearly within the range from 5 to 35 min as it follows $y = 1.970x + 31.23$; $R^2 = 0.9991$, $n = 3$, RSD = 4.8. In contrast, the ODN signal (CA peak) was changed quadratically as it follows $y = 0.1266x^2 - 1.945x + 11.52$; $R^2 = 0.9926$, $n = 3$, RSD = 5.1.

The third changing condition of hybridization process was concentration of ODN-SH-Cd complex. The concentration was changed within the interval from 2.5 to 20 μg mL^{-1} and both CA and Cd peaks were determined (Fig. 6b). As for previous parameters, the concentration of ODN-SH-Cd complex influenced measured peaks in the same way. Response of Cd peak increased linearly as it follows $y = 2.202x + 56.61$; $R^2 = 0.9958$, $n = 3$, RSD = 3.8, and ODN peak quadratically as it follows $y = -0.2013x^2 + 7.412x + 32.04$; $R^2 = 0.9838$, $n = 3$, RSD = 5.6 with the increasing concentration of ODN-SH-Cd

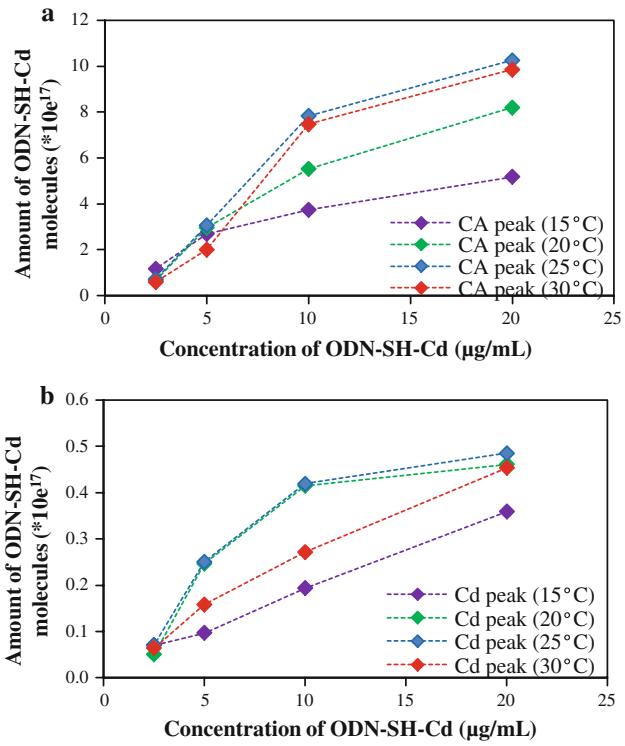

Fig. 5 **a** Detected amount of ODN-SH-Cd molecules ($\times 10e^{17}$) as a function of start concentration of ODN-SH-Cd (μg mL^{-1}) after separation process referenced for CA peak. **b** Amount of ODN-SH-Cd molecules ($\times 10e^{17}$) as a function of start concentration of ODN-SH-Cd (μg mL^{-1}) referenced for Cd peak. CA peak was measured by SWV and Cd peak by DPV. First hybridization step was carried out for 30 min at 25 °C

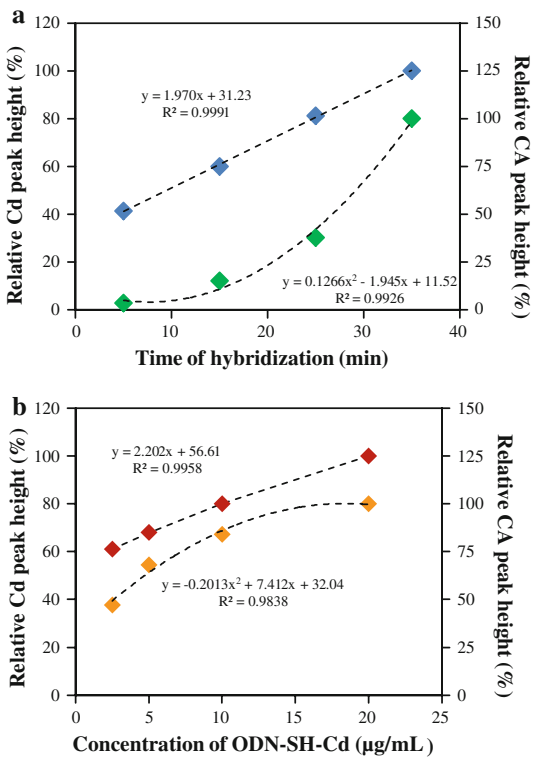

Fig. 6 **a** Change of relative peak height (relate to maximum value of CA and Cd peak) with the increasing of time of second hybridization (5, 15, 25 and 35 min). (*Green diamonds*) Change of CA peak (determined by SWV) and (*blue diamonds*) of Cd peak (determined by DPV). **b** Dependence of relative peak height (relate to maximum value of CA and Cd peak) on concentration of ODN-SH-Cd complex (2.5, 5, 10 and 20 µg mL^{-1}) at 25 °C. (*Orange diamonds*) Change of CA peak (determined by SWV) and (*red diamonds*) of Cd peak (determined by DPV)

complex. It clearly follows from the obtained results that the optimized conditions were temperature of hybridization 25 °C, time of hybridization 35 min and concentration of ODN-SH-Cd complex 20 µg mL^{-1}. Under these conditions, we can obtain the best efficiency in isolation and detection of influenza oligonucleotide.

The obtained results show that suggested method of isolation and detection of Cd labelled influenza-derived oligonucleotide is functional and provide electrochemically measurable signal of target molecule. Cd peak gives us the information about successful hybridization process, and ODN peak relates with the presence of ODNs in solution after hybridization process. The number of molecules determined from CA peak is approximately ten times higher than the number from Cd peak. This effect might be explained from breakage of creating complex after second hybridization in the other place that we assumed. Based on our previously published articles, the breakage of complex can proceed at A-T place [28–30]. We assumed that this situation can be explained from binding of more oligonucleotides to one CdS QD particle. This reasoning is in accordance with studies of Nolan et al. [42] and Ho et al. [43] who reported the use of QDs labelling oligo probes for hybridization with target DNA. Yet another published study is based on DNA-cross-linked CdS nanoparticles array [44] and shows similar effect.

Conclusion

Nowadays, research is directed towards finding methods for simultaneous detection of multiple DNA targets. The electrochemical coding technology is thus expected to open up new opportunities for DNA diagnostics [17, 45]. In this study, an optimized method for automated isolation of Cd-labelled influenza oligonucleotide using automated pipetting station has been proposed. The effects of hybridization temperature, hybridization time, and concentration of ODN-SH-Cd complex on CA and Cd peak height, which were determined electrochemically using SWV and DPV, were also demonstrated. The system proposed in this study can be used as electroanalytical tool for rapid detection of target oligonucleotide based on isolation by probe conjugated MPs.

Acknowledgments Financial support from the projects NANIMEL GA CR 102/08/1546 and CEITEC CZ.1.05/1.1.00/02.0068 is gratefully acknowledged.

References

1. Peiris JSM, Poon LLM, Guan Y (2012) Science 335:1173–1174
2. Osterholm MT, Henderson DA (2012) Science 335:801–802
3. Feng ZL, Towers S, Yang YD (2011) AAPS J 13:427–437
4. Ghendon Y (1994) Eur J Epidemiol 10:451–453
5. Fouchier RAM, Herfst S, Osterhaus A (2012) Science 335:662–663
6. Karlas A, Machuy N, Shin Y, Pleissner KP, Artarini A, Heuer D, Becker D, Khalil H, Ogilvie LA, Hess S, Maurer AP, Muller E, Wolff T, Rudel T, Meyer TF (2010) Nature 463:818–822
7. Elghanian R, Storhoff JJ, Mucic RC, Letsinger RL, Mirkin CA (1997) Science 277:1078–1081
8. Katz E, Willner I (2004) Angew Chem Int Ed 43:6042–6108
9. Hsing IM, Xu Y, Zhao WT (2007) Electroanalysis 19:755–768
10. Drbohlavova J, Hrdy R, Adam V, Kizek R, Schneeweiss O, Hubalek J (2009) Sensors 9:2352–2362
11. Pumera M (2011) Chem Commun 47:5671–5680
12. Ahmed ARH, Olivier GWJ, Adams G, Erskine ME, Kinsman RG, Branch SK, Moss SH, Notarianni LJ, Pouton CW (1992) Biochem J 286:377–382
13. Ossendorp FA, Bruning PF, Vandenbrink JAM, Deboer M (1989) J Immunol Methods 120:191–200
14. Xu HX, Sha MY, Wong EY, Uphoff J, Xu YH, Treadway JA, Truong A, O Brien E, Asquith S, Stubbins M, Spurr NK, Lai EH, Mahoney W (2003) Nucleic Acids Res 31:e43
15. Lim SH, Bestvater F, Buchy P, Mardy S, Yu ADC (2009) Sensors 9:5590–5599
16. Hicks JM (1984) Hum Pathol 15:112–116

17. Wang J, Liu GD, Merkoci A (2003) J Am Chem Soc 125:3214–3215
18. Cao YWC, Jin RC, Mirkin CA (2002) Science 297:1536–1540
19. Taton TA, Mirkin CA, Letsinger RL (2000) Science 289:1757–1760
20. Nicewarner-Pena SR, Freeman RG, Reiss BD, He L, Pena DJ, Walton ID, Cromer R, Keating CD, Natan MJ (2001) Science 294:137–141
21. Bakalova R, Zhelev Z, Ohba H, Baba Y (2005) J Am Chem Soc 127:11328–11335
22. Agrawal A, Sathe T, Nie SM (2007) J Agric Food Chem 55:3778–3782
23. Peterson AW, Heaton RJ, Georgiadis RM (2001) Nucleic Acids Res 29:5163–5168
24. Steel AB, Levicky RL, Herne TM, Tarlov MJ (2000) Biophys J 79:975–981
25. Ryvolova M, Chomoucka J, Janu L, Drbohlavova J, Adam V, Hubalek J, Kizek R (2011) Electrophoresis 32:1619–1622
26. Krejcova L, Dospivova D, Ryvolova M, Kopel P, Hynek D, Krizkova S, Hubalek J, Adam V, Kizek R (2012) Electrophoresis. doi:10.1002/elps.201200304
27. Li H, Shih WY, Shih WH (2007) Ind Eng Chem Res 46:2013–2019
28. Adam V, Huska D, Hubalek J, Kizek R (2010) Microfluid Nanofluid 8:329–339
29. Huska D, Hubalek J, Adam V, Vajtr D, Horna A, Trnkova L, Havel L, Kizek R (2009) Talanta 79:402–411
30. Janicek Z, Huska D, Trnkova L, Provaznik I, Hubalek J, Kizek R (2010) J Biochem Technol 2:S87–S88
31. Long GL, Winefordner JD (1983) Anal Chem 55:A712–A724
32. Huska D, Adam V, Trnkova L, Kizek R (2009) J Magn Magn Mater 321:1474–1477
33. Ju HX, Zhang XJ, Wang J (2011) In: Nanobiosensing: principles, development and application. Springer, New York, pp 535–567
34. Nam JM, Park SJ, Mirkin CA (2002) J Am Chem Soc 124:3820–3821
35. Nam JM, Thaxton CS, Mirkin CA (2003) Science 301:1884–1886
36. Rosi NL, Mirkin CA (2005) Chem Rev 105:1547–1562
37. Wang J (2009) ACS Nano 3:4–9
38. Huska D, Zitka O, Krystofova O, Adam V, Babula P, Zehnalek J, Bartusek K, Beklova M, Havel L, Kizek R (2010) Int J Electrochem Sci 5:1535–1549
39. Kleckerova A, Sobrova P, Krystofova O, Sochor J, Zitka O, Babula P, Adam V, Docekalova H, Kizek R (2011) Int J Electrochem Sci 6:6011–6031
40. Slinker JD, Muren NB, Renfrew SE, Barton JK (2011) Nat Chem 3:228–233
41. Halfpenny KC, Wright DW (2010) Wiley Interdiscip Rev Nanomed Nanobiotechnol 2:277–290
42. Nolan RL, Cai H, Nolan JP, Goodwin PM (2003) Anal Chem 75:6236–6243
43. Ho YP, Kung MC, Yang S, Wang TH (2005) Nano Lett 5:1693–1697
44. Willner I, Patolsky F, Wasserman J (2001) Angew Chem Int Ed 40:1861–1864
45. Chomoucka J, Drbohlavova J, Masarik M, Ryvolova M, Huska D, Prasek J, Horna A, Trnkova L, Provaznik I, Adam V, Hubalek J, Kizek R (2012) Int J Nanotechnol 9:746–783

5.2.2 Vědecký článek IV

KREJCOVA, L.; HYNEK, D.; KOPEL, P.; RODRIGO, M. A. M.; ADAM, V.; HUBALEK, J.; BABULA, P.; TRNKOVA, L.; KIZEK, R. Development of a Magnetic Electrochemical Bar Code Array for Point Mutation Detection in the H5N1 Neuraminidase Gene.

Viruses-Basel, 2013, roč. 5. č. 7, s. 1719-1739. ISS 1999-4915. IF: 3.279

Podíl autorky Krejčová L.: 75 % textové části práce, 80 % experimentální části práce

Vysoce patogenní ptačí chřipka (HPAI), subtypu H5N1 představuje pro lidstvo hrozbu od roku 1997, kdy byl diagnostikován první smrtelný případ *(Dankar, a kol., 2013)*. Dodnes subtyp H5N1 způsobil ztrátu milionů kusů drůbeže a zapříčinil úmrtí přibližně 650 lidí *(Zhang, a kol., 2014)*. HPAI nemá schopnost šíření z člověka na člověka, z toho důvodu je její šíření v lidské populaci omezené *(Poovorawan, a kol., 2013)*. Chřipkové viry snadno a rychle podléhají mutacím, což sebou přináší dvě rizika. Jednak je to zisk schopnosti přenosu mezi lidmi a jednak je to vznik rezistence vůči ativirotikům, jejichž současně nejvíce používanou skupinou jsou inhibitory neuraminidázy (NAIs). Řada autorů se ve svých pracích zaměřila na vývoj metod pro detekci mutantních forem H5N1 *(Xie, a kol., 2014)*. Analýza genomu, evoluce a fylogenetická analýza poukazují na to, že virus H5N1 vykazuje přítomnost mutací spojovaných s rezistencí jak v genu kódujícím matrixový protein tak neuraminidázu, tedy proteiny pro cílenou léčbu antivirotiky *(Tisdale, 2009, Volz, a kol., 2013, Wolf, a kol., 2006, Yen, a kol., 2013)*. Současné studie se především zaměřují na jednobodovou mutaci H275Y, odpovědnou za rezistenci vůči NAIs *(Pinilla, a kol., 2012, Samson, a kol., 2013, Tong, a kol., 2011)*. Pro navržený experiment byly vybrány tři specifické sekvence H5N1 kódující neuraminidázu, které se vzájemně lišily jednobodovou mutací, jako model pro mutaci H275Y. Předmětem experimentu byl popis hybridizačního testu založeného na automatické izolaci tří specifických chřipkových sekvencí pomocí anti-sense modifkikovaných MPs. Izolovaná cílová molekula byla pro účely elektrochemické analýzy konjugována s QDs (ZnS, PbS a CdS). Pro bare code test byly navrženy tři různé sekvece ve dvou délkách (12 a 28 nukleotidů), lišicí se jednobodouvou mutací, každá sekvence byla značena jiným typem QDs. Cílem experimentu bylo sestavit rychlý „screeningový“ test tvořený krátkými sekvencemi a

senzitivnější test tvořený delšími sekvencemi. Pro obě série cílových sekvencí byla optimalizována teplota hybridizace. Největší výtežnosti izolace bylo dosaženo při teplotě 25 °C (krátké sekvence) a 50 °C (pro dlouhé sekvence). Efetk teploty na výtežnost izolace byl zkoumán i při změně pomerů v zastoupení jednotlivých sekvencí ve vzorku. V této práci jsme popsali současnou detekci tří různých sekvencí, které se lišili bodovými mutacemi, v jednom vzorku. Bare code test (identifikace tří různých specifických sekvencí v jednom vzorku) byl založený na izolaci a elektrochemické detekci třech různých QDs (CdS, PbS a ZnS), které byly použity k označení mutantních forem specifické sekvence kódující gen pro neuraminidázu. Optimalizace teploty hybridizace a úspěšná identifikace tří různých sekvencí v jednom vzorku jsou hlavními úspěchy této práce. Rozpoznání mutace způsobující rezistenci NaiS je totiž nezbytné pro správný výběr antivirotika a úspěšnou léčbu těžkých případů chřipky, a to zejména v případě HPAI.

Viruses **2013**, *5*, 1719-1739; doi:10.3390/v5071719

OPEN ACCESS

viruses

ISSN 1999-4915

www.mdpi.com/journal/viruses

Article

Development of a Magnetic Electrochemical Bar Code Array for Point Mutation Detection in the H5N1 Neuraminidase Gene

Ludmila Krejcova [1], David Hynek [1,2], Pavel Kopel [1,2], Miguel Angel Merlos Rodrigo [1,2], Vojtech Adam [1,2], Jaromir Hubalek [2,3], Petr Babula [2,4], Libuse Trnkova [1,2,5] and Rene Kizek [1,2,*]

1 Department of Chemistry and Biochemistry, Faculty of Agronomy, Mendel University in Brno, Zemedelska 1, Brno CZ-613 00, Czech Republic; E-Mails: lidakrejcova@seznam.cz (L.K.); d.hynek@email.cz (D.H.); paulko@centrum.cz (P.K.); merlos19792003@hotmail.com (M.A.M.R.); vojtech.adam@mendelu.cz (V.A.); libuse@chemi.muni.cz (L.T.)

2 Central European Institute of Technology, Brno University of Technology, Technicka 3058/10, Brno CZ-616 00, Czech Republic; E-Mails: hubalek@feec.vutbr.cz (J.H.); petr_babula@email.cz (P.B.)

3 Department of Microelectronics, Faculty of Electrical Engineering and Communication, Brno University of Technology, Technicka 10, Brno CZ-616 00, Czech Republic

4 Department of Natural Drugs, Faculty of Pharmacy, University of Veterinary and Pharmaceutical Sciences, Palackeho 1-3, Brno CZ-612 42, Czech Republic

5 Department of Chemistry, Faculty of Science, Masaryk University, Kotlarska 2, Brno CZ-611 37, Czech Republic

* Author to whom correspondence should be addressed; E-Mail: kizek@sci.muni.cz; Tel.: +420-545-133-350; Fax: +420-545-212-044.

Received: 17 May 2013; in revised form: 10 June 2013 / Accepted: 1 July 2013 / Published: 15 July 2013

Abstract: Since its first official detection in the Guangdong province of China in 1996, the highly pathogenic avian influenza virus of H5N1 subtype (HPAI H5N1) has reportedly been the cause of outbreaks in birds in more than 60 countries, 24 of which were European. The main issue is still to develop effective antiviral drugs. In this case, single point mutation in the neuraminidase gene, which causes resistance to antiviral drug and is, therefore, subjected to many studies including ours, was observed. In this study, we developed magnetic electrochemical bar code array for detection of single point mutations (mismatches in up to four nucleotides) in H5N1 neuraminidase gene. Paramagnetic particles Dynabeads® with covalently bound oligo $(dT)_{25}$ were used as a tool for isolation

of complementary H5N1 chains (H5N1 Zhejin, China and Aichi). For detection of H5N1 chains, oligonucleotide chains of lengths of 12 (+5 adenine) or 28 (+5 adenine) bp labeled with quantum dots (CdS, ZnS and/or PbS) were used. Individual probes hybridized to target molecules specifically with efficiency higher than 60%. The obtained signals identified mutations present in the sequence. Suggested experimental procedure allows obtaining further information from the redox signals of nucleic acids. Moreover, the used biosensor exhibits sequence specificity and low limits of detection of subnanogram quantities of target nucleic acids.

Keywords: voltammetry; highly pathogenic influenza; antiviral resistance; paramagnetic particles; hybridization; quantum dots; automated separation; electrochemistry

1. Introduction

Highly pathogenic avian influenza A (HPAI), subtype H5N1, represents a threat to the human population [1]. While respiratory symptoms and fever are typical signs of influenza, H5N1 has a high incidence of neurological sequelae in many animal species and sporadically in humans, but it represents a continuous danger of global pandemic associated with high mortality [2,3]. HPAI viruses have caused millions of deaths in domestic poultry, and hundreds of deaths in humans [4]. Circulating of influenza viruses in wild animals poses the risk to human health [5,6]. Humans can be infected also by animal subtypes, such as avian influenza virus H5N1 and H9N2 and swine influenza virus H1N1 and H3N2 [7–9]. The primary risk factor for human infection appears to be direct or indirect exposure to infected live or dead animals or contaminated environments [10]. H5N1 occurs in two distinct pathotypes in bird population, seasonal low pathogenic avian influenza (LPAI), and highly pathogenic avian influenza (HPAI) [11–14]. LPAI may become HPAI to poultry through mutations after introduction from wild birds to poultry, but only two subtypes (H5 and H7) can become HPAI [15–17]. These viruses may result in 100% mortality within a susceptible poultry species [16]. The mechanism of mutation of LPAI to HPAI is based on passage in susceptible animals, typically poultry during several months. New generated HPAI virus has broken out in flocks of poultry as so as in wild birds, and caused devastation with huge economic and ecologic impact [3,18]. HPAI poses risk not only for birds, there were also reported sporadic human infections with low morbidity but high mortality, nearly 60% [19–21].

HPAI is not capable of droplet infection from human to human. For this reason, spread of H5N1 virus in the human population is limited [22]. There is a concern that H5N1 may obtain this ability and become pose a potential pandemic hazard to public health worldwide [23–27]. Influenza viruses can develop resistance to pharmacological mechanism of neuraminidase inhibitors (NAIs) that is based on the loss of binding affinity of these drugs. Antiviral resistance in influenza may not develop entirely during treatment but also sometimes transmit widely to replace susceptible strains in the absence of drug pressure [28]. Recently, different authors showed different methods for determination of mutations in H5N1. Sparse learning method was developed to identify antigenicity-associated sites in highly pathogenic H5N1 influenza virus HA based on immunologic data sets [29]. The analysis of

complete genome sequences, genetic evolution and phylogenetic analyses showed that the sequence analysis of H5N1 influenza virus displayed the drug-resistant mutations in the matrix protein and NA genes [30]. This fact is important for better understanding the prevalence and adaptation of H5N1 influenza viruses in different countries [31,32]. The continuous mutations in NA gene give rise to a great necessity to monitor its sequence for detection of any possibilities to drug resistance in H5N1 [33–36].

The current study was targeted to detect possible mutations in NA gene for both diagnosis and treatment purposes. Neuraminidase inhibitors resistance is based on single-point mutations of neuraminidase gene (H 275 Y) [37,38]. Our choice of three various gene sequences for neuraminidase of H5N1 influenza was based on this assumption. There was chosen sections, in which the sequences differed from each other. This way was considered as a model of point mutation. Further, we report multi-target detection of point mutation in H5N1 NA gene. As a model real sample RNA oligonucleotide (RNA ODN) labeled with CdS was tested. Isolation and detection was carried out under conditions optimized by labeled DNA oligonucleotide. In addition, we described hybridization assay based on automatic isolation by modified paramagnetic particles (MPs). Isolated target molecule labeled by quantum dots (QDs) was detected by electrochemical analysis.

2. Experimental Section

2.1. Chemicals

All used chemicals in ACS purity were purchased from Sigma Aldrich (Sigma-Aldrich, St. Louis, MO 3050 Spruce St., St. Louis, MO 63103, USA) unless noted otherwise. Stock solutions were prepared with ACS water. The pH value was measured using inoLab Level 3 (Wissenschaftlich-Technische Werkstatten GmbH; Weilheim, Germany). Deionized water underwent demineralization by reverse osmosis using Aqua Osmotic 02 (Aqua Osmotic, Tisnov, Czech Republic) and was subsequently purified using Millipore RG (MiliQ water, 18 MΩ, Millipore Corp., Billerica, MA 3050 Spruce St., St. Louis, MO 63103, USA). Deionized water was used for rinsing, washing and buffer preparation.

2.2. Preparation of QDs (CdS, PbS and ZnS)

All chemicals were purchased from Sigma-Aldrich (St. Louis, MO, USA) and used without further purification. CdS quantum dots (QDs) were prepared with a slightly modified method published in [39]. Briefly, cadmium nitrate tetrahydrate $Cd(NO_3)_2 \cdot 4H_2O$ (0.0309 g, 0.1 mM) was dissolved in ACS water (25 mL). 3-mercaptopropionic acid (35 μL, 0.4 mM) was slowly added to stirred solution. Afterwards, pH was adjusted to 9.11 with 1 M ammonia solution (NH_4OH, 1.5 mL). Sodium sulphide nanohydrate $Na_2S \cdot 9H_2O$ (0.0240 g, 0.1 mM) in 23 mL of ACS water was poured into the first solution with vigorous stirring. Obtained yellow solution was stirred for 1 h. ZnS QDs were prepared similarly to CdS QDs; zinc nitrate hexahydrate $Zn(NO_3)_2 \cdot 6H_2O$ (0.0298 g, 0.1 mM) was used in the preparation. Colorless solution was obtained.

PbS QDs were prepared by modified method of Hennequin [40]. Lead acetate trihydrate $Pb(OAc)_2 \cdot 3H_2O$ (0.0379 g, 0.1 mM) was dissolved in ACS water (25 mL). 3-mercaptopropionic acid

(60 µL, 0.69 mM) was slowly added to stirred solution. White precipitate, which disappeared after addition of 3.8 mL of 1 M ammonia solution (pH 9.88), was formed. Sodium sulfide nonahydrate $Na_2S \cdot 9H_2O$ (0.0120 g, 0.05 mM) in 21.2 mL of ACS water was added under vigorous stirring. Color of solution was brown. All QDs solutions were stored in dark at 4 °C prior to use.

2.3. Labeling of Influenzas' Derived DNA and RNA Oligonucleotides with QDs (CdS, PbS and ZnS)

Probes were found in the GenBank database at NCBI ([41], Tables 1,2) and synthesized by Sigma-Aldrich. The number for Zhejiang, China and Aichi ODN were DQ643810, EU263982, and AB684120, respectively. Briefly, ODN-SH (DNA or RNA) (100 µL, 100 $\mu g.mL^{-1}$) was mixed with a solution of NPs (100 µL, 100 $\mu g.mL^{-1}$). This mixture was shaken for 24 h at room temperature (Vortex Genie2, Scientific Industries, 70 Orville Drive, Bohemia, NY, USA). Subsequently, solution was dialyzed against 2000 ML of miliQ water (24 h, 4 °C) using a Millipore membrane filter 0.025 µm VSWP. During dialysis the sample was diluted to 800 µL. Diluted sample was concentrated to the final volume of 500 µL on a centrifuge filter device Amicon Ultra 3k (Millipore, Merck Millipore Headquarters 290 Concord Road, Billerica, MA 01821, USA). Centrifuge 5417R (Eppendorf, Hamburg, Germany) was set to the following parameters: 15 min, 4,500 rpm, 15 °C.

Table 1. Probes and target DNA oligonucleotides derived from influenza gene for neuraminidase.

Probe	Target
Zhejiang 5′ TCTGCATTCCAA AAAAA 3′	Zhejiang 5′ TTGGAATGCAGA (Th) 3′
China 5′ TCTGCATTCCAG AAAAA 3′	China 5′ CT GGAATGCAGA (Th) 3′
Aichi 5′ CCTGCATTCCAT AAAAA 3′	Aichi 5′ ATGGAATGCAGG (Th) 3′
Zhejiang 5′ TCTGCATTCCAAGTGGGAGCATGAGATGAAAAA 3′	Zhejiang 5′ CATCTCATGCTCCCACTTGGAATGCAGA (Th) 3′
China 5′ TCTGCATTCCAGATGGGAGCATGAGATGAAAAA 3′	China 5′ CATCTCATGCTCCCATCTGGAATGCAGA (Th) 3′
Aichi 5′ CCTGCATTCCATATGGGAGCATGAGATAAAAAA 3′	Aichi 5′ TATCTCATGCTCCCATATGGAATGCAGG (Th) 3′

Red highlighted nucleotides represent a point mutation in the gene of H5N1 influenza for neuraminidase.

Table 2. Probes and target RNA oligonucleotides derived from influenza gene for neuraminidase.

Probe	Target
China 5′ UCUGCAUUCCAG AAAAA 3′	China 5′ CU GGAAUGCAGA (Th) 3′
China 5′ UCUGCAUUCCAGAUGGGAGCAUGAGAUGAAAAA 3′	China 5′ CAUCUCAUGCUCCCAUCUGGAAUGCAGA (Th) 3′

2.4. Characterization of ODN-QDs by MALDI-TOF/TOF

The ODN-SH-QDs were characterized using MALDI-TOF/TOF mass spectrometer Bruker Ultraflextreme (Bruker Daltonik GmbH, Bremen, Germany) equipped with a laser operating at wavelength of 355 nm with an accelerating voltage of 25 kV, cooled with nitrogen and a maximum energy of 50.4 µJ with repetition rate 2,000 Hz in reflector and positive mode, and with software for data acquisition and processing of mass spectra flexControl and flexAnalysis Version 3.4. 3-hydroxypicolinic acid (3-HPA) was used as a matrix. The matrix 3-HPA was dissolved in ACS water to the concentration of 25 $mg.mL^{-1}$ and 10 $mg.mL^{-1}$ diammonium citrate (DAC) was added. Mixture was thoroughly vortexed for 2 min at room temperature. Working standard solutions were prepared daily by dilution of the stock solutions. The samples were prepared by dissolving with ACS

water. 1 μL of matrix was applied on the anchorchip target plate (Bruker) and dried under atmospheric pressure and room temperature. 1 μL oligo sample at a concentration of 40 $\mu g.mL^{-1}$ was applied on top of this thin layer and dried under atmospheric pressure and room temperature. A mixture of oligo calibrations standard (15-mer, 20-mer and 25-mer) was used for calibration of the instrument.

2.5. Automatic Isolation of ODN-QDs

Automatic pipetting station EP Motion 5075 (Eppendorf, Germany) with original devices (microplate holder, tips holder, tips (1,000, 300, 50 μL), rack tubes, reservoir holder, container for used tips, thermo adapter, PCR plate 96, magnetic adapter) was used for the fully automated target nucleic acids isolation process (Figure 1). Volume of 10 μL of Dynabeads® Oligo $(dT)_{25}$ (Invitrogen, Oslo) was dispensed in selected wells in the plate (PCR 96, Eppendorf, Germany). Plate was subsequently transferred to the magnet and MPs storing solution was aspirated to waste. Subsequently, beads were further washed three times with 20 μL of phosphate buffer I (pH 6.5, 0.1 M NaCl + 0.05 M Na_2HPO_4 + 0.05 M NaH_2PO_4). The first hybridization was the next step. 10 μL of polyA-modified anti-sense oligonucleotides and 10 μL of hybridization buffer (0.1 M phosphate buffer, 0.6 M guanidinium thiocynate, 0.15 M Tris, pH 7.5) were added in each well and then the plate was incubated (15 min, 25 °C, mixing). This procedure was followed by a washing (three times) with 20 μL of phosphate buffer I. The second hybridization was the next step. 10 μL of QDs-labeled oligonucleotide and 10 μL of hybridization buffer (0.1 M phosphate buffer, 0.6 M guanidinium thiocynate, 0.15 M Tris, pH = 7.5) were added to selected wells and the plate was incubated (15 min, 25 °C, mixing). This procedure was followed by washing (three times) with 20 μL of phosphate buffer I. Then, 30 μL of elution solution (phosphate buffer II 0.2 M NaCl + 0.1 M Na_2HPO_4 + 0.1 M NaH_2PO_4) was added into selected wells and plate was subsequently incubated (5 min, 85 °C, mixing). After the elution step, the plate was transferred to the magnet, and the product from selected wells was transferred to separate wells after 120 s of elution step. This isolation assay was described previously [42–45].

2.6. Electrochemical Method for Detection of CA and Metal Peak of ODN-QDs

Electrochemical analyses were performed using a 663 VA Stand (Metrohm, Herisau, Switzerland) and a standard cell with three electrodes. It was equipped with a standard cell consisting of three electrodes, a cooled sample holder and a measurement cell set at 4 °C (Julabo F25, JulaboDE, Seelbach, Germany). The three-electrode system consisted of a hanging mercury drop electrode (HMDE) with a drop area of 0.4 mm^2 as the working electrode, a Ag/AgCl/3M KCl reference electrode and a platinum electrode acting as the auxiliary. VA Database 2.2 by Metrohm was used for data acquisition and subsequent analysis. Acetate buffer (0.2 M CH_3COOH + 0.2 M CH_3COONa, pH 5.0) was used as a background electrolyte. Measurements were carried out at room temperature. The analyzed samples were deoxygenated prior to measurements by purging with argon (99.999%) saturated with water for 120 s. GPES 4.9 software was employed for data processing.

Cytosine-adenine reduction (CA peak) was detected by square wave voltammetry coupled with adsorptive transfer technique (AdTS SWV) [45–50]. The parameters of the electrochemical determination were as it follows: initial potential 0 V; end potential –1.85 V; frequency 80 Hz; potential step 0.005 V; amplitude 0.025 V. Time of accumulation was optimized.

Figure 1. Scheme of fully automated paramagnetic particles (MPs)-based isolation followed by electrochemical detection of target ODN labeled with QDs. As a target, three different ODNs derived from point-mutated neuraminidase gene of influenza H5N1 were used. (**i**) Covalent binding between oligo $(dT)_{25}$ and anti-sense sequence of different H5N1-derived ODNs; (**ii**) Target influenza ODNs labeled with QDs (China ODN with CdS, Aichi with PbS and Zhejiang with ZnS); (**iii**) Hybridization between anti-sense sequence bound to MPs and target sequence labeled with QDs; (**iv**) Isolation of target sequence ODN-QDs and elution from MPs (elution temperature 85 °C); (**v**) Electrochemical detection of ODN-QDs complex, ODN (CA peak) was measured by adsorptive transfer technique coupled with square wave voltammetry (AdTS SWV) and metal part of QDs (Cd, Pb and Zn peak) was measured by differential pulse anodic stripping voltammetry (DPASV).

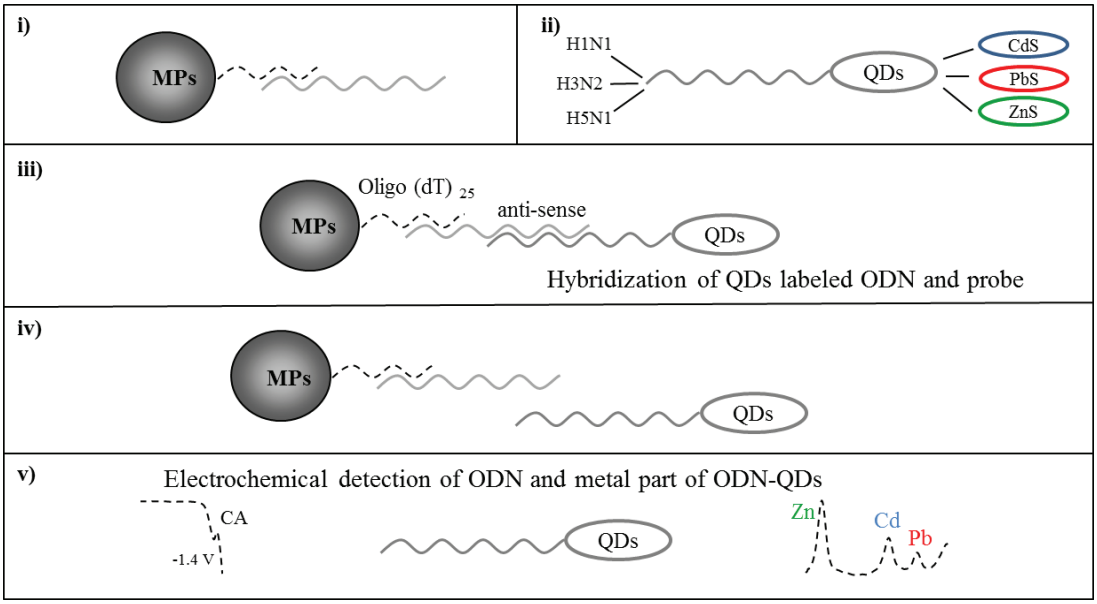

Metal part of the ODN-QDs complex was detected by differential pulse anodic stripping voltammetry (DPASV). In this case the parameters of electrochemical determination were as it follows: Cd (initial potential –0.9 V; end potential –0.45 V, deposition potential –0.9 V); Zn (initial potential –1.2 V; end potential –0.85 V, deposition potential –1.2 V); Pb (initial potential –0.6 V; end potential –0.25 V, deposition potential –0.6 V); others parameters were same: equilibration time 5 s; modulation time 0.06; time interval 0.2 s; potential step 0.002 V; modulation amplitude 0.025. Time of accumulation was optimized.

2.7. Descriptive Statistics

Data were processed using MICROSOFT EXCELs (USA) and STATISTICA.CZ Version 8.0 (Czech Republic). The results are expressed as mean ±SD unless noted otherwise. Statistical significances of the differences were determined using STATISTICA.CZ. Differences with $p < 0.05$ were considered significant and were determined by using of one way ANOVA test (particularly Scheffe test), which was applied for means comparison.

3. Results and Discussion

Detection of a specific nucleic acid (NA) sequence is one of the most important markers of clinical medicine. Knowledge of a specific sequence of nucleic acid may be applied in modern therapeutic approaches [51,52]. Based on these facts, it is clear that there is a plenty of methods that have been suggested for NA analysis. Electrochemical methods are especially important due to low costs, rapidity, simplicity, and especially selectivity for specific NA sequences. Our system of isolation and detection requires less than one hour for one sample determination. Due this fact it is obvious that it is very quick way of determination opposite the other methods. Nanoparticles-based electrochemical NA analysis represents an important tool in the detection of specific NA sequences [53]. In addition, using nanoparticles provides us the possibility to use not only electrochemistry but also spectrometry. Moreover, nanoparticles have found application as oligonucleotide labels for electrochemical detection of viruses. Sun *et al.* used lead sulfide (PbS) nanoparticles as oligonucleotide labels for electrochemical detection of the 35 S promoter from cauliflower mosaic virus (CaMV) sequence [54]. Quantum dots (QDs)-labeled RNA oligonucleotide was used by Roh *et al.* for detection of hepatitis C virus nonstructural protein 5B (NS5B) [55]. In this study, magnetic particles with covalently boundoligooligo$(dT)_{25}$ were used as a tool for isolation of complementary H5N1 chains (H5N1 Zhejin, China and Aichi, Figure 1). For detection of the isolated H5N1 chains, we used oligonucleotide chains of lengths of 12 (+5 adenine) or 28 (+5 adenine) bp labeled with quantum dots (CdS, ZnS and/or PbS, Figure 1). The scheme of the isolation and detection is shown in Figure 1.

3.1. Characterization of DNA Oligonucleotide Labeled with QDs (CdS, PbS and ZnS) by MALDI-TOF/TOF

MALDI-TOF/TOF was used to characterize mass spectra of ODN-QDs in 3-hydroxypicolinic acid (3-HPA) and diammonium citrate as a matrix for testing the binding of H5N1 neuraminidase gene with quantum dots (CdS, ZnS and/or PbS). The spectra of each labeled ODN with different QDs are shown in Figure 2. The signals shown in Figure 2 were assigned as follows: (A) $[ODN]^+$ of m/z 3,938.7 corresponding to unlabeled and $[ODN/CdS]^+$ of m/z 4,050.8 corresponding to labeled complex with CdS in China H5N1 neuraminidase gene, (B) $[ODN]^+$ of m/z 3,993.1 corresponding to unlabeled and $[ODN/PbS]^+$ of m/z 4,200.1 corresponding to labeled complex with PbS in Aichi H5N1 neuraminidase gene and (C) $[ODN]^+$ of m/z 3,864.2 corresponding to unlabeled and $[ODN/ZnS]^+$ of m/z 3,954.3 corresponding to labeled with ZnS in Zhejiang H5N1 neuraminidase gene. It is evident that the suggested labeling of different ODNs with QDs was carried out correctly, as it is shown in Figure 1.

3.2. Scheme of Fully Automated MPs Isolation Followed by Electrochemical Detection of Target ODN Labeled with QDs

Nanoparticles have found their application in the rapid and simple isolation of nucleic acids from various biological matrixes. Magnetic nanoparticles represent an especially important improvement in these techniques due to very easy manipulation [56,57]. However, data about application of NPs in isolation of viral nucleic acid are very limited. Anti-sense oligonucleotides specific for conserved region of AIV PA protein of H5N1 avian influenza virus were used by Zhang *et al.* [58]. Nevertheless,

the authors focused on the antiviral properties of these anti-sense oligonucleotides. In this study, we designed the protocol for multi-target isolation and detection of ODNs molecules (derived from neuraminidase gene of influenza H5N1) labeled with QDs. The first step consisted of hybridization (covalent binding) of the complementary anti-sense sequence modified with the polyA sequence on MPs modified with the polyT sequence (Figure 1i). This step was followed by influenza ODNs labeling with QDs. China ODNs (short and long) was labeled with CdS, Aichi with PbS and Zhejiang with ZnS (Figure 1ii) Hybridization between anti-sense and target ODN-QDs was the most important step (Figure 1iii). This step was the subject of study of effects of hybridization temperature and length of target ODN(s)-QDs on the hybridization, respectively the yield of isolated molecules. ODN-QDs elution was the last step of the isolation (temperature 85 °C, Figure 1iv). The isolation process was followed by electrochemical detection of ODN-QDs complex. Two voltammetry methods were used. ODN (CA peak) was determined by square wave voltammetry coupled with the adsorptive transfer technique (AdTS SWV) and metal peak (Cd, Pb and Zn) was determined by differential pulse anodic stripping voltammetry (DPASV), as it is shown in Figure 1v. Time of accumulation (t_A) of both methods was optimized.

Figure 2. MALDI-TOF/TOF mass spectra of oligonucleotide (ODN) derived from H5N1 gene for neuraminidase labeled with QDs (CdS, PbS and ZnS). (**A**) Spectra of ODN and ODN labeled with CdS in China H5N1 sequence; (**B**) spectra of ODN and ODN labeled with PbS in Aichi H5N1 sequence; and (**C**) spectra of ODN and ODN labeled with ZnS in Zhejiang H5N1 influenza virus. 3-hydroxypicolinic acid (3-HPA) and diammonium citrate were used as matrix.

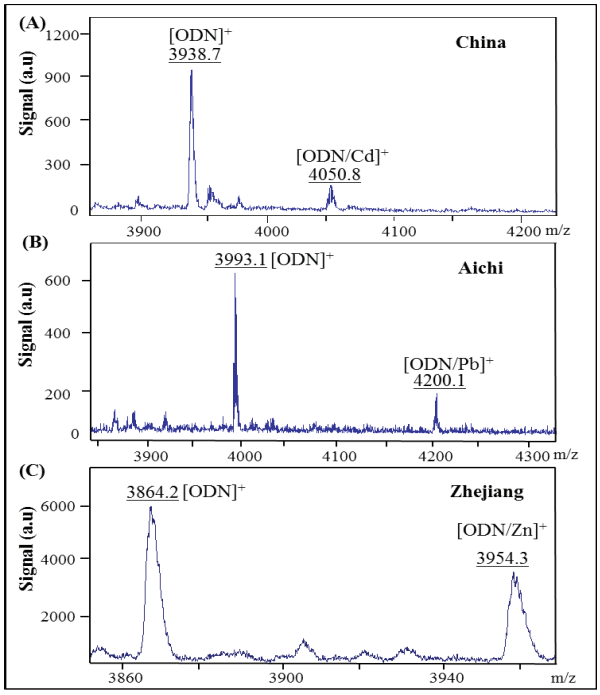

3.3. Optimization of AdTS SWV and DPASV Method

Time of accumulation (t_A) was optimized for detection of lead(II), cadmium(II) and zinc(II) ions using DPASV (Figure 3A–C, respectively). Different accumulation times (30, 60, 120, 240, 360, 480

and 600 s) were tested. Height of metal peak of ODN-QDs increased linearly up to 600 s, but the time of accumulation of 300 s was selected due to the time consuming measurements at t_A longer than 300 s. Time of accumulation (t_A) was optimized also in the case of CA peak detection in various ODN-QDs complexes formed from Pb, Cd and Zn (Figure 3D–F, respectively). Tested time intervals were 0, 30, 60, 90, 120, 180 and 240 s. Time of accumulation 120 s was chosen as an optimal t_A as the highest peak at the lowest time of accumulation.

Figure 3. Optimization of electrochemical determination. The influence of time of accumulation on the heights of metal and CA peaks. (**A**–**C**) Dependence of relative height of metal peak (%) on the time of accumulation of ODN(s) labeled with QDs; (**D**–**E**) Dependence of relative height of CA peak (%) on the time of accumulation of ODN(s) labeled by QDs. In the optimization step, these ODN(s) labeled with QDs were used: (**A**+**D**) Aichi (Ai) was labeled with PbS (Ai 1 is short ODN–12 nucleotides, Ai 2 is long ODN–28 nucleotides), (**B**+**E**) China (Ch) was labeled with CdS (Ch 1 is short ODN–12 nucleotides, Ch 2 is long ODN–28 nucleotides), (**C**+**D**) Zhejiang (Zh) was labeled with ZnS (Zh 1 is short ODN–12 nucleotides, Zh 2 is long ODN–28 nucleotides). DPASV was used to determine metal, parameters were as it follows: initial potential –1.2 V (Zn), –0.8 V (Cd), –0.65 V (Pb); end potential –0.9 V (Zn), –0.5 V (Cd), –0.3 V (Pb), deposition potential –1.2 V (Zn), –0.8 V (Cd), –0.65 V (Pb); equilibration time 5 s; modulation time 0.06 s; time interval 0.2 s; potential step 0.002 V; modulation amplitude 0.025 V. Optimized parameter was time of accumulation (a → h): a 30 s, b 60 s, c 120 s, d 240 s, e 360 s, f 480 s, g 600 s, h 700 s. AdTS SWV method was used to determine CA peak, parameters were as it follows: purge time 60 s, initial potential –1.85 V; end potential 0 V; frequency 100 Hz; potential step 0.005 V; amplitude 0.025 V. Optimized parameter was time of accumulation (a → g): a 0 s, b 30 s, c 60 s, d 90 s, e 120 s, f 180 s, g 240 s.

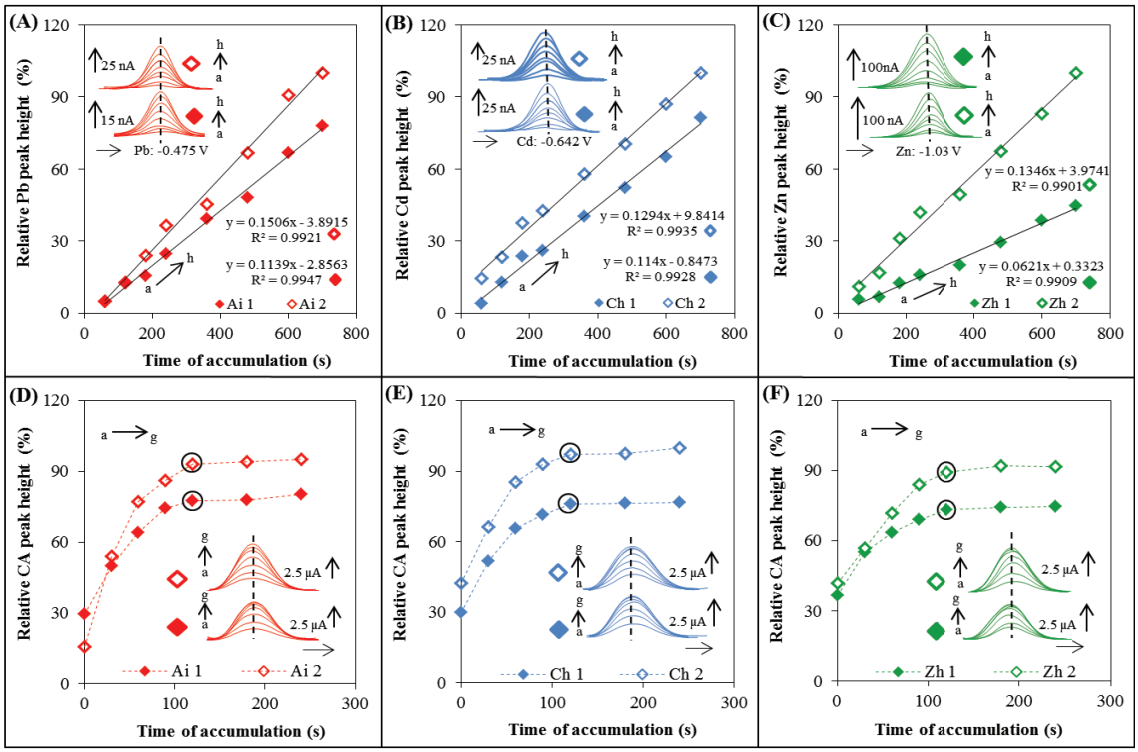

Calibration of the metal peak (Pb, Cd and Zn) in ODN-QDs using DPASV was carried out and it is shown in Figure 4A–C, respectively. Ai ODN labeled with PbS demonstrated the highest coefficient of reliability followed with Zn and Cd. Further, we aimed at calibration of CA peak measured by AdTS SWV. CA peak was measured in various ODN-QDs complexes formed from Pb, Cd and Zn (Figure 4D–F, respectively). The highest coefficient of reliability was demonstrated by Zh ODN labeled with ZnS.

Figure 4. Calibration curves of metal and CA peaks. (**A**–**C**) Dependences of height of metal peak (nA) on concentration of ODN-QDs (μg/mL): (**A**) ODN Ai 1+2 (labeled with PbS), (**B**) Ch 1+2 (labeled with CdS), (**B**) Zh 1+2 (labeled with ZnS). Ai 1, Ch 1 and Zh 1 are 12 nucleotides long sequences labeled with QDs, Ai 2, Ch 2 and Zh 2 are 28 nucleotides long sequences labeled with QDs. To measure metal(s) in QDs, DPASV method was used (parameters are in caption in Figure 3); (**D**–**F**) Dependences of height of CA peak (nA) on concentration of ODN-QDs (μg/mL): (**D**) ODN Ai 1+2 (labeled with PbS), (**E**) Ch 1+2 (labeled with CdS), (**F**) Zh 1+2 (labeled with ZnS). AdTS SWV method was used for measurements (parameters are in caption in Figure 3).

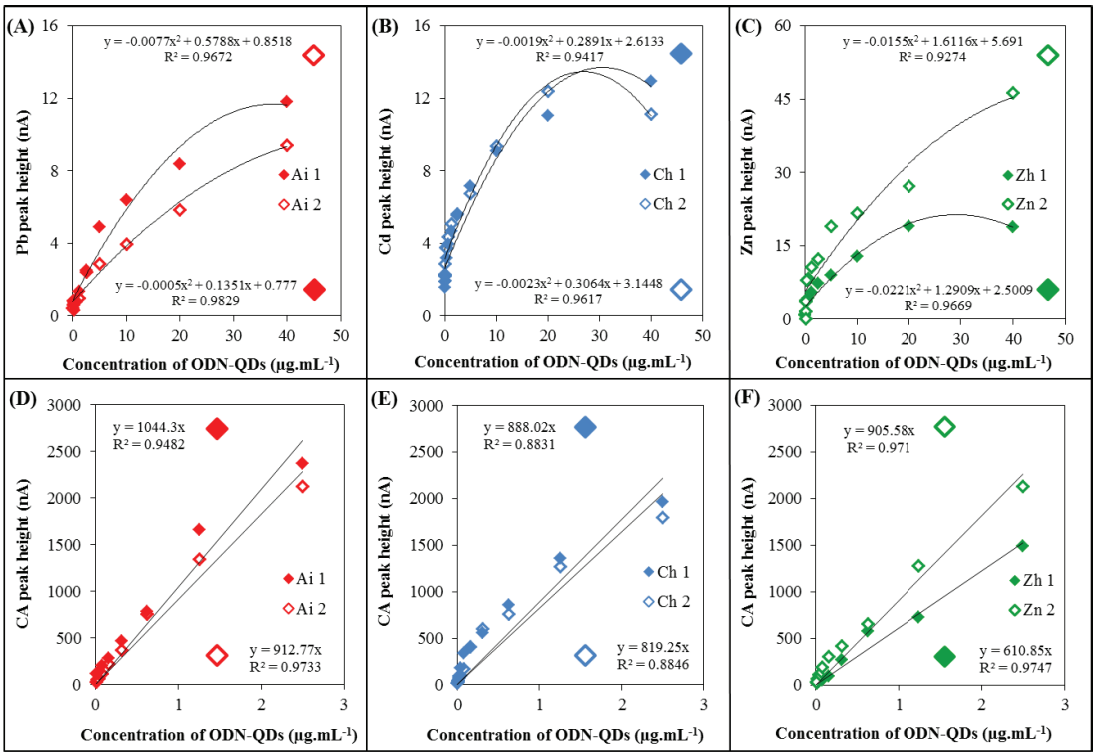

3.4. Hybridization Experiments–Influence of Different Hybridization Condition of Hybridization Efficiency

3.4.1. Influence of Temperature and Different Length of ODN-QDs on Hybridization

Firstly, we investigated the effect of length of ODN and temperature of hybridization on an amount of isolated ODN-QDS (effectiveness of hybridization) in accordance with the scheme introduced in Figure 5A,D, where hybridization of short (12 nucleotides + 5A tail; Ai 1, Ch 1 a Zh 1) and long (28 nucleotides + 5A tail; Ai 2, Ch 2 a Zh 2) nucleotide sequences is shown, respectively. Double

hybridization represents a substantial part of isolation. The first step was based on the hybridization of anti-sense chain of MPs (oligo $(dT)_{25}$), and the second one consisted in the second hybridization between anti-sense chain and target ODN-QDs molecule (Aichi 1, 2 labeled by PbS; China 1, 2 labeled by CdS a Zhejiang 1, 2 labeled by ZnS).

Figure 5. The effect of different temperatures on hybridization of short and long ODN-QDs derived from H5N1 gene for neuraminidase. (**A**) Short and/or (**D**) long ODN anti-sense (anti-H5N1 Zhejiang, China and Aichi) modified MPs with covalently bound oligo$(dT)_{25}$ were used as a tool for isolation of complementary H5N1 strands (H5N1 Zhejin, China and Aichi) labeled with QDs (CdS, ZnS and/or PbS). (**B**+**C**) The effect of the temperature of hybridization (20, 25 and 30 °C) on number of hybridized molecules of short ODN-QDs abbreviated as Ai 1, Ch 1 and Zh 1; (**B**) Number of H5N1 molecules was calculated from the height of CA peak; (**C**) Number of H5N1 molecules was calculated from the height of metal peak. (**E**+**F**) The effect of the temperature of hybridization (45 °C, 50 °C and 55 °C) on number of hybridized molecules of long ODN-QDs abbreviated as Ai 2, Ch 2 and Zh 2; (**E**) Number of H5N1 molecules was calculated from the height of CA peak; (**F**) Number of H5N1 molecules was calculated from the height of metal peak. AdTS SWV method was used to measure the height of CA peak was used (parameters are in caption in Figure 3). DPASV method was used to measure the height of metal peak (parameters are in caption in Figure 3). Blue color: minimal temperature of hybridization was 20 °C for 12 nucleotides long ODNs and/or 45 °C for 28 nucleotides long ODNs, red color: optimal temperature of hybridization was 25 °C for 12 nucleotides long ODNs and/or 50 °C for 28 nucleotides long ODNs, violet color: minimal temperature of hybridization was 30 °C for 12 nucleotides long ODNs and/or 55 °C for 28 nucleotides long ODNs.

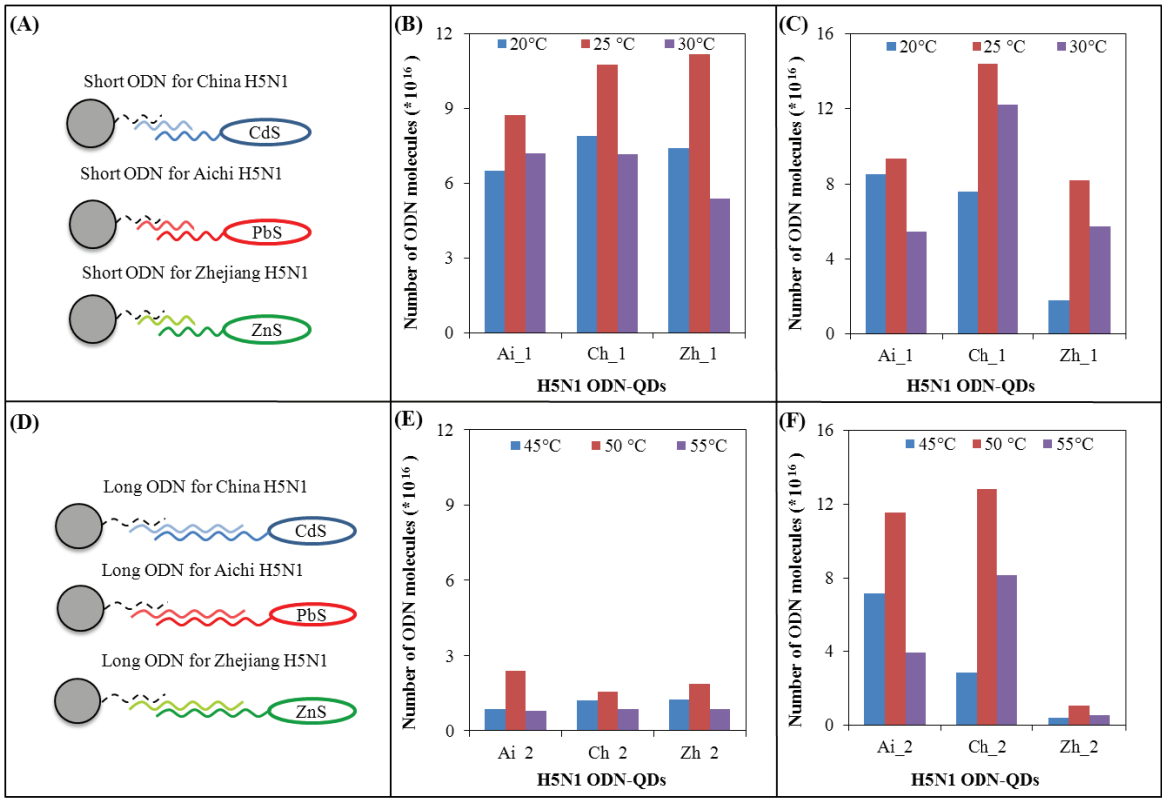

Effectiveness of the hybridization of short nucleotide sequences was monitored at different temperatures: 20 °C, 25 °C and 30 °C. Effectiveness of the hybridization of long nucleotide sequences was monitored at 45 °C, 50 °C and 55 °C. These temperatures were suggested in accordance with a calculation of T_m for given length and sequence of nucleotide. For short nucleotide sequences (12 nucleotides + 5A tail), the Tm value was $T_m = (wA+xT) \times 2 + (yG + zC) \times 4$, for long nucleotide sequences the TM value was $T_m = 64.9 +41 \times (yG + zC-16.4)/(wA + xT + yG + zC)$, where w, x, y, and z are the numbers of the bases A, T, G, and C in the sequence of ODN, respectively. Temperature of hybridization (T_{hyb}) was calculated according to $T_{hyb} = T_m–10$ °C (hybridization temperature specific to the probe is typically 5 °C–10 °C low than T_m). Subsequently, hybridization minimal, optimal and maximal values were suggested. Number of the isolated molecules was determined indirectly according to the height of peak that was measured using DPASV and AdTS SWV. CA peak that corresponds to the signals of cytosine and adenine was measured using AdTS SWV (Figure 5B,E) and metal peak was measured by DPASV (Figure 5C,F).

Effectiveness of the hybridization of short nucleotide sequences. To detect the highest CA and metal peaks, temperature of hybridization of 25 °C was selected as the most suitable for the short nucleotide sequences. Effectiveness of hybridization calculated according to the height of CA peak between three different ODN-QDs (Ai1, Ch1, Zh1) showed no significant differences (Figure 5B). Effectiveness of hybridization calculated according to the height of metal peak showed significant differences at $p < 0.05$ (the most effective Ch1-labeled CdS and the least effective Zh1-labeled ZnS), as it is shown in Figure 5C.

Effectiveness of the hybridization of long nucleotide sequences. According to CA and metal peaks heights, the temperature of hybridization of 50 °C was chosen as the most suitable for the hybridization of long nucleotide sequences. Effectiveness of hybridization calculated according the height of CA peak between three different ODN-QDs (Ai2, Ch2, Zh2) is not comparable to short ODN (Figure 5E). The most effective isolation was determined in the case of Ai 2 (labeled by PbS), on the other hand the least effective in the case of Ch2 and Zh2 that were labeled with CdS (Ch2) and ZnS (Zh2), respectively (Figure 5F). According to the number of the isolated molecules calculated from the height of metal peak, the most effective ODN were Ai2 and Ch2 and the least effective Zh2.

In conclusion, the largest number of short ODN-QDS molecules was isolated at 25 °C and the largest number of long ODN-QDS molecules was isolated at 50 °C. These temperatures were used in the subsequent experiment, where effectiveness of hybridization of mixture of short and long ODN-QDs was investigated.

3.4.2. Effect of Different Lengths of Mixture of Short and Long ODN-QDS on Hybridization

Hybridization of both mixtures was carried out according to the scheme introduced in Figure 6A. This experiment focused on the comparison of effectiveness of hybridization of mixture of ODN-ODs with short and long nucleotide sequences. Calculation of number of isolated molecules was carried out according to formula for Ai 1 (short ODN-QDs) and Ai 2 (long ODN-QDs). Mixtures of ODN-QDs were prepared at different rates of all three components as 1:1:1–the same ratio of oligonucleotides, and 1:2:1 oligonucleotides labeled with CdS were in twofold ratio than that labeled with ZnS and PbS.

This was done due to evaluation of the suggested procedure, because we expected the increase of peaks corresponding to CdS labeled ODNs.

Figure 6. The effect of optimal temperature on hybridization of short, long and mixture of short and long ODN-QDs derived from H5N1 gene for neuraminidase. (**A**) Experimental scheme: bar code array for detection of three different (long and/or short) point-mutated H5N1 neuraminidase gene. (**B**+**C**) The effect of optimal temperature on hybridization (optimal temperature: 25 °C for mixture of short ODN-QDs and 50 °C for mixture of long ODN-QDs) on number of hybridized short ODN-QDs molecules. Two ratios of oligonucleotides (1:1:1–the same ratio of oligonucleotides, 1:2:1 oligonucleotides labeled with CdS were in twofold ratio than ODN labeled with ZnS and PbS; (**B**) The effectiveness of hybridization determined by the height of CA peak. Number of molecules calculated from the height of CA peak (light grey–CA peak of short ODN, dark grey–CA peak of long ODN); (**C**) The effectiveness of hybridization was monitored using the height of Cd, Pb and Zn peaks. Number of molecules calculated from the height of metal peak (light color–metal peak(s) of short ODN, dark color–metal peak(s) of long ODN; (**D**–**F**) The effect of optimal temperature of hybridization (optimal temperature: 25 °C in light color and 50 °C in dark color, mixture of short and long ODN-QDs) on mixture of short and long ODN-QDs (12+28 nucleotides) molecules. Two ratios of oligonucleotides (1:1:1–the same ratio of oligonucleotides, 1:2:1 oligonucleotides labeled with CdS were in twofold ratio than that labeled with ZnS and PbS) were investigated; (**D**) The effectiveness of hybridization determined using the height of CA peak. (**E**+**F**) The number of molecules calculated from the height of metal peak (light color—metal peak of short ODN, dark color–metal peak of long ODN); (**E**) The effectiveness of hybridization was calculated from short ODN-QDs; (**F**) effectiveness of hybridization was calculated from long ODN-QDs.

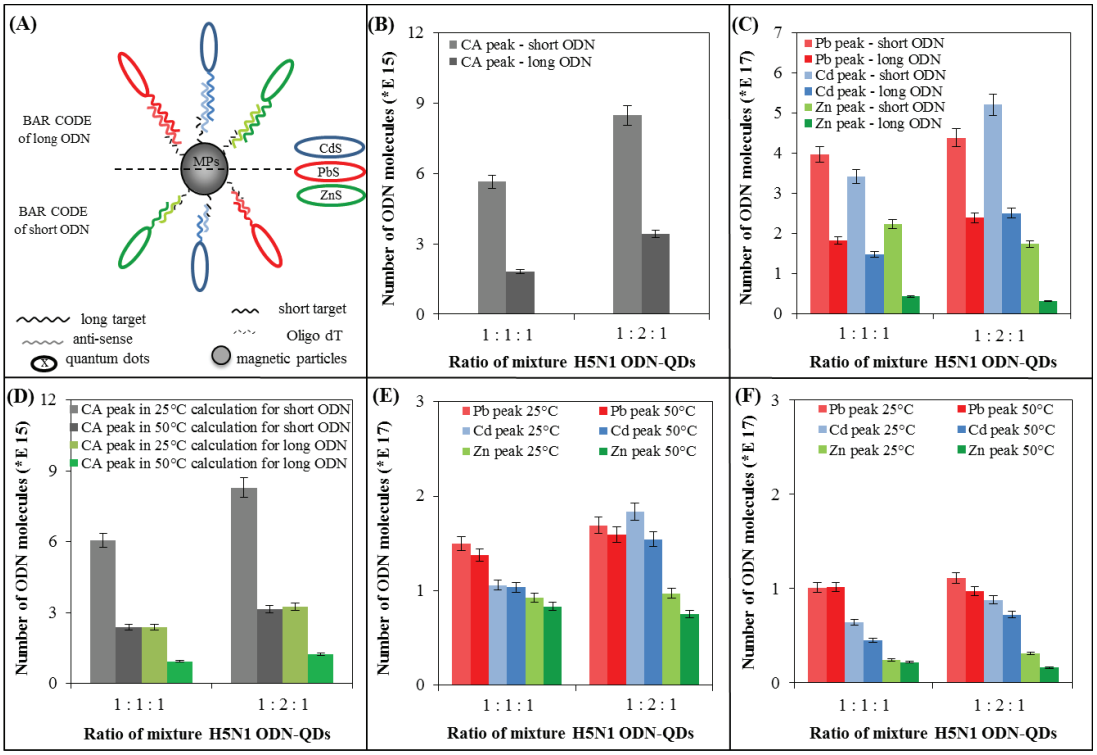

Comparison of results of effectiveness of hybridization of mixture of short and long ODN-QDs is shown in Figure 6B,C. The effect of hybridization was calculated based on the number of the isolated molecules calculated from the height of CA peak (Figure 6B) and from the height of metal peak (Figure 6C), where resulting values of the isolation of mixture of short molecules (lighter color) and mixture of long molecules (darker color) is shown. We monitored the effect of length in the mixture of short and long ODN-QDs as well as different ratios of individual components of ODN-QDs mixture. More effective is hybridization of the mixture of short ODN due to the better and rapid hybridization. In addition, they probably exhibit lower specificity. We proved also the effect of the ratio of different components in ODN-QDs mixture on the hybridization. Ratio 1:2:1 brought larger number of the isolated molecules compared to ratio 1:1:1. Similarly, we monitored the effect of the length of nucleotide sequence and their different ratios on number of the isolated molecules. More effective hybridization (larger number of isolated molecules) is observable for short ODN-QDs.

3.4.3. Influence of Two Optimal Hybridization Temperatures (25 °C and 50 °C) on Efficiency of Hybridization of Mixture of Short and Long ODN-QDs

Figure 6D–F introduces the effect of two temperatures of hybridization (25 °C and 50 °C) on the hybridization of mixture containing all ODN-QDs (Ai1+2, Ch 1+2, Zh 1+2). The number of isolated molecules was calculated from the height of CA peak (Figure 6D) and from the height of metal peak (Figure 6E,F). For the calculating of number of the isolated ODNs, formulas for Ai 1 (Figure 6D, E, grey columns) and for Ai 2 (Figure 6D, F, green columns) were used. Light color columns indicate results of hybridization at 25 °C, dark color columns at 50 °C. We tested two different ratios of mixture of short and long ODN-QDs. Ratio 1:1:1 represents mixture of all short and long ODN-QDs, where individual components occur at the same rate (columns on the left). Ratio 1:2:1 represents mixture of all short and long ODN-QDs, where ODN labeled with CdS (Ch1 and Ch2) occur at double rate compared to that labeled with PbS and ZnS (columns on the right).

Figure 6D shows effectiveness of hybridization (number of isolated molecules) at 25 °C that is larger compared to 50 °C. This is caused by the fact that short ODNs are not able of hybridization at 50 °C, because their T_m is almost for 20 °C lower. On the other hand, long ODN-QDs hybridized only at 50 °C. In conclusion, short sequences were hybridized at 25 °C specifically and long sequences nonspecifically, thus, the yield of the isolated molecules was higher at 25 °C compared to 50 °C. Calculation of number of isolated molecules was carried out according to the formula for short ODN-QDs (Figure 6D, grey columns) or for long ODN-QDs (Figure 6D, green columns). Columns on the right indicate increase in number of the isolated molecules. This fact is based on the increased ratio of ODNs labeled with CdS (Ch1 and Ch2).

Figure 6E shows results of hybridization calculated from the height of metal peak. Formula for Ai 1 was used for the calculation of effectiveness of hybridization. Differences between light and dark columns (hybridization at 25 °C and 50 °C) are not so evident in comparison with those that are shown in Figure 6D, where the yield was calculated from the height of CA peak. At 25 °C both short and long ODNs are hybridized, whereas at 50 °C long ODNs giving smaller signal are hybridized only. Method for detection of individual metals is not influenced by this effect. Significant difference is well evident in the increase in Cd peak in column with the ratio of 1:2:1 ($p < 0.05$).

Figure 6F shows results of hybridization calculated from the height of metal peak. However, the formula for Ai 2 was used for calculation compared to Figure 6E. Differences between light and dark columns (hybridization at 25 °C and 50 °C) are not so evident compared to Figure 6D, where the yield was calculated from the height of CA peak. In addition, the increase in the number of isolated molecules is well evident also in the case of columns calculated from Pb peak at the ratio of 1:1:1. Increase in the Cd peak in column with the ratio of 1:2:1 is well evident compared to ratio of 1:1:1; otherwise the values of isolated molecules between two different ratios are similar.

3.4.4. Isolation and Detection of RNA ODN-QDs

Above mentioned results showed that suggested procedure allowed to distinguish individual point mutations and therefore could be applicable for detecting of the point mutation in real samples. Influenza viruses belong to the RNA viruses group and therefore we were interested in the issue whether we would be able to detect RNA sequence as a model of the real sample using the suggested procedure. The detection of RNA sequences was performed under the optimal conditions (determined for DNA sequences). Application of the same experimental conditions for DNA and RNA sequences is in accordance with numerous published papers [59–70]. The RNA ODN are much more sensitive to external conditions and optimization of detection is usually provided with DNA ODN (DNA analogues), also in the case of RNA pathogens [59–70].

For our purposes, we decided to use two length China RNA ODN-CdS to confirm that the method is applicable to analysis of real sample. In accordance with above experimental design, one short (12 nucleotides) and one long (28 nucleotides) RNA ODN-CdS were tested. The differences between DNA and RNA experimental design were in number of isolated sequences (DNA: three different short and three different long ODN in combination with three different QDs and on the other hand RNA: one short, one long RNA sequence and one QDs type. The RNA ODNs were labeled with CdS quantum dots as in the case of DNA ODNs. The comparison of various detection ways is shown in Figure 7A. This picture shows number of RNA ODN molecules due to the detection via CA and Cd peaks. The comparison for short and long RNA ODNs is presented too. It is evident that the detection of short RNA ODN led to the same results compared to DNA ODNs. Analyzing long RNA ODNs showed various results, because Cd peak gave higher number of target molecules. This is in accordance with the results shown in Figure 5 for DNA ODNs. The changes of detected signals caused by the changing length of ODNs were compared too. The similarity assessment of these between RNA and DNA ODNs is shown in Figure 7B. There is the influence of RNA or DNA ODNs on detected signals quantified. Here is the percentage of signal intensity of the long ODN sequence related to the short ODN sequence detected due to CA and Cd peak. It is obvious that the compared signals reach the similar values with differences to ten percentages.

Presented results also show that the application of RNA ODNs to the suggested procedure brings no issues and behavior of the RNA ODNs and DNA analogues is similar. Due these facts, one may suggest that the optimized procedure is applicable for real sample analysis.

Figure 7. (**A**) The effect of the RNA-ODN length on the number of hybridized molecules. Two long varieties of China RNA ODN sequences were tested due to CA and Cd peak detection. Short RNA ODN sequence was hybridized at 25 °C and long RNA ODN sequence was hybridized at 50 °C; (**B**) Percentage of signal intensity of the long ODN sequence related to the short ODN sequence detected due to CA and Cd peak for RNA and DNA ODN sequence.

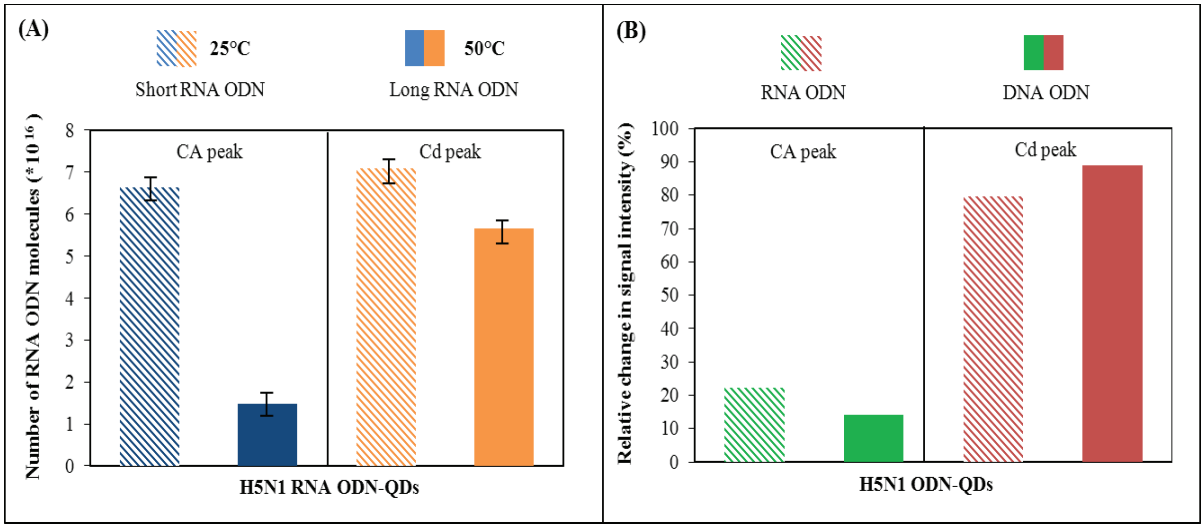

4. Conclusions

Mutations of the influenza virus in combination with the global increasing of the use of anti-influenza specific drugs allows for the selection of antiviral drug-resistant viruses. Therefore, there is imperative to have faster and more sensitive assays for detection of antiviral drug-resistant strains of the influenza virus. New assays are important for the surveillance of HPAI H5N1 and for decisions to use specific antiviral drugs in the treatment of human patients suspected or suffering from H5N1 influenza. In this study, we demonstrate methods for multi-target detection of NAIs-resistant influenza subtypes. This multi target bar code assay is based on the electrochemical analysis of isolated target molecules labeled with QDs. Based on previously published papers [42,43], we designed and optimized hybridization assay for multi-target isolation and detection of influenza H5N1 neuraminidase gene, respectively point-mutated neuraminidase gene. These point mutations are responsible for the resistance to NAIs. Revealing NAIs' resistance is important for targeted and successful treatment of severe human influenza cases, and for preventing the occurrence of severe influenza disease, especially HPAI H5N1.

Acknowledgments

Financial support from NanoBioTECell GA CR P102/11/1068, NanoBioMetalNet CZ.1.07/2.4.00/31.0023 and IGA IP16/2013 is greatly acknowledged.

Conflict of Interest

The authors declare no conflict of interest.

References and Notes

1. Shoham, D. Influenza type A virus: An outstandingly protean pathogen and a potent modular weapon. *Crit. Rev. Microbiol.* **2013**, *39*, 123–138.
2. Plourde, J.R.; Pyles, J.A.; Layton, R.C.; Vaughan, S.E.; Tipper, J.L.; Harrod, K.S. Neurovirulence of H5N1 infection in ferrets is mediated by multifocal replication in distinct permissive neuronal cell regions. *PLoS One* **2012**, *7*, 1–11.
3. Gilbert, M.; Jambal, L.; Karesh, W.B.; Fine, A.; Shiilegdamba, E.; Dulam, P.; Sodnomdarjaa, R.; Ganzorig, K.; Batchuluun, D.; Tseveenmyadag, N.; *et al.* Highly pathogenic avian influenza virus among wild birds in mongolia. *PLoS One* **2012**, *7*, 1–9.
4. Wei, K.F.; Chen, Y.F.; Chen, J.; Wu, L.J.; Xie, D.X. Evolution and adaptation of hemagglutinin gene of human H5N1 influenza virus. *Virus Genes* **2012**, *44*, 450–458.
5. Abdelwhab, E.M.; Hafez, H.M. Insight into alternative approaches for control of avian influenza in poultry, with emphasis on highly pathogenic H5N1. *Viruses* **2012**, *4*, 3179–3208.
6. Zhang, J.F. Advances and future challenges in recombinant adenoviral vectored H5N1 influenza vaccines. *Viruses* **2012**, *4*, 2711–2735.
7. Weinheimer, V.K.; Becher, A.; Tonnies, M.; Holland, G.; Knepper, J.; Bauer, T.T.; Schneider, P.; Neudecker, J.; Ruckert, J.C.; Szymanski, K.; *et al.* Influenza A viruses target type II pneumocytes in the human lung. *J. Infect. Dis.* **2012**, *206*, 1685–1694.
8. Chen, F.; Yan, Z.Q.; Liu, J.; Ji, J.; Chang, S.; Liu, D.; Qin, J.P.; Ma, J.Y.; Bi, Y.Z.; Xie, Q.M. Phylogenetic analysis of hemagglutinin genes of 40 H9N2 subtype avian influenza viruses isolated from poultry in China from 2010 to 2011. *Virus Genes* **2012**, *45*, 69–75.
9. Zhao, J.Q.; Wang, X.; Ragupathy, V.; Zhang, P.H.; Tang, W.; Ye, Z.P.; Eichelberger, M.; Hewlett, I. Rapid detection and differentiation of swine-origin influenza A virus (H1N1/2009) from other seasonal influenza A viruses. *Viruses* **2012**, *4*, 3012–3019.
10. Alberts, B. INTRODUCTION H5N1. *Science* **2012**, *336*, 1521–1521.
11. Takekawa, J.Y.; Prosser, D.J.; Newman, S.H.; Bin Muzaffar, S.; Hill, N.J.; Yan, B.P.; Xiao, X.M.; Lei, F.M.; Li, T.X.; Schwarzbach, S.E.; *et al.* Victims and vectors: Highly pathogenic avian influenza H5N1 and the ecology of wild birds. *Avian Biol. Res.* **2010**, *3*, 51–73.
12. Leung, Y.H.C.; Cheung, P.; Zhang, L.J.; Wu, Y.O.; Chow, K.C.; Ho, C.K.; Chow, C.K.; Ng, C.F.; Li, B.; Tsang, C.L.; *et al.* Influenza viruses in wild birds in Hong Kong, 2003–2010. *Influenza Other Respir. Viruses* **2011**, *5*, 77–78.
13. Capua, I.; Alexander, D.J. Ecology, epidemiology and human health implications of avian influenza viruses: Why do we need to share genetic data? *Zoonoses Public Health* **2008**, *55*, 2–15.
14. Neumann, G.; Chen, H.; Gao, G.F.; Shu, Y.L.; Kawaoka, Y. H5N1 influenza viruses: Outbreaks and biological properties. *Cell Res.* **2010**, *20*, 51–61.
15. Bragstad, K.; Jorgensen, P.H.; Handberg, K.; Hammer, A.S.; Kabell, S.; Fomsgaard, A. First introduction of highly pathogenic H5NI avian influenza A viruses in wild and domestic birds in Denmark, Northern Europe. *Virol. J.* **2007**, *4*, 1–10.
16. Rebel, J.M.J.; Peeters, B.; Fijten, H.; Post, J.; Cornelissen, J.; Vervelde, L. Highly pathogenic or low pathogenic avian influenza virus subtype H7N1 infection in chicken lungs: Small differences in general acute responses. *Vet. Res.* **2011**, *42*, 1–11.

17. Comin, A.; Klinkenberg, D.; Marangon, S.; Toffan, A.; Stegeman, A. Transmission dynamics of low pathogenicity avian influenza infections in Turkey flocks. *PLoS One* **2011**, *6*, 1–9.
18. Kabir, S.M.L. Avian flu (H5N1): Threat of "global pandemic" is growing and it's impact on the developing countries' economy. *Afr. J. Microbiol. Res.* **2010**, *4*, 1192–1194.
19. Yamada, S.; Suzuki, Y.; Suzuki, T.; Le, M.Q.; Nidom, C.A.; Sakai-Tagawa, Y.; Muramoto, Y.; Ito, M.; Kiso, M.; Horimoto, T.; *et al.* Haemagglutinin mutations responsible for the binding of H5N1 influenza A viruses to human-type receptors. *Nature* **2006**, *444*, 378–382.
20. Fauci, A.S.; Collins, F.S. Benefits and risks of influenza research: lessons learned. *Science* **2012**, *336*, 1522–1523.
21. Nguyen, T.; Rivailler, P.; Davis, C.T.; Hoa, D.T.; Balish, A.; Dang, N.H.; Jones, J.; Vui, D.T.; Simpson, N.; Huong, N.T.; *et al.* Evolution of highly pathogenic avian influenza (H5N1) virus populations in Vietnam between 2007 and 2010. *Virology* **2012**, *432*, 405–416.
22. Tang, D.J.; Lam, Y.M.; Siu, Y.L.; Lam, C.H.; Chu, S.L.; Peiris, J.S.M.; Buchy, P.; Nal, B.; Bruzzone, R. A single residue substitution in the receptor-binding domain of H5N1 hemagglutinin is critical for packaging into pseudotyped lentiviral particles. *PLoS One* **2012**, *7*, 1–12.
23. Park, A.W.; Glass, K. Dynamic patterns of avian and human influenza in east and southeast Asia. *Lancet Infect. Dis.* **2007**, *7*, 543–548.
24. Rao, S.S.; Styles, D.; Kong, W.; Andrews, C.; Gorres, J.P.; Nabel, G.J. A gene-based avian influenza vaccine in poultry. *Poult. Sci.* **2009**, *88*, 860–866.
25. Webster, R.G.; Govorkova, E.A. Focus on research: H5N1 influenza–Continuing evolution and spread. *N. Engl. J. Med.* **2006**, *355*, 2174–2177.
26. Peiris, J.S.M.; de Jong, M.D.; Guan, Y. Avian influenza virus (H5N1): A threat to human health. *Clin. Microbiol. Rev.* **2007**, *20*, 243–267.
27. Uyeki, T.M.; Bresee, J.S. Detecting human-to-human transmission of avian influenza a (H5N1). *Emerg. Infect. Dis.* **2007**, *13*, 1969–1970.
28. Hayden, F.G.; de Jong, M.D. Emerging influenza antiviral resistance threats. *J. Infect. Dis.* **2011**, *203*, 6–10.
29. Cai, Z.P.; Ducatez, M.F.; Yang, J.L.; Zhang, T.; Long, L.P.; Boon, A.C.; Webby, R.J.; Wan, X.F. Identifying antigenicity-associated sites in highly pathogenic H5N1 influenza virus hemagglutinin by using sparse learning. *J. Mol. Biol.* **2012**, *422*, 145–155.
30. Zhao, G.; Zhong, L.; Lu, X.L.; Hu, J.; Gu, X.B.; Kai, Y.; Song, Q.Q.; Sun, Q.; Liu, J.B.; Peng, D.X.; *et al.* Characterisation of a highly pathogenic H5N1 clade 2.3.2 influenza virus isolated from swans in Shanghai, China. *Virus Genes* **2012**, *44*, 55–62.
31. Nidom, C.A.; Yamada, S.; Nidom, R.V.; Rahmawati, K.; Alamudi, M.Y.; Kholik; Indrasari, S.; Hayati, R.S.; Horimoto, K.I.; Kawaoka, Y. Genetic characterization of H5N1 influenza viruses isolated from chickens in Indonesia in 2010. *Virus Genes* **2012**, *44*, 459–465.
32. Huang, K.; Zhu, H.V.; Fan, X.H.; Wang, J.; Cheung, C.L.; Duan, L.; Hong, W.S.; Liu, Y.M.; Li, L.F.; Smith, D.K.; *et al.* Establishment and lineage replacement of H6 influenza viruses in domestic ducks in Southern China. *J. Virol.* **2012**, *86*, 6075–6083.
33. Miyoshi-Akiyama, T.; Akasaka, Y.; Oogane, T.; Kondo, Y.; Matsushita, T.; Funatogawa, K.; Kirikae, T. Development and evaluation of a line probe assay for rapid typing of influenza viruses and detection of the H274Y mutation. *J. Virol. Methods* **2012**, *185*, 276–280.

34. Redlberger-Fritz, M.; Aberle, S.W.; Strassl, R.; Popow-Kraupp, T. Rapid identification of neuraminidase inhibitor resistance mutations in seasonal influenza virus A(H1N1), A(H1N1)2009, and A(H3N2) subtypes by melting point analysis. *Eur. J. Clin. Microbiol. Infect. Dis.* **2012**, *31*, 1593–1601.
35. Bao, J.R.; Huard, T.K.; Piscitelli, A.E.; Tummala, P.R.; Aleemi, V.E.; Coon, S.L.; Master, R.N.; Lewinski, M.A.; Clark, R.B. Reverse-transcription polymerase chain reaction/pyrosequencing to characterize neuraminidase H275 residue of influenza A 2009 H1N1 virus for rapid and specific detection of the viral oseltamivir resistance marker in a clinical laboratory. *Diagn. Microbiol. Infect. Dis.* **2011**, *71*, 396–402.
36. Deng, Y.M.; Caldwell, N.; Hurt, A.; Shaw, T.; Kelso, A.; Chidlow, G.; Williams, S.; Smith, D.; Barr, I. A comparison of pyrosequencing and neuraminidase inhibition assays for the detection of oseltamivir-resistant pandemic influenza A(H1N1) 2009 viruses. *Antivir. Res.* **2011**, *90*, 87–91.
37. Leang, S.K.; Deng, Y.M.; Shaw, R.; Caldwell, N.; Iannello, P.; Komadina, N.; Buchy, P.; Chittaganpitch, M.; Dwyer, D.E.; Fagan, P.; *et al.* Influenza antiviral resistance in the Asia-Pacific region during 2011. *Antivir. Res.* **2013**, *97*, 206–210.
38. Chairat, K.; Tarning, J.; White, N.J.; Lindegardh, N. Pharmacokinetic properties of anti-influenza neuraminidase inhibitors. *J. Clin. Pharmacol.* **2013**, *53*, 119–139.
39. Li, H.; Shih, W.Y.; Shih, W.H. Synthesis and characterization of aqueous carboxyl-capped CdS quantum dots for bioapplications. *Ind. Eng. Chem. Res.* **2007**, *46*, 2013–2019.
40. Hennequin, B.; Turyanska, L.; Ben, T.; Beltran, A.M.; Molina, S.I.; Li, M.; Mann, S.; Patane, A.; Thomas, N.R. Aqueous near-infrared fluorescent composites based on apoferritin-encapsulated PbS quantum dots. *Adv. Mater.* **2008**, *20*, 3592–3596.
41. Genbank. Available online: http://www.ncbi.nlm.nih.gov/genbank/ (accessed on 1 July 2013).
42. Krejcova, L.; Huska, D.; Hynek, D.; Kopel, P.; Adam, V.; Hubalek, J.; Trnkova, L.; Kizek, R. Using of paramagnetic microparticles and quantum dots for isolation and electrochemical detection of influenza viruses' specific nucleic acids. *Int. J. Electrochem. Sci.* **2013**, in press.
43. Krejcova, L.; Hynek, D.; Kopel, P.; Adam, V.; Hubalek, J.; Trnkova, L.; Kizek, R., Paramagnetic particles isolation of influenza oligonucleotide labelled with CdS QDs. *Chromatographia* **2013**, *76*, 355–362.
44. Huska, D.; Adam, V.; Babula, P.; Trnkova, L.; Hubalek, J.; Zehnalek, J.; Havel, L.; Kizek, R. Microfluidic robotic device coupled with electrochemical sensor field for handling of paramagnetic micro-particles as a tool for determination of plant mRNA. *Microchim. Acta* **2011**, *173*, 189–197.
45. Huska, D.; Hubalek, J.; Adam, V.; Vajtr, D.; Horna, A.; Trnkova, L.; Havel, L.; Kizek, R. Automated nucleic acids isolation using paramagnetic microparticles coupled with electrochemical detection. *Talanta* **2009**, *79*, 402–411.
46. Krejcova, L.; Dospivova, D.; Ryvolova, M.; Kopel, P.; Hynek, D.; Krizkova, S.; Hubalek, J.; Adam, V.; Kizek, R. Paramagnetic particles coupled with an automated flow injection analysis as a tool for influenza viral protein detection. *Electrophoresis* **2012**, *33*, 3195–3204.

47. Zitka, O.; Krizkova, S.; Krejcova, L.; Hynek, D.; Gumulec, J.; Masarik, M.; Sochor, J.; Adam, V.; Hubalek, J.; Trnkova, L.; *et al.* Microfluidic tool based on the antibody-modified paramagnetic particles for detection of 8-hydroxy-2'-deoxyguanosine in urine of prostate cancer patients. *Electrophoresis* **2011**, *32*, 3207–3220.
48. Prasek, J.; Huska, D.; Jasek, O.; Zajickova, L.; Trnkova, L.; Adam, V.; Kizek, R.; Hubalek, J. Carbon composite micro- and nano-tubes based electrodes for detection of nucleic acids. *Nanoscale Res. Lett.* **2011**, *6*, 1–5.
49. Huska, D.; Zitka, O.; Krystofova, O.; Adam, V.; Babula, P.; Zehnalek, J.; Bartusek, K.; Beklova, M.; Havel, L.; Kizek, R. Effects of cadmium(II) ions on early somatic embryos of Norway spruce studied by using electrochemical techniques and nuclear magnetic resonance. *Int. J. Electrochem. Sci.* **2010**, *5*, 1535–1549.
50. Chomoucka, J.; Drbohlavova, J.; Masarik, M.; Ryvolova, M.; Huska, D.; Prasek, J.; Horna, A.; Trnkova, L.; Provaznik, I.; Adam, V.; *et al.* Nanotechnologies for society. New designs and applications of nanosensors and nanobiosensors in medicine and environmental analysis. *Int. J. Nanotechnol.* **2012**, *9*, 746–783.
51. Berton, M.; Turelli, P.; Trono, D.; Stein, C.A.; Allemann, E.; Gurny, R. Inhibition of HIV-1 in cell culture by oligonucleotide-loaded nanoparticles. *Pharm. Res.* **2001**, *18*, 1096–1101.
52. Schneider, T.; Becker, A.; Ringe, K.; Reinhold, A.; Firsching, R.; Sabel, B.A. Brain tumor therapy by combined vaccination and antisense oligonucleotide delivery with nanoparticles. *J. Neuroimmunol.* **2008**, *195*, 21–27.
53. Cai, H.; Zhu, N.N.; Jiang, Y.; He, P.G.; Fang, Y.Z. Cu@Au alloy nanoparticle as oligonucleotides labels for electrochemical stripping detection of DNA hybridization. *Biosens. Bioelectron.* **2003**, *18*, 1311–1319.
54. Sun, W.; Zhong, J.H.; Qin, P.; Jiao, K. Electrochemical biosensor for the detection of cauliflower mosaic virus 35 S gene sequences using lead sulfide nanoparticles as oligonucleotide labels. *Anal. Biochem.* **2008**, *377*, 115–119.
55. Roh, C.; Lee, H.Y.; Kim, S.E.; Jo, S.K. A highly sensitive and selective viral protein detection method based on RNA oligonucleotide nanoparticle. *Int. J. Nanomed.* **2010**, *5*, 323–329.
56. Bandyopadhyay, A.; Chatterjee, S.; Sarkar, K. Rapid isolation of genomic DNA from E. coli XL1 Blue strain approaching bare magnetic nanoparticles. *Curr. Sci.* **2011**, *101*, 210–214.
57. Trachtova, S.; Kaman, O.; Spanova, A.; Veverka, P.; Pollert, E.; Rittich, B. Silica-coated La0.75Sr0.25MnO3 nanoparticles for magnetically driven DNA isolation. *J. Sep. Sci.* **2011**, *34*, 3077–3082.
58. Zhang, T.; Zhao, P.S.; Zhang, W.; Liang, M.; Gao, Y.W.; Yang, S.T.; Wang, T.C.; Qin, C.; Wang, C.Y.; Xia, X.Z. Antisense oligonucleotide inhibits avian influenza virus H5N1 replication by single chain antibody delivery system. *Vaccine* **2011**, *29*, 1558–1564.
59. Malecka, K.; Grabowska, I.; Radecki, J.; Stachyra, A.; Gora-Sochacka, A.; Sirko, A.; Radecka, H. Voltammetric detection of a specific DNA sequence of avian influenza virus H5N1 using HS-ssDNA probe deposited onto gold electrode. *Electroanalysis* **2012**, *24*, 439–446.
60. Ganbold, E.O.; Kang, T.; Lee, K.; Lee, S.Y.; Joo, S.W. Aggregation effects of gold nanoparticles for single-base mismatch detection in influenza A (H1N1) DNA sequences using fluorescence and Raman measurements. *Colloid Surf. B-Biointerfaces* **2012**, *93*, 148–153.

61. Liu, X.G.; Cheng, Z.Q.; Fan, H.; Ai, S.Y.; Han, R.X. Electrochemical detection of avian influenza virus H5N1 gene sequence using a DNA aptamer immobilized onto a hybrid nanomaterial-modified electrode. *Electrochim. Acta* **2011**, *56*, 6266–6270.
62. Lai, W.A.; Lin, C.H.; Yang, Y.S.; Lu, M.S.C. Ultrasensitive and label-free detection of pathogenic avian influenza DNA by using CMOS impedimetric sensors. *Biosens. Bioelectron.* **2012**, *35*, 456–460.
63. Tian, J.P.; Zhao, H.M.; Liu, M.; Chen, Y.Q.; Quan, X. Detection of influenza A virus based on fluorescence resonance energy transfer from quantum dots to carbon nanotubes. *Anal. Chim. Acta* **2012**, *723*, 83–87.
64. Chung, D.J.; Kim, K.C.; Choi, S.H. Electrochemical DNA biosensor based on avidin-biotin conjugation for influenza virus (type A) detection. *Appl. Surf. Sci.* **2011**, *257*, 9390–9396.
65. Fan, H.; Ju, P.; Ai, S.Y. Controllable synthesis of CdSe nanostructures with tunable morphology and their application in DNA biosensor of Avian Influenza Virus. *Sens. Actuator B-Chem.* **2010**, *149*, 98–104.
66. Adam, V.; Huska, D.; Hubalek, J.; Kizek, R. Easy to use and rapid isolation and detection of a viral nucleic acid by using paramagnetic microparticles and carbon nanotubes-based screen-printed electrodes. *Microfluid. Nanofluid.* **2010**, *8*, 329–339.
67. Chen, X.J.; Xie, H.; Seow, Z.Y.; Gao, Z.Q. An ultrasensitive DNA biosensor based on enzyme-catalyzed deposition of cupric hexacyanoferrate nanoparticles. *Biosens. Bioelectron.* **2010**, *25*, 1420–1426.
68. Lim, S.H.; Buchy, P.; Mardy, S.; Kang, M.S.; Yu, A.D.C. Specific nucleic acid detection using photophysical properties of quantum dot probes. *Anal. Chem.* **2010**, *82*, 886–891.
69. Tam, P.D.; Hieu, V.N.; Chien, N.D.; Le, A.T.; Tuan, M.A. DNA sensor development based on multi-wall carbon nanotubes for label-free influenza virus (type A) detection. *J. Immunol. Methods* **2009**, *350*, 118–124.
70. Kim, S.A.; Kim, S.J.; Lee, S.H.; Park, T.H.; Byun, K.M.; Kim, S.G.; Shuler, M.L. Detection of avian influenza-DNA hybridization using wavelength-scanning surface plasmon resonance biosensor. *J. Opt. Soc. Korea* **2009**, *13*, 392–397.

5.2.3 Vědecký článek V

KREJCOVA, L.; HUSKA, D.; HYNEK, D.; KOPEL, P.; ADAM, V.; HUBALEK, J.; TRNKOVA, L.; KIZEK, R. Using of Paramagnetic Microparticles and Quantum Dots for Isolation and Electrochemical Detection of Influenza Viruses' Specific Nucleic Acids.

International Journal of Electrochemical Science, 2013, roč. 8. č. 1, s. 689-702. ISS 1452-3981. IF: 1.956

Podíl autorky Krejčová L.: 75 % textové části práce, 85 % experimentální části práce

Článek popisuje návrh a realizaci metody pro identifikaci tří různých subtypů chřipky v jednom vzorku současně. Cílovými molekulami byly od chřipky odvozené oligonukleotidy (ODN), se sekvencemi charakteristickými pro tři různé subtypy chřipky typu A (H1N1, H3N2 a H5N1). Každá cílová sekvence (ODN) byla pro účely elektrochemické detekce značena jiným typem NPs (H1N1: ZnS, H3N2: PbS a H5N1: CdS). Nanočástice mají řadu unikátních vlastností, jako je poměrně velký aktivní povrch, velká mechanická odolnost, dobré elektrické, optické a magnetické vlastnosti, snadná interakce s biomolekulami *(Akbarzadeh, a kol., 2012, Liu, a kol., 2011, Liu, a kol., 2014)*, a z toho důvodu jsou považovány za nástroj rozšiřující možnosti detekce biomolekul *(Wei, a kol., 2014, Xie, a kol., 2014)*.

Experimentální část byla rozdělena do dvou kroků. Prvním krokem byla izolace pomocí MPs spojená s dvojitou hybridizací. Jako platforma pro izolaci byly zvoleny MPs, které jsou v současné době pro účely izolace nukleových kyselin široce používané *(Hsing, a kol., 2007, van Reenen, a kol., 2014)*. První hybridizace představovala vazbu anti-sense řetězců na MPs, druhá pak vazbu mezi anti-sense řetězci a cílovými ODN konjugovanými NPs. Izolované komplexy ODN-SH-NPs byly detekovány pomocí voltametrie a to pomocí dvou metod. ODN část komplexu (CA pík) byla detekována pomocí square wave voltametrie (SWV) ve spojení s přenosovou adsorptivní technikou při potenciálu -1,4 V. Kovová část NPs (Cd, Pb a Zn píky) byla detekována pomocí diferenční pulzní voltametrie (DPV) při potenciálech -1,03V (Zn), -0,63V (Cd) a -0,45V (Pb). Podstatou vzájemného rozlišení třech různých ODN sekvencí bylo jejich značení pomocí NPs a rozdíl v potenciálech píků kovových částí NPs. Nejprve byly optimalizovány parametry elektrochemických metod pro detekci CA píku a píků kovových částí NPs, následně byly sestaveny příslušné kalibrační závislosti pro všechny

sledované molekuly (ODN a NPs). Poté byla optimalizována teplota druhé hybridizace. Jako optimum bylo vybráno 25 °C. Při této teplotě bylo dosaženo největšího výtěžku izolace. Efekt izolace byl sledován elektrochemicky, na základě analýzy CA píků a píků kovových částí NPs. Lze tedy říci, že se podařily splnit všechny vytýčené úkoly a že námi navržená metoda může být modifikována a aplikována i pro detekci dalších infekčních nebo podmíněně dědičných onemocnění.

Int. J. Electrochem. Sci., 8 **(2013)** 689 - 702

International Journal of
ELECTROCHEMICAL
SCIENCE
www.electrochemsci.org

Using of Paramagnetic Microparticles and Quantum Dots for Isolation and Electrochemical Detection of Influenza Viruses' Specific Nucleic Acids

Ludmila Krejcova[1], *Dalibor Huska*[1], *David Hynek*[1,2], *Pavel Kopel*[1,2], *Vojtech Adam*[1,2], *Jaromir Hubalek*[2,3], *Libuse Trnkova*[1,2] *and Rene Kizek*[1,2*]

[1] Department of Chemistry and Biochemistry, Faculty of Agronomy, Mendel University in Brno, Zemedelska 1, CZ-613 00 Brno, Czech Republic, European Union
[2] Central European Institute of Technology, Brno University of Technology, Technicka 3058/10, CZ-616 00 Brno, Czech Republic, European Union
[3] Department of Microelectronics, Faculty of Electrical Engineering and Communication, Brno University of Technology, Technicka 3058/10, CZ-616 00 Brno, Czech Republic, European Union
[*]E-mail: kizek@sci.muni.cz

Received: 30 October 2012 / *Accepted:* 28 November 2012 / *Published:* 1 January 2013

The aim of this study was to suggest isolation protocol based on paramagnetic microparticles and multicolour electrochemical detection of three various influenza oligonucleotides (H1N1 influenza subtype, H3N2 influenza subtype and H5N1 influenza subtype) modified with nanoparticles (NPs) called quantum dots (QDs), which are made from zinc, cadmium or lead. Particularly, we described hybridization assay based on paramagnetic microparticles (MPs) and coupled with detection of three different influenza derived oligonucleotides (ODNs) labelled with QDs. Hybridization efficiency between NPs conjugated anti-senses and target nucleic acid hybrids was optimized and evaluated by the electrochemical analysis. The highest response of ODN-SH-NPs was determined for the hybridization temperature of 25 °C. Further, we tested detection of the complexes via peak coming from the presence of ODNs and/or from the presence of metal ions in QDs. Under the optimized conditions, LODs (3 S/N) based on the determination of metal ions in QDs label were estimated as follows: 0.1 ng/ml of ODN-SH-CdNPs, 0.5 ng/ml of ODN-SH-ZnNPs and 1 ng/ml of ODN-SH-PbNPs. Besides this we also correlated the results from ODNs and metal ions signals.

Keywords: Influenza; Nanoparticles; Quantum Dots; Multi Target Detection; Voltammetry; Magnetic Particles; Hybridization; Automated Separation; Electrochemistry

1. INTRODUCTION

Influenza is an infectious disease, which affect respiratory system and is often associated with the high morbidity in the common population and mortality in a group of high-risk patients

(immunosuppressed, geriatrics or very young etc.). Currently, vaccination is the most common way of the influenza control. Influenza vaccine exists, however, it must be prepared year after year again because of the constant mutational changes in the antigenic structure of the influenza virus (hemagglutinin and neuraminidase antigens). In collaboration with World Health Organization (WHO), two vaccines are prepared every year in a six-month interval between the Southern and Northern hemisphere due to seasonal occurrence in the winter months [1]. Except the common subtypes that are responsible for mortality only in a high-risk patients group, highly virulent subtypes, such as H5N1 (highly pathogenic avian influenza) with mortality of about 60%, occur [2,3]. Constant mutational changes of antigens represent a high risk, especially in the connection with a possibility of origination of the highly virulent subtype(s). Global travelling can successfully potentiate extension of the global pandemic. Rapid and well-timed diagnostics is one of the most effective tools in the fight against emergence and spread of the epidemic. Multi target analyses have a great potential as a tool for the diagnosis of commonly occurring and new influenza subtypes [4-6]. Obviously applied analytical methods for identification of nucleic acids (NAs) require highly sensitive analytical tools. Microarrays, as one of the tested tools, are based on the fluorescent probes; however, they are limited by their sensitivity, range of the emission spectrum and demands on data evaluation [7-11]. In the light of the above-mentioned facts, methods of nucleic acids detection and isolation have become the crucial part of nucleic acids analysis [12-19]. Presently, paramagnetic particles are widely used in the NAs isolation [20-25]. They may be applied for the isolation of RNA, DNA and proteins as well as for the isolation of specific nucleic acids or specific antigens [11,24,26-29]. Paramagnetic particles (MPs) enable automation of the whole process; in addition, paramagnetic particles' surface may be effectively modified by interactions with target biomolecules [23]. Target DNA is usually isolated and detected by probe hybridization and by using different compounds such as biotin-avidin system, substrate-enzyme systems, antigen-antibody system and fluorescent dyes or quantum dots (which has vast spectrum of application in microarrays as fluorescent probes) [30-32]. Recently, a plenty of assays uses oligo (probe) conjugated MPs for the isolation of target DNA [26,33-35].

Nanoparticles (NPs) have significantly improved the techniques based on the paramagnetic particles. Through the nano size (scale) dimensions ranging from 1 to 100 nm, NPs have a quite large active surface, high mechanical resistance, excellent electrical, catalytic and eventually magnetic properties with the possibility to interact with a wide range of biological as well as chemical compounds [36-41]. They extended possibilities in the NAs isolation and especially detection [12,14,23,24,29,42-46]. Gold, silver and iron NPs are the most used NPs for this purpose [14,47,48]. However, isolation itself is not sufficient for the diagnosis. Isolated targeting NA must be detected by the use an appropriate method. Detection of hybridised target NANAs is important for a diagnosis of viral and bacterial pathogens as well as diagnosis of genetic diseases or for forensic analyses [11,49]. Nowadays, research is directed to the finding the methods for the simultaneous detection of multiple target DNA. The research is focused on the methods using optical detection with application of fluorescently active labels [50-52]. Wang et al. describes multi-target electrochemical DNA detection based on the application of different quantum dots tags, multi-target electrochemical detection scheme incorporates the high sensitivity and selectivity advantages of the NPs-based electrochemical assays [53]. The great advantage of electrochemical methods is based on their high sensitivity, low costs and

possibility of automation and connection with other analytical methods [54-59]. In addition, they can be miniaturized into nanoscale dimensions [60-64].

The aim of this study was to suggest isolation protocol based on paramagnetic particles and multicolour electrochemical detection of three various influenza ODNs (H1N1 influenza subtype, H3N2 influenza subtype and H5N1 influenza subtype) modified with nanoparticles (NPs) called quantum dots, which are made from zinc, cadmium or lead according to scheme shown in Fig. 1/Part 1.

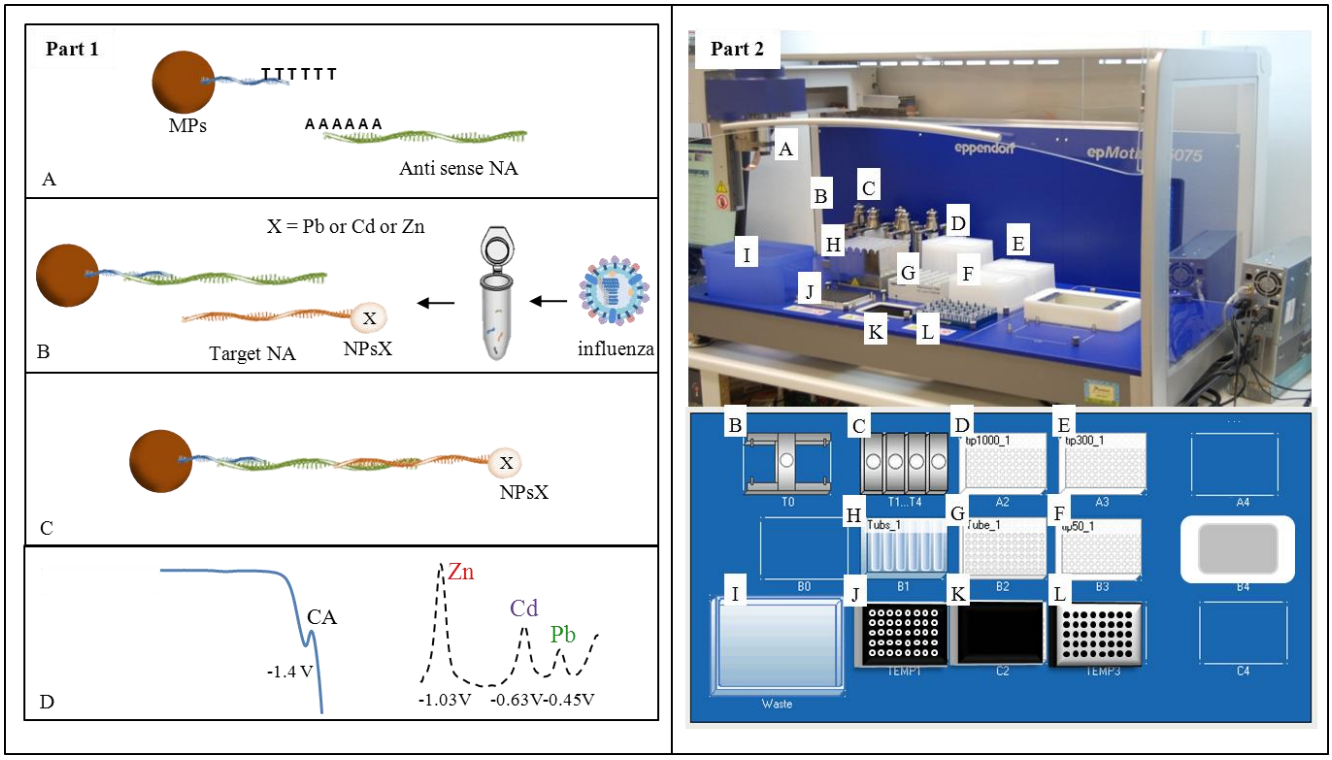

Figure 1. (**Part 1**) Scheme of isolation and detection of specific influenza sequences by using paramagnetic microparticles (MPs), nanoparticles labels as quantum dots (NPs) and electrochemistry. (**A**) Paramagnetic particle modified by poly thymine strand oligonucleotide and addition of probe modified by poly adenine strand. (**B**) Addition of target to: ODN-SH-XNPs. X= Pb or Cd or Zn. (**C**) Hybridization ODN-SH-XNPs to anti sense on MPs. (**D**) Electrochemical detection of XNPs and target influenza ODN. (**Part 2**) (**A**) arm for tips and microplate holder with optic sensor, (**B**) microplate holder, (**C**) tips holders, (**D**) tips (1000 µl), (**E**) tips (300 µl), (**F**) tips (50 µl), (**G**) rack tubes (Eppendorf 1.5 ml, MPs, antisense, specific ODN labelled by NPs, hybridization buffer, phosphate buffer II), (**H**) reservoir holder (30 ml, phosphate buffer I and waste), (**I**) container for used tips, (**J**) thermo adapter, (**K**) start position for microplate – PCR plate 96, (**L**) magnetic adapter.

2. EXPERIMENTAL PART

2.1 Preparation of nanoparticles (NPs)

All chemicals were purchased from Sigma Aldrich (USA) in ACS purity and used without further purification. CdS QDs were prepared with a slightly modified method published in [34].

Briefly, cadmium nitrate tetrahydrate $Cd(NO_3)_2 \cdot 4H_2O$ (0.03085 g, 0.1mM) was dissolved in ACS water (25 ml). 3-mercaptopropionic acid (35 µl, 0.4mM) was slowly added to stirred solution. Afterwards, pH was adjusted to 9.11 using 1M NH_4OH (1.5 ml). Sodium sulphide nonahydrate $Na_2S \cdot 9H_2O$ (0.02402 g, 0.1mM) in 23 ml of ACS water was poured into the first solution with vigorous stirring. Obtained yellow solution was stirred for 1 h. CdS QDs were stored in dark at 4ºC. ZnS QDs were prepared similarly to CdS QDs; zinc nitrate hexahydrate $Zn(NO_3)_2 \cdot 6H_2O$ (0.02975 g, 0.1 mM) was used for this preparation. Obtained colourless solution was stirred for 1 h and stored in dark at 4ºC. PbS QDs were prepared by modified method of Hennequin [65]. Lead acetate trihydrate $Pb(OAc)_2 \cdot 3H_2O$ (0.03794 g, 0.1mM) was dissolved in ACS water (25 ml). 3-mercaptopropionic acid (60 µl, 0.69mM) was slowly added to stirred solution. White precipitate was formed, which disappeared after addition of 3.8 ml of 1M NH_4OH (pH = 9.88). $Na_2S \cdot 9H_2O$ (0.01201 g, 0.05mM) in 21.2 ml of ACS water was added with vigorous stirring. The obtained brown solution was stirred for 1 h and stored in dark at 4 ºC.

2.2 Preparation of NPs-labelled oligonucleotide (ODN-SH-NPs)

ODN-SH (100 µl, 100 µg/ml, Tab. 1) was mixed with a solution of NPs (100 µl). This mixture was shaken for 24 h at room temperature (Vortex Genie2, Scientific Industries, USA). Subsequently, solution was dialysed against 2000 ml of miliQ water (24 h, 4ºC) using a Millipore membrane filter 0.025 µm VSWP. During dialysis the sample was diluted to 800 µl. Diluted sample was concentrated to the final volume of 500 µl on a centrifuge filter device Amicon Ultra 3k (Millipore, USA). Centrifuge 5417R (Eppendorf, Germany) set to the following parameters: 15 min, 4,500 rpm, 15 ºC.

Table 1. Probes and targets oligonucleotide (ODN) [66].

Probes	Target oligonucleotide
H1N1- 5′ (AAAAA) CCA TTG GTT C 3′	H1N1- 5′ (Th) GAA CCA ATG G 3′
H3N2- 5′ (AAAAA) CCC GTT ACA C 3′	H3N2- 5′ (Th) GTG TAA CGG G 3′
H5N1- 5′ (AAAAA) CCT CAA GGA G 3′	H5N1- 5′ (Th) CTC CTT GA GG 3′

2.3 Automatic isolation of ODN-SH-NPs

Automatic pipetting station epMotion 5075 (Eppendorf, Germany) with original devices (microplate holder, tips holder, tips (1000, 300, 50 µl), rack tubes, reservoir holder, container for used tips, thermo adapter, PCR plate 96, magnetic adapter) was used for the fully automated target nucleic acids isolation process (Fig. 1/Part 2). Volume of 10 µl of Dynabeads Oligo $(dT)_{25}$ (Invitrogen, Oslo) was dispensed in each well in the plate (PCR 96, Eppendorf, Germany). The plate was subsequently transferred to the magnet and NPs storing solution was aspirated to waste. Subsequently, beads were further washed three times with 20 µl of phosphate buffer I (pH = 6.5, 0.1 M NaCl + 0.05 M Na_2HPO_4 + 0.05 M NaH_2PO_4). The *first hybridization* according to the following protocol was the next step. 10 µl of polyA-modified anti sense oligonucleotide and 10 µl of hybridization buffer (0.1 M phosphate

buffer, 0.6 M guanidinium thiocyanate, 0.15 M Tris, pH = 7.5) were added in each well and then the plate was incubated (15 min, 25°C, mixing). This procedure was followed by a washing (three times) with 20 µl of phosphate buffer I. The *second hybridization* according to the following protocol was the next step. 10 µl of NPs-labelled oligonucleotide and 10 µl of hybridization buffer (0.1 M phosphate buffer, 0.6 M guanidinium thiocyanate, 0.15 M Tris, pH = 7.5) were added to each well and the plate was incubated (15 min, 25°C, mixing). Procedure was followed by a washing (three times) with 20 µl of phosphate buffer I. Then, 30 µl of elution solution (phosphate buffer II - 0.2 M NaCl + 0.1 M Na_2HPO_4 + 0.1 M NaH_2PO_4) was added into each well and plate was subsequently incubated (5 min, 85°C, mixing). After elution step, the plate was transferred to the magnet, and elution product from each well was transferred to a separate well.

2.4 Method for detection of CA and metal peak of ODN-SH-NPs

Electrochemical measurements were performed with 747 VA Stand instrument connected to 746 VA Trace Analyzer and 695 Autosampler (Metrohm, Switzerland), using a standard cell with three electrodes and cooled sample holder (4 °C). A hanging mercury drop electrode (HMDE) with a drop area of 0.4 mm^2 was the working electrode. An Ag/AgCl/3M KCl electrode was the reference and glassy carbon electrode was auxiliary electrode. GPES 4.9 supplied by EcoChemie was employed for data processing. All measurements were performed in the presence of acetate buffer 0.2M CH_3COOH + 0.2M CH_3COONa (pH 5.0) at 25°C. The analysed samples were deoxygenated prior to measurements by purging with argon (99.99%) for 120 s.

For detection of CA signal, square wave voltammetry (SWV) method was applied [23]. The parameters of the electrochemical determination were as follows: initial potential 0 V; end potential - 1.85 V; frequency 10 Hz; potential step 0.005 V; amplitude 0.025 V. Differential pulse voltammetry (DPV) was applied for electrochemical detection of metal part of the complex. In this case the parameters of electrochemical determination were as follows: Cd (initial potential -0.9 V; end potential -0.45 V); Zn (initial potential -1.2 V; end potential -0.85 V); Pb (initial potential -0.6 V; end potential -0.25 V); others parameters were the same: deposition potential -0.9 V; duration 240 s; equilibration time 5 s; modulation time 0.06 s; time interval 0.2 s; potential step 0.002 V; modulation amplitude 0.025 V.

2.5 Mathematical treatment of data and estimation of detection limits

Mathematical analysis of the data and their graphical interpretation was realized by MICROSOFT EXCEL® (USA). Results are expressed as mean ± standard deviation (S.D.) unless noted otherwise (EXCEL®). The detection limits (3 signal/noise, S/N) were calculated according to Long and Winefordner [67], whereas N was expressed as standard deviation of noise determined in the signal domain unless stated otherwise.

3. RESULTS AND DISCUSSION

We suggested and developed hybridization kit for the isolation and detection of three different influenzas' nucleic acids sequence from one sample. Procedure is based on the detection of metal-based NPs (ZnNPs, PbNPs and/or CdNPs) complex with NAs. Generally, metals can be very sensitively and selectively determined using the electrochemical techniques. NPs from different metals provide signals at different potentials -1.03 ± 0.005 V (Zn), -0.63 ± 0.005 V (Cd) and -0.45 ± 0.005 V (Pb) [40,63,68,69]. The suggested procedure is shown in Fig.1/Part 1. Firstly, separation step as isolation of target sequences from sample was provided by anti-sense modified MPs (Fig. 1/Part 1A). After hybridization of target sequence to MPs, the washing step followed. After removing the interfering compounds (unbound MPs, proteins and other residues of matrix), detection of the elution of bound target influenzas' sequences could be carried out. However, we would obtain information only about the total amount of isolated NAs without details about their sequence or influenza subtypes. For the simultaneous three influenza subtypes differentiation and their quantification, target NAs (influenzas' derived oligonucleotides) were incubated with the ZnNPs, CdNPs, and PbNPs (Fig. 1/Part 1B). MPs used in isolation part were modified with three different probes (anti sense chain), which are able to bind the target sequences by hybridisation reaction between anti sense chain and target influenza ODN (Fig. 1/Part 1C). Complex NPs with target ODN was designated as ODN-SH-ZnNPs; ODN-SH-CdNPs and/or ODN-SH-PbNPs (connection due to-S-S- bond). After complex formation due to recognizing the specific target sequence, this can be determined electrochemically (Fig. 1/Part 1D).

ODN-SH-NPs enable simultaneous quantification of three different target NAs. Application of two different electrochemical methods (SWV and DPV) brought two diverse signals. The first one corresponds to ODN-SH (CA peak) measured by SWV and the second one to metal part of QDs (metal peak) measured by DPV. In the case of application of both methods, we obtain information about the presence of NPs corresponding to one of the three target molecules (influenza subtype) which coresponded to one of three specific influenzas**'** derived ODNs. However, in the case of the only one signal detection, we can assume that the probe has not been linked with the target sequence or the linkage has failed. Signal of metal part NPs cannot be evaluated in this case. In addition to above-mentioned facts, all steps were fully automated by the use of an automated pipetting system modified for the hybridisation assay and for manipulation with paramagnetic and nano particles (Fig.1/Part 2).

3.1 Electrochemical detection of ODN-SH-NPs – CA and metal peaks

In general, electrochemical determination of oligonucleotides is based on the measurement of electroactivity of DNA (respectively cytosine and adenine bases), or the measurement of electroactivity of labels that has been used for modifying the oligonucleotides. Measurement of direct electroactivity (label-free) of oligonucleotides is the easiest and low cost variant, which is available [58,70-73]. The second possibility of DNA detection is DNA modifying by the electroactive label (indirect detection). The widely used compounds are methylene blue [74], Meldola's blue [75],

ferrocene and organic ligand complexes with osmium, ruthenium and copper [76-78]. Recently, quantum dots were used for this purpose also [30,79,80].

Labeling of oligonucleotides with nanoparticles as quantum dots is the basic requirement for theirs detection in our suggested system. Therefore, it was necessary to optimize all steps for the correct function of hybridization kit. Isolation of target sequences using anti sense modified MPs was carried out in accordance with the following paper [23]. Due to this fact, we focused on the optimization of ODN-SH-NPs detection. Effect of ODN-SH-NPs accumulation and ODN-SH accumulation on the working electrode is shown in Fig. 2A. We detected CA signal at -1.4V. This signal corresponds to reduction of adenine and cytosine bases, why it is called CA peak. The highest signal of CA peak was obtained at detection of ODN-SH without NPs (ODN-SH signal in blue) linkage at the time of accumulation 120 – 180 s (Fig. 2A). Signals of all ODN-SH-NPs are app. 50% lower compared to ODN-SH at the same time of accumulation (Fig. 2A). However, they provide sufficient signal (signal of metal part NPs) for their determination. Therefore we detected signals of individual NPs corresponding to metals (Zn, Cd and Pb) at potentials of -1.03V (Zn), -0.63V (Cd) and -0.45V (Pb). The main advantage of the NPs detection (compared to CA signal determination) is the fact that this way of detection is more sensitive with the lower limit of detection. Evaluated signals corresponding to individual NPs metals (Zn signal in red); (Pb signal in green) and (Cd signal in violet) are demonstrated in Figs. 2B, C and D. The increasing time of accumulation lead to the increase in response. Various NPs achieved saturation of electrode surface at various times. The highest responses were detected at time of accumulation 900 s for Zn and at 1000 s for Pb (Figs. 2B and C). ODN-SH-CdNPs required the shorter time of accumulation. The highest response of Cd peak was determined at 390 s (Fig. 2D).

We were subsequently focused on the possibility to bind various amounts of ODN onto NPs and to detect these amounts. Effect of ODN concentration on the CA peak height is shown in Figs. 3A and B. We used ODNs, which was linked to NPs via -SH groups, within the concentration range from 0.002 to 2 μg/ml. The increasing concentration led to the increase of the detected signal in all targets. The dependences had polynomial character in all cases (Fig. 3A). However, in lower concentration range (0.002 μg/ml to 0.125 μg/ml) it was possible to detect linear course too (Fig. 3B). Regression equations for individual probes with the coefficient of determination R^2=0.99 are shown in Fig. 3A. If we compare ODN-SH and ODN-SH-NPs, we can determine the effect of bounded NPs on the response of CA signal. The most significant effect on the signal response was determined for PbNPs, the least for CdNPs. Due to differences in the sensitivity, LODs (3 S/N) were estimated as follows: 0.1 ng/ml of ODN-SH-CdNPs, 0.5 ng/ml of ODN-SH-ZnNPs and 1 ng/ml of ODN-SH-PbNPs.

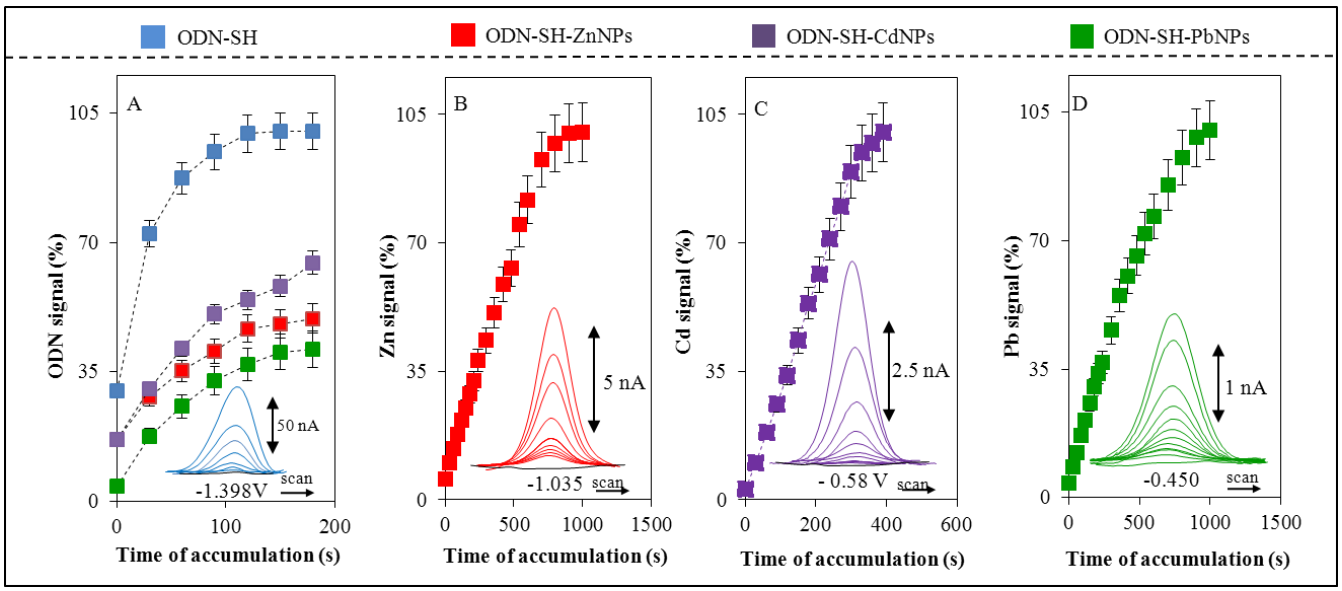

Figure 2. Optimization of accumulation time: (**A**) CA peaks of ODN-SH (♦); ODN-SH-ZnNPs (♦); ODN-SH-PbNPs (♦); and ODN-SH-CdNPs (♦). (**B**) Zn peak of ODN-SH-ZnNPs (♦). (**C**) Pb peak of ODN-SH-PbNPs (♦). (**D**) Cd peak of ODN-SH-CdNPs (♦); concentration of ODN-SH and ODN-SH-NPs was 2 µg/ml. CA peak was measured by SWV. Zn, Cd and Pb peaks were measured by DPV.

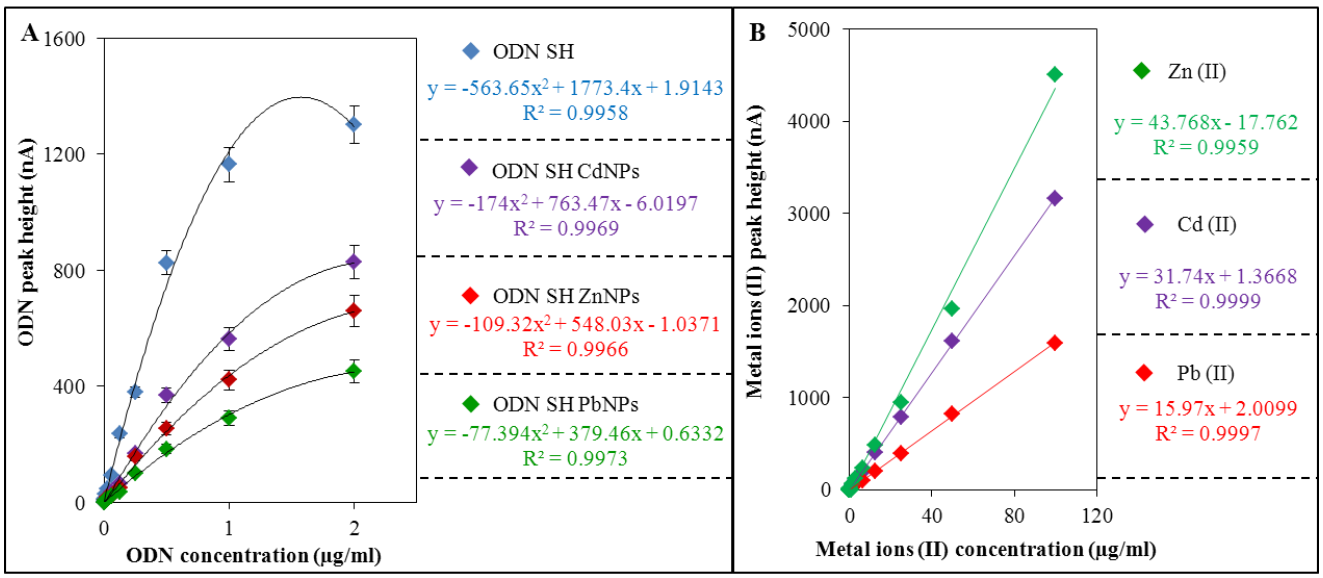

Figure 3. (**A**) Dependence of CA peak height on concentration of ODN (µg/ml) as ODN-SH (♦); ODN-SH-ZnNPs(♦); ODN-SH-PbNPs(♦) and ODN-SH-CdNPs (♦). (**B**) Dependence of metal ions peak height on concentration of metal ions (µg/ml) as Pb(II): (♦); Zn(II): (♦) and Cd(II): (♦).

3.2 Optimization of hybridization temperature

It was necessary to determine the effect of hybridization temperature on the binding of ODN-SH-NPs with the target NAs linked with magnetic NPs for the optimum hybridization (Fig. 4). Target

NAs interacted for 30 min with 2.5; 5; 10 and 20 µg/ml of ODN-SH-NPs at the temperature of 15 °C, 20 °C, 25 °C and 30 °C. Subsequently, the CA signal (Figs. 4. A, C and E) and Cd, Zn and Pb responses were determined (Figs. 4 B, D and F). It clearly follows from the results shown in Fig. 4 that the highest response of ODN-SH-NPs was determined for the hybridization temperature of 25 °C. On the other hand, the lowest ODN-SH-NPs response was detected for the hybridization temperature of 30 °C. ODN-SH-CdNPs represented exception. In this case, hybridization temperature of 30 °C led to the binding of the second higher amount of labelled oligonucleotides in the studied concentrations 10 and 20 µg/ml compared to other temperatures. We expected that the higher temperature of hybridization increased hybridization effect. This direct correlation can be applied only to the temperature of 25 °C because the oligonucleotide T_m was 28 °C.

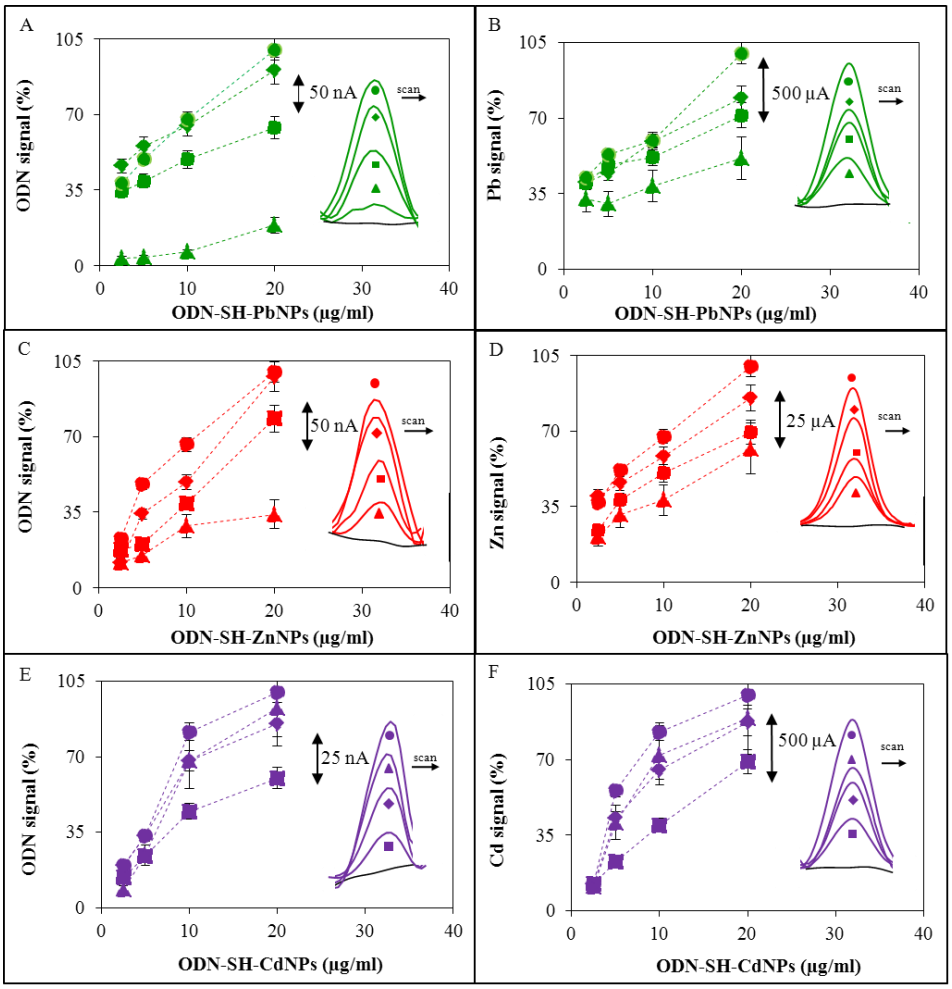

Figure 4. Dependence of relative peak heights (%) on concentration of ODN-SH-NPs (µg/ml), (left side – ODN peak height; right side – metal peak height); (**A+B**) ODN-SH-PbNPs; (**C+D**) ODN-SH-ZnNPs; (**E+F**) ODN-SH-CdNPs. Hybridisation temperatures: ■15 °C; ♦20 °C; ● 25 °C; and ▲30 °C.

3.3 Correlation Analysis

For the evaluation of dependence between CA signal and signal corresponding to NPs, correlation analysis was carried out (Fig. 5/Part 1/A, B and C). We used percentage values of signals

for individual NPs, temperatures and concentrations. The correlation was 77% in the case of PbNPs, 89% at ZnNPs and 91% at CdNPs. Further, the Spearman Rank-Order Correlation analysis was proved. In this case, the correlation coefficient for PbNPs was 0.90, for ZnNPs 0.89 and for CdNPs 0.96. Correlation analysis provided sufficient data, which showed that measuring both ODN-SH and NPs gave us similar results.

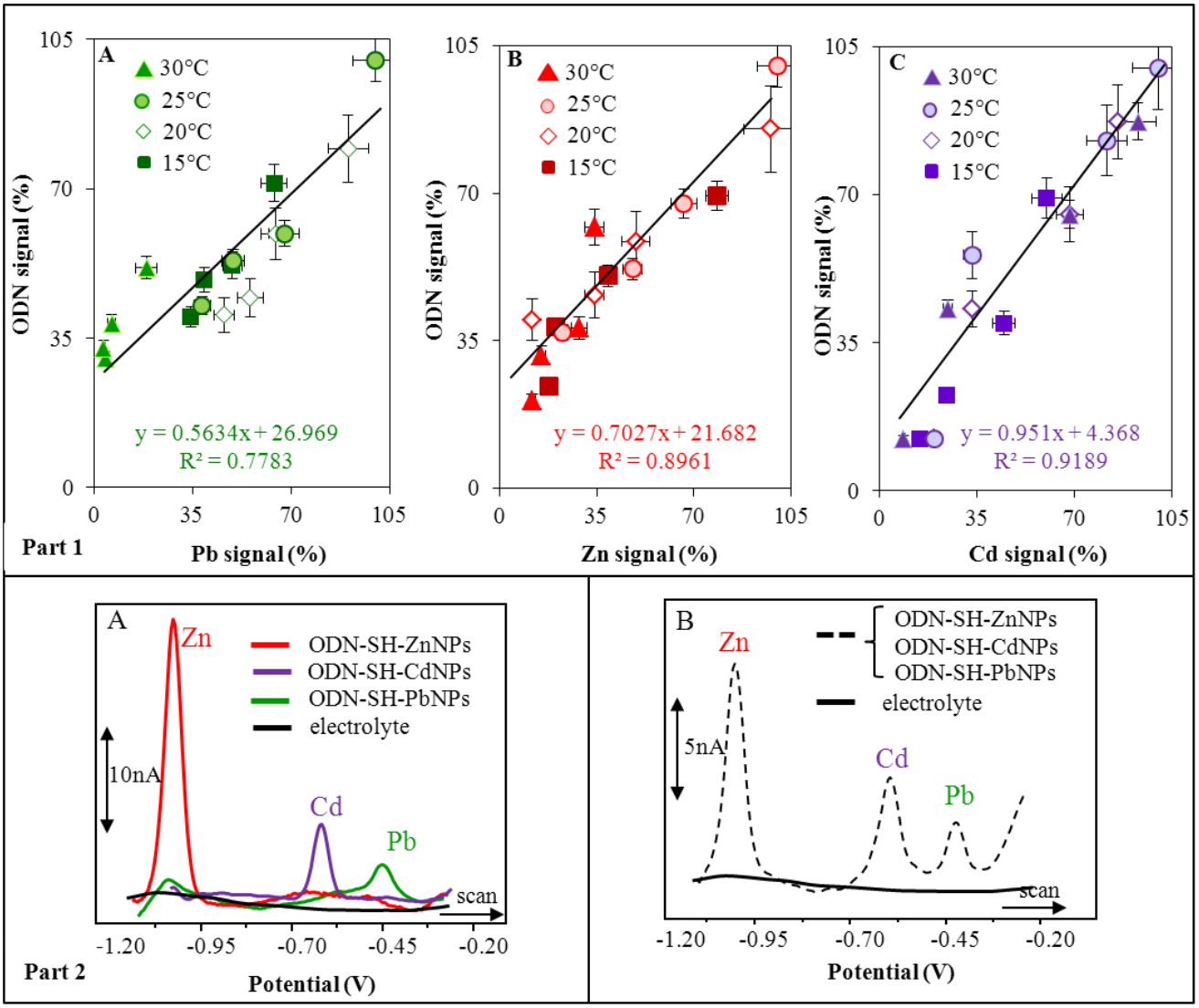

Figure 5. (**Part 1**) Correlation between the peak height of ODN and metal ions peak for hybridization temperatures: 15 °C, 20 °C, 25 °C and 30°C and concentrations of ODN-SH-NPs: 2.5; 5; 10 and 20 µg/ml for (**A**) ODN-SH-PbNPs (♦); (**B**) ODN-SH-ZnNPs (♦) and (**C**) ODN-SH-CdNPs. (**Part 2**) (**A**) voltamograms of Zn, Cd and Pb peak from complex ODN-SH-ZnNPs (-); ODN-SH-PbNPs (-) and ODN-SH-CdNPs (-), measured by DPV (concentration of ODN was 2 µg/ml). (**B**) Mixture of oligonucleotides (concentration of all ODNs was 2 µg/ml).

The results showed that both ODN-SH-ZnNPs and ODN-SH-PbNPs had optimal hybridization temperature 25 °C for 25 µg/ml. Further, ODN-SH-CdNPs provided optimal hybridization temperature as 25 °C also, but the other hybridization temperature provided almost similar data like hybridization at 25 °C. This we observed only in ODN-SH-CdNPs for 25 µg/ml concentration. We conclude from

the results that hybridization between ODN-SH and NPs within the range from 20 °C to 25 °C is suitable for the whole tested concentration interval.

3.4 Multi target determination

All above-mentioned experiments led to the optimization of the experimental conditions for individual experimental steps of the whole experiment. After it, we applied this procedure on the preparation samples containing mixture of specific probes and target sequence for the given specific sequence of ODN labelled by NPs. Test tubes with these reagents were placed in the automated pipetting system, where the isolation of target influenzas' ODN using the MPs, hybridization and washing steps take place. The resulted samples were determined using DPV. Voltammograms of individual signals for individual NPs are shown in Fig. 5/Part 2A. Red curve indicates record of ZnNPs with Zn signal in the potential area of -1.03 ± 0.005V. Violet curve indicates record of CdNPs and Cd signal at the potential of -0.63 ± 0.005V. Green curve represents PbNPs and Pb signal in the potential area of -0.45 ± 0.005V. The obtained signals are well separated and they are symmetric and well repeatable. In addition, we focused on the detection of individual ODN-SH-NPs in the mixture in test tube. Voltammogram of this measurement is shown in Fig. 5/Part 1B. In given potential areas all three signals are well evident and they correspond to ZnNPs – H1N1 influenza subtype (on the left), CdNPs – H3N2 influenza subtype (in the middle) and PbNPs H5N1 influenza subtype (on the right). This result confirmed our main goal of this study to suggest electrochemical nanobiosensor that enables identification of three specific influenza sequences without demands on special apparatus equipment.

4. CONCLUSIONS

We suggested fully functional hybridization kit for the identification of specific nucleic acids based on the hybridization and electrochemical detection. Due to the various NPs based on the different metals that provide signals at the specific potential areas, we can simultaneously determine three different influenzas subtypes in one sample. Connecting between paramagnetic particles, nanoparticles, automated pipetting system and electrochemical detection enable proposition of unique tool for the detection of specific NAs sequences. Electrochemical bionanosensors brings new possibilities into this field. High sensitivity of the suggested sensing device with the possibility of miniaturization, compatibility with modern technologies, low price and low demands on the power (possibility of *in situ* application) represent the excellent properties for detection of specific NAs in the field of pathogen and genetic disease diagnostics.

ACKNOWLEDGEMENTS
Financial support from NANIMEL GA CR 102/08/1546, NanoBioTeCell GA CR P102/11/1068 and CEITEC CZ.1.05/1.1.00/02.0068 is highly acknowledged.

References

1. M. L. Perdue and T. Nguyen, *Bull. World Health Organ.*, 90 (2012) 246.
2. T. Zhang, T. C. Wang, P. S. Zhao, M. Liang, Y. W. Gao, S. T. Yang, C. Qin, C. Y. Wang and X. Z. Xia, *Int. Immunopharmacol.*, 11 (2011) 2057.
3. M. T. Osterholm and D. A. Henderson, *Science*, 335 (2012) 801.
4. Y. Ghendon, *Eur. J. Epidemiol.*, 10 (1994) 451.
5. M. C. Christman, A. Kedwaii, J. Xu, R. O. Donis and G. Lu, *Infect. Genetics Evol.*, 11 (2011) 803.
6. S. E. Hensley, S. R. Das, A. L. Bailey, L. M. Schmidt, H. D. Hickman, A. Jayaraman, K. Viswanathan, R. Raman, R. Sasisekharan, J. R. Bennink and J. W. Yewdell, *Science*, 326 (2009) 734.
7. A. Hadidi, H. Czosnek and M. Barba, *J. Plant Pathol.*, 86 (2004) 97.
8. R. M. Lee and P. J. Tranel, *Weed Sci.*, 56 (2008) 283.
9. M. Seidel and R. Niessner, *Anal. Bioanal. Chem.*, 391 (2008) 1521.
10. M. Uttamchandani, J. L. Neo, B. N. Z. Ong and S. Moochhala, *Trends Biotechnol.*, 27 (2009) 53.
11. J. Wang, Y. F. Bai, T. X. Li and Z. Lu, *J. Biochem. Biophys. Methods*, 55 (2003) 215.
12. J. Wang, *Electroanalysis*, 19 (2007) 769.
13. H. Hanne, H. Ghourchian and A. A. Ziaee, *Anal. Biochem.*, 370 (2007) 195.
14. J. Wang, *Anal. Chim. Acta*, 500 (2003) 247.
15. V. Adam, D. Huska, J. Hubalek and R. Kizek, *Microfluid. Nanofluid.*, 8 (2010) 329.
16. R. M. Iost, J. M. Madurro, A. G. Brito-Madurro, I. L. Nantes, L. Caseli and F. N. Crespilho, *Int. J. Electrochem. Sci.*, 6 (2011) 2965.
17. D. N. Jiang, G. M. Xiang, J. H. Wu, C. Liu, F. Liu and X. Y. Pu, *Int. J. Electrochem. Sci.*, 7 (2012) 5273.
18. J. Chomoucka, J. Drbohlavova, M. Masarik, M. Ryvolova, D. Huska, J. Prasek, A. Horna, L. Trnkova, I. Provaznik, V. Adam, J. Hubalek and R. Kizek, *Int. J. Nanotech.*, 9 (2012) 746.
19. L. Trnkova, I. Fabrik, D. Huska, H. Skutkova, M. Beklova, J. Hubalek, V. Adam, I. Provaznik and R. Kizek, *J. Environ. Monit.*, 13 (2011) 2763.
20. I. M. Hsing, Y. Xu and W. T. Zhao, *Electroanalysis*, 19 (2007) 755.
21. D. Huska, V. Adam, J. Hubalek, L. Trnkova, T. Eckschlager, M. Stiborova, I. Provaznik and R. Kizek, *Chim. Oggi-Chem. Today*, 28 (2010) 18.
22. D. Huska, V. Adam, L. Trnkova and R. Kizek, *Chem. Listy*, 104 (2010) 177.
23. D. Huska, J. Hubalek, V. Adam, D. Vajtr, A. Horna, L. Trnkova, L. Havel and R. Kizek, *Talanta*, 79 (2009) 402.
24. D. Huska, O. Krystofova, V. Adam, J. Zehnalek, P. Babula, L. Havel, L. Trnkova and R. Kizek, *FEBS J.*, 276 (2009) 281.
25. B. Rittich, A. Spanova, D. Horak, M. J. Benes, L. Klesnilova, K. Petrova and A. Rybnikar, *Colloid Surf. B-Biointerfaces*, 52 (2006) 143.
26. J. Kukacka, D. Huska, V. Adam, R. Prusa, M. Kreidlova, J. Hubalek and R. Kizek, *Clin. Chem.*, 55 (2009) A42.
27. E. Palecek and M. Fojta, *Talanta*, 74 (2007) 276.
28. L. Krejcova, D. Dospivova, M. Ryvolova, P. Kopel, D. Hynek, S. Krizkova, J. Hubalek, V. Adam and R. kizek, *Electrophoresis*, 33 (2012) 3195.
29. L. Krejcova, D. Hynek, P. Kopel, V. Adam, J. Hubalek, L. Trnkova and R. Kizek, *Chromatographia*, in press, DOI 10.1007/s10337-012-2327-0 (2012).
30. S. H. Lim, F. Bestvater, P. Buchy, S. Mardy and A. D. C. Yu, *Sensors*, 9 (2009) 5590.
31. J. M. Hicks, *Hum. Pathol.*, 15 (1984) 112.
32. D. Huska, J. Hubalek, V. Adam and R. Kizek, *Electrophoresis*, 29 (2008) 4964.
33. R. Elghanian, J. J. Storhoff, R. C. Mucic, R. L. Letsinger and C. A. Mirkin, *Science*, 277 (1997) 1078.

34. E. Katz and I. Willner, *Angew. Chem.-Int. Edit.*, 43 (2004) 6042.
35. R. Prusa, J. Kukacka, D. Vajtr, D. Huska, J. Alba, V. Adam and R. Kizek, *Clin. Chem.*, 54 (2008) A156.
36. H. W. Gu, K. M. Xu, C. J. Xu and B. Xu, *Chem. Commun.* (2006) 941.
37. I. Koh and L. Josephson, *Sensors*, 9 (2009) 8130.
38. A. Akbarzadeh, M. Samiei and S. Davaran, *Nanoscale Res. Lett.*, 7 (2012) 1.
39. P. A. He, Y. Xu and Y. Z. Fang, *Anal. Lett.*, 38 (2005) 2597.
40. T. Neuberger, B. Schopf, H. Hofmann, M. Hofmann and B. von Rechenberg, *J. Magn. Magn. Mater.*, 293 (2005) 483.
41. F. J. Liu, S. Laurent, H. Fattahi, L. V. Elst and R. N. Muller, *Nanomedicine*, 6 (2011) 519.
42. J. Chomoucka, J. Drbohlavova, D. Huska, V. Adam, R. Kizek and J. Hubalek, *Pharmacol. Res.*, 62 (2010) 144.
43. J. Drbohlavova, R. Hrdy, V. Adam, R. Kizek, O. Schneeweiss and J. Hubalek, *Sensors*, 9 (2009) 2352.
44. M. Fojtikova, J. Bartoskova, S. Holubova, E. Kaletova, L. Trnkova and R. Kizek, Use of Paramagnetic Particles for the Isolation of Oligonucleotides with Different Sequence and Chain Length, 2010.
45. D. Huska, V. Adam, P. Babula, L. Trnkova, J. Hubalek, J. Zehnalek, L. Havel and R. Kizek, *Microchim. Acta*, 173 (2011) 189.
46. D. Huska, V. Adam, L. Trnkova and R. Kizek, *J. Magn. Magn. Mater.*, 321 (2009) 1474.
47. J. Wang, *Microchim. Acta*, 177 (2012) 245.
48. G. Doria, J. Conde, B. Veigas, L. Giestas, C. Almeida, M. Assuncao, J. Rosa and P. V. Baptista, *Sensors*, 12 (2012) 1657.
49. J. Hubalek, V. Adam and R. Kizek, New Approach in Rapid Viruses Detection and its Implementation on a Chip, IEEE Computer Soc, Los Alamitos, 2009.
50. Y. W. C. Cao, R. C. Jin and C. A. Mirkin, *Science*, 297 (2002) 1536.
51. T. A. Taton, C. A. Mirkin and R. L. Letsinger, *Science*, 289 (2000) 1757.
52. S. R. Nicewarner-Pena, R. G. Freeman, B. D. Reiss, L. He, D. J. Pena, I. D. Walton, R. Cromer, C. D. Keating and M. J. Natan, *Science*, 294 (2001) 137.
53. J. Wang, G. D. Liu and A. Merkoci, *J. Am. Chem. Soc.*, 125 (2003) 3214.
54. R. P. Bowater, R. J. H. Davies, E. Palecek and M. Fojta, *Chim. Oggi-Chem. Today*, 27 (2009) 50.
55. M. Fojta, F. Jelen, L. Havran and E. Palecek, *Curr. Anal. Chem.*, 4 (2008) 250.
56. E. Palecek, *Talanta*, 56 (2002) 809.
57. E. Palecek, *Electroanalysis*, 21 (2009) 239.
58. E. Palecek and M. Bartosik, *Chem. Rev.*, 112 (2012) 3427.
59. E. Palecek and F. Jelen, *Crit. Rev. Anal. Chem.*, 32 (2002) 261.
60. V. N. Goral, N. V. Zaytseva and A. J. Baeumner, *Lab Chip*, 6 (2006) 414.
61. S. Laschi and M. Mascini, *Med. Eng. Phys.*, 28 (2006) 934.
62. T. M. H. Lee and I. M. Hsing, *Anal. Chim. Acta*, 556 (2006) 26.
63. S. Martic, M. Labib and H. B. Kraatz, *Talanta*, 85 (2011) 2430.
64. M. Mir, A. Homs and J. Samitier, *Electrophoresis*, 30 (2009) 3386.
65. B. Hennequin, L. Turyanska, T. Ben, A. M. Beltran, S. I. Molina, M. Li, S. Mann, A. Patane and N. R. Thomas, *Adv. Mater.*, 20 (2008) 3592.
66. M. Redlberger-Fritz, S. W. Aberle, R. Strassl and T. Popow-Kraupp, *Eur. J. Clin. Microbiol. Infect. Dis.*, 31 (2012) 1593.
67. G. L. Long and J. D. Winefordner, *Anal. Chem.*, 55 (1983) A712.
68. A. B. Moghaddam, T. Nazari, J. Badraghi and M. Kazemzad, *Int. J. Electrochem. Sci.*, 4 (2009) 247.
69. Y. F. Qiao, J. S. Zhang, T. H. Lu and C. Li, *Chin. J. Inorg. Chem.*, 22 (2006) 1282.
70. J. D. Feng, W. J. Zhao, B. Su and J. M. Wu, *Biosens. Bioelectron.*, 30 (2011) 21.

71. L. Trnkova, M. Studnickova and E. Palecek, *Bioelectrochem. Bioenerg.*, 7 (1980) 643.
72. M. Fojta, *Collect. Czech. Chem. Commun.*, 69 (2004) 715.
73. V. Adam, D. Huska, S. Krizkova, J. Hubalek and R. Kizek, *FEBS J.*, 276 (2009) 95.
74. M. Q. Liu, C. H. Luo and H. Peng, *Talanta*, 88 (2012) 216.
75. S. Girousi and V. Kinigopoulou, *Cent. Eur. J. Chem*, 8 (2010) 732.
76. Q. Wang, L. J. Yang, X. H. Yang, K. M. Wang, L. L. He and J. Q. Zhu, *Anal. Chim. Acta*, 688 (2011) 163.
77. M. Fojta, P. Kostecka, H. Pivonkova, P. Horakova and L. Havran, *Curr. Anal. Chem.*7 (2011) 35.
78. M. Trefulka, M. Bartosik and E. Palecek, *Electrochem. Commun.*, 12 (2010) 1760.
79. Y. Zhang and T. H. Wang, *Theranostics*, 2 (2012) 631.
80. K. E. Sapsford, T. Pons, I. L. Medintz and H. Mattoussi, *Sensors*, 6 (2006) 925

5.3 Izolace a detekce chřipkového antigenu

5.3.1 Vědecký článek VI

KREJCOVA, L.; DOSPIVOVA, D.; RYVOLOVA, M.; KOPEL, P.; HYNEK, D.; KRIZKOVA, S.; HUBALEK, J.; ADAM, V.; KIZEK, R. Paramagnetic particles coupled with an automated flow injection analysis as a tool for influenza viral protein detection.

Electrophoresis, 2012, roč. 33. č. 21, s. 3195-3204. ISS 0173-0835. IF: 3.161

Podíl autorky Krejčová L.: 65 % textové části práce, 70 % experimentální části práce

Chřipkové viry mají na svém povrchu dva typy antigenů: hameglutinin (HA) a neuraminidázu (NA), které mají důležité role v životním cyklu viru *(Stevens, a kol., 2006)*. HA inicijuje infekci a je odpovědný za vstup viru do hostitelské buňky. NA ukončuje proces infekce a umožňuje uvolnění nově replikovaným virionům z hostitelské buňky *(Russell, a kol., 2008, Watanabe, a kol., 2010)*. Oba antigeny snadno a rychle podléhají mutacím, které jsou důvodem vzniku chřipkových epidemií a pandemií. Detekce epidemiologicky a pandemicky významných subtypů je nezbytná pro prevenci a kontrolu chřipkových onemocnění *(Schutten, a kol., 2013, Singh, a kol., 2014)*.

Cílem studie bylo navrhnout alternativní metodu pro detekci chřipkového hemaglutininu, biosenzor založený na izolaci a následné detekci chřipkového proteinu A/H5N1 (A/H5N1/Vietnam/1203/2004) značeného pomocí CdS QDs. HA byl izolován pomocí glykanem modifikovaných MPs (tento proces byl automatizován pomocí pipetovací stanice EP motion 5075). Izolovaná molekula (HA-QDs komplex) byla detekována pomocí dvou typů elektrod: skelná uhlíková elektroda (GC) a rtuťová kapková elektroda (HMDE). V případě detekce pomocí HMDE byly vzorky měřeny v klasickém tříelektrodovém zapojení a byl detekován jak signál kovu (Cd) pomocí DPV metody, tak signál HA pomocí AdTS DPV metody. Detekce HA proíhala v prostředí brdičkova elektrolytu a byly detekovány tři píky (odezva na interakci pomocného elektrolytu s HA proteinem). Z výsledků vyplívá, že se zvyšující se koncentrací HA se zvyšovala výrazně i výška píku v poloze -1,55 V a stejný trend byl zaznamenán i se zvyšující se koncentrací HA-QDs komplexu. Tvorba komplexu HA-

QDs byla potvrzena fluorescenčními metodami. Kromě detekce HA-CdS komplexu na rtuti byl komplex (respektive kovová část QDs) detekován pomocí SFIA analýzy na elektrodě ze skelného uhlíku (GC), i zde byla pro detekci Cd píku použita metoda DPV. Závěrem lze říci, že byla navržena a optimalizována metoda pro izolaci a detekci chřipkového hemaglutininu značeného pomocí Cd QDs. Pomocí navržené metody jsme byly schopni detekovat 10 ng/mg Cd (v komplexu HA-CdS), což ukazuje na možnost detekce submikrogramových množství HA. Navržený a optimalizovaný postup detekce HA-QDs komplexu spojený s jeho izolací pomocí glykanem modifikovaných MPs představuje citlivý a miniaturizovaný nástroj pro rychlou detekci hemaglutininu. Výhodou této metody je modifikovatelnost pro detekci ostatních proteinů, které mohou sloužit jako markery onemocnění.

Ludmila Krejcova[1]
Dana Dospivova[1]
Marketa Ryvolova[1,2]
Pavel Kopel[1,2]
David Hynek[1,2]
Sona Krizkova[1,2]
Jaromir Hubalek[1,2]
Vojtech Adam[1,2]
Rene Kizek[1,2]

[1]Department of Chemistry and Biochemistry, Faculty of Agronomy, Mendel University in Brno, Czech Republic, European Union
[2]Central European Institute of Technology, Brno University of Technology, Czech Republic, European Union

Received April 15, 2012
Revised July 2, 2012
Accepted July 3, 2012

Research Article

Paramagnetic particles coupled with an automated flow injection analysis as a tool for influenza viral protein detection

Currently, the influenza virus infects millions of individuals every year. Since the influenza virus represents one of the greatest threats, it is necessary to develop a diagnostic technique that can quickly, inexpensively, and accurately detect the virus to effectively treat and control seasonal and pandemic strains. This study presents an alternative to current detection methods. The flow-injection analysis-based biosensor, which can rapidly and economically analyze a wide panel of influenza virus strains by using paramagnetic particles modified with glycan, can selectively bind to specific viral A/H5N1/Vietnam/1203/2004 protein-labeled quantum dots. Optimized detection of cadmium sulfide quantum dots (CdS QDs)-protein complexes connected to paramagnetic microbeads was performed using differential pulse voltammetry on the surface of a hanging mercury drop electrode (HMDE) and/or glassy carbon electrode (GCE). Detection limit (3 S/N) estimations based on cadmium(II) ions quantification were 0.1 μg/mL or 10 μg/mL viral protein at HMDE or GCE, respectively. Viral protein detection was directly determined using differential pulse voltammetry Brdicka reaction. The limit detection (3 S/N) of viral protein was estimated as 0.1 μg/mL. Streptavidin-modified paramagnetic particles were mixed with biotinylated selective glycan to modify their surfaces. Under optimized conditions (250 μg/mL of glycan, 30-min long interaction with viral protein, 25°C and 400 rpm), the viral protein labeled with quantum dots was selectively isolated and its cadmium(II) content was determined. Cadmium was present in detectable amounts of 10 ng per mg of protein. Using this method, submicrogram concentrations of viral proteins can be identified.

Keywords:
Electrochemical detection / Hemagglutinin / Influenza / Magnetic separation / Voltammetry
DOI 10.1002/elps.201200304

1 Introduction

Influenza represents one of the greatest threats in society today. It is not surprising that the World Health Organization (WHO) initiated the Global Influenza Program, which provides member states with strategic guidance, technical support, and coordination of activities essential to better prepare healthcare systems against seasonal, zoonotic, and pandemic influenza threats to populations and individuals (http://www.who.int/influenza/en/) [1, 2]. According to WHO, seasonal influenza is responsible for several million cases of acute illnesses and between 250 000 and 500 000 deaths each year [3].

There are three genera of the influenza virus: Influenza virus A, Influenza virus B, and Influenza virus C. They are RNA viruses that make up three of the five genera of the *Orthomyxoviridae* family. Type A virus, the most virulent human pathogens among the three influenza types, causes the most severe disease. This virus can be further subdivided into different serotypes based on antibody responses. The influenza virus contains two major surface proteins: hemagglutinin (HA) and neuraminidase. HA mediates glycan receptor binding and membrane fusion for viral entry. Neuraminidase conducts receptor-destroying enzyme activity important for virus release [4]. Subtypes of influenza viruses are classified according to these proteins [5, 6].

More than 500 cases of avian H5N1 influenza infections in humans have been reported from 15 countries, of which nearly 60% have resulted in death (Fig. 1). Recently published meta-analysis in Science shows 12 677 participants in 20 studies that have been infected with the avian H5N1 have mild

Correspondence: Professor Rene Kizek, Department of Chemistry and Biochemistry, Mendel University in Brno, Zemedelska 1, CZ-613 00 Brno, Czech Republic
E-mail: kizek@sci.muni.cz
Fax: +420-5-4521-2044

Abbreviations: **CdS QDs**, cadmium sulfide quantum dots; **FIA**, flow injection analysis; **GCE**, glassy carbon electrode; **HA**, hemagglutinin; **HMDE**, hanging mercury drop electrode; **QD**, quantum dots; **WHO**, World Health Organization

Colour Online: See the article online to view Figs. 1–8 in colour.

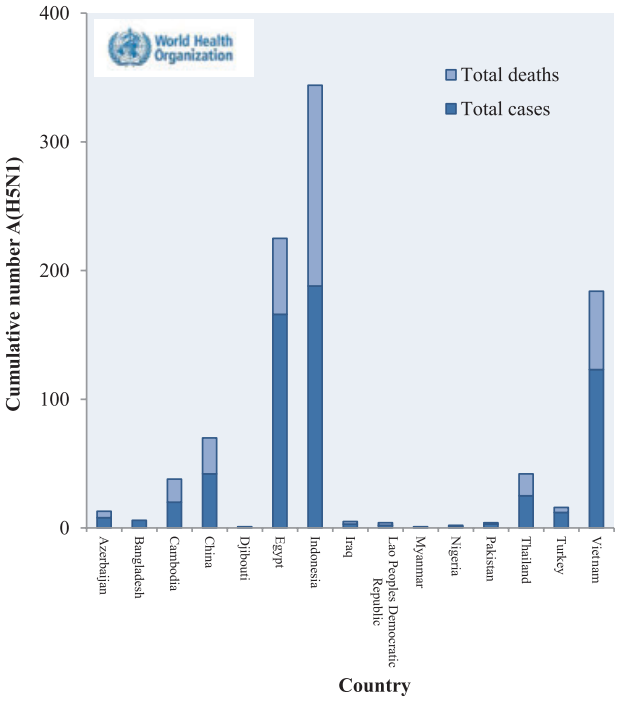

Figure 1. Affected areas with confirmed cases of H5N1 avian influenza since April 5, 2003, modified according to http://www.who.int/influenza/human_animal_interface/avian_influenza/en/.

symptoms or subclinical infections that are not currently accounted for; thus, the true fatality rate for H5N1 influenza viruses is likely to be less than the frequently reported rate of more than 50% [7]. It is possible that deaths caused by H5N1 infections, as documented by WHO, are also underestimated. A portable and robust standardized approach for large-scale studies is examined.

Nanoparticles have numerous possible applications in biosensors and bioassays. Electrochemical biosensors and bioassays have attracted considerable interest due to their high performance, miniaturized construction, and low cost [8]. Conventional enzyme and electroactive labels have incorporated nanoparticles, nanotubes, and nanowires due to their improved sensitivity in small molecule and protein detection. Gold nanoparticles electrodes used to build immunosensors were the first target materials studied in electrochemical immunosensors and DNA biosensors [9–11]. Semiconductor nanoparticles, inorganic compounds, and apoferritin or liposomes-labeled complexes can be applied as electrochemical targets for bioassays. Semiconductor nanoparticles also called quantum dots are of particular interest because of their size and tuneable fluorescence emission. Owing to their unique properties, semiconductor nanoparticles have generated considerable interest for optical biodetection. The intrinsic redox properties and sensitive electrochemical stripping analysis of the metal components of semiconductor nanoparticles cause labels in the electrochemical biosensors to be very sensitive; thus, low detection limits can be achieved. Liu et al. introduced an electrochemical immunoassay protocol for simultaneously measuring multiple protein targets based on the use of CdS, ZnS, and PbS quantum dots (QDs). Each protein gives a distinct voltammetric peak whose position and size reflects the identity and amount of the corresponding antigen with fmol detection limits [12, 13].

This study aimed to develop a low-cost isolation and rapid CdS quantum dots-based biosensor to detect viruses. Viral quantity was determined through cadmium(II) ion concentrations abstracted from quantum dots. The results were confirmed by differential pulse voltammetry Brdicka reaction. Particular attention was focused on the application of streptavidin-coated paramagnetic particles modified with biotinylated glycan and its selective binding properties to the influenza virus.

2 Materials and methods

2.1 Chemicals

Tris(2-carboxyethyl)phosphine was from Molecular Probes (Eugene, OR, USA). $Co(NH_3)_6Cl_3$ and other chemicals used were purchased from Sigma Aldrich (St. Louis, MA, USA) unless otherwise noted. Stock solutions were prepared from ACS water. pH value and conductivity was measured using inoLab Level 3 (Wissenschaftlich-Technische Werkstatten; Weilheim, Germany). Deionized water underwent demineralization by reverse osmosis using Aqua Osmotic 02 (Aqua Osmotic, Tisnov, Czech Republic) and was subsequently purified using Millipore RG (MilliQ water, 18 MΩ, Millipore, Billerica, MA, USA). Deionized water was used for rinsing, washing, and buffer preparation.

2.2 Preparation of CdS QDs

CdS QDs were prepared using a slightly modified version of a published method [14]. Cadmium nitrate tetrahydrate $Cd(NO_3)_2 \cdot 4H_2O$ (0.1 mM) was dissolved in ACS water (25 mL). A 3-mercaptopropionic acid (35 μL, 0.4 mM) was slowly added to the stirred solution. Afterward, the pH was adjusted to 9.11 with 1 M NH_3 (1.5 mL). Sodium sulfide monohydrate $Na_2S{\cdot}9H_2O$ (0.1 mM) in ACS water was poured into the solution while vigorously stirring. The acquired yellow solution was stirred for 1 h. Prepared CdS-quantum dots were stored in the dark at 4°C.

2.3 Preparation of samples

A/H5N1/Vietnam/1203/2004 protein (accession no. ISDN 38687, Prospec-Tany TechoGene, Tel Aviv, Israel) (200 μL, 100 μg/mL) was mixed with a solution of CdS QDs (100 μL). This mixture was shaken for 24 h at room temperature (Vortex Genie2 [Scientific Industries, Bohemia, NY, USA]). The volume of solution was reduced to 100 μL on an Amicon

Ultra 3k centrifugal filter device (Millipore). Centrifuge 5417R (Eppendorf, Hamburg, Germany) was performed under the following parameters 15 min, 6000 rpm, 20°C. The obtained concentrate was diluted with 400 μL of ACS water and reduced on centrifuge to 100 μL. The process was repeated five times. The washed sample was diluted to 300 μL and used for succeeding measurements.

2.4 Magnetic nanoparticle separation

Streptavidin Dynabeads M-270 was purchased from Life Technologies (Carlsbad, CA, USA). Biotinylated multivalent glycans (01–078 [Neu5Acα2–3Galβ1–3GlcNAcβ1-PAA-biotin]) were obtained from GlycoTech (Gaithersburg, MD, USA). Soluble forms of HA derived from newly emerging influenza viruses expressed in baculovirus, were purchased from Prospec-Tany TechnoGene. Streptavidin Dynabeads M-270 (10 μL) was pipetted to microplates (PCR 96, Eppendorf), then subsequently transferred to a magnet plate. Stored solution was drained from the magnetic particles. Magnetic particles were washed three times with 100 μL of phosphate buffer (0.3 M, pH 7.4, made from NaH_2PO_4 and Na_2HPO_4). Twenty microliters of biotinylated glycan were added to each of the wells and incubated (30 min, 25°C, 400 rpm). After the incubation, the sample was washed three times with phosphate buffer (0.3 M, pH 7.4). Subsequently 20 μL of H5N1-Cd-labeled protein was added. It was further incubated (30 min, 25°C, 400 rpm) and washed with 100 μL of phosphate buffer (0.3 M, pH 7.4). Thirty-five microliters of phosphate buffer (0.3 M, pH 7.4) was added followed by the treatment of ultrasound needle (2 min). The plate was transferred to the magnet plate and the supernatant (product) was measured using differential pulse voltammetry. The detected substance was identified as cadmium (quantum dots).

2.5 Determination of proteins by Brdicka reaction

Differential pulse voltammetric measurements were performed with a 747 VA Stand instrument connected to a 693 VA Processor and 695 Autosampler (Metrohm, Herisau, Switzerland). It was equipped with a standard cell consisting of three electrodes, a cooled sample holder, and a measurement cell set at 4°C (Julabo F25, JulaboDE, Seelbach, Germany). The three-electrode system consisted of a hanging mercury drop electrode (HMDE) with a drop area of 0.4 mm^2 as the working electrode, an Ag/AgCl/3M KCl reference electrode, and a platinum electrode acting as the auxiliary. VA Database 2.2 by Metrohm was used for data acquisition and subsequent analysis. The analyzed samples were deoxygenated prior to measurements by purging with argon (99.999%) saturated with water for 120 s. Brdicka-supporting electrolyte containing 1 mM $Co(NH_3)_6Cl_3$ and 1M ammonia buffer (NH_3(aq) + NH_4Cl, pH = 9.6) was used. The supporting electrolyte was exchanged after each analysis. The parameters of the measurement were as follows: initial potential of −0.7 V, end potential of −1.75 V, modulation time 0.057 s, time interval 0.2 s, step potential 2 mV, modulation amplitude −250 mV, E_{ads} = 0 V. The volume of injected sample was 5 μL with a total volume of 2 mL in the measurement cell (5 μL of sample + 1995 μL Brdicka solution).

2.6 Electrochemical determination of cadmium

Determination of cadmium by differential pulse voltammetry was performed using a 663 VA Stand (Metrohm) and a standard cell with three electrodes. The three-electrode system consisted of an HMDE with a drop area of 0.4 mm^2 as the working electrode, an Ag/AgCl/3M KCl reference electrode, and a glassy carbon acting as the auxiliary electrode. GPES 4.9 software was employed for data processing. The analyzed samples were deoxygenated prior to measurements by purging with argon (99.999%). Acetate buffer (0.2 M CH_3COONa + CH_3COOH, pH 5) was used as a supporting electrolyte. The supporting electrolyte was replaced after each analysis. The parameters of the measurement were as follows: purging time 120 s, deposition potential −0.9 V, accumulation time 240 s, equilibration time 5 s, modulation time 0.057 s, interval time 0.2 s, initial potential −0.9 V, end potential −0.3 V, step potential 0.00195 V, modulation amplitude 0.02505 V, volume of injected sample: 10 μL, volume of measurement cell 1 mL (10 μL of sample; 990 μL acetate buffer).

2.7 Flow injection analysis (FIA)

An automated FIA system with electrochemical detection was proposed. The system consisted of a solvent delivery automated analytical syringe operating in a working volume of 1–50 μL, with variable speeds ranging from 1.66 to 50 μL/s (Model eVol, SGE Analytical Science, Kiln Farm Milton Keynes, UK), a 3-way 2-position selector valve (made from 6-way valve) (Valco Instruments, Schenkon, Switzerland), and a dosing capillary that directly entered the electrochemical flow cell (CH Instruments, Austin, TX, USA). To prepare a fully automated system, a switching valve that enabled alternating between the off waste and sample flow was placed in the system. The sample (10 μL) was injected by an automated syringe (SGE Analytical Science) through a flow cell at a speed of 1.66 μL/s. The flow cell was first rinsed clean with 200 μL of ethanol in water (75% *v*/*v*), then with 200 μL of 100% ethanol, and stabilized with 200 μL of supporting electrolyte. Cleaning procedures were applied after every 50 measurements. The electrochemical flow cell includes a low volume (1.5 μL) flow-through analytical cell (CH Instruments, Austin, TX, USA), which consisted of a doubled glassy carbon working electrode, Ag/AgCl reference electrode, and an output steel tubing as an auxiliary electrode. An electrochemical flow cell was connected to a miniaturized control module, potentiostat 910 PSTAT mini (Metrohm). The differential pulse

voltammetry was used as the measuring method with the following parameters: initial potential −1.2 V, end potential −0.2 V, modulation amplitude 0.05 V, step potential 0.001 V. Acetate buffer (0.2 M, pH 5) was used as the supporting electrolyte. Each sample solution of 10 μL was diluted in acetate buffer. The data obtained were processed by the PSTAT software 1.0 (Metrohm). The experiments were carried out at 20°C.

2.8 Fluorescence measurement

Fluorescence spectra were acquired by a multifunctional microplate reader called Tecan Infinite 200 PRO (TECAN, Männedorf, Switzerland). The excitation wavelength was set at 350 nm and the fluorescence scan was measured every 5 nm within a 400 to 850 nm wavelength range. Each intensity value was based on an average of five repeated measurements. The detector gain was set at 100. The sample (50 μL) was placed in a transparent 96-well microplate with a flat bottom (Nunc). Fluorescence monitoring was performed using In vivo Xtreme system by Carestream (Rochester, NY, USA). This instrument was equipped with a 400 W xenon light source and 28 excitation filters (410–760 nm). The emitted light is captured by a 4MP CCD camera. The excitation wavelength was set at 410 nm and the emission was measured at 700 nm. The exposition time was 4.5 s. Sample volumes of 25 μL were placed in microtitrate plates (Eppendorf).

2.9 Robotic pippeting station

Computer controlled automated pipetting station, Ep-Motion 5075 (Eppendorf) was used for automated sample handling prior to electrochemical analysis. Positions C1 and C4 were thermostated (Epthermoadapter PCR96). At position B1, module reservoir for washing solutions and waste were placed. Tips were placed in positions A4 (ePtips 50), A3 (ePtips 300), and A2 (ePtips 1000). Transfer was ensured by a robotic arm with pipetting adaptors (TS50, TS300, TS1000–numeric labeling refers to maximal pipetting volume in μL) and a gripper for platform transport (TG-T). The program sequence was edited and the station was controlled in pEditor 4.0. For sample preparation, two platforms were used. A thermorack for 24 × 1.5–2 mL microtubes (Position C3) was used to store working solutions and a 96-well DPW (low binding DNA) thermostated plate with a well volume of 200 μL (Position C1) was also available. After separation, the magnetic particles were forced apart using a Promega magnetic pad (Promega, Madison, WI, USA) (position B4). The solutions were then transferred to a new DPW plate.

2.10 Descriptive statistics

Data were processed using MICROSOFT EXCEL (Microsoft, Redmond, WA, USA) and STATISTICA.CZ Version 8.0 (StatSoft CR, Prague, Czech Republic). The results are expressed as mean ±SD unless otherwise noted. The detection limits (3 S/N) were calculated according to Long and Winefordner [15], whereas *N* was expressed as a standard deviation of noise determined in the signal domain unless otherwise stated.

3 Results and discussion

At the beginning of 2009, the influenza A (H1N1) virus emerged and spread to most parts of the world. WHO considered this virus a potentially dangerous strain that could lead to a pandemic with high mortality. Transmission of swine H1N1 virus into the human population probably occurred due to changes in HA and their sialyl glycan-based receptors. Other contributing factors include its distribution in tissues of different species, host range, and tissue tropism and its capacity to initiate a human pandemic. Based on previous studies, H5N1 consists of homology-based HA-glycan structural complexes with human-type oligosaccharide receptors (*N*-acetylneuraminic acid α2–6-linked to galactose) and avian-type (*N*-acetylneuraminic acid α2–3-linked to galactose) [16–21]. However, these receptors and interactions can also be used as tools for successful isolation of various types of influenza viruses [22]. Current studies attempted to design a biosensor, which consists of paramagnetic particles-based isolation of viral proteins modified with QDs and subsequent electrochemical detection of both protein and QDs as a new type of labeling.

3.1 Characterization of QD labeling

Aqueous CdS QDs displayed long lifetimes accompanied by excellent stability [14]. The current study affirmed the stability of synthesized CdS QDs longer than 1 month. The emission spectrum of CdS QDs is shown (green line) in Fig. 2A with

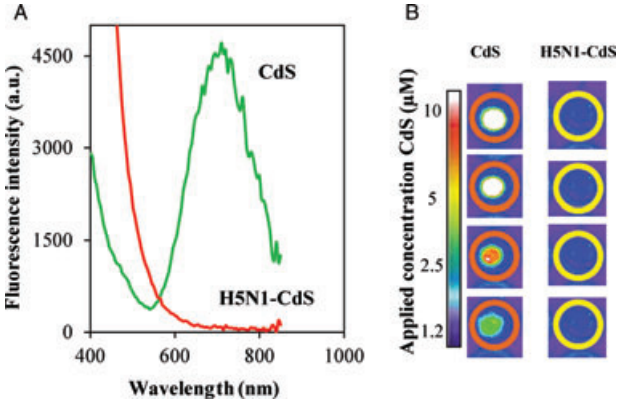

Figure 2. (A) Fluorescence intensity of CdS QD (green line) and complex H5N1-CdS (red line), excitation wavelength was 350 nm. (B) Picture of CdS QDs fluorescence (orange rings) and complex H5N1-CdS (yellow rings) measured on In vivo Xtreme system. Presented position creates concentration line in half part dilution.

an emission maximum at 710 nm. Moreover, it was found that the interaction of CdS QDs with H5N1 (red line) caused significant fluorescence quenching within the 560–850 nm range. In vivo imaging was utilized to confirm increasing concentrations of CdS QDs, which resulted in higher fluorescence intensity (Fig. 2B). The increasing fluorescence intensity of CdS QDs with corresponding increasing QDs concentrations (1.2–10 μM) are shown in Fig. 2B. The relative intensity scale is added designating the white color as of highest intensity. Fluorescence quenching after QDs interaction with H5N1 was observed. No fluorescence was detected after the interaction (H5N1-CdS, Fig. 2B). The results of gradual fluorescence quenching suggest there is a very strong interaction between CdS QDs and viral proteins apparently through disulfide bonds with free protein sulfhydryl groups (CdS-S-viral protein) and/or via binding of cadmium(II) atoms with cysteine, histidine, or lysine. Observed effects conclude the CdS quantum dot–protein interaction is strong and significant enough to be further used for other processes and applications.

3.2 Determination of cadmium(II) ions at mercury and glassy carbon electrode (GCE)

For quantification purposes, the determination of the presence of formed CdS QDs and proteins complexes by electrochemical quantification of cadmium(II) ions is advantageous in that electro-analysis of metal ions is a sensitive and robust technique routinely used for various types of real sample analysis [23, 24]. Differential pulse voltammetry was used in cadmium(II) ion detection. Two types of working electrodes were tested. HMDE was used for standard purposes. The obtained dependence was linear within a 0.1–100 μM range as follows: $y = 1.6958x$; $R^2 = 0.9911$, $n = 5$, RSD = 4.8. An automated FIA system in combination with electrochemical detection and miniaturized micropotentiostat for detection of cadmium(II) ions [25] was suggested. Cadmium(II) ions within the same concentration interval as HMDE were detected at a GCE in the presence of acetate buffer (pH 5.0). When cadmium(II) ions were detected using FIA technique coupled with GCE (FIA-GCE), well repeatable responses were obtained with the following calibration equation $y = 0.7710x - 0.2621$, $R^2 = 0.9982$, $n = 5$, RSD = 6.3. Both working electrodes were tested and cadmium(II) ions were quantified at the synthesized QDs. The obtained signals of cadmium(II) ions were recalculated to a concentration according to the calibration dependences mentioned above. HMDE calibration dependence was strictly linear within the whole tested concentration range up to 100 μM; however, GCE dependence was of quadratic course. Thus, the correlation of both dependences within the concentration interval 0.25 μM to 30 μM of cadmium(II) ions was tested. The correlation of both methods was favorable with R^2 exceeding 0.99; however, the sensitivity of GCE to cadmium(II) ions was 30% lower than HMDE.

Based on our findings, both HMDE and GCE can be utilized for QDs quantification. Therefore, interest in whether these electrodes could be utilized for quantification of CdS QDs-viral protein complexes was further examined. Viral proteins (A/H5N1/Vietnam/1203/2004; 100 μg/mL) were incubated in the presence of CdS (for other experimental conditions, see Section 2). The modified protein was purified and the unbound CdS was removed. Based on fluorimetric analysis, which confirmed QDs-viral protein complexes (Fig. 2), studies were attempted to determine the complexes through cadmium(II) ions content using differential pulse voltammetry at HMDE and GCE. The following protein concentrations (from 0.5 to 45 μg/mL) were applied to CdS QDs. Typical dependence of cadmium(II) concentration on protein concentration incubated with CdS QDs and measured at HMDE and/or GCE are shown in Fig. 3A and B, respectively. Dependence measured at HMDE had strictly linear characteristics ($y = 0.2871x$, $R^2 = 0.9973$, $n = 5$, RSD 2.1%). The observed voltammetric signals were

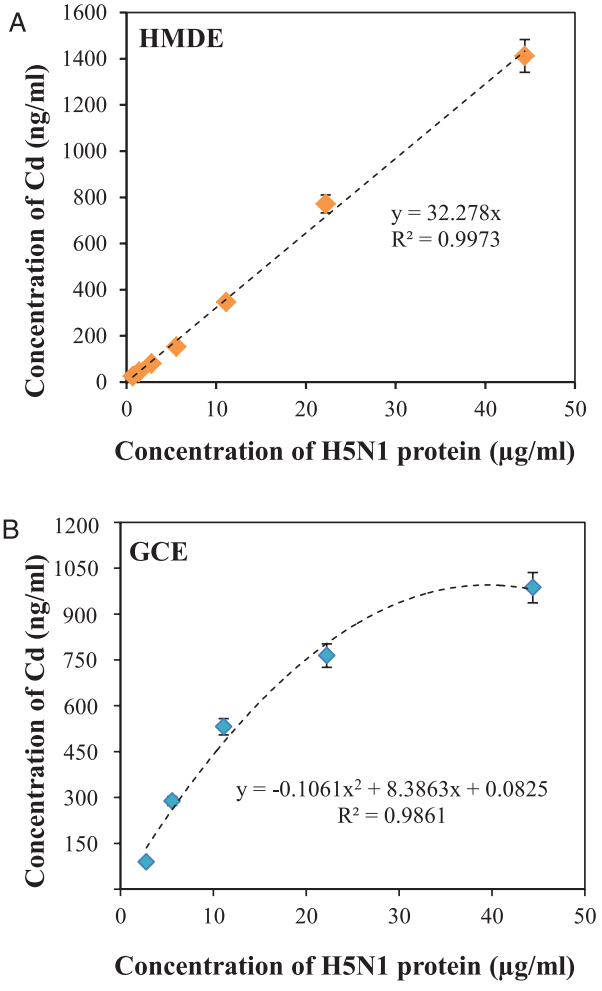

Figure 3. Dependences of cadmium ions concentration (related to protein amount) on various concentrations of complex H5N1-CdS (1: 100; 2: 50; 3: 25; 4: 12.5; 5: 6.2; 6: 3.1 7: 1.0 μM measured at (A) HMDE and (B) and FIA-GCE.

well developed and distinguishable at potential −0.6 V. Moreover, ratio of cadmium content in the formed complexes was calculated. There were approximately 20 cadmium(II) ions per complex. The ability to detect cadmium based on an indirect approach of detecting QDs-protein complexes shows great promise and pertinence. Based on obtained results, the detection limit for viral protein (3 S/N) was estimated as 0.1 μg/mL. The FIA-GCE exhibited nonlinear dependence. A mathematical approach in the form of a quadratic function (RSD 4.8%) determined protein concentration. In spite of the nonlinear dependence, the ratio of cadmium content in QDs-protein complexes demonstrated a repeated value of 20:1. The detection limit (3 S/N) of viral protein was estimated as 1 μg/mL. Both estimated detection limits pertain to real concentrations of cadmium ions that could be detected when analyzing protein-modified QDs.

3.3 Analysis of CdS QDs viral proteins complex

In addition to detecting cadmium(II) ions, this study investigated the presence of complexes in relation to viral proteins. Differential pulse voltammetry Brdicka reaction, a highly sensitive technique, was utilized to detect Cd QDs-protein complexes [26, 27]. The reaction's mechanism is based on the catalytic evolution of hydrogen on mercury electrodes from protein solutions containing SH groups in ammonia buffer and hexaamminecobalt chloride complexes ($Co(NH_3)_6Cl_3$) [28]. The mechanism of the reaction is annotated in detail, but it is believed that the cobalt(II) protein, peptide, and basic nitro compounds play important roles in the catalytic process. This method is highly recommended for sensitive analysis of peptides and proteins [29]. Communication between cobalt(II) ions and protein causes a decrease in cobalt peak and the occurrence of two new voltammetric peaks between

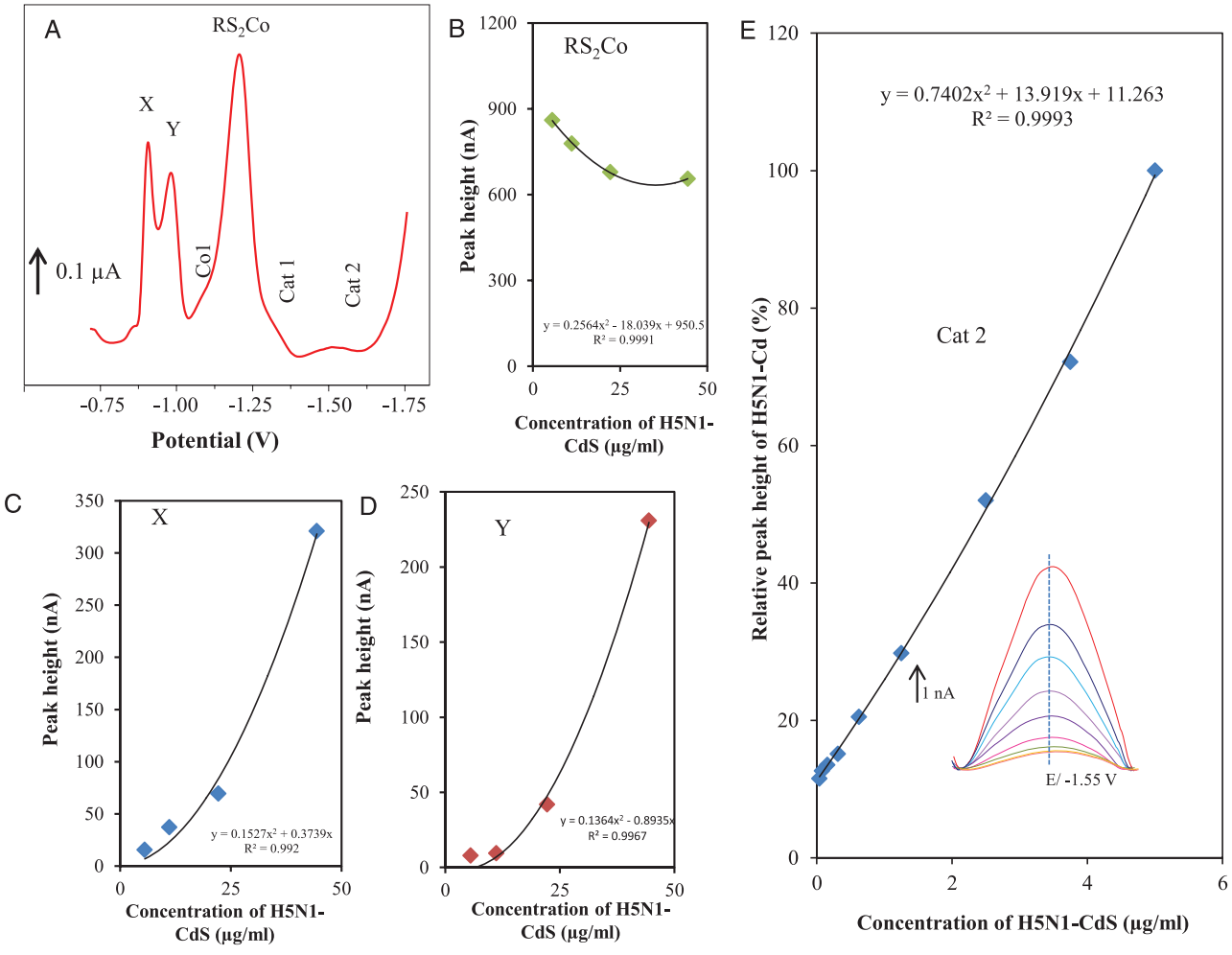

Figure 4. (A) Typical differential pulse Brdicka voltammogram of H5N1-CdS (10 μg/mL protein). Dependences of heights of (B) RS2Co, (C) signal X and (D) signal Y on concentration of H5N1-CdS QDs complex. (E) Dependences of Cat2 peak height on concentration of H5N1-CdS QDs complex; in inset: typical catalytic signal Cat2. The parameters of the measurement were as follows: initial potential of −0.7 V, end potential of −1.75 V, modulation time 0.057 s, time interval 0.2 s, step potential 2 mV, modulation amplitude −250 mV, E_{ads} = 0 V, volume of sample: 5 μL.

−1.2 and −1.5 V. The reduction of complex $R(SH)_2$ and Co(II) at potential −1.35 V corresponds to the first catalytic signal (RS_2Co). Cat1 and Cat2 signals correspond to the reduction of hydrogen at the mercury electrode. These two signals can be used to quantify complexes because height is proportional to the concentration of protein. In addition, the signal, Co1, could occasionally result from the reduction of $[Co(H_2O)_6]^{2+}$ [30]. Under current conditions, formation of catalytic signals was present between −1.0 and −1.1 V for first catalytic signal (RS_2Co) and −1.2 and −1.5 V for Cat1 and Cat2 signals, respectively (Fig. 4A). Varied strength of signal Co1 was observed at potential −0.8V. Dependence of the RS_2Co peak height on viral protein concentration is shown in Fig. 4B. Results clearly show peak height decreased with the increasing concentrations of viral protein. This phenomenon is the best explained with the formation of a complex between an SH group, Brdicka solution (cobalt ions), and CdS QD. Along with standard Brdicka peaks, two new peaks labeled X and Y were present owing to the complex formation between CdS QDs and viral protein's -SH groups. This was apparent from the obtained dependences on the concentration of protein, which are shown in Fig. 4C and D. From an analytical point of view, Cat2 is the most important detected signal. The signal increased with increasing concentrations of protein, which is shown in Fig. 4E. The detection limit (3 S/N) of viral protein was estimated as 100 ng/mL (more details will be published elsewhere).

3.4 Magnetic particles for viral isolation

The isolation procedure utilized a microfluidic instrument to perform paramagnetic particle detection. Similar approaches have implemented microfluidic platforms that can detect pathogenic avian influenza virus H5N1 in a throat swab sample. The technique coupled with polymerase chain reaction uses magnetic forces to manipulate a free droplet containing superparamagnetic particles [31–33]. These approaches are so sensitive, as Mizutani et al. showed, that they were able to isolate five particles from the influenza virus [34]. Magnetic particles can also be used for viral infection characterization. Virion immunosorting with magnetic nanobeads is direct, efficient, and adaptable to viral characterization at a nanometric resolution [35]. Another approach involved an immunomagnetic bead-based microfluidic system. By performing a simple two-step diagnostic process that includes a magnetic bead-based fluorescent immunoassay and an endpoint optical analysis the technique allows rapid detection of influenza A virus. Influenza A was targeted with magnetic particles and then labeled with a fluorescent signal

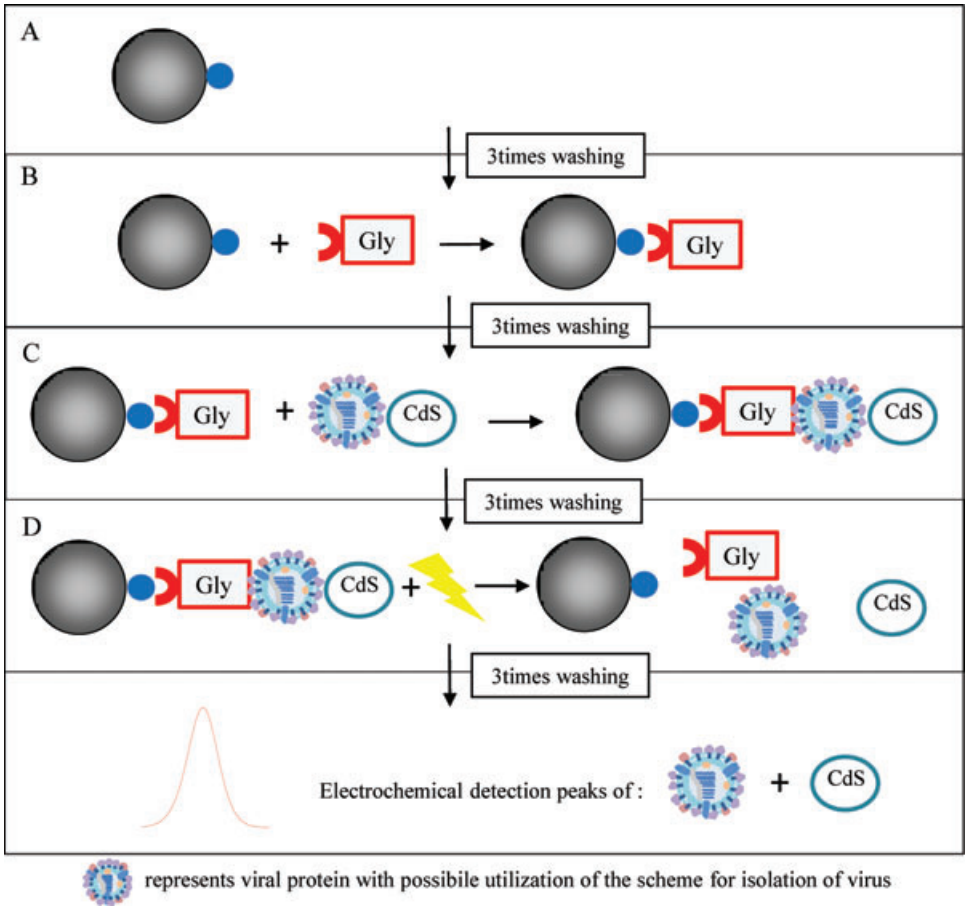

Figure 5. Scheme of a fully automated method of detection H5N1 using paramagnetic-based isolation and QD-based detection. (A) Paramagnetic streptavidin-modified particles are prepared by washing in buffer. (B) Biotinylated glycan binds to paramagnetic streptavidin-modified particles due to biotin-streptavidin affinity [45,46]. (C) Preparation of complex of CdS QDs-viral protein with the paramagnetic particles. (D) Washing and releasing of protein and cadmium(II) ions from the particles using ultrasonic pulse. (E) Electrochemical detection of HA protein and Cd.

using mAb with R-phycoerythrin [36]. Taking advantage of the large surface area-to-volume ratio, antibody-conjugated magnetic nanoparticles can act as an effective probe to extract influenza virus for gel electrophoresis and on-bead mass spectrometric analysis [37]. An approach describing sandwich design hybridization probes consisting of magnetic particles and quantum dots with target DNA, and their application in the detection of avian influenza virus (H5N1) sequences were also published [38]. Based on the previously published results, a combination of several approaches was integrated to sensitively select and determine H5N1 viral protein. Streptavidin-modified paramagnetic particles were mixed with biotinylated selective glycan. Glycan-binding proteins are often expressed by viruses, bacteria, and protozoa on their surfaces to facilitate their attachment to host cells and establish colonization and infection. The first key step in the process of infection, transmission, and virulence of influenza viruses involves HA, a trimeric glycoprotein expressed on the influenza virus membrane [5], which binds to a host cell's surface glycans via a terminal sialic acid (Sia) with α2–3 and α2–6 linkages [39, 40]. A fully automated setup was developed using a pipetting robot as described in Fig. 5. (PCR 96) 10 μL of Dynabeads M-270 Streptavidin were pipetted (Fig. 5A) out of each well of a plate. The plate was then transferred to a magnet plate where the stored solution was extracted from the beads. Beads were washed three times with 100 μL of phosphate buffer (0.3 M; pH 7.4) followed by the addition of 20 μL biotinylated glycan to each well. In the following step, 20 μL of H5N1-Cd-labeled protein was added proceeded by incubation (30 min, 25°C, 400 rpm) and washing with 100 μL of phosphate buffer (0.3 M; pH 7.4) (Fig. 5C). Samples were treated with ultrasound needle (2 min.) (Fig. 5D). The plate was transferred to a magnet, and the product from each well was analyzed using electrochemical analysis. Cadmium was detected by differential pulse voltammetry and H5N1 protein was confirmed present using Brdicka reaction (Fig. 5).

3.5 Optimization of biosensing system parameters

Selected components and their effect were tested to design a biosensor. The influence of varying concentrations of glycan on the amount of isolated H5N1 CdS QDs-viral protein complex was investigated. Changes in cadmium(II) ions peak height showed increasing dependency on the concentration of biotinylated glycan. Thirty-minute treatments with viral protein (5 μg/mL) at 25°C and 400 rpm showed a maximum response with 250 μg/mL of glycan (Fig. 6A). Maximum capacity of particles was not achieved until concentrations reached 1 mg/mL, but this in some biosensing applications is economically disadvantageous. Increasing the surface coverage of coated paramagnetic particles can also be achieved by imposing longer interaction time. Thirty to sixty minutes of incubation treatments (up to 60%), show a dramatic increase in signal as shown in Fig. 6B. The cadmium peaks are shown in Fig. 6B. Treatments lasting 120 min augment the

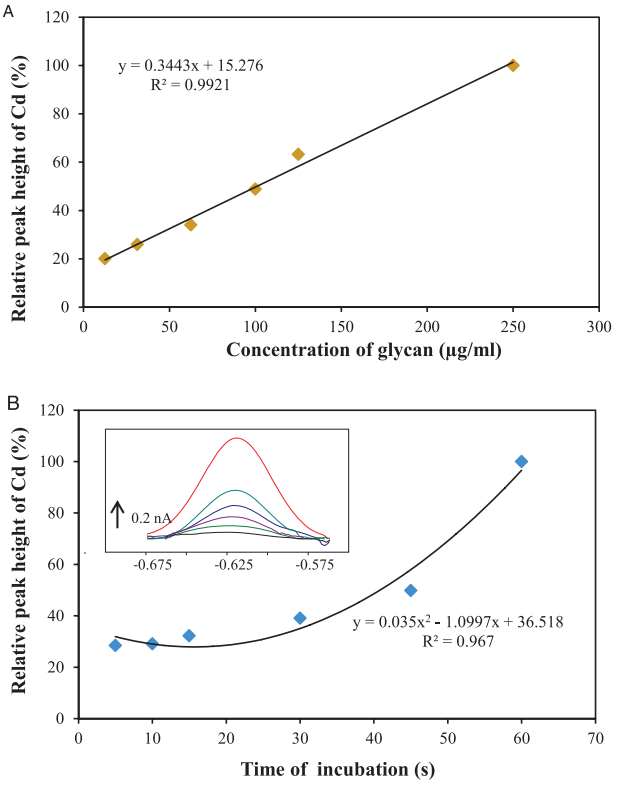

Figure 6. Isolation of complex H5N1-CdS (5 μg/mL) on paramagnetic particles in connection with glycan binding. Influence of (A) glycan concentration and (B) time of interaction on measured cadmium signal; inset: cadmium peaks. For other experimental conditions, see Section 2.

cadmium(II) ion signal by more than 30%. Protein concentrations were also determined using Brdicka reaction. The obtained voltammograms are shown in inset of Fig. 7. Cat2 peak height increased with increasing viral protein concentration (Fig. 7). The greater intercept value of the curve is associated with streptavidin release from paramagnetic particles' surface during ultrasound needle.

3.6 Calibration of the assay

The effects of viral protein concentrations on H5N1 fully automated isolation procedure were monitored. Under optimized conditions (250 μg/mL of glycan, 30-min long interaction, 25°C and 400 rpm), the typical dependence of the cadmium content per mg H5N1 viral protein is shown in Fig. 8. Individual signals of applied varying concentrations (0.625, 1.25, 2.5, 3.75, and 5 μg/mL H5N1-CdS QDs) measured at HMDE (blue rhombus) and GCE (red square) exhibited good linearity, $y = 0.0284x + 0.0054$, with $R^2 = 0.9904$ for HMDE and, $y = 0.024x + 0.0017$, with $R^2 = 0.9923$ for FIA GCE. Detectable amounts of cadmium in the protein were 10 ng per mg, which meant submicrograms quantities of viral protein could be identified.

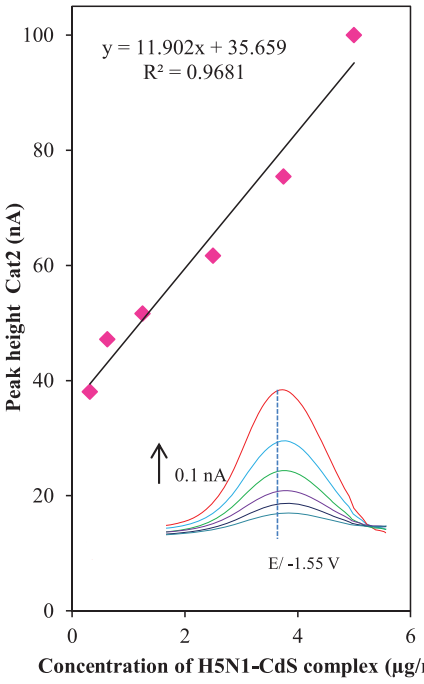

Figure 7. Dependence of Cat2 viral protein H5N1-CdS peak on applied concentration of H5N1 protein; inset: typical voltammograms of Cat2 peal measured at −1.55 V. Volume of measured sample was 3 µL. For other experimental conditions, see Fig. 4.

4 Conclusions

Most cases of human infection due to avian influenza viruses have involved close contact with infected poultry, particularly ill or dying chickens. During the 1997 outbreak in Hong Kong, one case-control study found exposure to live poultry within a week before the onset of illness was associated with human disease, but no significant risk was related to traveling, eating, or preparing poultry products or being exposed to people infected by the H5N1 virus [41]. Effective routine surveillance may be impossible in countries lacking basic public health resources. For a global containment strategy to be successful, low-cost, easy-to-use handheld units that permit decentralized testing are vital. Moreover, a protocol that allows rapid detection of the virus is critical to prevent pandemic spread [42]. A rapid detection method using an automated FIA and particle-based technology in micro-analysis systems may provide laboratories with solutions that enhance laboratory system productivity and test accuracy for the detection of a broad range of disease markers. Techniques using micro- and nanotechnology are used to fabricate lab-on-a-chip devices [43–47]. The paramagnetic particles are modified using biotechnology to make separation and electrochemical detection of viral nucleic acids and proteins easier to measure.

Financial support from NANOSEMED GA AV KAN208130801 and CEITEC CZ.1.05/1.1.00/02.0068 is greatly acknowledged.

The authors have declared no conflict of interest.

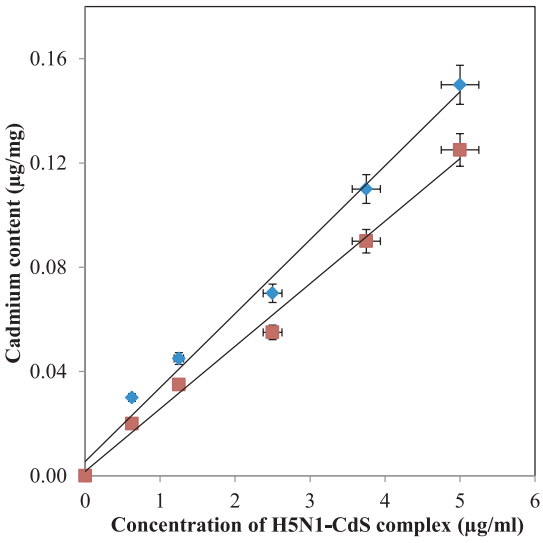

Figure 8. Cadmium content in H5N1-CdS QDs proteins captured on paramagnetic particles determined at (blue rhombus) HMDE and (red square) and FIA-GCE.

5 References

[1] Perdue, M. L., Nguyen, T., *Bull. World Health Organ.* 2012, *90*, 246.

[2] Shindo, N., Briand, S., *Bull. World Health Organ.* 2012, *90*, 247.

[3] Jones, B., *Bull. World Health Organ.* 2012, *90*, 252–253.

[4] WHO, *Bull. WHO* 1980, *58*, 585–591.

[5] Garten, R. J., Davis, C. T., Russell, C. A., Shu, B., Lindstrom, S., Balish, A., Sessions, W. M., Xu, X. Y., Skepner, E., Deyde, V., Okomo-Adhiambo, M., Gubareva, L., Barnes, J., Smith, C. B., Emery, S. L., Hillman, M. J., Rivailler, P., Smagala, J., de Graaf, M., Burke, D. F., Fouchier, R. A. M., Pappas, C., Alpuche-Aranda, C. M., Lopez-Gatell, H., Olivera, H., Lopez, I., Myers, C. A., Faix, D., Blair, P. J., Yu, C., Keene, K. M., Dotson, P. D., Boxrud, D., Sambol, A. R., Abid, S. H., George, K. S., Bannerman, T., Moore, A. L., Stringer, D. J., Blevins, P., Demmler-Harrison, G. J., Ginsberg, M., Kriner, P., Waterman, S., Smole, S., Guevara, H. F., Belongia, E. A., Clark, P. A., Beatrice, S. T., Donis, R., Katz, J., Finelli, L., Bridges, C. B., Shaw, M., Jernigan, D. B., Uyeki, T. M., Smith, D. J., Klimov, A. I., Cox, N. J., *Science* 2009, *325*, 197–201.

[6] Kaleta, E. F., Hergarten, G., Yilmaz, A., *Dtsch. Tierarztl. Wochenschr.* 2005, *112*, 448–456.

[7] Wang, T. T., Parides, M. K., Palese, P., *Science* 2012, *335*, 1463–1463.

[8] Liu, G. D., Wang, J., Wu, H., Lin, Y. Y., Lin, Y. H., *Electroanalysis* 2007, *19*, 777–785.

[9] Dequaire, M., Degrand, C., Limoges, B., *Anal. Chem.* 2000, *72*, 5521–5528.

[10] Gonzalez-Garcia, M. B., Fernandez-Sanchez, C., Costa-Garcia, A., *Biosens. Bioelectron.* 2000, *15*, 315–321.

[11] Wang, J., Xu, D. K., Kawde, A. N., Polsky, R., *Anal. Chem.* 2001, *73*, 5576–5581.

[12] Liu, G. D., Wang, J., Kim, J., Jan, M. R., Collins, G. E., *Anal. Chem.* 2004, *76*, 7126–7130.

[13] Liu, G. D., Lin, Y. H., *Talanta* 2007, *74*, 308–317.

[14] Li, H., Shih, W. Y., Shih, W. H., *Ind. Eng. Chem. Res.* 2007, *46*, 2013–2019.

[15] Long, G. L., Winefordner, J. D., *Anal. Chem.* 1983, *55*, A712–A724.

[16] Chandrasekaran, A., Srinivasan, A., Raman, R., Viswanathan, K., Raguram, S., Tumpey, T. M., Sasisekharan, V., Sasisekharan, R., *Nat. Biotechnol.* 2008, *26*, 107–113.

[17] Stevens, J., Blixt, O., Paulson, J. C., Wilson, I. A., *Nat. Rev. Microbiol.* 2006, *4*, 857–864.

[18] Stevens, J., Corper, A. L., Basler, C. F., Taubenberger, J. K., Palese, P., Wilson, I. A., *Science* 2004, *303*, 1866–1870.

[19] Stevens, J., Blixt, O., Tumpey, T. M., Taubenberger, J. K., Paulson, J. C., Wilson, I. A., *Science* 2006, *312*, 404–410.

[20] Yamada, S., Suzuki, Y., Suzuki, T., Le, M. Q., Nidom, C. A., Sakai-Tagawa, Y., Muramoto, Y., Ito, M., Kiso, M., Horimoto, T., Shinya, K., Sawada, T., Usui, T., Murata, T., Lin, Y. P., Hay, A., Haire, L. F., Stevens, D. J., Russell, R. J., Gamblin, S. J., Skehel, J. J., Kawaoka, Y., *Nature* 2006, *444*, 378–382.

[21] Bewley, C. A., *Nat. Biotechnol.* 2008, *26*, 60–62.

[22] Suenaga, E., Mizuno, H., Penmetcha, K. K. R., *Biosens. Bioelectron.* 2012, *32*, 195–201.

[23] Huska, D., Zitka, O., Krystofova, O., Adam, V., Babula, P., Zehnalek, J., Bartusek, K., Beklova, M., Havel, L., Kizek, R., *Int. J. Electrochem. Sci.* 2010, *5*, 1535–1549.

[24] Kleckerova, A., Sobrova, P., Krystofova, O., Sochor, J., Zitka, O., Babula, P., Adam, V., Docekalova, H., Kizek, R., *Int. J. Electrochem. Sci.* 2011, *6*, 6011–6031.

[25] Krystofova, O., Trnkova, L., Adam, V., Zehnalek, J., Hubalek, J., Babula, P., Kizek, R., *Sensors* 2010, *10*, 5308–5328.

[26] Adam, V., Baloun, J., Fabrik, I., Trnkova, L., Kizek, R., *Sensors* 2008, *8*, 2293–2305.

[27] Petrlova, J., Potesil, D., Mikelova, R., Blastik, O., Adam, V., Trnkova, L., Jelen, F., Prusa, R., Kukacka, J., Kizek, R., *Electrochim. Acta* 2006, *51*, 5112–5119.

[28] Heyrovsky, M., *Electroanalysis* 2000, *12*, 935–939.

[29] Adam, V., Fabrik, I., Eckschlager, T., Stiborova, M., Trnkova, L., Kizek, R., *TRAC-Trends Anal. Chem.* 2010, *29*, 409–418.

[30] Raspor, B., Paic, M., Erk, M., *Talanta* 2001, *55*, 109–115.

[31] Pipper, J., Inoue, M., Ng, L. F. P., Neuzil, P., Zhang, Y., Novak, L., *Nat. Med.* 2007, *13*, 1259–1263.

[32] Chui, L., Drebot, M., Andonov, A., Petrich, A., Glushek, M., Mahony, J., *Diagn. Microbiol. Infect. Dis.* 2005, *53*, 47–55.

[33] Deng, M. J., Long, L., Xiao, X. Z., Wu, Z. X., Zhang, F. J., Zhang, Y. M., Zheng, X. L., Xin, X. Q., Wang, Q., Wu, D. L., *Vet. Immunol. Immunopathol.* 2011, *141*, 183–189.

[34] Mizutani, H., Suzuki, M., Fujiwara, K., Shibata, S., Arishima, K., Hoshino, M., Ushijima, H., Honma, H., Kitamura, T., *Microbiol. Immunol.* 1991, *35*, 717–727.

[35] Bonnafous, P., Perrault, M., Le Bihan, O., Bartosch, B., Lavillette, D., Penin, F., Lambert, O., Pecheur, E. I., *J. Gen. Virol.* 2010, *91*, 1919–1930.

[36] Lien, K. Y., Hung, L. Y., Huang, T. B., Tsai, Y. C., Lei, H. Y., Lee, G. B., *Biosens. Bioelectron.* 2011, *26*, 3900–3907.

[37] Chou, T. C., Hsu, W., Wang, C. H., Chen, Y. J., Fang, J. M., *J. Nanobiotechnol.* 2011, *9*, 52.

[38] Lim, S. H., Bestvater, F., Buchy, P., Mardy, S., Yu, A. D. C., *Sensors* 2009, *9*, 5590–5599.

[39] Skehel, J. J., Wiley, D. C., *Annu. Rev. Biochem.* 2000, *69*, 531–569.

[40] Russell, R. J., Kerry, P. S., Stevens, D. J., Steinhauer, D. A., Martin, S. R., Gamblin, S. J., Skehel, J. J., *Proc. Natl. Acad. Sci. USA* 2008, *105*, 17736–17741.

[41] Hayden, F., Croisier, A., *J. Infect. Dis.* 2005, *192*, 1311–1314.

[42] Adam, V., Huska, D., Hubalek, J., Kizek, R., *Microfluid. Nanofluid.* 2010, *8*, 329–339.

[43] Manz, A., Graber, N., Widmer, H. M., *Sens. Actuator B-Chem.* 1990, *1*, 244–248.

[44] Janasek, D., Franzke, J., Manz, A., *Nature* 2006, *442*, 374–380.

[45] Kizek, R., Masarik, M., Kramer, K. J., Potesil, D., Bailey, M., Howard, J. A., Klejdus, B., Mikelova, R., Adam, V., Trnkova, L., Jelen, F., *Anal. Bioanal. Chem.* 2005, *381*, 1167–1178.

[46] Masarik, M., Kizek, R., Kramer, K. J., Billova, S., Brazdova, M., Vacek, J., Bailey, M., Jelen, F., Howard, J. A., *Anal. Chem.* 2003, *75*, 2663–2669.

[47] Hubalek, J., Adam, V., Kizek, R., in: Conley, E. C., Dini, P., Doarn, C., Holopainen, A. (Eds.), *International Conference on eHealth, Telemedicine, and Social Medicine, eTELEMED*, Institute of Electrical and Electronics Engineers (IEEE), Cancun, Mexico 2009, pp. 108–112, Article 4782641.

5.3.2 Vědecký článek VII

KREJCOVA, L.; NEJDL, L.; HYNEK, D.; KRIZKOVA, S.; KOPEL, P.; ADAM, V.; KIZEK, R. Beads-Based Electrochemical Assay for the Detection of Influenza Hemagglutinin Labeled with CdTe Quantum Dots.

Molecules, 2013, roč. 18. č. 12, s. 15573-15586. ISS 1420-3049. IF: 2.095

Podíl autorky Krejčová L.: 70 % textové části práce, 80 % experimentální části práce

Paramagnetické částice (MPs) jsou vynikajícím nástrojem pro izolaci s mnoha unikátními vlastnostmi, jako je snadná manipulace a separace pomocí magnetického pole *(van Reenen, a kol., 2014)*. Další výhodou je jejich velký aktivní povrch (vzhledem k malým rozměrům), který může být snadno modifikován *(Gooding, 2002)*. Vzhledem k výše uvedeným vlastnostem mají MPs využití v řadě detekčních systémů, jelikož zvyšují jejich selektivitu, citlivost a rychlost *(Kim a Poudel, 2013, Liu, a kol., 2011, Ramadan a Gijs, 2012)*. Kombinace pokročilých metod detekce biomolekul (detekce nukleových kyselin, imunologické metody) s mikrofluidními a imunomagnetickými separačními technikami, které využívají modifikovaných MPs, má obrovský potenciál pro realizaci integrovaného systému pro detekci patogenů *(Ramadan a Gijs, 2012, Sin, a kol., 2014)*.

V této studii byl popsán detekční systém založený na magnetické izolaci HA, značeného QDs (CdTe) a elektrochemické detekci izolovaného HA-QDs komplexu. Cílovou molekulou byl chřipkový antigen (HA). Jako vzorek byla použita vakcína proti chřipce, obsahující tři chřipkové viry (a tudíž tři typy HA). Nejprve byly vakcinační HA (vaxi HA) konjugovány s kademnatými QDs (CdTe), tento komplex byl charakterizován elektrochemicky a pomocí gelové elektroforézy. Následně byl komplex izolován pomocí glykanem modifikovaných MPs, přičemž celý proces izolace byl optimalizován a automatizován. Optimalizovanými podmínkami byla koncentrace glykanu, teplota a čas izolační reakce. Produkt izolace byl detekován elektrochemicky, dvěma voltametrickými metodami. Kovová část QDs (Cd(II)) byla detekována pomocí anodické rozpouštěcí diferenční pulzní voltametrie (DPASV) v prostředí acetátového pufru. Signál kademnatého iontu z QDs (Cd pík) byl detekován při potenciálu -0.66 V. HA byl detekován pomocí diferenční pulzní voltametrie spojené s přenosovou adsorptivní techikou (AdTS DPV) v prostředí amonného pufru, při potenciálu -1.5 V. Největšího výtěžku bylo dosaženo při těchto izolačních podmínkách: koncentrace

glykanu 100 μg/ml, teplota izolační reakce 45°C, doba izolace 20 min. Při optimalizovaných podmínkách byl sledován vliv koncentrace vakcinačního HA v komplexu HA-CdTe na výšku Cd a HA píku. Naměřené hodnoty obou píků byly vzájemě korelovány. V této studii jsme popsali metodu pro rychlou a automatiozovanou izolaci cílového HA-QDs komplexu, propojenou s elektrochemickou detekcí HA a QDs částí.

Molecules **2013**, *18*, 15573-15586; doi:10.3390/molecules181215573

OPEN ACCESS

molecules

ISSN 1420-3049

www.mdpi.com/journal/molecules

Article

Beads-Based Electrochemical Assay for the Detection of Influenza Hemagglutinin Labeled with CdTe Quantum Dots

Ludmila Krejcova [1], Lukas Nejdl [1], David Hynek [1,2], Sona Krizkova [1,2], Pavel Kopel [1,2], Vojtech Adam [1,2] and Rene Kizek [1,2,*]

[1] Department of Chemistry and Biochemistry, Faculty of Agronomy, Mendel University in Brno, Zemedelska 1, Brno CZ-613 00, Czech Republic

[2] Central European Institute of Technology, Brno University of Technology, Technicka 3058/10, Brno CZ-616 00, Czech Republic

* Author to whom correspondence should be addressed; E-Mail: kizek@sci.muni.cz; Tel.: +420-5-4513-3350; Fax: +420-5-4521-2044.

Received: 10 October 2013; in revised form: 25 November 2013 / Accepted: 5 December 2013 / Published: 13 December 2013

Abstract: In this study we describe a beads-based assay for rapid, sensitive and specific isolation and detection of influenza vaccine hemagglutinin (HA). Amplification of the hemagglutinin signal resulted from binding of an electrochemical label as quantum dots (QDs). For detection of the metal and protein part of the resulting HA-CdTe complex, two differential pulse voltammetric methods were used. The procedure includes automated robotic isolation and electrochemical analysis of the isolated product. The isolation procedure was based on the binding of paramagnetic particles (MPs) with glycan (Gly), where glycan was used as the specific receptor for linkage of the QD-labeled hemagglutinin.

Keywords: influenza hemagglutinin; electrochemical detection; paramagnetic particles; glycan; quantum dot labeling

1. Introduction

These days are characterized by rapid population growth, international trade and globalization, and for this reason the risk of influenza pandemics looms larger and larger [1]. Influenza is one of the most frequently occurring respiratory diseases, which causes approximately 500,000 deaths every year. The influenza virus is subject to genetic mutations, mainly due to the lack of proof-reading activity of its

polymerase [2]. Influenza infections mostly occur as seasonal epidemics or less frequently, as influenza pandemics. During twentieth century there were three, with shortening delays between them: Spanish flu in 1918, Asian flu in 1957 and Hong-Kong flu in 1968. The twenty first century has also been marked by a few cases of pandemics (swine and avian influenza) with a small number of victims, but with much larger economic impact.

Antigenic drift results from an accumulation of point mutations leading to minor antigenic changes, while antigenic shift involves major antigenic changes by introduction of new hemagglutinin (HA) and/or neuraminidase (NA) subtypes into the human population [2]. Combinations of HA (1-17) and NA (1-9) subtypes affect the biological properties of influenza viruses, especially their host range and virulence. HA is responsible for the initiation of the infection and it binds sialic acid on the host cell surface. NA removes sialic acid from the host receptor and thus enables the release of the replicated virion [3,4]. Sialic acids (SAs) are located on the terminal positions of glycans on the host cell surface, which is important for the spread of pathogens [5,6].

Vaccination is the most effective way of preventing influenza epidemics and the emergence of pandemics [7–9], however, influenza vaccines are only effective one year, because the limiting factors are the antigens' mutational changes, which mean that reuse of the previous year's vaccine would not be effective [10]. In 2006, World Health Organization (WHO) published an action plan to increase the current supplies of influenza vaccines. Inactivated vaccines induce protective levels of serum antibodies to influenza HA surface proteins [9] and are regarded as the most effective prophylactic method. Before the presentation of the influenza vaccine on the pharmaceutical market rapid and sensitive analysis of vaccination antigens is necessary, especially for human immunization. As a detection system, electrochemical biosensors and bioassays have attracted considerable interest due to their high performance, miniaturized construction, and low costs [11–15]. In spite of the fact that quantum dots (QDs) and magnetic nanoparticles (MPs) are currently utilized, especially for *in vivo* and *in vitro* imaging, their application in the field of biosensing devices for influenza viruses could be also considered [16–18].

The aim of this study was to design and to test a method for indirect detection of hemagglutinin for the purposes of quantification of vaccine antigen or for the detection of influenza virus. We suggest a method based on the isolation of QD-labeled HA by glycan-modified MPs and on electrochemical detection of the MPs-HA-glycan-QDs complex, which is formed due to the specific and selective binding between glycans and HA.

2. Results and Discussion

Influenza type A can be subtyped by different variants of NA (1-9) and HA (1-17), which differ from each other in virulence, host specificity and binding of HAs subtypes on human and/or avian glycan receptors [19–24]. Specific HA-glycan affinity has been exploited as the basis for isolation of various types of influenza viruses [25]. In our previous study we described a MPs-based isolation method for standard viral proteins labeled with CdS [26]. The current study was moved forward by the isolation of real samples (influenza vaccines) instead of the HA standard. Labeling of HA with CdTe QDs was used because of their better electrochemical properties.

2.1. Characterization of vaxi HA, CdTe and HA-CdTe Complex by Gel Electrophoresis

The beads-based isolation of HA-CdS complex is the cornerstone of the proposed procedure. Glycan-conjugated (modified) beads bind vaccine HAs, which could be recognized specifically and linked onto the surface of the glycan-modified MPs. This design is based on the hemagglutinin as the basic element. Therefore the protein characterization of influenza vaccine by gel electrophoresis is very important. The complexity of work with such sample is due to the many proteins present in samples. The interpretation of the gel electropherogram (Figure 1A) is based on the results presented in literature [27–29]. The proportions of several influenza proteins have been found to be similar for various strains of the virus [28]. One band at 28 kDa corresponds to the matrix protein 1 (M1). The band at 38 kDa represents the hemagglutinin fragment from influenza B virus. The band at 48 kDa was assigned to the glycosylated HA [30]. The band at 56 kDa is connected with the presence of nucleocapsid protein (NP). The predicted molecular mass of HA is approximately 63 kDa, however, the band pattern of HA is affected by glycosylation and proteolytic cleavage under *in vivo* conditions [31].

2.2. Characterization of CdTe by Electrochemical Analysis

Further, we aimed our attention at determination of the metal part of the label used in this study to mark the virus. Cd in CdTe and HA-CdTe complex was determined by differential pulse anodic stripping voltammetry (DPASV) at the potential −0.66 ± 0.005 V (bottom inset in Figure 1B). Optimization of the electrochemical procedure was done due to the testing of accumulation time (upper inset in Figure 1B). Dependence of relative Cd peak height (%) on time of accumulation is linear within the whole testing interval from 0 to 600 s. As the optimum time, 360 s was selected (due to the time consuming nature of measurements with longer accumulation times). The dependence of the peak height on concentration of CdTe had a sigmoidal shape with the following regression curve: Cd in CdTe $y = -0.0008x^2 + 0.724x + 3.8864$, $R^2 = 0.9953$, n = 4 (Figure 1B).

2.3. Characterization of Influenza Vaccine by the Brdicka Reaction

Proteins from influenza vaccine were characterized by differential pulse voltammetry (AdT DPV) measured in the Brdicka solution and coupled with the adsorptive transfer technique. As the targer peak the so called Cat2 peak at potential −1.56 ± 0.005 V was choosen (bottom inset in Figure 1C). Apply the same concept as above, we also optimized the time of accumulation. From the obtained dependence of relative detected peak height (%) on time of accumulation, 120 s was selected (upper inset in Figure 1C) as the optimum. The calibration curve of the obtained concentration dependence was as follows: $y = 215.18x + 10.747$, $R^2 = 0.9943$, n = 4 (Figure 1C).

2.4. Electrochemical Characterization of HA-CdTe Complex

HA-CdTe complex formed due to the specific and selective binding between glycan and HA was characterized by two electrochemical methods. Each method serves for the detection of one part of the complex. Characterization of the metal part of the complex, namely the cadmium ions, was done by the DPASV method. The cadmium peak was detected at the potential −0.66 V. For this purpose the method was optimized through determination of the optimal accumulation time (Figure 2A). As it was

mentioned above, the value of 360 s was confirmed. Concentration dependence was as follows: $y = -0.04x^2 + 0.637x + 0.0419$, $R^2 = 0.9983$, n = 4 (Figure 2B).

Figure 1. Characterization of QDs and hemagglutinin by gel electrophoresis and electrochemical analysis. (**A**) Characterization of vaxi HA, CdTe and vaxi HA-CdTe by gel electrophoresis (SDS PAGE). Concentration of labeled and non-labeled vaxi HA was 22.5 µg/mL, concentration of CdTe was 500 µM; (**B**) Electrochemical detection of individual parts of HA-CdTe complex. Dependence of Cd peak height on Cd (CdTe) concentration. Inset: dependence of relative Cd peak height (related to the maximum value) on time of accumulation. Cd was determined by DPASV with parameters as it follows: initial potential −0.8 V; end potential -0.5 V; deposition potential -0.8 V; equilibration time 5 s; modulation time 0.06 s; time interval 0.2 s; potential step 0.002 V; modulation amplitude 0.025 V. Time of accumulation was optimized (a → k): *a* 30 s, *b* 60 s, *c* 120 s, *d* 180 s, *e* 240 s, *f* 300 s, *g* 360 s, *h* 420 s, *i* 480 s, *j* 540 s, and *k* 600 s; (**C**) Dependence of HA peak height on HA (vaxi HA) concentration. Inset: dependence of relative HA peak height (related to the maximum value) on time of accumulation. For measurement AdT DPV Brdicka reaction was used under following parameters: purge time 30 s; initial potential −0.7 V; end potential −1.8 V; potential step 0.002 V; amplitude 0.025 V. Time of accumulation was optimized (a → g): *a* 0 s, *b* 30 s, *c* 60 s, *d* 90 s, *e* 120 s, *f* 240 s, and *g* 360 s. Concentration of vaxi HA was 2.25 µg/mL, initial concentration of CdTe was 500 µM.

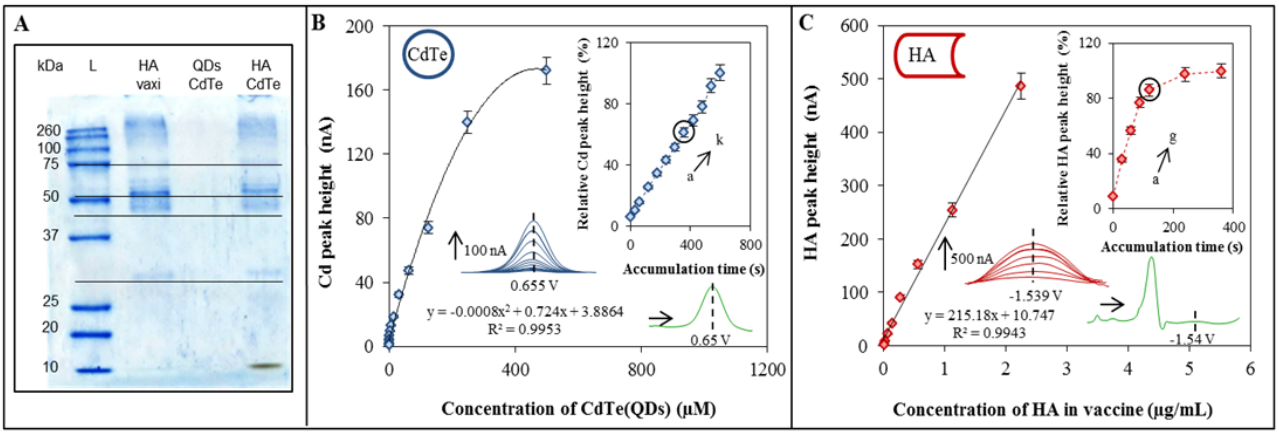

Characterization of HA part of the complex was done by the AdT DPV method connected with the Brdicka reaction. The detected peak was recorded at a potential near −1.56 V. The method optimization included the optimal accumulation time determination too (Figure 2C). As it was mentioned above, the value of 120 s was confirmed. The calibration curve of the obtained concentration dependence was as follows: $y = 122.97x + 3.3705$, $R^2 = 0.9979$, n = 4 (Figure 2D).

2.5. Optimization of the Automated Isolation Procedure

The isolation procedure was done according to the previously published paper [26]. The isolation procedure scheme is shown in Figure 3. Briefly, streptavidin-modified MPs bind biotinyled glycan and in the other step the hemagglutinin binds quantum dots. In the next step the final complex is created

from all four parts. This complex is subsequently disordered by sonication and the individual parts are detected.

Figure 2. Electrochemical characterization of HA-QDs complex. *Optimization and detection of the metal part of HA-CdTe complex*. (**A**) Dependence of relative Cd peak height (related to the maximum value) on time of accumulation; (**B**) Dependence of Cd peak height on concentration of CdTe. For Cd determination DPASV was used under the following parameters: initial potential −0.8 V; end potential −0.5 V; deposition potential −0.8 V; equilibration time 5 s; modulation time 0.06 s; time interval 0.2 s; potential step 0.002 V; modulation amplitude 0.025 V. Time of accumulation was optimized (a → g): *a* 30 s, *b* 60 s, *c* 120 s, *d* 240 s, *e* 360 s, *f* 480 s, and *g* 600 s. *Optimization and detection of HA (protein part of the HA-QDs complex)*; (**C**) Dependence of relative HA peak height (related to the maximum value) on time of accumulation; (**D**) Dependence of HA peak height on HA(HA-QDs) concentration. For HA determination AdT DPV Brdicka reaction was used under the following parameters: purge time 30 s, initial potential −0.7 V; end potential −1.8 V; potential step 0.002 V; amplitude 0.025 V. Time of accumulation was optimized (a → g): *a* 0 s, *b* 30 s, *c* 60 s, *d* 90 s, *e* 120 s, *f* 240 s, and *g* 360 s.

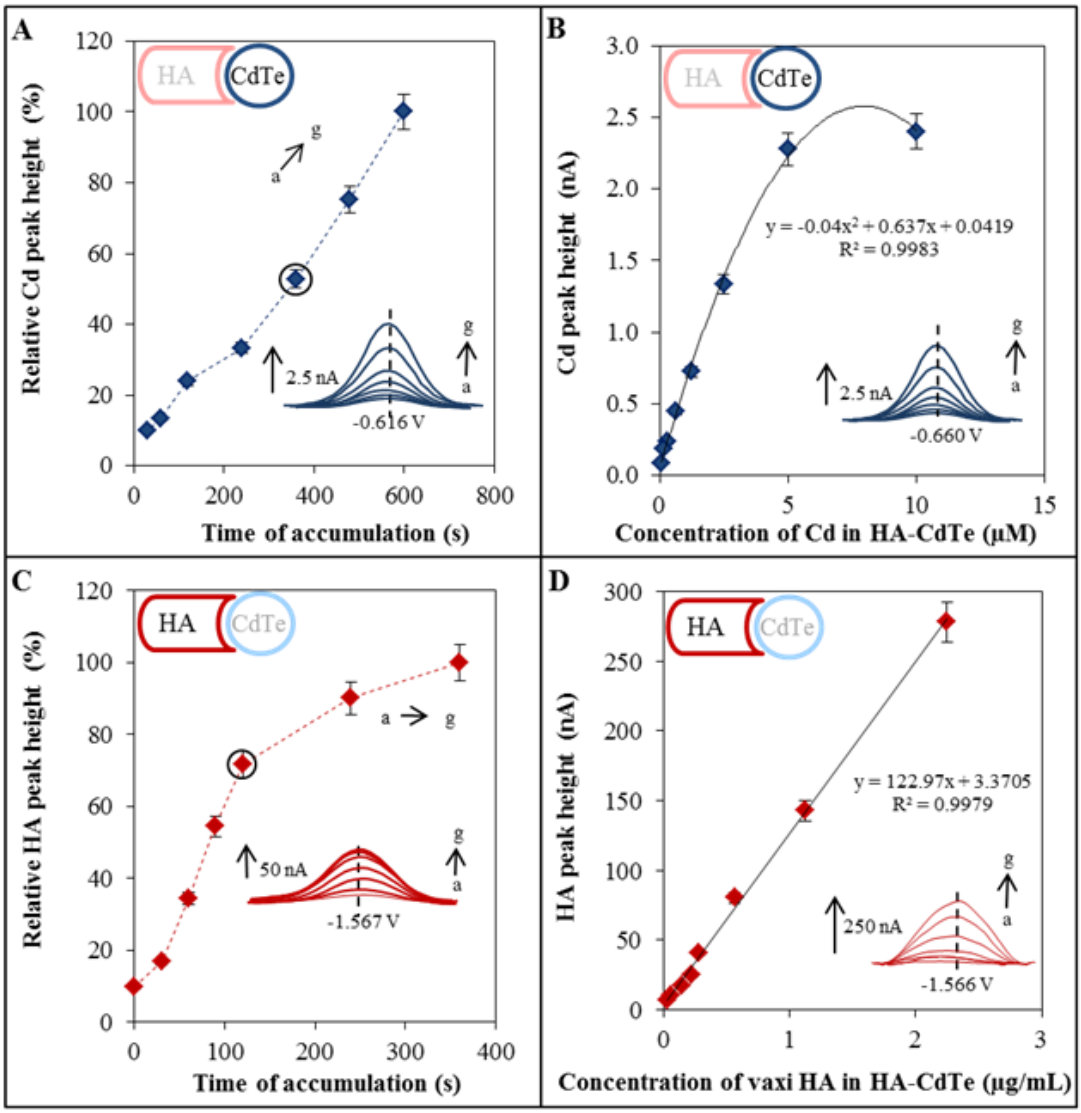

Figure 3. Scheme of isolation (**A**+**B**+**C**) and electrochemical detection (**D**) of vaccine hemagglutinin (vaxi HA) labeled with CdTe quantum dots (QDs); (**A**) Biotinyled glycan binding on streptavidin modified paramagnetic particles (MPs) based on biotin-streptavidin affinity, (**B**) HA labelling by CdTe, (**C**) magnetic isolation of HA-CdTe complex (based on glycan-HA affinity), followed by sonication and (**D**) electrochemical detection of HA and QDs parts. HA was detected by differential pulse voltammetry (DPV) connected with adsorptive transfer technique (AdT DPV) Brdicka reaction. QDs (Cd respectively) were detected by DPASV. Other experimental conditions see in Figure 2.

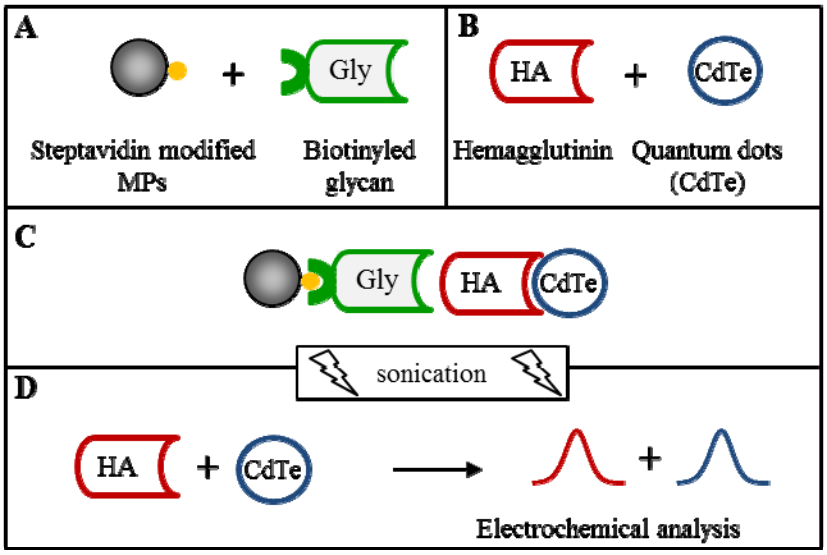

This procedure was optimized to increase the HA-CdTe yield. The effect of different conditions such as the amount of glycan, time and temperature of isolation was tested using an automatic isolation procedure performed by an ep*Motion* 5075 device. The influence of different conditions was investigated by the optimized electrochemical detection. The effect of glycan amount was investigated first. Figure 4A shows the increasing dependency of HA and Cd relative peak height on the glycan amount, but only up to a concentration of 50 µg/mL (this concentration was established as the best). Blue columns show the dependence of Cd relative peak height on glycan concentration, and red rhombi show the dependence of HA relative peak height on glycan concentration. The other two conditions optimized directly included the labeled HA isolation reaction. Tested conditions included six temperatures (5, 25, 35, 45, 55 and 65 °C) and reaction times (5, 10, 15, 20, 30, 45 and 60 min). From the results it follows that best signals were obtained at temperatures higher than 35 °C and the temperature of 45 °C was established as the best, based on the Cd peak results (blue columns in Figure 4B) and HA peak (red rhombi in Figure 4B), which correspond to the range of body temperatures of humans and small animals, especially birds, which serve as influenza reservoirs [32]. The highest effect of reaction time was observed based on the Cd peak (blue columns in Figure 4C) and HA peak (blue columns in Figure 4C) after 45 min of incubation of glycan-modified MPs with HA-Cd-Te. If we summarize the results of the optimization, the best conditions was glycan concentration 50 µg/mL, reaction time of 45 min., and the reaction temperature 45 °C. The observed distinct temperature dependence of HA-Cd-Te interaction is in accordance with previously published data on the thermostability of hemagglutinin, whereby at temperatures higher than 60 °C the loss of HA secondary

structure occurs and at temperatures below 30 °C HA conformational changes affecting the functionality of the virion are observed [28,33,34].

Figure 4. Optimization of isolation procedure. (**A**) Dependence of relative Cd peak height (related to the maximum value) on optimized condition (blue column). Dependence of relative HA peak height (related to the maximum value) on optimized condition (red rhomb). Dependence of relative Cd/HA peak height on concentration of glycan; (**B**) Dependence of relative Cd/HA peak height on temperature of reaction between HA-CdTe and glycan modified MPs; (**C**) Dependence of relative Cd/HA peak height on time of reaction (HA-CdTe and glycan-MPs). Other experimental conditions see in Figure 2.

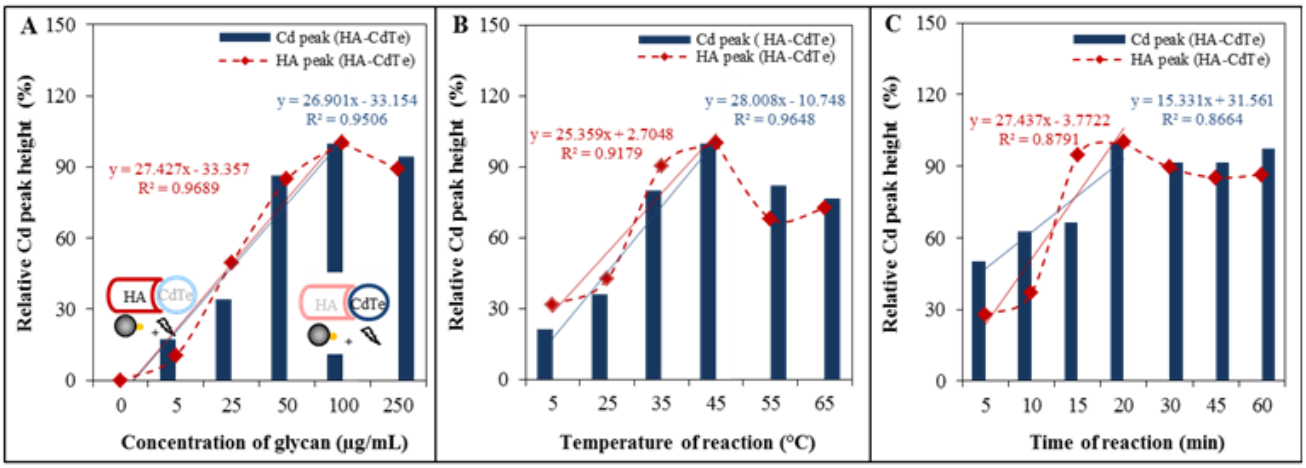

2.6. Hemagglutinin Detection from the Influenza Vaccine

Usage of influenza vaccine as a source of hemagglutinin for the proof of the suggested concept was tested. The whole isolation procedure was done according to the optimized conditions and as the next step the HA-CdTe complex was detected. Electrochemical detection was applied to both parts of the complex. The dependencies of the individually detected electrochemical signals on the concentration of HA-CdTe complex are shown in Figure 5. For electrochemical determination two different electrochemical methods were utilized, individually focused on the Cd and HA part of the complex. Both dependencies have polynomial character. The CdTe part had dependence as follows: $y = 0.005x^2 + 1.634x + 15.60$, $R^2 = 0.986$, n = 4. The HA part had a dependence as follows: $y = 0.039x^2 - 0.328x + 35.09$, $R^2 = 0.999$, n = 4. The lowest concentration of HA in the vaccine (10 µg/mL) refers to 0.2 µmol/L HA. When electrochemical detection of HA-CdTe was tested, the lowest detectable concentration was 62.5 pmol/L. The obtained results are comparable with other nanoparticle-based influenza (immuno)sensors with terminal HA quantification [15], such as an electrically active magnetic nanoparticle-based biosensor for the detection of pandemic influenza with a detection limit of 1.4 µmol/L [35] or the detection of the hemagglutinin molecules of influenza virus by combining an electrochemiluminescence sensor with an immunoliposome encapsulating a Ru complex with a detection limit on the order of atomoles per 50 µL of sample volume, which corresponds to 120 pmol/L [36]. The vaccine is prepared by splitting and inactivating influenza virions. If the vaccine HA is able to immunize humans, the structure of the HA would not be significantly changed, and it will be possible to also apply this

method for the isolation and detection of influenza virions. For this reason this method should be applicable both for isolation and detection of vaccine antigen—hemagglutinin as well as influenza virus—because hemagglutinin is found on the surface of the influenza virion [37]. Some other authors also described the importance of methods for quantification of vaccine hemagglutinin. *Legastelois et al.* described ELISA assays, where HA detection was 1.9 μg/mL, as opposed to the 5 μg/mL quantitation limit generally accepted for the standard single-radial-immunodiffusion (SRID) assay, the approved technique for quantifying HA content in influenza vaccines [38]. *Bousse et al.* described a method which was applied to quantitate type A influenza viruses in solution, and focused on two early steps of vaccine preparation, firstly, detection and quantitation of virus harvested from eggs and cell cultures and, secondly, virus quantitation following inactivation [39].

Figure 5. Detection of isolated HA-CdTe complex by electrochemical analysis. Dependence of relative peak height (related to the maximum value, Cd peak - blue colour, HA peak - red colour) on concentration of isolated HA-CdTe complex. Other experimental conditions see in Figure 2.

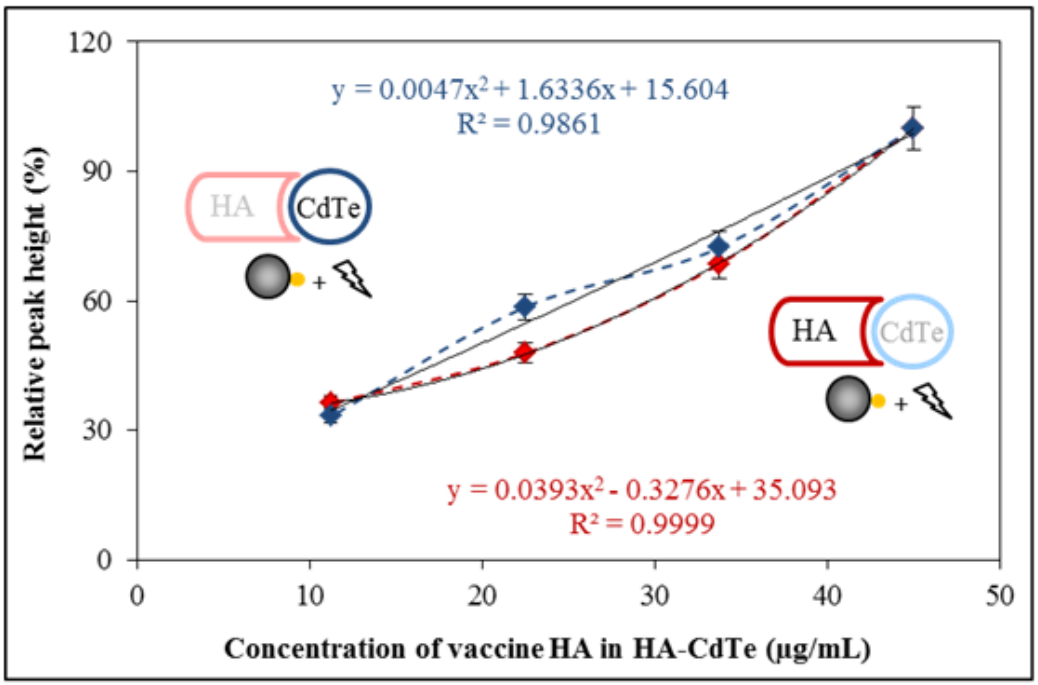

3. Experimental

3.1. Chemicals

Tris(2-carboxyethyl)phosphine (TCEP) was supplied by Molecular Probes (Eugene, OR, USA). $Co(NH_3)_6Cl_3$ and other chemicals were supplied by Sigma Aldrich (St. Louis, MO, USA) unless indicated otherwise. Deionised water passed demineralization by reverse osmosis using Aqua Osmotic 02 (Aqua Osmotic, Tisnov, Czech Republic) and further it was purified using Millipore RG (MiliQ water, 18 MΩ, Millipore Corp., Billerica, MA USA). Deionized water was used to rinse, wash and prepare buffers. Stock solutions were prepared with water of ACS purity.

3.2. Hemagglutinin

The vaccine Vaxigrip® (Sanofi Pasteur, Lyon, France) was used as the sample of influenza hemagglutinin. Vaxigrip® is inactivated trivalent influenza vaccine. Sterile suspension contain three influenza strains (A/California/7/2009 (H1N1), A/Victoria/361/2011 (H3N2) and B/Wisconsin/1/2010), cultivated on fertilised eggs, concentrated, purified by zone centrifugation in a sucrose gradient, split, inactivated and diluted in phosphate buffered saline solution. Vaxigrip® contains 15 micrograms of all three HAs per 0.5 mL (90 μg/mL HA).

3.3. Preparation of QDs (CdTe)

CdTe QDs were prepared according to a slight modification of the method published by Duan *et al.* [40]. Briefly, cadmium acetate dihydrate ($Cd(OAc)_2 \cdot 2H_2O$, 0.0267 g) was dissolved in ACS water (44 mL) and trisodium citrate dihydrate (100 mg) was added with stirring. A solution of Na_2TeO_3 (0.0055 g) in water (1.25 mL) was poured into the first solution, followed by 3-mercaptopropionic acid (100 μL, 1.14 mM). Afterwards, solid $NaBH_4$ (50 mg) was added with vigorous stirring and hydrogen evolution was observed, followed by a color change of the solution to slightly yellow. After 30 min of stirring, an aliquot of solution (2 mL) was heated in a glass vial in a Multiwave 3000 Microwave Reaction System (Anton Paar, Graz, Austria) using a 64MG5 rotor. Reaction conditions were as follows: power 300 W, temperature 120 °C and time 18 min. Obtained CdTe QDs were stored in the dark at 4 °C.

3.4. Labelling of Vaxigrip® HA by CdTe QDs

Vaxigrip® (500 μL containing 45 μg of HA) was reduced and washed with water (5 × 400 μL) on an Amicon 3k centrifugal filter device (Millipore) and mixed with a solution of prepared QDs (500 μL). This mixture was shaken for 24 h at room temperature (Biosan Orbital Shaker OS-10, Biosan Ltd. Riga, Latvia). The volume of solution was reduced to 100 μL on an Amicon Ultra 3k centrifugal filter, diluted with water and washed five times using a 5417R centrifuge (Eppendorf, Hamburg, Germany). The washed sample was diluted to 1 mL with ACS water and used for measurements.

3.5. Characterization of vaxi HA and HA-CdTe Complex by Gel Electrophoresis

Sodium dodecyl sulphate polyacrylamide gel electrophoresis (SDS-PAGE) was performed using a Mini Protean Tetra apparatus with gel dimensions of 8.3 × 7.3 cm (Bio-Rad, Hercules, CA, USA). First 12.5% (m/V) running, then 5% (m/V) stacking gel was poured. The gel was prepared from 30% (m/V) acrylamide stock solution with 1% (m/V) bisacrylamide. The polymerization of the running or stacking gels was performed at room temperature for 30 min. Prior to analysis the samples were mixed with non-reduction sample buffer in a 2:1 ratio. The samples were incubated at 93 °C for 3 min, and the sample was loaded onto a gel. For determination of the molecular mass, the "Precision plus Protein Standards" protein ladder from Bio-Rad was used. The electrophoresis was run at 150 V for 1 h at laboratory temperature (23 °C) (Power Basic, Bio-Rad) in tris-glycine buffer (0.025 M trizma-base, 0.19 M glycine and 3.5 mM SDS, pH = 8.3). Then the gels were stained Coomassie-blue. The rapid Coomassie-blue staining procedure was adopted from Wong *et al.* [41].

3.6. Isolation of HA-QDs by Glycan Modified MPs Using a Robotic Pipetting Station

3.6.1. Robotic Pipetting Station

An ep*Motion* 5075 (Eppendorf, Hamburg, Germany) automated pipetting station, was used for CdTe labeled HA isolation prior to electrochemical analysis. The isolation process was computer controlled. The program sequence was edited and the station was supervised by pEditor 4.0. Transfer of species was provided by a robotic arm with pipetting adaptors (TS50, TS300 – numeric labeling refers to the maximal pipetting volume in μL) and a gripper for microplate transport (TG-T), was placed at the A1 position. Tips were placed in positions A3 (300 μL tips) and A2 (50 μL tips). At position A4 a Thermo mixer was located. At position B1, a module reservoir for washing solutions and waste were placed. Position C1 was thermostated (PCR 96 thermoadapter). A thermorack for 24 × 1.5–2 mL microtubes (Position B3) was used to store working solutions (buffers). For sample preparation 96-well PCR plates (microplates) with a maximal well volume of 200 μL were used. The principal position of the microplate was C1. During washing and at the end of isolation, the MPs were forced to the well bottoms using a magnetic adapter (Promega, Madison, WI, USA) (position C4).

3.6.2. The Automated Isolation Procedure

The first step of the automatic isolation involved pipetting of Dynabeads® M-270 Streptavidin (10 μL), supplied by Life Technologies (Carlsbad, CA, USA), into microplate wells (PCR 96, Eppendorf). Then the plate was subsequently transferred to a magnet. Stored solution was aspirated out of the MPs and the MPs were washed three times with phosphate buffer (PB, 0.3 M, pH 7.4, made from NaH_2PO_4 and Na2HPO4, 100 μL). After that biotinyled multivalent-glycan (01-039a [Neu5Acα2-6Galβ1-4GlcNAcβ1-PAA-biotin], 20 μL) which was used according to *Suenaga at al.* [25], supplied by GlycoTech (Gaithersburg, MD, USA), were added to each of the wells and incubated (30 min, 25 °C, 400 rpm). In the next step each well was washed three times with PB (100 μL and sample (vaccine HA labeled by CdTe, 20 μL) was added. The mixture in each well was further incubated (400 rpm, optimized conditions) and washed three-times with PB (100 μL). In the last step PB (35 μL) was added followed by ultrasound needle treatment (2 min). The plate was transferred to the magnet, where the supernatant was pipetted out of MPs into the new wells and electrochemically analyzed.

3.7. Electrochemical Detection of CdTe and HA-CdTe Complex

Cd (CdTe) itself and Cd from HA-CdTe complex was detected by differential pulse anodic stripping voltammetry (DPASV). Measurements were carried on a 663 VA Stand (Metrohm, Herisau, Switzerland) with an electrochemical cell with a three electrode set-up. A hanging mercury drop electrode (HMDE) with a drop area of 0.4 mm^2 was used as the working electrode, an Ag/AgCl/3M KCl as a reference electrode and a platinum electrode was the auxiliary electrode. Samples were deoxygenated prior to each measurement by purging with argon (99.999%). Acetate buffer (0.2 M CH_3COONa + CH_3COOH, pH 5.0) was used as a background electrolyte and was replaced after each measurement. The parameters of the measurement were as it follows: purging time 100 s; deposition potential −0.85 V; equilibration time 2 s; modulation time 0.057 s; interval time 0.2 s; initial potential

−0.85 V; end potential −0.4 V; step potential 0.005 V; modulation amplitude 0.0250 V; volume of measurement cell: 1 mL (5 μL sample; 995 μL acetate buffer). GPES 4.9 software was used for data processing.

3.8. Electrochemical Detection of vaxi HA and HA-CdTe Complex

HA itself and HA from HA-CdTe complex were detected by the adsorptive transfer technique connected with a differential pulse voltammetric method (AdT DPV) Brdicka reaction [42]. All measurements were performed with a 663 VA Stand instrument (Metrohm) with a cooled electrochemical cell, equipped with a three electrode set-up. The temperature of the measurement cell was controlled at 4 °C by a Julabo F25 instrument (JulaboDE, Seelbach, Germany). The three-electrode setup was composed of a hanging mercury drop electrode (HMDE) with a drop area of 0.4 mm^2 as the working electrode, an Ag/AgCl/3M KCl reference electrode and a platinum electrode as the auxiliary one. Prior to measurements the analysed samples were deoxygenated by purging with argon (99.999%) for 120 s. The Brdicka supporting electrolyte contained 1 mM $Co(NH_3)_6Cl_3$ and 1 M ammonia buffer (NH_3(aq) and NH_4Cl, pH = 9.6) and was changed after each analysis. The parameters of the measurement were as it follows: initial potential −0.7 V; end potential −1.75 V; modulation time 0.057 s; time interval 0.2 s; step potential 0.002 V; modulation amplitude 0.025 V; sample volume 5 μL; buffer volume 1500 μL. Software GPES 4.9 was used for data analysis.

3.9. Descriptive Statistics

Data were processed using MICROSOFT EXCELs (Microsoft Corp., Redmond, WA, USA) and STATISTICA.CZ Version 8.0 (StatSoft, Prague, Czech Republic). The results are expressed as mean ± SD unless noted otherwise. The detection limits (3 signal/noise, S/N) were calculated according to Long and Winefordner [43], where N was expressed as a standard deviation of noise determined in the signal domain, unless stated otherwise.

4. Conclusions

In this study we designed and optimized method for automated isolation and detection of vaccine influenza hemagglutinin labeled with CdTe quantum dots. For the detection of HA-CdTe complex two voltammetric methods were used. The effect of various conditions (glycan concentration, time and temperature of glycan and HA-CdTe mixing on the detected HA and Cd signals were investigated. These results demonstrate that the automatic isolation procedure coupled with the usage of quantum dots as an electrochemical label is suitable for vaccine influenza detection. Our platform may be applied for analysis of other pathogens, based on specific receptor binding and magnetic isolation processes.

Acknowledgments

Financial support from CEITEC CZ.1.05/1.1.00/02.0068, PGS03/2012 and IGA IP16/2013 is greatly acknowledged.

Conflicts of Interest

The authors declare no conflict of interest.

References

1. Shoji, Y.; Farrance, C.E.; Bautista, J.; Bi, H.; Musiychuk, K.; Horsey, A.; Park, H.; Jaje, J.; Green, B.J.; Shamloul, M.; *et al.* A plant-based system for rapid production of influenza vaccine antigens. *Influenza Other Respir. Viruses* **2012**, *6*, 204–210.
2. Ding, X.F.; Jiang, L.F.; Ke, C.W.; Yang, Z.; Lei, C.L.; Cao, K.Y.; Xu, J.; Xu, L.; Yang, X.F.; Zhang, Y.H.; *et al.* Amino acid sequence analysis and identification of mutations under positive selection in hemagglutinin of 2009 influenza A (H1N1) isolates. *Virus Genes* **2010**, *41*, 329–340.
3. Chen, Q.J.; Huang, S.P.; Chen, J.J.; Zhang, S.Q.; Chen, Z. NA proteins of influenza A viruses H1N1/2009, H5N1, and H9N2 show differential effects on infection initiation, virus release, and cell-cell fusion. *PLoS One* **2013**, *8*, e54334.
4. Samson, M.; Pizzorno, A.; Abed, Y.; Boivin, G. Influenza virus resistance to neuraminidase inhibitors. *Antivir. Res.* **2013**, *98*, 174–185.
5. Rudrawar, S.; Pascolutti, M.; Bhatt, B.; Thomson, R.J.; von Itzstein, M. An efficient synthesis of C3 C-alkylated Neu5Ac2en derivatives. *Tetrahedron Lett.* **2013**, *54*, 1198–1201.
6. Cho, S.; Lee, B.R.; Cho, B.K.; Kim, J.H.; Kim, B.G. *In vitro* selection of sialic acid specific RNA aptamer and its application to the rapid sensing of sialic acid modified sugars. *Biotechnol. Bioeng.* **2013**, *110*, 905–913.
7. Feng, Z.L.; Towers, S.; Yang, Y.D. Modeling the effects of vaccination and treatment on pandemic influenza. *AAPS J.* **2011**, *13*, 427–437.
8. Couch, R.B. Seasonal inactivated influenza virus vaccines. *Vaccine* **2008**, *26*, D5–D9.
9. Lanthier, P.A.; Huston, G.E.; Moquin, A.; Eaton, S.M.; Szaba, F.M.; Kummer, L.W.; Tighe, M.P.; Kohlmeier, J.E.; Blair, P.J.; Broderick, M.; *et al.* Live attenuated influenza vaccine (LAIV) impacts innate and adaptive immune responses. *Vaccine* **2011**, *29*, 7849–7856.
10. Thompson, C.M.; Petiot, E.; Lennaertz, A.; Henry, O.; Kamen, A.A. Analytical technologies for influenza virus-like particle candidate vaccines: Challenges and emerging approaches. *Virol. J.* **2013**, *10*, 1–14.
11. Adam, V.; Sileny, A.; Hubalek, J.; Beklova, M.; Zehnalek, J.; Havel, L.; Kizek, R. Microsensors as a tool to detect heavy metals. *Toxicol. Lett.* **2008**, *180*, S227-S228.
12. Huska, D.; Zitka, O.; Adam, V.; Beklova, M.; Krizkova, S.; Zeman, L.; Horna, A.; Havel, L.; Zehnalek, J.; Kizek, R. A sensor for investigating the interaction between biologically important heavy metals and glutathione. *Czech J. Anim. Sci.* **2007**, *52*, 37–43.
13. Liu, G.D.; Lin, Y.H. Nanomaterial labels in electrochemical immunosensors and immunoassays. *Talanta* **2007**, *74*, 308–317.
14. Majzlik, P.; Prasek, J.; Trnkova, L.; Zehnalek, J.; Adam, V.; Havel, L.; Hubalek, J.; Kizek, R. Biosensors for detection of heavy metals. *Listy Cukrov. Reparske* **2010**, *126*, 413–414.
15. Amano, Y.; Cheng, Q. Detection of influenza virus: Traditional approaches and development of biosensors. *Anal. Bioanal. Chem.* **2005**, *381*, 156–164.

16. Hubalek, J.; Adam, V.; Kizek, R. New Approach in Rapid Viruses Detection and Its Implementation on a Chip. In Proceedings of the 2009 International Conference on eHealth, Telemedicine, and Social Medicine, Los Alamitos, CA, USA, 1–7 February 2009; IEEE Computer Society: Washington, DC, USA, 2009; pp. 108–112.
17. Miller, S.A.; Hiatt, L.A.; Keil, R.G.; Wright, D.W.; Cliffel, D.E. Multifunctional nanoparticles as simulants for a gravimetric immunoassay. *Anal. Bioanal. Chem.* **2011**, *399*, 1021–1029.
18. Zhao, W.; Zhang, W.P.; Zhang, Z.L.; He, R.L.; Lin, Y.; Xie, M.; Wang, H.Z.; Pang, D.W. Robust and highly sensitive fluorescence approach for Point-of-Care virus detection based on immunomagnetic separation. *Anal. Chem.* **2012**, *84*, 2358–2365.
19. Chandrasekaran, A.; Srinivasan, A.; Raman, R.; Viswanathan, K.; Raguram, S.; Tumpey, T.M.; Sasisekharan, V.; Sasisekharan, R. Glycan topology determines human adaptation of avian H5N1 virus hemagglutinin. *Nat. Biotechnol.* **2008**, *26*, 107–113.
20. Stevens, J.; Blixt, O.; Paulson, J.C.; Wilson, I.A. Glycan microarray technologies: Tools to survey host specificity of influenza viruses. *Nat. Rev. Microbiol.* **2006**, *4*, 857–864.
21. Stevens, J.; Corper, A.L.; Basler, C.F.; Taubenberger, J.K.; Palese, P.; Wilson, I.A. Structure of the uncleaved human H1 hemagglutinin from the extinct 1918 influenza virus. *Science* **2004**, *303*, 1866–1870.
22. Stevens, J.; Blixt, O.; Tumpey, T.M.; Taubenberger, J.K.; Paulson, J.C.; Wilson, I.A. Structure and receptor specificity of the hemagglutinin from an H5N1 influenza virus. *Science* **2006**, *312*, 404–410.
23. Takahashi, Y.; Hirano, Y.; Yasukawa, T.; Shiku, H.; Yamada, H.; Matsue, T. Topographic, electrochemical, and optical images captured using standing approach mode scanning electrochemical/optical microscopy. *Langmuir* **2006**, *22*, 10299–10306.
24. Bewley, C.A. Illuminating the switch in influenza viruses. *Nat. Biotechnol.* **2008**, *26*, 60–62.
25. Suenaga, E.; Mizuno, H.; Penmetcha, K.K.R. Monitoring influenza hemagglutinin and glycan interactions using surface plasmon resonance. *Biosens. Bioelectron.* **2012**, *32*, 195–201.
26. Krejcova, L.; Dospivova, D.; Ryvolova, M.; Kopel, P.; Hynek, D.; Krizkova, S.; Hubalek, J.; Adam, V.; kizek, R. Paramagnetic particles coupled with an automated flow injection analysis as a tool for influenza viral protein detection. *Electrophoresis* **2012**, *33*, 3195–3204.
27. Garcia-Canas, V.; Lorbetskie, B.; Cyr, T.D.; Hefford, M.A.; Smith, S.; Girard, M. Approach to the profiling and characterization of influenza vaccine constituents by the combined use of size-exclusion chromatography, gel electrophoresis and mass spectrometry. *Biologicals* **2010**, *38*, 294–302.
28. Epand, R.M.; Epand, R.F. Thermal denaturation of influenza virus and its relationship to membrane fusion. *Biochem. J.* **2002**, *365*, 841–848.
29. Schwarzer, J.; Rapp, E.; Hennig, R.; Genzel, Y.; Jordan, I.; Sandig, V.; Reichl, U. Glycan analysis in cell culture-based influenza vaccine production: Influence of host cell line and virus strain on the glycosylation pattern of viral hemagglutinin. *Vaccine* **2009**, *27*, 4325–4336.
30. Chou, T.C.; Hsu, W.; Wang, C.H.; Chen, Y.J.; Fang, J.M. Rapid and specific influenza virus detection by functionalized magnetic nanoparticles and mass spectrometry. *J. Nanobiotechnol.* **2011**, *9*, 1–13.

31. Hoffman, L.R.; Kuntz, I.D.; White, J.M. Structure-based identification of an inducer of the low-pH conformational change in the influenza virus hemagglutinin: Irreversible inhibition of infectivity. *J. Virol.* **1997**, *71*, 8808–8820.
32. Doneley, B. *Avian Medicine and Surgery in Practice: Companion and Aviary Birds*; Manson Publishing Ltd.: London, UK, 2010; p. 330.
33. Korte, T.; Ludwig, K.; Booy, F.P.; Blumenthal, R.; Herrmann, A. Conformational intermediates and fusion activity of influenza virus hemagglutinin. *J. Virol.* **1999**, *73*, 4567–4574.
34. Ruigrok, R.W.H.; Martin, S.R.; Wharton, S.A.; Skehel, J.J.; Bayley, P.M.; Wiley, D.C. Conformational-changes in the hemagglutinin of influenza-virus which accompany heat-induced fusion of virus with liposomes. *Virology* **1986**, *155*, 484–497.
35. Kamikawa, T.L.; Mikolajczyk, M.G.; Kennedy, M.; Zhang, P.; Wang, W.; Scott, D.E.; Alocilja, E.C. Nanoparticle-based biosensor for the detection of emerging pandemic influenza strains. *Biosens. Bioelectron.* **2010**, *26*, 1346–1352.
36. Egashira, N.; Morita, S.; Hifumi, E.; Mitoma, Y.; Uda, T. Attomole detection of hemagglutinin molecule of influenza virus by combining an electrochemiluminescence sensor with an immunoliposome that encapsulates a Ru complex. *Anal. Chem.* **2008**, *80*, 4020–4025.
37. Wagner, R.; Matrosovich, M.; Klenk, H.D. Functional balance between haemagglutinin and neuraminidase in influenza virus infections. *Rev. Med. Virol.* **2002**, *12*, 159–166.
38. Legastelois, I.; Chevalier, M.; Bernard, M.C.; de Montfort, A.; Fouque, M.; Pilloud, A.; Serraille, C.; Devard, N.; Engel, O.; Sodoyer, R.; *et al.* Avian glycan-specific IgM monoclonal antibodies for the detection and quantitation of type A and B haemagglutinins in egg-derived influenza vaccines. *J. Virol. Methods* **2011**, *178*, 129–136.
39. Bousse, T.; Shore, D.A.; Goldsmith, C.S.; Hossain, M.J.; Jang, Y.; Davis, C.T.; Donis, R.O.; Stevens, J. Quantitation of influenza virus using field flow fractionation and multi-angle light scattering for quantifying influenza A particles. *J. Virol. Methods* **2013**, *193*, 589–596.
40. Duan, J.L.; Song, L.X.; Zhan, J.H. One-pot synthesis of highly luminescent CdTe quantum dots by microwave irradiation reduction and their Hg^{2+}-sensitive properties. *Nano Res.* **2009**, *2*, 61–68.
41. Wong, C.; Sridhara, S.; Bardwell, J.C.A.; Jakob, U. Heating greatly speeds Coomassie blue staining and destaining. *Biotechniques* **2000**, *28*, 426–428.
42. Skalickova, S.; Zitka, O.; Nejdl, L.; Krizkova, S.; Sochor, J.; Janu, L.; Ryvolova, M.; Hynek, D.; Zidkova, J.; Zidek, V.; *et al.* Study of interaction between metallothionein and CdTe quantum dots. *Chromatographia* **2013**, *76*, 345–353.
43. Long, G.L.; Winefordner, J.D., Limit of detection. *Anal. Chem.* **1983**, *55*, A712–A724.

Sample Availability: Samples of the quantum dots are available from the authors.

5.4 Využití 3D technologie pro tvorbu čipů

5.4.1 Vědecký článek VIII

KREJCOVA, L.; NEJDL, L.; RODRIGO, M. A. M.; ZUREK, M.; MATOUSEK, M.; HYNEK, D.; ZITKA, O.; KOPEL, P.; ADAM, V.; KIZEK, R. 3D printed chip for electrochemical detection of influenza virus labeled with CdS quantum dots.

Biosensors & bioelectronics, 2014, roč. 54. č., s. 421-427. ISS 0956-5663; 1873-4235. IF: 6.451

Podíl autorky Krejčová L.: 60 % textové části práce, 65 % experimentální části práce

Pomocí 3D tisku může být vyrobeno téměř cokoliv, z toho důvodu nalezla technologie 3D tisku využití téměř ve všech odvětvích zahrnující průmysl *(Bonyar, a kol., 2014)*, zdravotnictví *(Dorey, 2014, Lee, a kol., 2014)*, dopravu *(Moon, a kol., 2014)* a značnou budoucnost má i její aplikace v oblasti výzkumu *(Dorey, 2014)*, včetně využití 3D tisku při výrobě mikrofluidních zařízení pro různé detekční systémy *(Kitson, a kol., 2012)*. Mezi výhody 3D techologie tisku patří extrémě rychlé zhotovení, cenově dostupné materiály a v neposlední řadě také možnost výroby přesných a precizních prototypů *(Bonyar, a kol., 2014)*. Cílem publikace byl návrh a aplikace trojrozměrného (3D) čipu, vyvinutého pro rychlou, citlivou a specifickou detekci chřipkového hemaglutininu, značeného CdS QDs. Princip stanovení byl založen na bázi mikrofluidního čipu, ve kterém probíhla jak izolace pomocí paramagnetických částic, tak vlastní elektrochemická detekce. Jako platforma pro izolaci byly použity streptavidinem modifikované MPs, na které byl nejprve navázán biotinylovaný glykan a následně komplex HA-QDs. Pro modifikaci povrchu MPs byl vybrán glykan představující syntetický analog silové kyseliny, která se běžně vyskytuje na povrchu hostitelských buňek a který slouží pro přichycení chřipkového virionu prostřednicvím HA. Jako vzorek HA byla použita vakcína proti chřipce obsahující tři chřipkové viry (H1N12, H3N2 a chřipku typu B). Vakcinační HA byly nejprve značeny CdS QDs. HA-QDs komplexy byly specificky izolovány díky vazbě na povrch MPs modifikovaných glykanem. Pro detekci produktu izolace (komplexu HA-QDs) byla vybrána skelná uhlíková elektroda, která byla zapojena jako pracovní elektroda. Popsaný proces izolace a detekce probíhal celý v čipu vytvořeném pomocí 3D tiskárny. Použití 3D technologií má v oblasti vývoje senzorů a biosenzorů značnou budoucnost. Navržený detekční

systém může být použit pro detekci dalších specifických látek, které jsou důležité pro prevenci, diagnózu nebo léčbu infekčních chorob.

Biosensors and Bioelectronics 54 (2014) 421–427

Contents lists available at ScienceDirect

Biosensors and Bioelectronics

journal homepage: www.elsevier.com/locate/bios

3D printed chip for electrochemical detection of influenza virus labeled with CdS quantum dots

Ludmila Krejcova [a], Lukas Nejdl [a], Miguel Angel Merlos Rodrigo [a,b], Michal Zurek [a], Miroslav Matousek [a], David Hynek [a,b], Ondrej Zitka [a,b], Pavel Kopel [a,b], Vojtech Adam [a,b], Rene Kizek [a,b,*]

[a] Department of Chemistry and Biochemistry, Faculty of Agronomy, Mendel University in Brno, Zemedelska 1, 613 00 Brno, Czech Republic
[b] Central European Institute of Technology, Brno University of Technology, Technicka 3058/10, 61600 Brno, Czech Republic

ARTICLE INFO

Article history:
Received 17 August 2013
Received in revised form
10 October 2013
Accepted 21 October 2013
Available online 1 November 2013

Keywords:
3D Printing
Microfluidic chip
Voltammetry
Paramagnetic particles
Influenza hemagglutinin
Quantum dots

ABSTRACT

In this study, we report a new three-dimensional (3D), bead-based microfluidic chip developed for rapid, sensitive and specific detection of influenza hemagglutinin. The principle of microfluidic chip is based on implementation of two-step procedure that includes isolation based on paramagnetic beads and electrochemical detection. As a platform for isolation process, streptavidin-modified MPs, which were conjugated via biotinylated glycan (through streptavidin–biotin affinity) followed by linkage of hemagglutinin to glycan, were used. Vaccine hemagglutinin (HA vaxi) was labeled with CdS quantum dots (QDs) at first. Detection of the isolation product by voltammetry was the end point of the procedure. The suggested and developed method can be used also for detection of other specific substances that are important for control, diagnosis or therapy of infectious diseases.

1. Introduction

Influenza is likely the most powerful member of the group of potential pandemic agents (Krasnoselsky and Katze, 2012), because of the continuous mutational changes in its surface antigens, hemagglutinin (HA) and neuraminidase (NA), which play the main role in the mechanism of their interaction with sialic acid (SA) receptors on a host cell (Chen et al., 2013).

Numerous analytical methods are used to detect influenza viruses including methods based on the direct isolation of viruses (Bui et al., 2013) followed by real time-polymerase chain reaction (RT-PCR) (Tong et al., 2012), or immunology tests (Hemmatzadeh et al., 2013; Shembekar et al., 2013). Most of them have some disadvantages (an isolation of virus is time consuming; RT-PCR requires appropriate equipment and well-trained staff). For this reason, new sensors and biosensors based on magnetic beads separation are coming to the forefront (Kamikawa et al., 2010; Lien et al., 2011). Its sensitivity, specificity, speed, and the ability to recognize a very low concentration of target molecules belong to the most important features of a biosensor (Xu and Wang, 2012). For this reason, wide range of methods, materials and substances to optimize developing biosensing instrument has been tested (Kim et al., 2013). Paramagnetic particles (MPs) are the excellent tool with many advantageous features, such as easy handling and possibility to be separated by the magnetic field (Gijs, 2004; Ramadan and Gijs, 2012). Currently, various bead-based assays implemented to microfluidic systems have been reported for biomedical applications (Lien et al., 2011; Tsai et al., 2013). Combination of advanced biological detection methods with microfluidic and immunomagnetic separation techniques exploiting functionalized magnetic particles has tremendous potential for realization of an integrated system for detection of pathogens (Casavant et al., 2013; Ramadan and Gijs, 2012).

In this study, the microfluidic assay based on MPs based isolation of HA was followed with the indirect detection of the isolated compound with QDs labels. Microfluidic device for isolation and detection of HA–QDs was fabricated using three-dimensional (3D) printing, which is an example of additive manufacturing or solid freeform fabrication technology (Polzin et al., 2013).

2. Experimental section

2.1. Chemicals

Streptavidin Dynabeads M-270 was purchased from Life Technologies (Norway), uniform and superparamagnetic beads are

* Corresponding author at: Mendel University in Brno, Department of Chemistry and Biochemistry, Faculty of Agronomy, Zemedelska 1, 613 00 Brno, Czech Republic. Tel.: +420 5 4513 3350; fax: +420 5 4521 2044.
E-mail address: kizek@sci.muni.cz (R. Kizek).

0956-5663/$ - see front matter © 2013 Elsevier B.V. All rights reserved.
http://dx.doi.org/10.1016/j.bios.2013.10.031

2.8 μm in diameter, with a monolayer of recombinant streptavidin covalently coupled to the surface. Biotinylated multivalent-glycan (01-039a [Neu5Acα2–6 Galβ1–4GlcNAcβ1-PAA-biotin]) from GlycoTech (USA), Vaxigrip® (HA) from Sanofi Pasteur (France), and tris(2-carboxyethyl)phosphine (TCEP) from Molecular Probes (USA). Sample of inactivated influenza H5N1 was donated by University of Veterinary and Pharmaceutical Sciences Brno. $Co(NH_3)_6Cl_3$ and other chemicals were purchased from Sigma Aldrich (USA) in ACS purity unless indicated otherwise. Stock solutions were prepared with ACS water. pH value was measured using an instrument inoLab Level 3 (Wissenschaftlich-Technische Werkstatten GmbH; Germany). Deionised water underwent demineralization by reverse osmosis using an apparatus Aqua Osmotic 02 (Aqua Osmotic, Czech Republic) and was subsequently purified using Millipore RG (Millipore Corp., USA). Deionised water was used for rinsing, washing, and preparation of buffers.

2.2. Hemagglutinin

Influenza vaccine Vaxigrip®, which contains inactivated and split influenza virions of the following strands: A/California/7/2009 (H1N1), A/Victoria/361/2011 (H3N2) and B/Wisconsin/1/2010, was used as the sample of Influenza A and B hemagglutinin. Vaxigrip contains 15 micrograms of all three HA per 0.5 mL (together 90 μg/mL HA).

2.3. Preparation of QDs (CdS)

CdS quantum dots were prepared according to modified previously published protocol (Li et al., 2007). Briefly, cadmium nitrate tetrahydrate $Cd(NO_3)_2 \cdot 4H_2O$ (0.1 mM) was dissolved in ACS water (25 ml). 3-mercaptopropionic acid (35 μL, 0.4 mM) was slowly added to the stirred solution. Afterwards, the pH was adjusted to 9.11 with 1 M NH_3 (1.5 mL). Sodium sulfide nonahydrate $Na_2S \cdot 9H_2O$ (0.1 mM) in ACS water was poured into the solution under vigorous stirring. The acquired yellow solution was stirred for 1 h. Prepared CdS quantum dots were stored in the dark at 4 °C and were used for labeling of HA.

2.4. Labeling of HA from Vaxigrip by QDs (CdS)

Two preparation procedures of HA–CdS complex were designed. The effect of complex fabrication was tested using an automatic isolation procedure (described in Section 2.6) with subsequent electrochemical detection using hanging mercury drop electrode (described in Section 2.7).

Procedure No. 1: Vaxigrip® (0.5 mL, containing 15 μg of H1N1, H3N2 and Brisbane virions) was mixed with QDs (0.5 mL) and shaken for 16 h in dark at room temperature on a Biosan OS-10 Orbital Shaker (Biosan Ltd., Latvia). Dialysis of the sample was performed on a Millipore filter 0.025 μm VSWP against 2 L of miliQ water at 4 °C. During dialysis volume of sample increased to 4.5 mL. Volume was reduced to 1 mL on an Amicon 3k on centrifuge 5417R (Eppendorf, Germany) at 6000 rpm for 15 min at 20 °C. Concentrations of HA and QDs (expressed as Cd content) were as it follows: 3 × 15 μg HA and 115 μg Cd/mL.

Procedure No. 2: Vaxigrip (500 μL) was reduced and washed with water (5 × 400 μL) on an Amicon 3k centrifugal filter device (Millipore, USA) and mixed with a solution of prepared QDs (500 μL). This mixture was shaken for 24 h at room temperature on a Biosan Orbital Shaker OS-10. The volume of solution was reduced to 100 μL on an Amicon Ultra 3k, diluted with water and washed 5 times using centrifuge 5417R. The washed sample was diluted to 1 mL and used for succeeding measurements. Concentrations of HA and QDs were the same as in the case of *Procedure no.* 1.

2.5. Characterization of vaxi HA, CdS and HA–CdS isolated by MPs

Characterization of vaxi HA, CdS and HA–CdS complex were provided by matrix-assisted laser desorption/ionization time of flight mass spectrometry (MALDI-TOF MS), gel electrophoresis and spectral analysis. MPs and HA–CdS complex isolated by MPs were characterized also by scanning electrochemical microscope (SCEM).

2.5.1. Characterization of vaxi HA, CdS and HA–CdS complex by spectral analysis

Fluorescence and/or absorption spectra of vaxi HA, CdS and HA–CdS were acquired by a multifunctional microplate reader Tecan Infinite 200 PRO (TECAN, Switzerland). 230, 320, 430, 450 and 550 nm were used as excitation wavelengths and the fluorescence scan was measured within the range from 290 to 850 nm per 5 nm steps. The detector gain was set to 100. Absorption scan was measured within the range from 230 to 630 nm. Samples (50 μL) were placed in UV-transparent 96 well microplate with flat bottom by CoStar (Corning, USA). All measurements were performed at 30 °C and controlled by a Tecan Infinite 200 PRO.

2.5.2. Characterization of vaxi HA by MALDI-TOF MS

The mass spectrometry characterization was performed by MALDI-TOF/TOF mass spectrometer Bruker Ultraflextreme (Bruker Daltonik GmbH, Germany) equipped with a laser operating with wavelength of 355 nm according to Nejdl et al. (in press).

2.5.3. Characterization of vaxi HA by gel electrophoresis

Sodium dodecyl sulfate polyacrylamide gel electrophoresis (SDS-PAGE) was performed using a Mini Protean Tetra apparatus with gel dimension of 8.3 × 7.3 cm^2 (Bio-Rad, USA) according to Vyslouzilova et al. (2013).

2.5.4. Characterization of MPs and MPs–glycan–HA–CdS by SECM

Characterization of MPs and MPs–glycan–HA–CdS was provided by SECM at CH Instruments Scanning electrochemical microscope 920C (Metrohm, Switzerland) in Amperometric mode. Working electrode was a disk shaped microelectrode with radius of the conductive core 10 μm. The dimensionless parameter RG defined as ratio of radii of conductive and isolated cores was 5.4. The following parameters were used for working and substrate electrode: WE (working electrode, Pt); applied potential: 0.3V, SA (substrate electrode, Au): applied potential −0.4 V Ferrocenemethanol concentration 1 mM was used as an electrochemical mediator. All the experiments were done at the same distance between tip and substrate (d = 30 μm).

The electrochemical cell was cleaned ultrasonically (in the mixture of acetone and ethanol in the same ratio) and furthermore was purified with hydrogen peroxide and sulfuric acid (also in the same ratio). The purification step took five minutes on the surface of electrode to purify it. The tip was cleaned ultrasonically only in ethanol. Afterwards the chemical cleaning was finished, when the cyclic voltammetry (CV) was started in the presence of 30% (v/v) sulfuric acid. Finally, all the above-mentioned parts were rinsed with double distilled water and dried with nitrogen. This procedure was repeated after each measurement. Firstly, electrochemical mediator (ferrocenemethanol with KCl in ratio 1:1) was identified. CV was initiated to determine what potential is responsible for reversible redox reaction of mediator. These potentials were applied to reach approach curves– determination of optimal tip–substrate distance (30 μm). The bare substrate electrode was scanned and after it MPs and MPs–HA–CdS were scanned too.

2.6. Isolation of HA-QDs by MPs modified with glycan using robotic pipetting station

A computer-controlled automated pipetting station, *ep-Motion* 5075 (Eppendorf) was used for automated sample handling prior to electrochemical analysis. Position C1 was thermostated (Epthermoadapter PCR96). After the separation, MPs were forced apart using a Promega magnetic pad (Promega, USA) at position C4. The program sequence was edited and the station was controlled with pEditor 4.0. Pipetting of 10 μL of streptavidin Dynabeads M-270 to microplates (PCR 96, Eppendorf) was the first step of isolation process. Subsequently, plate was transferred to magnet. Stored solution was aspirated from the MPs and MPs were washed three times with 100 μL of phosphate buffer (PB) (0.3 M, pH 7.4, made from NaH_2PO_4 and Na_2HPO_4). Thereafter volume of 20 μL of biotinylated glycan was added to each of the wells and incubated (30 min, 25 °C, 400 rpm). After the incubation, the sample was washed three times with PB (0.3 M, pH 7.4). Subsequently 20 μL of HA-QDs was added. Mixture in each well was further incubated (400 rpm, time and temperature was optimized) and washed three-times with 100 μL of PB (0.3 M, pH 7.4). In the last step, 35 μL of PB (0.3 M, pH 7.4) was added. This step was followed by the treatment of a sample using ultrasound needle (2 min). The plate was transferred to the magnet and the supernatant was analyzed using voltammetry. The detected substance was identified as cadmium (CdS QDs) and protein (HA from Vaxigrip).

2.7. Electrochemical analysis of HA–CdS isolated by robotic pipetting station

For electrochemical analysis of both parts of isolated HA–CdS complex two different techniques and supporting electrolytes were applied.

2.7.1. Determination of vaxi HA from HA–CdS complex by Brdicka reaction

Adsorptive transfer technique differential pulse voltammetric measurements (AdT DPV) were performed with a 663 VA Stand instrument (Metrohm, Switzerland) according to experimental conditions indicated by Sochor et al. (2012).

2.7.2. Determination of cadmium from HA–QDs complex in acetate buffer

Determination of cadmium by differential pulse anodic stripping voltammetry (DPASV) was performed using a 663 VA Stand (Metrohm, Switzerland) and a standard cell with three electrodes according to experimental conditions indicated by Krejcova et al. (2012).

2.8. Fabrication of 3D microfluidic chip and its application

The first step in fabrication of microfluidic chip was its 3D processing in the modeling program Blender 2.65 (available on the http://www.blender.org/community/get-involved). Product of this software was exported in STL format and further edited in netFabb program (Parsberg, Germany), which allows elimination of cranny or wrongly oriented triangles. The corrected model (in STL format) was opened in the program G3DMAKER (DO-IT, Czech Republic) and 3D printing was controlled by EASY 3D MAKER (DO-IT). After the above-mentioned corrections, the model was ready for printing. Chip of the size [x, y and z] 42.64/14.95 and 4.87 mm was printed with an accuracy of [x, y and z] 0.1/0.1 and 0.08 mm for 94 min. As material polylactide (PLA) from DO-IT, which was applied by extrusion (melting head) at temperature 210 °C on a heated surface (40 °C), was used. Each printed chip was machined from minor impurities, fitted with tubes with a diameter of 2.1 mm and with three electrodes (working glassy carbon microelectrode, reference graphite electrode and auxiliary platinum wire) for detail description see Section 2.8.2. Attachment the plastic film (thickness 0.7 mm) at top of chip was the last step of procedure.

2.8.1. Microfluidic analysis

A microfluidic analysis system (3D chip) equipped with devices for electrochemical detection was suggested and constructed. Procedure included two basic steps: isolation and electrochemical detection. Isolation procedure was based on glycan conjugated MPs, which was used for binding of HA (vaccination or real sample) labeled by QDs (Fig. S2, Part 1). The isolation procedure was done as it follows: 10 μL of MPs was dosed by a peristaltic pump (Pump Amersham Biosciences, Sweden). Using an external magnet it was anchored on the reaction chamber, stored solution from the MPs was aspirated and MPs were washed with 1500 μL of PB. Thereafter, MPs were modified with 20 μL of biotinyled Glycan (50 μg/mL). This step was followed by washing with 1500 μl of PB. The last part of the isolation was binding of HA–CdS (20 μL, concentration 45 μg/mL) onto glycan-modified MPs, again followed by a washing with 1500 μL of PB. After it, chip with MPs-glycan-HA–CdS was immersed in an ultrasonic bath and MPs–glycan–HA–CdS complex was fractionated. Isolated HA was detected indirectly due to electroactivity of Cd(II), respectively CdS in the isolated HA–CdS complex.

2.8.2. Electrochemical detection of the isolated HA–CdS complex by glassy carbon microelectrode

Measurements were carried out using three-electrode set up. As the working electrode a glassy carbon microelectrode (GCm) was used, as the quasi-reference electrode a graphite lead was used and as the auxiliary electrode a platinum electrode with diameter 0.5 mm (CH Instruments, USA) was used. GCm was purchased from (Sensolytics, Germany). The pencil leads (diameter = 500 μm, length = 60 mm) were purchased from Koh-I-Noor (Czech Republic). Immersing 3 mm of the pencil lead into a solution resulted in an active electrode area of 4.91 mm^2. The electrodes were used without any pre-treatments except GCm, which was polished by 0.3 m polishing paper.

The differential pulse voltammetry (DPV) was used as the measuring method for detection of cadmium part of the complex under the following parameters: initial potential −1.3 V, end potential −0.1 V, deposition potential −1.3 V, deposition time 85 s, modulation amplitude 0.1 V, step potential 0.005 V, scan rate 0.05 V/s. Acetate buffer (0.2 M, pH 5) was used as the supporting electrolyte. The experiments were carried out at 20 °C. The electrochemical signal was detected by PGSTAT101 Autolab potentiostat (Metrohm, The Netherlands) and the results were evaluated by the Software NOVA 1.8 (Metrohm). The cadmium signal was detected at potential −0.9 V.

2.9. Descriptive statistics

Data were processed using MICROSOFT EXCELs (USA) and STATISTICA.CZ Version 8.0 (Czech Republic). The results are expressed as mean ± SD unless noted otherwise. The detection limits (3 signal/noise, S/N) were calculated according to Long and Winefordner (1983).

3. Results and discussion

Influenza A surface antigen, hemagglutinin, occurs in different host specific subtypes, which binds human and/or avian type

receptors with high specificity (Stevens et al., 2006). Those highly specific affinities of HA-receptors were utilized as a basic pattern for isolation of various types of influenza viruses (Suenaga et al., 2012). In our previous study a biosensor for influenza detection was designed. It consists from automatic MPs-based isolation process of standard viral protein modified with CdS QDs with subsequent electrochemical detection of HA (direct detection of virus) and QDs (indirect detection of virus) (Krejcova et al., 2012). This study is based on the previously published concept, but the main idea was to develop 3D fabricated microfluidic chip and applied it for analysis of a real sample (vaxi HA). Primarily, we focused on the designing and implementation of the method for isolation and detection of HA–CdS by magnetic field controllable microfluidic 3D chip. The isolation was stable due to the continual washing process at a flow rate of 480 μL/min. The flow was discontinued in two isolation steps: (i) conjugation of glycan on MPs surface and (ii) conjugation of HA–CdS on surface of glycan-modified MPs. Under these conditions, the isolation process was very specific because non-specifically bounded substances were eliminated by the washing process compared to stationary measurements. The beads-based isolation of HA–CdS complex was the cornerstone of the procedure. Glycan-conjugated (modified) beads bound vaccine HAs, which could be recognized specifically and linked onto the surface of the glycan-modified MPs.

In the first step, different method for characterization of reactants (spectral analysis, matrix-assisted laser desorption/ionization time of flight mass spectrometry, gel electrophoresis, scanning electrochemical microscope) were used.

3.1. Characterization of reactant by different method

3.1.1. Spectral characterization of vaxi HA, CdS, and HA–CdS complex

In this section, we focused on UV/VIS and fluorescence spectrometric characterization of HA–CdS complex. Spectral characteristics of nanoparticles hold a special place among properties of these materials. Differences (sometimes very considerable) between compact semiconductor materials and the corresponding nanoparticles are the most distinct in this context, and a theoretical basis was created to interpret many of the observed effects (Shalyapina et al., 2013). The first recorded absorption scan of CdS showed the absorption maximum at $\lambda = 450$ nm (Fig. S1A and a). Formation of the HA–CdS complex resulted in a change in absorption spectrum and in a decrease of the absorption maximum, as shown in Fig. S1A and b. The absorption maximum was not observed in the case of HA (Fig. S1A and c). Furthermore, the fluorescence intensities of CdS (Fig. S1B) and HA–CdS (Fig. S1C) complexes were compared, whereas different excitation wavelength were tested ($\lambda = 230$, 320, 430, 450, and 550 nm). The highest intensity of fluorescence was observed at $\lambda = 430$ nm (Fig. S1B and e). Formation of HA–CdS complex was reflected by a decrease in fluorescence by 25 % on the average (Fig. S1C and e). Differences between water, CdS, and HA–CdS complex were also visualized by UV and are shown in Fig. S1D.

3.1.2. Characterization of influenza vaccine by matrix-assisted laser desorption/ionization time of flight mass spectrometry and gel electrophoresis

After that we characterized the spectral properties of the complexes used in this study, we followed with their further characterization, mainly, with characterization of isolation design. The beads-based isolation of HA–CdS complex was the cornerstone of the procedure. Glycan-conjugated (modified) beads bound vaccine HAs, which could be recognized specifically and linked onto the surface of the glycan-modified MPs (Fig. S2/Part 1). This design is based on the hemagglutinin as the basic element. Therefore, the protein characterization of influenza vaccine by MALDI-TOF MS and gel electrophoresis was the further key step.

MALDI-TOF MS was used to characterize vaccine (Vaxigrip) mass spectra. Vaccine consists of three influenza's HAs (A/California/7/2009 (H1N1), A/Victoria/361/2011 (H3N2) and B/Wisconsin/1/2010), which were cultivated on embryonated eggs, concentrated, purified by zone centrifugation in a sucrose gradient, split, inactivated, and then diluted in phosphate buffered saline solution. The MALDI-TOF spectra showed three distinct peaks corresponding to vaccine HAs as indicated by the manufacturer. Fig. S2/Part 2 shows the detected proteins in the spectra of vaccine represented by three peaks (28 000 m/z, 48 000 m/z and 56 000 m/z). These results were compared with the SDS-PAGE gel (showed in insert in Fig. S2/Part 2) and the comparison brings the identical results, which is in good agreement with the published data (Epand and Epand, 2002; Garcia-Canas et al., 2010; Schwarzer et al., 2009). The proportions of several influenza proteins were found to be similar for various strains of the virus (Epand and Epand, 2002). One peak at 28 kDa corresponds to the matrix protein 1 (M1). The peak at 38 kDa represents the hemagglutinin fragment from influenza B virus. The peak at 48 kDa was assigned to the glycosylated HA (Chou et al., 2011). The highest peak in MALDI-TOF record at 56 kDa is connected with the presence of nucleocapsid protein (NP). The HA peak is necessary to search for at 63 kDa. This peak was also detected as expected (Fig. S2/Part 2).

3.1.3. Characterization of MPs–HA–CdS complex by scanning electrochemical microscope

It clearly follows from the obtained results that we successfully characterized all materials need for construction of beads-based isolation of virus. As further step, verification of MPs binding to HA–CdS was performed. SECM was used to characterize the MPs itself and HA–CdS complex bounded to MPs modified by glycan. Scan of the structure of the sample is performed in the SECM conventional feedback mode. Fig. S2/Part 3A shows the SECM images of MPs itself and Fig. S2/Part 2B shows MPs–glycan–HA–CdS complex formed during the isolation procedure. Current level of MPs itself was −0.6 nA, current level of the MPs–glycan–HA–CdS complex was −0.45 nA. Differences between current levels of both samples are caused by the formation of MPs–HA–CdS complex, because the presence of cadmium(II) enables to increase the level of current.

3.2. Optimization of the isolation procedure in stationary design connected with HMDE detection

Various conditions of isolation procedure were tested by automatic isolation procedure by ep Motion 5075 coupled with electrochemically detection at HMDE electrode to apply this procedure for the 3D chip microfluidic setup. The influence of four parameters (the way of HA–CdS complex preparation, concentration of glycan, interaction temperature and time of binding between glycan and HA–CdS) on the yield of the isolated CdS labeled viral protein was investigated.

Firstly, the influence of two preparation ways differing in the specific parameters (Section 2.4) on the isolation of HA–CdS complex was tested. Better way of preparation was confirmed for HA–CdS complex prepared by the second procedure, according to the result based on the detection of HA peak (Fig. 1A, blue color) as well as Cd peak (Fig. 1A, violet color).

Further, we aimed our attention at the optimization of the concentration of the glycan. Fig. 1B, blue color shows the dependence of Cd relative peak height on glycan concentration, and Fig. 1B, violet color shows the dependence of HA peak on the concentration of glycan. Changes in cadmium peak height showed the increasing dependence on the concentration of biotinylated

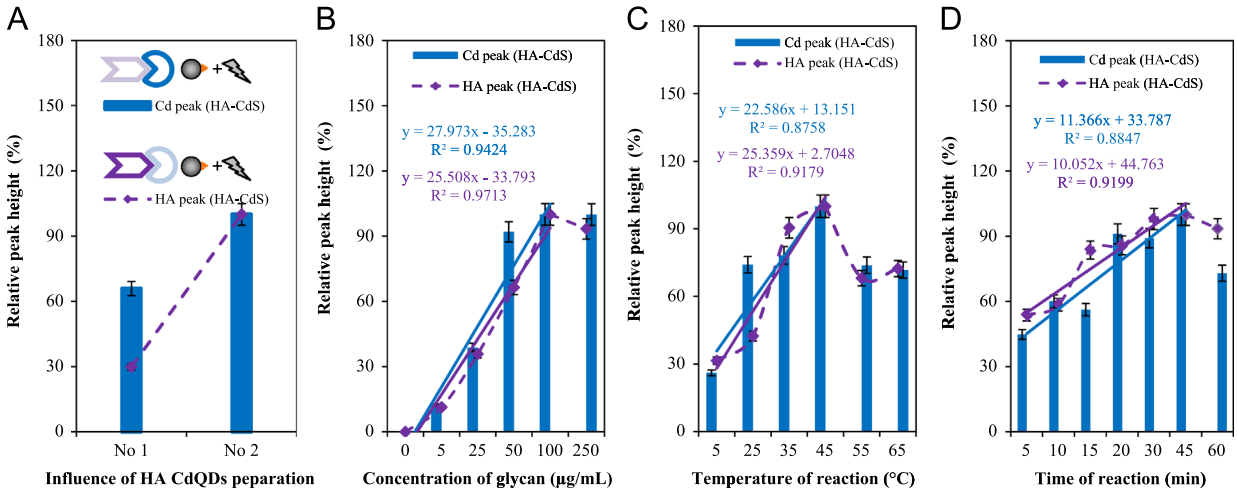

Fig. 1. Optimization of isolation procedure of HA–CdS complex by epMotion 5075 detected by electrochemical analysis of HA and Cd part of isolated HA–CdS complex. Cd peak was measured by DPASV. HA peak was measured by AdT DPV (for methods parameters see Section 2). Cd signal was described by columns and/or straight line and HA signal by points and/or dashed line. (**A**) Influence of the preparation way on detected signal of Cd and HA. (**B**) Influence of glycan concentration on detected signal of Cd and HA. (**C**) Influence of temperature on the linkage between glycan and HA–CdS. (**D**) Influence of reaction time on the linkage between glycan and HA–CdS. (For interpretation of the references to color in this figure legend, the reader is referred to the web version of this article.)

glycan, but only up to concentration of 50 μg/mL and this concentration was found as the optimal.

The further two optimized parameters (time and temperature of reaction) were directly connected with binding of glycan with HA–CdS. We tested six different values of temperature (5, 25, 35, 45, 55, and 65 °C) and seven different times of reaction (5, 10, 15, 20, 30, 45, and 60 min). Temperature of 45 °C was established as the best according to the Cd peak height (Fig. 1C, blue color) and HA peak (Fig. 1C, violet color). The highest effect of reaction time was observed for Cd peak (Fig. 1D, blue color) and HA peak (Fig. 1D, violet color) after 45 min of the incubation of glycan modified MPs with HA–CdS. If we summarize the results of the optimization, the best conditions were as it follows: concentration of glycan 50 μg/mL, preparation of HA–CdS complex by the second procedure, reaction time 45 min, and the reaction temperature 45 °C. These optimized conditions were applied for the 3D microfludic chip procedure.

3.3. Microfluidic analysis

Microfluidic devices have many advantages compared to their macro-scale counterparts, including a reduced reaction solution and cell consumption, an improved analysis speed, a greater portability, lower fabrication and operating costs, and the potential for parallel processing and integration with other miniaturized devices (Rios et al., 2012; Young, 1996). In this study we suggested, designed and fabricated the microfluidic device for the influenza detection (Fig. 2A). Optimized conditions for virus isolation were applied in the analysis process using 3D fabricated microfluidic chip. However, some further optimization steps aimed at chip detection parameters were done. The optimization of the electrochemical detection of Cd(II) under microfluidic conditions was the first step. Flow rate and time of accumulation were the optimized parameters. Sample was dosed by peristaltic pump in the operating range from 0 to 1200 μL/min (determined according to a flow number of peristaltic pump). With growing flow rate there was no enhancement in the yield of the isolation product over 480 μL/min (Fig. 2B). Between 134 and 480 μL/min there was the most efficient shift towards products detection and therefore the highest change of detected signal. The highest response of signal was achieved by the flow rate 480 μL/min (Fig. 2B). Thus, this optimized parameter was closely related to the next important parameter of electrochemical detection, time of accumulation. During the accumulation time there is a reaction between Cd and the surface of electrode, and due to the sensitivity of detection it was essential to test the effect of time of the accumulation on Cd peak height. Because the peak height did not markedly increase with higher time of accumulation of Cd (II), as the optimum 65 s was selected (Fig. 2C). Due to the fact that we obtained the optimal parameters for microfluidic device, it was possible to determine the accuracy. The system stability (including the isolation and detection process) was monitored (Fig. 2D) and Cd peak height was determined for five individual processes performed at five various chips. The presented error bars represent measurement error in the detection of the one specific isolation process. The accuracy of method was higher than 80 %. The influence of HA–CdS concentration (Cd concentration respectively) within the range from 0.06 to 0.5 mM on cadmium signal was investigated too. The increasing dependence in this concentration interval has parameters as it follows: $y=158.9x$, $R^2=0.9842$, $n=4$ (Fig. 2E) with RSD 5.2 %.

3.4. Application of suggested device to the influenza vaccine detection

Isolation and detection of influenza vaccine is introduced as a model of real sample detection in microfluidic device. Inactivated avian influenza viruses H5N1 labeled with CdS was isolated and detected by above-mentioned optimized procedure using 3D chip with three-electrode setup. For this experiment four equal samples and two negative controls were used. Each sample was used for the individual isolation and detection process. Electrochemical determination of the presence of formed HA–CdS complex by electrochemical quantification of cadmium(II) ions was used. The obtained results are shown in Fig. 3, where it is obvious the good accordance between samples and negative control, which gives no signal.

4. Conclusions

3D microfluidic chip was tested using CdS quantum dots labeled vaccine hemagglutinines. Our experiment demonstrated that the electrochemical analysis of isolated hemagglutinin using CdS quantum dots is very effective. Due to this fact, Cd signal has a great potential to become an alternative option as a rapid,

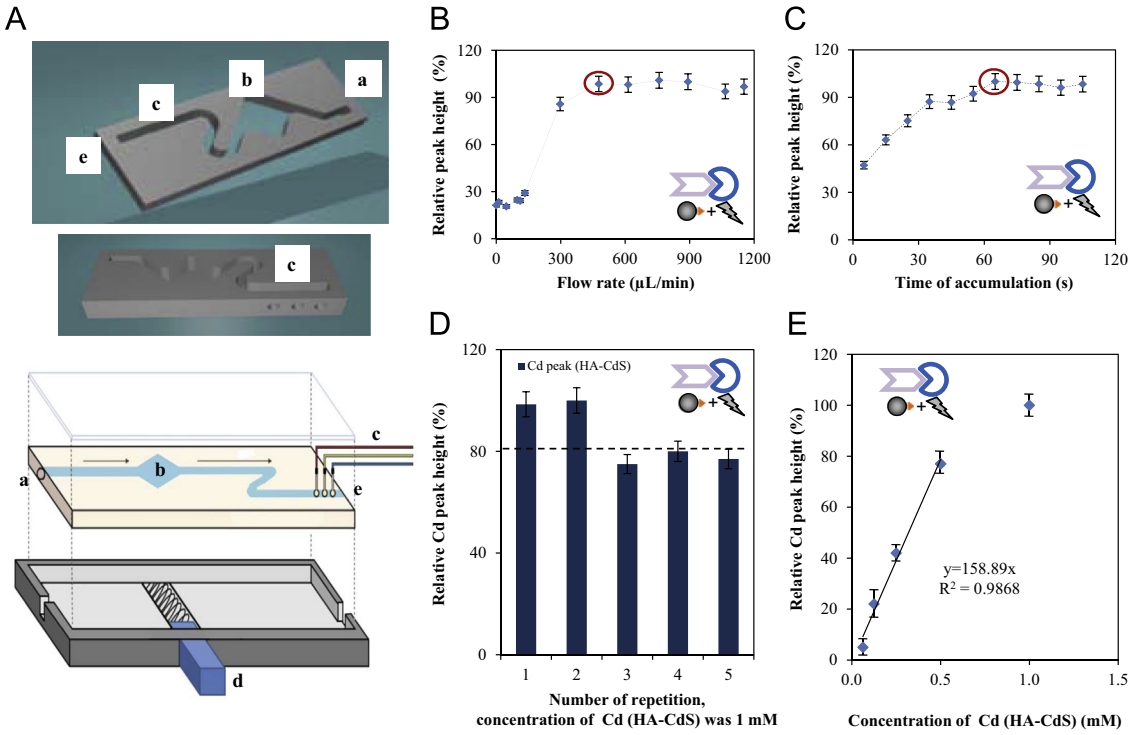

Fig. 2. (**A**) Scheme and model of 3D fabricated chip: (**a**) injection (influx) was used for dispensing the samples, buffer and electrolyte, (**b**) reaction cell, where whole process of isolation and magnetic pad, (d) was placed. (**c**) Three electrode setup, with working glassy carbon microelectrode, and efflux (**e**) for removing of reactants from the reaction chamber. Optimization of parameters for isolation and detection procedure. (**B**) Influence of flow rate (μL/min) on Cd relative peak height (%). (**C**) Dependence of relative peak height (%) on time of accumulation (s). (**D**) Dependence of relative Cd peak height (%) on concentration of Cd (HA–CdS) (1 mM). (**E**) Dependence of relative Cd peak height (%) on different concentration of Cd (HA–CdS). All measurements were provided by three electrode setup with working glassy carbon microelectrode. Differential pulse voltammetry (DPV) was a used for Cd signal detection (for methods parameters see Section 2).

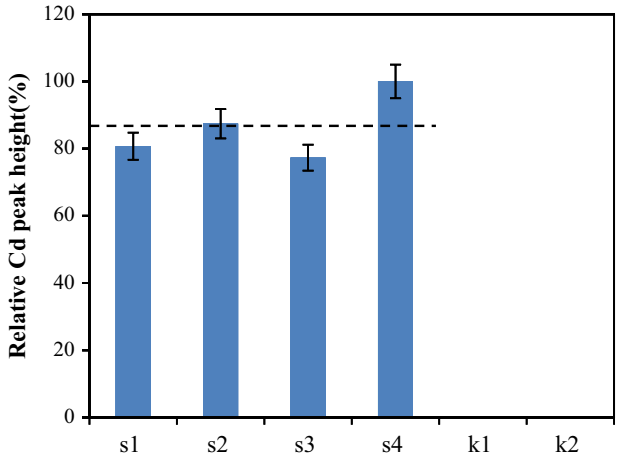

Fig. 3. Effect of isolation and detection procedure on the real sample detection. Real sample is inactivated avian influenza virus H5N1(295/Turkey/Canada/6213/66) labeled with CdS. The results were obtained through the electrochemical detection of Cd, using 3D chip. s1–s4 are the same samples and k1 and k2 are the negative controls.

sensitive, and specific detection of influenza hemagglutinin or influenza virus, and this 3D microfluidic system may be considered as a promising and powerful platform for the rapid diagnosis of influenza antigens and may be extended for diagnosis of other pathogens. As a future perspective, using of QDs with magnetic properties could be considered (Koole et al., 2009).

Acknowledgment

Financial support from CEITEC CZ.1.05/1.1.00/02.0068 and IGA IP16/2013 is highly acknowledged. We also thank to Assoc. Prof. Petr Lány from Department of Microbiology, Virology and Immunology, University of Veterinary and Pharmaceutical Sciences Brno for providing real sample of inactivated influenza.

Appendix A. Suppolementary material

Supplementary data associated with this article can be found in the online version at http://dx.doi.org/10.1016/j.bios.2013.10.031.

References

Bui, V.N., Ogawa, H., Ngo, L.H., Baatartsogt, T., Abao, L.N.B., Tamaki, S., Saito, K., Watanabe, Y., Runstadler, J., Imai, K., 2013. Arch. Virol. 158 (2), 451–455.
Casavant, B.P., Guckenberger, D.J., Berry, S.M., Tokar, J.T., Lang, J.M., Beebe, D.J., 2013. Lab Chip 13 (3), 391–396.
Chen, Q.J., Huang, S.P., Chen, J.J., Zhang, S.Q., Chen, Z., 2013. PLoS One 8 (1), 1–8.
Chou, T.C., Hsu, W., Wang, C.H., Chen, Y.J., Fang, J.M., 2011. J. Nanobiotechnol. 9, 1–13.
Epand, R.M., Epand, R.F., 2002. Biochem. J. 365, 841–848.
Garcia-Canas, V., Lorbetskie, B., Cyr, T.D., Hefford, M.A., Smith, S., Girard, M., 2010. Biologicals 38 (2), 294–302.
Gijs, M.A.M., 2004. Microfluid. Nanofluid. 1 (1), 22–40.
Hemmatzadeh, F., Sumarningsih, S., Tarigan, S., Indriani, R., Dharmayanti, N., Ebrahimie, E., Igniatovic, J., 2013. PLoS One 8 (2), 1–9.
Kamikawa, T.L., Mikolajczyk, M.G., Kennedy, M., Zhang, P., Wang, W., Scott, D.E., Alocilja, E.C., 2010. Biosens. Bioelectron. 26 (4), 1346–1352.
Kim, J.Y., Choi, K., Moon, D.I., Ahn, J.H., Park, T.J., Lee, S.Y., Choi, Y.K., 2013. Biosens. Bioelectron. 41, 867–870.
Koole, R., Mulder, W.J.M., van Schooneveld, M.M., Strijkers, G.J., Meijerink, A., Nicolay, K., 2009. Wiley Interdiscip. Rev.-Nanomed. Nanobiotechnol. 1 (5), 475–491.
Krasnoselsky, A.L., Katze, M.G., 2012. Nature 483 (7390), 416–417.
Krejcova, L., Dospivova, D., Ryvolova, M., Kopel, P., Hynek, D., Krizkova, S., Hubalek, J., Adam, V., Kizek, R., 2012. Electrophoresis 33 (21), 3195–3204.
Li, H., Shih, W.Y., Shih, W.H., 2007. Ind. Eng. Chem. Res. 46 (7), 2013–2019.
Lien, K.Y., Hung, L.Y., Huang, T.B., Tsai, Y.C., Lei, H.Y., Lee, G.B., 2011. Biosens. Bioelectron. 26 (9), 3900–3907.
Long, G.L., Winefordner, J.D., 1983. Anal. Chem. 55 (7), A712–A724.

Nejdl, L., Merlos, M.A.R., Kudr, J., Ruttkay-Nedecky, B., Konecna, M., Kopel, P., Zitka, O., Hubalek, J., Kizek, R., Adam, V., Electrophoresis. http://dx.doi.org/10.1002/elps.201300197, (inpress).
Polzin, C., Spath, S., Seitz, H., 2013. Rapid Prototyping J. 19 (1), 37–43.
Ramadan, Q., Gijs, M.A.M., 2012. Microfluid. Nanofluid. 13 (4), 529–542.
Rios, A., Zougagh, M., Avila, M., 2012. Anal. Chim. Acta 740, 1–11.
Shalyapina, A.Y., Zaporozhets, M.A., Volkov, V.V., Zhigalina, O.M., Nikolaichik, V.I., Gubin, S.P., Avilov, A.S., 2013. Russ. J. Inorg. Chem. 58 (1), 74–77.
Shembekar, N., Mallajosyula, V.V.A., Mishra, A., Yeolekar, L., Dhere, R., Kapre, S., Varadarajan, R., Gupta, S.K., 2013. PLoS One 8 (1), 1–13.
Schwarzer, J., Rapp, E., Hennig, R., Genzel, Y., Jordan, I., Sandig, V., Reichl, U., 2009. Vaccine 27 (32), 4325–4336.
Sochor, J., Hynek, D., Krejcova, L., Fabrik, I., Krizkova, S., Gumulec, J., Adam, V., Babula, P., Trnkova, L., Stiborova, M., Hubalek, J., Masarik, M., Binkova, H., Eckschlager, T., Kizek, R., 2012. Int. J. Electrochem. Sci. 7 (3), 2136–2152.
Stevens, J., Blixt, O., Tumpey, T.M., Taubenberger, J.K., Paulson, J.C., Wilson, I.A., 2006. Science 312 (5772), 404–410.
Suenaga, E., Mizuno, H., Penmetcha, K.K.R., 2012. Biosens. Bioelectron. 32 (1), 195–201.
Tong, S.X., Li, Y., Rivailler, P., Conrardy, C., Castillo, D.A.A., Chen, L.M., Recuenco, S., Ellison, J.A., Davis, C.T., York, I.A., Turmelle, A.S., Moran, D., Rogers, S., Shi, M., Tao, Y., Weil, M.R., Tang, K., Rowe, L.A., Sammons, S., Xu, X.Y., Frace, M., Lindblade, K.A., Cox, N.J., Anderson, L.J., Rupprecht, C.E., Donis, R.O., 2012. Proc. Natl. Acad. Sci. USA 109 (11), 4269–4274.
Tsai, S.S.H., Wexler, J.S., Wan, J.D., Stone, H.A., 2013. Lab Chip 13 (1), 119–125.
Vyslouzilova, L., Krizkova, S., Anyz, J., Hynek, D., Hrabeta, J., Kruseova, J., Eckschlager, T., Adam, V., Stepankova, O., Kizek, R., 2013. Electrophoresis 34 (11), 1637–1648.
Xu, Y.H., Wang, E.K., 2012. Electrochim. Acta 84, 62–73.
Young, J., 1996. Forbes 158 (7), 210–211.

6 ZÁVĚR

Disertační práce byla zaměřena na konstrukci senzorů a biosenzorů pro detekci ptačí chřipky. Pro tento účel byly zvoleny dvě cílové části chřipkového virionu: nukleová kyselina a povrchový antigen. Tyto dvě molekuly byly v detekčních systémech zastoupeny syntetickým hemaglutininem nebo vakcínou s obsahem hemaglutininů (v případě detekce povrchového antigenu) a syntetickými DNA oligonukleotidy, odvozenými od genomu chřipky (v případě detekce nukleové kyseliny). Obě cílové molekuly byly modifikované pomocí kvantových teček (QDs), za účelem citlivé a specifické elektrochemické detekce. Veškeré detekční systémy publikované v přiložených textech byly založené na využití magnetické izolace a elektrochemické detekce cílových molekul. Izolace byla založena na selektivitě modifikovaných paramagnetických částic (MPs). Pro detekci izolovaných cílových molekul byly použity metody diferenční pulzní voltametrie, square wave voltametrie a cyklické voltametrie.

V úvodní části práce je obecně popsána problematika chřipkových onemocnění. Teoretická část se zabývá podrobným popisem chřipkových virů, jejich životního cyklu a struktury chřipkového virionu. Další kapitoly pojednávají o mutačních změnách a jejich důsledcích v podobě epidemií a pandemií. Dále je popisována chřipka, jako onemocnění s podkapitolami věnovanými klinickým příznakům, komplikacím, prevenci a terapii. Teoretickou část uzavírají kapitoly popisující standardně používané metody detekce chřipkových virů a nové přístupy v podobě senzorů a biosenzorů.

V metodické části práce jsou blíže popsány přístroje a metody, požívané při experimentální práci.

Všechny výsledky této práce jsou shrnuty v kapitole výsledky a diskuze. Základem této kapitoly je osm vědeckých prací v ISI impaktovaných časopisech, ke kterým je připojen shrnující komentář. Pojítkem všech článků je použití elektrochemických detekčních metod k prokázání přítomnosti chřipkového viru.

Cílem této práce bylo nalézt způsoby pro izolaci a detekci dvou klíčových struktur chřipkového virionu a to nukleové kyseliny a povrchového antigenu. Publikované práce dokazují, že spojení nanomateriálů s elektrochemickými metodami, má svoje místo v oblasti diagnostiky. Popsané senzory založené na magnetické izolaci a následné elektrochemické detekci jsou slibným nástrojem pro detekci chřipky a ostatních patogenů. Poslední z publikovaných prací představuje využití 3D tiskové technologie

pro výrobu mikrofluidních čipů a jejich aplikaci pro detekci dalších specifických látek, které jsou klíčovými v oblasti prevence, diagnostiky nebo léčby infekčních chorob.

7 LITERATURA

ADAM, V.; HUSKA, D.; HUBALEK, J.; KIZEK, R. Easy to use and rapid isolation and detection of a viral nucleic acid by using paramagnetic microparticles and carbon nanotubes-based screen-printed electrodes. *Microfluidics and Nanofluidics*, 2010, roč. 8. č. 3, s. 329-339. ISS 1613-4982.

AIR, G. M. Influenza neuraminidase. *Influenza and Other Respiratory Viruses*, 2012, roč. 6. č. 4, s. 245-256. ISS 1750-2640.

AKARSU, H.; IWATSUKI-HORIMOTO, K.; NODA, T.; KAWAKAMI, E.; KATSURA, H.; BAUDIN, F.; HORIMOTO, T.; KAWAOKA, Y. Structure-based design of NS2 mutants for attenuated influenza A virus vaccines. *Virus Research*, 2011, roč. 155. č. 1, s. 240-248. ISS 0168-1702.

AKBARZADEH, A.; SAMIEI, M.; JOO, S. W.; ANZABY, M.; HANIFEHPOUR, Y.; NASRABADI, H. T.; DAVARAN, S. Synthesis, characterization and in vitro studies of doxorubicin-loaded magnetic nanoparticles grafted to smart copolymers on A549 lung cancer cell line. *Journal of Nanobiotechnology*, 2012, roč. 10. č., s. ISS 1477-3155.

ANSUMANA, R.; BONWITT, J.; STENGER, D. A.; JACOBSEN, K. H. Ebola in Sierra Leone: a call for action. *Lancet*, 2014, roč. 384. č. 9940, s. 303. ISS 1474-547X.

ARRANZ, R.; COLOMA, R.; CHICHON, F. J.; CONESA, J. J.; CARRASCOSA, J. L.; VALPUESTA, J. M.; ORTIN, J.; MARTIN-BENITO, J. The Structure of Native Influenza Virion Ribonucleoproteins. *Science*, 2012, roč. 338. č. 6114, s. 1634-1637. ISS 0036-8075.

ARZEY, G. G.; KIRKLAND, P. D.; ARZEY, K. E.; FROST, M.; MAYWOOD, P.; CONATY, S.; HURT, A. C.; DENG, Y.-M.; IANNELLO, P.; BARR, I.; DWYER, D. E.; RATNAMOHAN, M.; MCPHIE, K.; SELLECK, P. Influenza Virus A (H10N7) in Chickens and Poultry Abattoir Workers, Australia. *Emerging Infectious Diseases*, 2012, roč. 18. č. 5, s. 814-816. ISS 1080-6040.

AYDINLIK, S.; OZKAN-ARIKSOYSAL, D.; KARA, P.; SAYINER, A. A.; OZSOZ, M. A nucleic acid-based electrochemical biosensor for the detection of influenza B virus from PCR samples using gold nanoparticle-adsorbed disposable graphite electrode and Meldola's blue as an intercalator. *Analytical Methods*, 2011, roč. 3. č. 7, s. 1607-1614. ISS 1759-9660.

BAGUELIN, M.; JIT, M.; MILLER, E.; EDMUNDS, W. J. Health and economic impact of the seasonal influenza vaccination programme in England. *Vaccine*, 2012, roč. 30. č. 23, s. 3459-3462. ISS 0264-410X.

BAHL, J.; VIJAYKRISHNA, D.; HOLMES, E. C.; SMITH, G. J. D.; GUAN, Y. Gene flow and competitive exclusion of avian influenza A virus in natural reservoir hosts. *Virology*, 2009, roč. 390. č. 2, s. 289-297. ISS 0042-6822.

BARKER, C. I. S.; SNAPE, M. D. Pandemic influenza A H1N1 vaccines and narcolepsy: vaccine safety surveillance in action. *Lancet Infectious Diseases*, 2014, roč. 14. č. 3, s. 227-238. ISS 1473-3099.

BELSER, J. A.; BLIXT, O.; CHEN, L.-M.; PAPPAS, C.; MAINES, T. R.; VAN HOEVEN, N.; DONIS, R.; BUSCH, J.; MCBRIDE, R.; PAULSON, J. C.; KATZ, J. M.; TUMPEY, T. M. Contemporary North American influenza H7 viruses possess human receptor specificity: Implications for virus

transmissibility. *Proceedings of the National Academy of Sciences of the United States of America*, 2008, roč. 105. č. 21, s. 7558-7563. ISS 0027-8424.

BELSER, J. A.; GUSTIN, K. M.; KATZ, J. M.; MAINES, T. R.; TUMPEY, T. M. Influenza Virus Infectivity and Virulence following Ocular-Only Aerosol Inoculation of Ferrets. *Journal of Virology*, 2014, roč. 88. č. 17, s. 9647-54. ISS 1098-5514.

BI, J. M.; DENG, G. C.; DONG, J.; KONG, F. L.; LI, X. Z.; XU, Q. A.; ZHANG, M. J.; ZHAO, L. H.; QIAO, J. A. Phylogenetic and Molecular Characterization of H9N2 Influenza Isolates from Chickens in Northern China from 2007-2009. *Plos One*, 2010, roč. 5. č. 9, s. ISS 1932-6203.

BLOOM, J. D.; GONG, L. I.; BALTIMORE, D. Permissive Secondary Mutations Enable the Evolution of Influenza Oseltamivir Resistance. *Science*, 2010, roč. 328. č. 5983, s. 1272-1275. ISS 0036-8075.

BODEWES, R.; MORICK, D.; DE MUTSERT, G.; OSINGA, N.; BESTEBROER, T.; VAN DER VLIET, S.; SMITS, S. L.; KUIKEN, T.; RIMMELZWAAN, G. F.; FOUCHIER, R. A. M.; OSTERHAUS, A. Recurring Influenza B Virus Infections in Seals. *Emerging Infectious Diseases*, 2013, roč. 19. č. 3, s. 511-512. ISS 1080-6040.

BONYAR, A.; SANTHA, H.; VARGA, M.; RING, B.; VITEZ, A.; HARSANYI, G. Characterization of rapid PDMS casting technique utilizing molding forms fabricated by 3D rapid prototyping technology (RPT). *International Journal of Material Forming*, 2014, roč. 7. č. 2, s. 189-196. ISS 1960-6206; 1960-6214.

BOUVIER, N. M.; LOWEN, A. C. Animal Models for Influenza Virus Pathogenesis and Transmission. *Viruses-Basel*, 2010, roč. 2. č. 8, s. 1530-1563. ISS 1999-4915.

BRAGSTAD, K.; VINNER, L.; HANSEN, M. S.; NIELSEN, J.; FOMSGAARD, A. A polyvalent influenza A DNA vaccine induces heterologous immunity and protects pigs against pandemic A(H1N1)pdm09 virus infection. *Vaccine*, 2013, roč. 31. č. 18, s. 2281-2288. ISS 0264-410X.

CAI, J.; ZHOU, Q.; CHEN, G.; LIU, S. Avian influenza virus piezoelectric biological sensor detecting instrument: Chongqing Inst Technology.

CAO, R. G.; SUAREZ, N. M.; OBERMOSER, G.; LOPEZ, S. M. C.; FLANO, E.; MERTZ, S. E.; ALBRECHT, R. A.; GARCIA-SASTRE, A.; MEJIAS, A.; XU, H.; QIN, H.; BLANKENSHIP, D.; PALUCKA, K.; PASCUAL, V.; RAMILO, O. Differences in antibody responses between trivalent inactivated influenza vaccine and live attenuated influenza vaccine correlate with the kinetics and magnitude of interferon signaling in children. *The Journal of infectious diseases*, 2014, roč. 210. č. 2, s. 224-33. ISS 1537-6613.

COBBIN, J. C. A.; ONG, C.; VERITY, E.; GILBERTSON, B. P.; ROCKMAN, S. P.; BROWN, L. E. Influenza Virus PB1 and Neuraminidase Gene Segments Can Cosegregate during Vaccine Reassortment Driven by Interactions in the PB1 Coding Region. *Journal of Virology*, 2014, roč. 88. č. 16, s. 8971-80. ISS 1098-5514.

COMIN, A.; TOFT, N.; STEGEMAN, A.; KLINKENBERG, D.; MARANGON, S. Serological diagnosis of avian influenza in poultry: is the haemagglutination inhibition test really the "gold standard"? *Influenza and Other Respiratory Viruses*, 2013, roč. 7. č. 3, s. 257-264. ISS 1750-2640.

CONENELLO, G. M.; TISONCIK, J. R.; ROSENZWEIG, E.; VARGA, Z. T.; PALESE, P.; KATZE, M. G. A Single N66S Mutation in the PB1-F2 Protein of

Influenza A Virus Increases Virulence by Inhibiting the Early Interferon Response In Vivo. *Journal of Virology*, 2011, roč. 85. č. 2, s. 652-662. ISS 0022-538X.

COSNIER, S.; MAILLEY, P. Recent advances in DNA sensors. *Analyst*, 2008, roč. 133. č. 8, s. 984-991. ISS 0003-2654.

CURRAN, J. W.; MORGAN, W. M.; HARDY, A. M.; JAFFE, H. W.; DARROW, W. W.; DOWDLE, W. R. THE EPIDEMIOLOGY OF AIDS - CURRENT STATUS AND FUTURE-PROSPECTS. *Science*, 1985, roč. 229. č. 4720, s. 1352-1357. ISS 0036-8075.

DANILENKO, D. M.; SMIRNOVA, T. D.; GUDKOVA, T. M.; PROKOPETZ, A. V.; BILDANOVA, E. R.; KADIROVA, R. A.; SLITA, A. V.; EROPKIN, M. Y. Comparative study of MDCK and CaCo-2 cell Lines for influenza virus isolation. *Voprosy Virusologii*, 2014, roč. 59. č. 2, s. 40-45. ISS 0507-4088.

DANKAR, S. K.; MIRANDA, E.; FORBES, N. E.; PELCHAT, M.; TAVASSOLI, A.; SELMAN, M.; PING, J. H.; JIA, J. J.; BROWN, E. G. Influenza A/Hong Kong/156/1997(H5N1) virus NS1 gene mutations F103L and M106I both increase IFN antagonism, virulence and cytoplasmic localization but differ in binding to RIG-I and CPSF30. *Virology Journal*, 2013, roč. 10. č., s. ISS 1743-422X.

DE CHASSEY, B.; AUBLIN-GEX, A.; RUGGIERI, A.; MEYNIEL-SCHICKLIN, L.; PRADEZYNSKI, F.; DAVOUST, N.; CHANTIER, T.; TAFFOREAU, L.; MANGEOT, P. E.; CIANCIA, C.; PERRIN-COCON, L.; BARTENSCHLAGER, R.; ANDRE, P.; LOTTEAU, V. The Interactomes of Influenza Virus NS1 and NS2 Proteins Identify New Host Factors and Provide Insights for ADAR1 Playing a Supportive Role in Virus Replication. *Plos Pathogens*, 2013, roč. 9. č. 7, s. ISS 1553-7374.

DE JONG, M. D.; VAN CAM, B.; QUI, P. T.; HIEN, V. M.; THANH, T. T.; HUE, N. B.; BELD, M.; PHUONG, L. T.; KHANH, T. H.; CHAU, N. V. V.; HIEN, T. T.; HA, D. Q.; FARRAR, J. Brief report: Fatal avian influenza A (H5N1) in a child presenting with diarrhea followed by coma. *New England Journal of Medicine*, 2005, roč. 352. č. 7, s. 686-691. ISS 0028-4793.

DEL POZO, P.; ABARCA, K.; CONCHA, I.; CERDA, J. Concordance of nasal swabs and nasopharyngeal swabs in the detection of respiratory viruses by direct immunofluorescence. *Revista Chilena De Infectologia*, 2014, roč. 31. č. 2, s. 160-164. ISS 0716-1018; 0717-6341.

DENIS, J.; ACOSTA-RAMIREZ, E.; ZHAO, Y.; HAMELIN, M.-E.; KOUKAVICA, I.; BAZ, M.; ABED, Y.; SAVARD, C.; PARE, C.; MACIAS, C. L.; BOIVIN, G.; LECLERC, D. Development of a universal influenza A vaccine based on the M2e peptide fused to the papaya mosaic virus (PapMV) vaccine platform. *Vaccine*, 2008, roč. 26. č. 27-28, s. 3395-3403. ISS 0264-410X.

DEY, R. S.; RAJ, C. R. Enzyme-integrated cholesterol biosensing scaffold based on in situ synthesized reduced graphene oxide and dendritic Pd nanostructure. *Biosensors & bioelectronics*, 2014, roč. 62. č., s. 357-64. ISS 1873-4235.

DOLLER, G.; DOLLER, P. C.; GERTH, H. J. SEROLOGICAL INFLUENZA DIAGNOSIS - COMPARISON BETWEEN CFT AND SUBTYPE AND IMMUNOGLOBULIN CLASS SPECIFIC IFT. *Zentralblatt Fur Bakteriologie Mikrobiologie Und Hygiene Series a-Medical Microbiology Infectious Diseases Virology Parasitology*, 1987, roč. 267. č. 1, s. 93-93. ISS 0174-3031.

DONG, L. B.; BO, H.; BAI, T.; GAO, R. B.; DONG, J.; ZHANG, Y.; GUO, J. F.; ZOU, S. M.; ZHOU, J. F.; ZHU, Y.; XIN, L.; LI, X. D.; XU, C. L.; WANG, D. Y.; SHU, Y. L. A Combination of Serological Assays to Detect Human Antibodies to the Avian Influenza A H7N9 Virus. *Plos One*, 2014, roč. 9. č. 4, s. ISS 1932-6203.

DOREY, E. Process technology 3D printing for drugs. *Chemistry & Industry*, 2014, roč. 78. č. 7, s. 7-7. ISS 0009-3068; 2047-6329.

EAMES, K. T. D.; WEBB, C.; THOMAS, K.; SMITH, J.; SALMON, R.; TEMPLE, J. M. F. Assessing the role of contact tracing in a suspected H7N2 influenza A outbreak in humans in Wales. *BMC infectious diseases*, 2010, roč. 10. č., s. ISS 1471-2334.

EDINGER, T. O.; POHL, M. O.; STERTZ, S. Entry of influenza A virus: host factors and antiviral targets. *Journal of General Virology*, 2014, roč. 95. č., s. 263-277. ISS 0022-1317.

ENSERINK, M. Pandemic influenza - Global update. *Science*, 2005, roč. 309. č. 5733, s. 371-+. ISS 0036-8075.

FADRNA, R.; CAHOVA-KUCHARIKOVA, K.; HAVRAN, L.; YOSYPCHUK, B.; FOJTA, M. Use of polished and mercury film-modified silver solid amalgam electrodes in electrochemical analysis of DNA. *Electroanalysis*, 2005, roč. 17. č. 5-6, s. 452-459. ISS 1040-0397.

FAUQUET, C. M.; PRINGLE, C. R. Revised Guidelines for the Preparation of Family Descriptions for the Seventh Report of the International Committee on Taxonomy of Viruses (ICTV) due to be published in mid-1999. *Archives of Virology*, 1997, roč. 142. č. 10, s. 2115-2120. ISS 0304-8608.

FERDINANDS, J. M.; OLSHO, L. E. W.; AGAN, A. A.; BHAT, N.; SULLIVAN, R. M.; HALL, M.; MOURANI, P. M.; THOMPSON, M.; RANDOLPH, A. G.; PEDIATRIC ACUTE LUNG, I.; SEPSIS INVESTIGATORS, N. Effectiveness of Influenza Vaccine Against Life-threatening RT-PCR-confirmed Influenza Illness in US Children, 2010-2012. *The Journal of infectious diseases*, 2014, roč. 210. č. 5, s. 674-83. ISS 1537-6613.

FERGUSON, N. M.; GALVANI, A. P.; BUSH, R. M. Ecological and immunological determinants of influenza evolution. *Nature*, 2003, roč. 422. č. 6930, s. 428-433. ISS 0028-0836.

FIALOVA, D.; KREJCOVA, L.; JANU, L.; BLAZKOVA, I.; KRYSTOFOVA, O.; HYNEK, D.; KOPEL, P.; DRBOHLAVOVA, J.; KONECNA, M.; VACULOVICOVA, M.; KYNICKY, J.; HUBALEK, J.; BABULA, P.; KIZEK, R.; ADAM, V. Flow Injection Electrochemical Analysis of Complexes of Influenza Proteins with CdS, PbS and CuS Quantum Dots. *International Journal of Electrochemical Science*, 2013, roč. 8. č. 8, s. 10805-10817. ISS 1452-3981.

FODOR, E. The RNA polymerase of influenza A virus: mechanisms of viral transcription and replication. *Acta Virologica*, 2013, roč. 57. č. 2, s. 113-122. ISS 0001-723X.

FOJTA, M.; HAVRAN, L.; HORAKOVA, P.; KOSTECKA, P.; PIVONKOVA, H.; SIMKOVA, E.; SPACEK, J.; VYCHODILOVA, Z.; VIDLAKOVA, P. Electrochemical Analysis of DNA: When, How and Why to Use Electroactive Labels and Indicators. *Modern Electrochemical Methods Xxx*, 2010, roč. č., s. 40-44. ISS

FONTANA, J.; STEVEN, A. C. At Low pH, Influenza Virus Matrix Protein M1 Undergoes a Conformational Change Prior to Dissociating from the Membrane. *Journal of Virology*, 2013, roč. 87. č. 10, s. 5621-5628. ISS 0022-538X.

FORBES, N.; SELMAN, M.; PELCHAT, M.; JIA, J. J.; STINTZI, A.; BROWN, E. G. Identification of Adaptive Mutations in the Influenza A Virus Non-Structural 1 Gene That Increase Cytoplasmic Localization and Differentially Regulate Host Gene Expression. *Plos One*, 2013, roč. 8. č. 12, s. ISS 1932-6203.

FORTES, P.; BELOSO, A.; ORTIN, J. INFLUENZA-VIRUS NS1 PROTEIN INHIBITS PREMESSENGER RNA SPLICING AND BLOCKS MESSENGER-RNA NUCLEOCYTOPLASMIC TRANSPORT. *Embo Journal*, 1994, roč. 13. č. 3, s. 704-712. ISS 0261-4189.

FREIDL, G. S.; MEIJER, A.; DE BRUIN, E.; DE NARDI, M.; MUNOZ, O.; CAPUA, I.; BREED, A. C.; HARRIS, K.; HILL, A.; KOSMIDER, R.; BANKS, J.; VON DOBSCHUETZ, S.; STARK, K.; WIELAND, B.; STEVENS, K.; VAN DER WERF, S.; ENOUF, V.; VAN DER MEULEN, K.; VAN REETH, K.; DAUPHIN, G.; KOOPMANS, M.; CONSORTIUM, F. Influenza at the animal-human interface: a review of the literature for virological evidence of human infection with swine or avian influenza viruses other than A(H5N1). *Eurosurveillance*, 2014, roč. 19. č. 18, s. 8-26. ISS 1560-7917.

GAMBLIN, S. J.; SKEHEL, J. J. Influenza Hemagglutinin and Neuraminidase Membrane Glycoproteins. *Journal of Biological Chemistry*, 2010, roč. 285. č. 37, s. 28403-28409. ISS 0021-9258.

GARCIA-SASTRE, A.; EGOROV, A.; MATASSOV, D.; BRANDT, S.; LEVY, D. E.; DURBIN, J. E.; PALESE, P.; MUSTER, T. Influenza A virus lacking the NS1 gene replicates in interferon-deficient systems. *Virology*, 1998, roč. 252. č. 2, s. 324-330. ISS 0042-6822.

GARCIA, V.; ARIS-BROSOU, S. Comparative Dynamics and Distribution of Influenza Drug Resistance Acquisition to Protein M2 and Neuraminidase Inhibitors. *Molecular Biology and Evolution*, 2014, roč. 31. č. 2, s. 355-363. ISS 0737-4038.

GARTEN, W.; KLENK, H. D. Understanding influenza virus pathogenicity. *Trends in Microbiology*, 1999, roč. 7. č. 3, s. 99-100. ISS 0966-842X.

GETHING, M. J.; BYE, J.; SKEHEL, J.; WATERFIELD, M. CLONING AND DNA-SEQUENCE OF DOUBLE-STRANDED COPIES OF HEMAGGLUTININ GENES FROM H2-STRAINS AND H3-STRAINS ELUCIDATES ANTIGENIC SHIFT AND DRIFT IN HUMAN INFLUENZA-VIRUS. *Nature*, 1980, roč. 287. č. 5780, s. 301-306. ISS 0028-0836.

GILBERT, S. C. Advances in the development of universal influenza vaccines. *Influenza and Other Respiratory Viruses*, 2013, roč. 7. č. 5, s. 750-758. ISS 1750-2640.

GLIKMANN, G.; MORDHORST, C. H.; KOCH, C. MONOCLONAL-ANTIBODIES FOR THE DIRECT-DETECTION OF INFLUENZA-A VIRUS BY ELISA IN CLINICAL SPECIMENS FROM PATIENTS WITH RESPIRATORY-INFECTIONS. *Clinical and Diagnostic Virology*, 1995, roč. 3. č. 4, s. 361-369. ISS 0928-0197.

GLODOWSKI, D. R.; CHEN, C. C. H.; SCHAEFER, H.; GRANT, B. D.; RONGO, C. RAB-10 regulates glutamate receptor recycling in a cholesterol-dependent endocytosis pathway. *Molecular Biology of the Cell*, 2007, roč. 18. č. 11, s. 4387-4396. ISS 1059-1524.

GOODING, J. J. Electrochemical DNA hyhridization biosensors. *Electroanalysis*, 2002, roč. 14. č. 17, s. 1149-1156. ISS 1040-0397.

GOU, Y.; SLAVIN, S.; GENG, J.; VOORHAAR, L.; HADDLETON, D. M.; BECER, C. R. Controlled Alternate Layer-by-Layer Assembly of Lectins and Glycopolymers Using QCM-D. *Acs Macro Letters*, 2012, roč. 1. č. 1, s. 180-183. ISS 2161-1653.

GRABOWSKA, I.; MALECKA, K.; STACHYRA, A.; GORA-SOCHACKA, A.; SIRKO, A.; ZAGORSKI-OSTOJA, W.; RADECKA, H.; RADECKI, J. Single Electrode Genosensor for Simultaneous Determination of Sequences Encoding Hemagglutinin and Neuraminidase of Avian Influenza Virus Type H5N1. *Analytical Chemistry*, 2013, roč. 85. č. 21, s. 10167-10173. ISS 0003-2700.

GRABOWSKA, I.; STACHYRA, A.; GORA-SOCHACKA, A.; SIRKO, A.; OLEJNICZAK, A. B.; LESNIKOWSKI, Z. J.; RADECKI, J.; RADECKA, H. DNA probe modified with 3-iron bis(dicarbollide) for electrochemical determination of DNA sequence of Avian Influenza Virus H5N1. *Biosensors & bioelectronics*, 2014, roč. 51. č., s. 170-176. ISS 0956-5663; 1873-4235.

GUO, L.; ZHANG, X.; REN, L. L.; YU, X. L.; CHEN, L. J.; ZHOU, H. L.; GAO, X.; TENG, Z.; LI, J. G.; HU, J. Y.; WU, C.; XIAO, X.; ZHU, Y. Y.; WANG, Q. Y.; PANG, X. H.; JIN, Q.; WU, F.; WANG, J. W. Human Antibody Responses to Avian Influenza A(H7N9) Virus, 2013. *Emerging Infectious Diseases*, 2014, roč. 20. č. 2, s. 192-200. ISS 1080-6040.

HAI, R.; SCHMOLKE, M.; LEYVA-GRADO, V. H.; THANGAVEL, R. R.; MARGINE, I.; JAFFE, E. L.; KRAMMER, F.; SOLORZANO, A.; GARCIA-SASTRE, A.; PALESE, P.; BOUVIER, N. M. Influenza A(H7N9) virus gains neuraminidase inhibitor resistance without loss of in vivo virulence or transmissibility. *Nature Communications*, 2013, roč. 4. č., s. ISS 2041-1723.

HALE, B. G.; RANDALL, R. E.; ORTIN, J.; JACKSON, D. The multifunctional NS1 protein of influenza A viruses. *Journal of General Virology*, 2008, roč. 89. č., s. 2359-2376. ISS 0022-1317.

HALL, J. S.; TESLAA, J. L.; NASHOLD, S. W.; HALPIN, R. A.; STOCKWELL, T.; WENTWORTH, D. E.; DUGAN, V.; IP, H. S. Evolution of a reassortant North American gull influenza virus lineage: drift, shift and stability. *Virology Journal*, 2013, roč. 10. č., s. ISS 1743-422X.

HASSEN, W. M.; DUPLAN, V.; FROST, E.; DUBOWSKI, J. J. Quantitation of influenza A virus in the presence of extraneous protein using electrochemical impedance spectroscopy. *Electrochimica Acta*, 2011, roč. 56. č. 24, s. 8325-8328. ISS 0013-4686.

HATADA, E.; SAITO, S.; FUKUDA, R. Mutant influenza viruses with a defective NS1 protein cannot block the activation of PKR in infected cells. *Journal of Virology*, 1999, roč. 73. č. 3, s. 2425-2433. ISS 0022-538X.

HEWA, T. M. P.; TANNOCK, G. A.; MAINWARING, D. E.; HARRISON, S.; FECONDO, J. V. The detection of influenza A and B viruses in clinical specimens using a quartz crystal microbalance. *Journal of Virological Methods*, 2009, roč. 162. č. 1-2, s. 14-21. ISS 0166-0934.

HILL, A.; COOKE, G. Medicine. Hepatitis C can be cured globally, but at what cost? *Science (New York, N.Y.)*, 2014, roč. 345. č. 6193, s. 141-2. ISS 1095-9203.

HOOPER, K. A.; BLOOM, J. D. A Mutant Influenza Virus That Uses an N1 Neuraminidase as the Receptor-Binding Protein. *Journal of Virology*, 2013, roč. 87. č. 23, s. 12531-12540. ISS 0022-538X; 1098-5514.

HOSAKA, Y. Structure and function of influenza virus nucleoprotein (NP). *Nihon rinsho. Japanese journal of clinical medicine*, 1997, roč. 55. č. 10, s. 2599-604. ISS 0047-1852.

HSING, I. M.; XU, Y.; ZHAO, W. Micro- and nano-magnetic particles for applications in biosensing. *Electroanalysis*, 2007, roč. 19. č. 7-8, s. 755-768. ISS 1040-0397.

HTTP://WWW.WHO.INT/INFLUENZA/EN/. 8/2014, 2014.

HYLAND, L.; WEBBY, R.; SANDBULTE, M. R.; CLARKE, B.; HOU, S. Influenza virus NS1 protein protects against lymphohematopoietic pathogenesis in an in vivo mouse model. *Virology*, 2006, roč. 349. č. 1, s. 156-163. ISS 0042-6822.

CHACHRA, R.; RIZZO, R. C. Origins of resistance conferred by the R292K neuraminidase mutation via molecular dynamics and free energy calculations. *Journal of Chemical Theory and Computation*, 2008, roč. 4. č. 9, s. 1526-1540. ISS 1549-9618.

CHAN, W. H.; NG, A. K. L.; ROBB, N. C.; LAM, M. K. H.; CHAN, P. K. S.; AU, S. W. N.; WANG, J. H.; FODOR, E.; SHAW, P. C. Functional Analysis of the Influenza Virus H5N1 Nucleoprotein Tail Loop Reveals Amino Acids That Are Crucial for Oligomerization and Ribonucleoprotein Activities. *Journal of Virology*, 2010, roč. 84. č. 14, s. 7337-7345. ISS 0022-538X.

CHEN, W. S.; CALVO, P. A.; MALIDE, D.; GIBBS, J.; SCHUBERT, U.; BACIK, I.; BASTA, S.; O'NEILL, R.; SCHICKLI, J.; PALESE, P.; HENKLEIN, P.; BENNINK, J. R.; YEWDELL, J. W. A novel influenza A virus mitochondrial protein that induces cell death. *Nature Medicine*, 2001, roč. 7. č. 12, s. 1306-1312. ISS 1078-8956.

CHENAVAS, S.; CREPIN, T.; DELMAS, B.; RUIGROK, R. W. H.; SLAMA-SCHWOK, A. Influenza virus nucleoprotein: structure, RNA binding, oligomerization and antiviral drug target. *Future Microbiology*, 2013, roč. 8. č. 12, s. 1537-1545. ISS 1746-0913.

CHENG, X.; ZENGEL, J. R.; XU, Q.; JIN, H. Surface glycoproteins of influenza A H3N2 virus modulate virus replication in the respiratory tract of ferrets. *Virology*, 2012, roč. 432. č. 1, s. 91-98. ISS 0042-6822.

IMAI, M.; HERFST, S.; SORRELL, E. M.; SCHRAUWEN, E. J. A.; LINSTER, M.; DE GRAAF, M.; FOUCHIER, R. A. M.; KAWAOKA, Y. Transmission of influenza A/H5N1 viruses in mammals. *Virus Research*, 2013, roč. 178. č. 1, s. 15-20. ISS 0168-1702.

IQBAL, M.; REDDY, K. B.; BROOKES, S. M.; ESSEN, S. C.; BROWN, I. H.; MCCAULEY, J. W. Virus Pathotype and Deep Sequencing of the HA Gene of a Low Pathogenicity H7N1 Avian Influenza Virus Causing Mortality in Turkeys. *Plos One*, 2014, roč. 9. č. 1, s. ISS 1932-6203.

ISIN, B.; DORUKER, P.; BAHAR, I. Functional motions of influenza virus hemagglutinin: A structure-based analytical approach. *Biophysical Journal*, 2002, roč. 82. č. 2, s. 569-581. ISS 0006-3495.

ITO, T.; COUCEIRO, J.; KELM, S.; BAUM, L. G.; KRAUSS, S.; CASTRUCCI, M. R.; DONATELLI, I.; KIDA, H.; PAULSON, J. C.; WEBSTER, R. G.; KAWAOKA, Y. Molecular basis for the generation in pigs of influenza A viruses with pandemic potential. *Journal of Virology*, 1998, roč. 72. č. 9, s. 7367-7373. ISS 0022-538X.

JACOBS, C. B.; PEAIRS, M. J.; VENTON, B. J. Review: Carbon nanotube based electrochemical sensors for biomolecules. *Analytica Chimica Acta*, 2010, roč. 662. č. 2, s. 105-127. ISS 0003-2670.

JAGGER, B. W.; WISE, H. M.; KASH, J. C.; WALTERS, K. A.; WILLS, N. M.; XIAO, Y. L.; DUNFEE, R. L.; SCHWARTZMAN, L. M.; OZINSKY, A.; BELL, G. L.; DALTON, R. M.; LO, A.; EFSTATHIOU, S.; ATKINS, J. F.; FIRTH, A. E.; TAUBENBERGER, J. K.; DIGARD, P. An Overlapping Protein-Coding Region in Influenza A Virus Segment 3 Modulates the Host Response. *Science*, 2012, roč. 337. č. 6091, s. 199-204. ISS 0036-8075.

JIAO, P. R.; TIAN, G. B.; LI, Y. B.; DENG, G. H.; JIANG, Y. P.; LIU, C.; LIU, W. L.; BU, Z. G.; KAWAOKA, Y.; CHEN, H. L. A single-amino-acid substitution in the NS1 protein changes the pathogenicity of H5N1 avian influenza viruses in mice. *Journal of Virology*, 2008, roč. 82. č. 3, s. 1146-1154. ISS 0022-538X.

JONES, B. Spreading the word about seasonal influenza. *Bull. World Health Organ.*, 2012, roč. 90. č., s. 253-253. ISS

JOSEPH, C.; TOGAWA, Y.; SHINDO, N. Bacterial and viral infections associated with influenza. *Influenza and Other Respiratory Viruses*, 2013, roč. 7. č., s. 105-113. ISS 1750-2640; 1750-2659.

KALTHOFF, D.; BOGS, J.; GRUND, C.; TAUSCHER, K.; TEIFKE, J. P.; STARICK, E.; HARDER, T.; BEER, M. Avian Influenza H7N9/13 and H7N7/13: a Comparative Virulence Study in Chickens, Pigeons, and Ferrets. *Journal of Virology*, 2014, roč. 88. č. 16, s. 9153-9165. ISS 0022-538X.

KANDEIL, A.; BAGATO, O.; ZARAKET, H.; DEBEAUCHAMP, J.; KRAUSS, S.; EL-SHESHENY, R.; WEBBY, R. J.; ALI, M. A.; KAYALI, G. Proteolytic enzymes in embryonated chicken eggs sustain the replication of egg-grown low-pathogenicity avian influenza viruses in cells in the absence of exogenous proteases. *Journal of Virological Methods*, 2014, roč. 202. č., s. 28-33. ISS 0166-0934; 1879-0984.

KATZ, J. M.; LIM, W.; BRIDGES, C. B.; ROWE, T.; HU-PRIMMER, J.; LU, X. H.; ABERNATHY, R. A.; CLARKE, M.; CONN, L.; KWONG, H.; LEE, M.; AU, G.; HO, Y. Y.; MAK, K. H.; COX, N. J.; FUKUDA, K. Antibody response in individuals infected with avian influenza A (H5N1) viruses and detection of anti-H5 antibody among household and social contacts. *Journal of Infectious Diseases*, 1999, roč. 180. č. 6, s. 1763-1770. ISS 0022-1899.

KIM, D. K.; POUDEL, B. Tools to Detect Influenza Virus. *Yonsei Medical Journal*, 2013, roč. 54. č. 3, s. 560-566. ISS 0513-5796.

KIM, H.; SCHOOFS, P.; ANDERSON, D. A.; TANNOCK, G. A.; ROCKMAN, S. P. Cold adaptation improves the growth of seasonal influenza B vaccine viruses. *Vaccine*, 2014, roč. 32. č. 21, s. 2474-2479. ISS 0264-410X.

KIM, J. H.; RESENDE, R.; WENNEKES, T.; CHEN, H. M.; BANCE, N.; BUCHINI, S.; WATTS, A. G.; PILLING, P.; STRELTSOV, V. A.; PETRIC, M.; LIGGINS, R.; BARRETT, S.; MCKIMM-BRESCHKIN, J. L.; NIIKURA, M.; WITHERS, S. G. Mechanism-Based Covalent Neuraminidase Inhibitors with Broad-Spectrum Influenza Antiviral Activity. *Science*, 2013, roč. 340. č. 6128, s. 71-75. ISS 0036-8075.

KIM, M. J.; LATHAM, A. G.; KRUG, R. M. Human influenza viruses activate an interferon-independent transcription of cellular antiviral genes: Outcome with influenza A virus is unique. *Proceedings of the National Academy of Sciences of the United States of America*, 2002, roč. 99. č. 15, s. 10096-10101. ISS 0027-8424.

KITSON, P. J.; ROSNES, M. H.; SANS, V.; DRAGONE, V.; CRONIN, L. Configurable 3D-Printed millifluidic and microfluidic 'lab on a chip'

reactionware devices. *Lab on a Chip*, 2012, roč. 12. č. 18, s. 3267-3271. ISS 1473-0197.

KOBASA, D.; TAKADA, A.; SHINYA, K.; HATTA, M.; HALFMANN, P.; THERIAULT, S.; SUZUKI, H.; NISHIMURA, H.; MITAMURA, K.; SUGAYA, N.; USUI, T.; MURATA, T.; MAEDA, Y.; WATANABE, S.; SURESH, M.; SUZUKI, T.; SUZUKI, Y.; FELDMANN, H.; KAWAOKA, Y. Enhanced virulence of influenza A viruses with the haemagglutinin of the 1918 pandemic virus. *Nature*, 2004, roč. 431. č. 7009, s. 703-707. ISS 0028-0836.

KOEL, B. F.; BURKE, D. F.; BESTEBROER, T. M.; VAN DER VLIET, S.; ZONDAG, G. C. M.; VERVAET, G.; SKEPNER, E.; LEWIS, N. S.; SPRONKEN, M. I. J.; RUSSELL, C. A.; EROPKIN, M. Y.; HURT, A. C.; BARR, I. G.; DE JONG, J. C.; RIMMELZWAAN, G. F.; OSTERHAUS, A.; FOUCHIER, R. A. M.; SMITH, D. J. Substitutions Near the Receptor Binding Site Determine Major Antigenic Change During Influenza Virus Evolution. *Science*, 2013, roč. 342. č. 6161, s. 976-979. ISS 0036-8075.

KOMADINA, N.; MCVERNON, J.; HALL, R.; LEDER, K. A Historical Perspective of Influenza A(H1N2) Virus. *Emerging Infectious Diseases*, 2014, roč. 20. č. 1, s. 6-12. ISS 1080-6040.

KOMAROVA, E.; ALDISSI, M.; BOGOMOLOVA, A. Direct electrochemical sensor for fast reagent-free DNA detection. *Biosensors & bioelectronics*, 2005, roč. 21. č. 1, s. 182-189. ISS 0956-5663.

KONGCHANAGUL, A.; SUPTAWIWAT, O.; BOONARKART, C.; KITPHATI, R.; PUTHAVATHANA, P.; UIPRASERTKUL, M.; AUEWARAKUL, P. Decreased Expression of Surfactant Protein D mRNA in Human Lungs in Fatal Cases of H5N1 Avian Influenza. *Journal of Medical Virology*, 2011, roč. 83. č. 8, s. 1410-1417. ISS 0146-6615.

KREJCOVA, L.; DOSPIVOVA, D.; RYVOLOVA, M.; KOPEL, P.; HYNEK, D.; KRIZKOVA, S.; HUBALEK, J.; ADAM, V.; KIZEK, R. Paramagnetic particles coupled with an automated flow injection analysis as a tool for influenza viral protein detection. *Electrophoresis*, 2012, roč. 33. č. 21, s. 3195-3204. ISS 0173-0835.

KREJCOVA, L.; NEJDL, L.; HYNEK, D.; KRIZKOVA, S.; KOPEL, P.; ADAM, V.; KIZEK, R. Beads-Based Electrochemical Assay for the Detection of Influenza Hemagglutinin Labeled with CdTe Quantum Dots. *Molecules*, 2013, roč. 18. č. 12, s. 15573-15586. ISS 1420-3049.

KUIKEN, T.; HOLMES, E. C.; MCCAULEY, J.; RIMMELZWAAN, G. F.; WILLIAMS, C. S.; GRENFELL, B. T. Host species barriers to influenza virus infections. *Science*, 2006, roč. 312. č. 5772, s. 394-397. ISS 0036-8075.

LAM DAI, T.; BINH HAI, N.; NGUYEN VAN, H.; HOANG VINH, T.; HUY LE, N.; PHUC XUAN, N. Electrochemical detection of short HIV sequences on chitosan/Fe3O4 nanoparticle based screen printed electrodes. *Materials Science & Engineering C-Materials for Biological Applications*, 2011, roč. 31. č. 2, s. 477-485. ISS 0928-4931.

LAMB, R. A.; CHOPPIN, P. W. THE GENE STRUCTURE AND REPLICATION OF INFLUENZA-VIRUS. *Annual Review of Biochemistry*, 1983, roč. 52. č., s. 467-506. ISS 0066-4154.

LASKOWSKI, M.; GREER, A. L.; MOGHADAS, S. M. Antiviral Strategies for Emerging Influenza Viruses in Remote Communities. *Plos One*, 2014, roč. 9. č. 2, s. ISS 1932-6203.

LAZZARI, S.; STOHR, K. Avian influenza and influenza pandemics. *Bulletin of the World Health Organization*, 2004, roč. 82. č. 4, s. 242-242. ISS 0042-9686.

LE, T. H.; NGUYEN, N. T. B. Evolutionary dynamics of highly pathogenic avian influenza A/H5N1 HA clades and vaccine implementation in Vietnam. *Clinical and experimental vaccine research*, 2014, roč. 3. č. 2, s. 117-27. ISS 2287-3651.

LEE, V. K.; KIM, D. Y.; NGO, H.; LEE, Y.; SEO, L.; YOO, S.-S.; VINCENT, P. A.; DAI, G. Creating perfused functional vascular channels using 3D bio-printing technology. *Biomaterials*, 2014, roč. 35. č. 28, s. 8092-8102. ISS 0142-9612; 1878-5905.

LEIKINA, E.; RAMOS, C.; MARKOVIC, I.; ZIMMERBERG, J.; CHERNOMORDIK, L. V. Reversible stages of the low-pH-triggered conformational change in influenza virus hemagglutinin. *Embo Journal*, 2002, roč. 21. č. 21, s. 5701-5710. ISS 0261-4189.

LI, C.; LI, X.; MIAO, Y.; WANG, Q.; JIANG, W.; XU, C.; LI, J.; HAN, J.; ZHANG, F.; GONG, B.; XU, L. SubpathwayMiner: a software package for flexible identification of pathways. *Nucleic Acids Research*, 2009, roč. 37. č. 19, s. ISS 0305-1048.

LI, J.-X.; FANG, S.-S.; CHENG, X.-W.; WANG, T.; WANG, X.; LV, X.; WU, C.-L.; ZHANG, R.-L.; CHENG, J.-Q.; YU, M.-H. Compare real-time RT-PCR with two culture methods for influenza virus detection. *Zhonghua shi yan he lin chuang bing du xue za zhi = Zhonghua shiyan he linchuang bingduxue zazhi = Chinese journal of experimental and clinical virology*, 2011, roč. 25. č. 1, s. 66-8. ISS 1003-9279.

LI, J. L.; DOHNA, H. Z.; CARDONA, C. J.; MILLER, J.; CARPENTER, T. E. Emergence and Genetic Variation of Neuraminidase Stalk Deletions in Avian Influenza Viruses. *Plos One*, 2011, roč. 6. č. 2, s. ISS 1932-6203.

LI, X.; CHEN, H.; WEI, J.; LV, N.; YOU, L. The evaluation of colloidal gold immunochromatographic assay (GICA) for rapid diagnosis of influenza A disease. *Clinical Chemistry and Laboratory Medicine*, 2011, roč. 49. č. 9, s. 1533-1537. ISS 1434-6621.

LI, X.; LU, D.; SHENG, Z.; CHEN, K.; GUO, X.; JIN, M.; HAN, H. A fast and sensitive immunoassay of avian influenza virus based on label-free quantum dot probe and lateral flow test strip. *Talanta*, 2012, roč. 100. č., s. 1-6. ISS 0039-9140.

LI, Z.-N.; LIN, S.-C.; CARNEY, P. J.; LI, J.; LIU, F.; LU, X.; LIU, M.; STEVENS, J.; LEVINE, M.; KATZ, J. M.; HANCOCK, K. IgM, IgG, and IgA Antibody Responses to Influenza A(H1N1)pdm09 Hemagglutinin in Infected Persons during the First Wave of the 2009 Pandemic in the United States. *Clinical and vaccine immunology : CVI*, 2014, roč. 21. č. 8, s. 1054-60. ISS 1556-679X.

LIN, Y. P.; GREGORY, V.; COLLINS, P.; KLOESS, J.; WHARTON, S.; CATTLE, N.; LACKENBY, A.; DANIELS, R.; HAY, A. Neuraminidase Receptor Binding Variants of Human Influenza A(H3N2) Viruses Resulting from Substitution of Aspartic Acid 151 in the Catalytic Site: a Role in Virus Attachment? *Journal of Virology*, 2010, roč. 84. č. 13, s. 6769-6781. ISS 0022-538X.

LIN, Y. P.; XIONG, X. L.; WHARTON, S. A.; MARTIN, S. R.; COOMBS, P. J.; VACHIERI, S. G.; CHRISTODOULOU, E.; WALKER, P. A.; LIU, J. F.; SKEHEL, J. J.; GAMBLIN, S. J.; HAY, A. J.; DANIELS, R. S.; MCCAULEY, J. W. Evolution of the receptor binding properties of the influenza A(H3N2)

hemagglutinin. *Proceedings of the National Academy of Sciences of the United States of America*, 2012, roč. 109. č. 52, s. 21474-21479. ISS 0027-8424.

LINA, B. History of influenza pandemics. In: RAOULT, D.; DRANCOURT M., eds. Paleomicrobiology: Past Human Infections: Springer-Verlag Berlin, Heidelberger Platz 3, D-14197 Berlin, Germany, 2008.

LIU, F.; CHOI, K. S.; PARK, T. J.; LEE, S. Y.; SEO, T. S. Graphene-based electrochemical biosensor for pathogenic virus detection. *Biochip Journal*, 2011, roč. 5. č. 2, s. 123-128. ISS 1976-0280.

LIU, F.; LAURENT, S.; FATTAHI, H.; ELST, L. V.; MULLER, R. N. Superparamagnetic nanosystems based on iron oxide nanoparticles for biomedical imaging. *Nanomedicine*, 2011, roč. 6. č. 3, s. 519-528. ISS 1743-5889.

LIU, J.; WU, J. Q.; WANG, B.; ZENG, S.; QI, F. F.; LU, C. L.; KIMURA, Y.; LIU, B. X. Oral vaccination with a liposome-encapsulated influenza DNA vaccine protects mice against respiratory challenge infection. *Journal of Medical Virology*, 2014, roč. 86. č. 5, s. 886-894. ISS 0146-6615.

LIU, R. H.; LODES, M. J.; NGUYEN, T.; SIUDA, T.; SLOTA, M.; FUJI, H. S.; MCSHEA, A. Validation of a fully integrated microfluidic array device for influenza A subtype identification and sequencing. *Analytical Chemistry*, 2006, roč. 78. č. 12, s. 4184-4193. ISS 0003-2700.

LIU, S.; CHEN, G.; ZHOU, Q.; WEI, Y. An immuno-biosensor system based on quartz crystal microbalance for avian influenza virus detection - art. no. 67943P. In: SASAKI, M.; SANG G. C.; LI Z.; IKEURA R.; KIM H.; XUE F., eds. Icmit 2007: Mechatronics, Mems, and Smart Materials, Pts 1 and 2, 2008 (vol 6794).

LIU, S.; ZHAO, Y.; PARKS, J. W.; DEAMER, D. W.; HAWKINS, A. R.; SCHMIDT, H. Correlated electrical and optical analysis of single nanoparticles and biomolecules on a nanopore-gated optofluidic chip. *Nano letters*, 2014, roč. 14. č. 8, s. 4816-20. ISS 1530-6992.

MALECKA, K.; GRABOWSKA, I.; RADECKI, J.; STACHYRA, A.; GORA-SOCHACKA, A.; SIRKO, A.; RADECKA, H. Voltammetric Detection of a Specific DNA Sequence of Avian Influenza Virus H5N1 Using HS-ssDNA Probe Deposited onto Gold Electrode. *Electroanalysis*, 2012, roč. 24. č. 2, s. 439-446. ISS 1040-0397.

MALECKA, K.; GRABOWSKA, I.; RADECKI, J.; STACHYRA, A.; GORA-SOCHACKA, A.; SIRKO, A.; RADECKA, H. Electrochemical Detection of Avian Influenza Virus Genotype Using Amino-ssDNA Probe Modified Gold Electrodes. *Electroanalysis*, 2013, roč. 25. č. 8, s. 1871-1878. ISS 1040-0397.

MARTCHEVA, M. An evolutionary model of influenza A with drift and shift. *Journal of Biological Dynamics*, 2012, roč. 6. č. 2, s. 299-332. ISS 1751-3758.

MARTINEZ-PAREDES, G.; GONZALEZ-GARCIA, M. B.; COSTA-GARCIA, A. Lead Sensor Using Gold Nanostructured Screen-Printed Carbon Electrodes as Transducers. *Electroanalysis*, 2009, roč. 21. č. 8, s. 925-930. ISS 1040-0397.

MATROSOVICH, M. N.; MATROSOVICH, T. Y.; GRAY, T.; ROBERTS, N. A.; KLENK, H. D. Neuraminidase is important for the initiation of influenza virus infection in human airway epithelium. *Journal of Virology*, 2004, roč. 78. č. 22, s. 12665-12667. ISS 0022-538X.

MCGETTIGAN, P.; POLLOCK, A.; HERXHEIMER, A. OSELTAMIVIR AND ZANAMIVIR FOR FLU Department of Health's misguided alert recommending

neuraminidase inhibitors for flu. *Bmj-British Medical Journal*, 2014, roč. 348. č., s. ISS 1756-1833.

MCLEOD, A.; GUERNE-BLEICH, E. Social, economic and policy issues in the long-term control of HPAI. In: SCHUDEL, A.; LOMBARD M., eds. OIE/FAO International Scientific Conference on Avian Influenza. Basel: Karger, 2006 (vol 124).

MERKOCI, A.; ALDAVERT, M.; TARRASON, G.; ERITJA, R.; ALEGRET, S. Toward an ICPMS-linked DNA assay based on gold nanoparticles immunoconnected through peptide sequences. *Analytical Chemistry*, 2005, roč. 77. č. 19, s. 6500-6503. ISS 0003-2700.

MILLS, C. E.; ROBINS, J. M.; BERGSTROM, C. T.; LIPSITCH, M. Pandemic influenza: Risk of multiple introductions and the need to prepare for them. *Plos Medicine*, 2006, roč. 3. č. 6, s. 769-773. ISS 1549-1277.

MIODEK, A.; SAURIAT-DORIZON, H.; CHEVALIER, C.; DELMAS, B.; VIDIC, J.; KORRI-YOUSSOUFI, H. Direct electrochemical detection of PB1-F2 protein of influenza A virus in infected cells. *Biosensors & bioelectronics*, 2014, roč. 59. č., s. 6-13. ISS 0956-5663; 1873-4235.

MISONO, T. S.; KUMAR, P. K. R. Selection of RNA aptamers against human influenza virus hemagglutinin using surface plasmon resonance. *Analytical Biochemistry*, 2005, roč. 342. č. 2, s. 312-317. ISS 0003-2697.

MITAMURA, K.; SHIMIZU, H.; YAMAZAKI, M.; ICHIKAWA, M.; NAGAI, K.; KATADA, J.; WADA, A.; KAWAKAMI, C.; SUGAYA, N. Clinical evaluation of highly sensitive silver amplification immunochromatography systems for rapid diagnosis of influenza. *Journal of Virological Methods*, 2013, roč. 194. č. 1-2, s. 123-128. ISS 0166-0934; 1879-0984.

MOELLER, A.; KIRCHDOERFER, R. N.; POTTER, C. S.; CARRAGHER, B.; WILSON, I. A. Organization of the Influenza Virus Replication Machinery. *Science*, 2012, roč. 338. č. 6114, s. 1631-1634. ISS 0036-8075.

MOOKKAN, P.; PADUBIDHRI, N. P.; VELUMANI, S.; KWANG, H.-S. J. Binding protein and epitope-blocking ELISA for the universal detection of H5-subtype influenza viruses: Temasek Life Sciences Laboratory Limited, 2013.

MOON, S. K.; TAN, Y. E.; HWANG, J.; YOON, Y.-J. Application of 3D Printing Technology for Designing Light-weight Unmanned Aerial Vehicle Wing Structures. *International Journal of Precision Engineering and Manufacturing-Green Technology*, 2014, roč. 1. č. 3, s. 223-228. ISS 2288-6206; 2198-0810.

MU, B.; HUANG, X.; BU, P.; ZHUANG, J.; CHENG, Z.; FENG, J.; YANG, D.; DONG, C.; ZHANG, J.; YAN, X. Influenza virus detection with pentabody-activated nanoparticles. *Journal of Virological Methods*, 2010, roč. 169. č. 2, s. 282-289. ISS 0166-0934.

MURAMOTO, Y.; NODA, T.; KAWAKAMI, E.; AKKINA, R.; KAWAOKA, Y. Identification of Novel Influenza A Virus Proteins Translated from PA mRNA. *Journal of Virology*, 2013, roč. 87. č. 5, s. 2455-2462. ISS 0022-538X.

MUSCATELLO, D. J.; AMIN, J.; MACINTYRE, C. R.; NEWALL, A. T.; RAWLINSON, W. D.; SINTCHENKO, V.; GILMOUR, R.; THACKWAY, S. Inaccurate Ascertainment of Morbidity and Mortality due to Influenza in Administrative Databases: A Population-Based Record Linkage Study. *Plos One*, 2014, roč. 9. č. 5, s. ISS 1932-6203.

MUTI, M.; KURALAY, F.; ERDEM, A. Single-walled carbon nanotubes-polymer modified graphite electrodes for DNA hybridization. *Colloids and Surfaces B-Biointerfaces*, 2012, roč. 91. č., s. 77-83. ISS 0927-7765.

MUTI, M.; KURALAY, F.; ERDEM, A.; ABACI, S.; YUMAK, T.; SINAG, A. Tin oxide nanoparticles-polymer modified single-use sensors for electrochemical monitoring of label-free DNA hybridization. *Talanta*, 2010, roč. 82. č. 5, s. 1680-1686. ISS 0039-9140.

NASREEN, S.; KHAN, S. U.; AZZIZ-BAUMGARTNER, E.; HANCOCK, K.; VEGUILLA, V.; WANG, D.; RAHMAN, M.; ALAMGIR, A. S. M.; STURM-RAMIREZ, K.; GURLEY, E. S.; LUBY, S. P.; KATZ, J. M.; UYEKI, T. M. Seroprevalence of Antibodies against Highly Pathogenic Avian Influenza A (H5N1) Virus among Poultry Workers in Bangladesh, 2009. *Plos One*, 2013, roč. 8. č. 9, s. ISS 1932-6203.

NG, A. K. L.; LAM, M. K. H.; ZHANG, H. M.; LIU, J. H.; AU, S. W. N.; CHAN, P. K. S.; WANG, J. H.; SHAW, P. C. Structural Basis for RNA Binding and Homo-Oligomer Formation by Influenza B Virus Nucleoprotein. *Journal of Virology*, 2012, roč. 86. č. 12, s. 6758-6767. ISS 0022-538X.

NG, A. K. L.; ZHANG, H. M.; TAN, K. M.; LI, Z. L.; LIU, J. H.; CHAN, P. K. S.; LI, S. M.; CHAN, W. Y.; AU, S. W. N.; JOACHIMIAK, A.; WALZ, T.; WANG, J. H.; SHAW, P. C. Structure of the influenza virus A H5N1 nucleoprotein: implications for RNA binding, oligomerization, and vaccine design. *Faseb Journal*, 2008, roč. 22. č. 10, s. 3638-3647. ISS 0892-6638.

NIDZWORSKI, D.; PRANSZKE, P.; GRUDNIEWSKA, M.; KROL, E.; GROMADZKA, B. Universal biosensor for detection of influenza virus. *Biosensors & bioelectronics*, 2014, roč. 59. č., s. 239-242. ISS 0956-5663.

NICHOLSON, K. G.; WOOD, J. M.; ZAMBON, M. Influenza. *Lancet*, 2003, roč. 362. č. 9397, s. 1733-1745. ISS 0140-6736.

NODA, T.; KAWAOKA, Y. Classification and virion structure of influenza virus. *Nihon rinsho. Japanese journal of clinical medicine*, 2006, roč. 64. č. 10, s. 1766-9. ISS 0047-1852.

NOISUMDAENG, P.; POORUK, P.; PRASERTSOPON, J.; ASSANASEN, S.; KITPHATI, R.; AUEWARAKUL, P.; PUTHAVATHANA, P. Homosubtypic and heterosubtypic antibodies against highly pathogenic avian influenza H5N1 recombinant proteins in.H5N1 survivors and non-H5N1 subjects. *Virology*, 2014, roč. 454. č., s. 254-262. ISS 0042-6822.

OH, D. Y.; HURT, A. C. A Review of the Antiviral Susceptibility of Human and Avian Influenza Viruses over the Last Decade. *Scientifica*, 2014, roč. 2014. č., s. 430629. ISS 2090-908X.

OKOMO-ADHIAMBO, M.; NGUYEN, H. T.; ABD ELAL, A.; SLEEMAN, K.; FRY, A. M.; GUBAREVA, L. V. Drug susceptibility surveillance of influenza viruses circulating in the United States in 2011-2012: application of the WHO antiviral working group criteria. *Influenza and Other Respiratory Viruses*, 2014, roč. 8. č. 2, s. 258-265. ISS 1750-2640.

OWEN, T. W.; AL-KAYSI, R. O.; BARDEEN, C. J.; CHENG, Q. Microgravimetric immunosensor for direct detection of aerosolized influenza A virus particles. *Sensors and Actuators B-Chemical*, 2007, roč. 126. č. 2, s. 691-699. ISS 0925-4005.

PALECEK, E.; BARTOSIK, M. Electrochemistry of Nucleic Acids. *Chemical Reviews*, 2012, roč. 112. č. 6, s. 3427-3481. ISS 0009-2665.

PALESE, P.; GARCIA-SASTRE, A. Influenza vaccines: present and future. *Journal of Clinical Investigation*, 2002, roč. 110. č. 1, s. 9-13. ISS 0021-9738.

PALESE, P.; SCHULMAN, J. L. MAPPING OF INFLUENZA-VIRUS GENOME - IDENTIFICATION OF HEMAGGLUTININ AND NEURAMINIDASE GENES. *Proceedings of the National Academy of Sciences of the United States of America*, 1976, roč. 73. č. 6, s. 2142-2146. ISS 0027-8424.

PARK, J. K. Immunochromatographic strip useful in kit for detecting e.g. hepatitis C, influenza, Syphilis, Chlamydia and malaria, comprises adhesive plastic support, liquid sample to-be-analyzed, analyte, detection signals, and sample of specimen: RAPIGEN INC (RAPI-Non-standard).

PERDUE, M. L.; NGUYEN, T. The WHO research agenda for influenza: two years later. *Bull. World Health Organ.*, 2012, roč. 90. č., s. 246-246. ISS

PEREZ, J. T.; VARBLE, A.; SACHIDANANDAM, R.; ZLATEV, I.; MANOHARAN, M.; GARCIA-SASTRE, A.; TENOEVER, B. R. Influenza A virus-generated small RNAs regulate the switch from transcription to replication. *Proceedings of the National Academy of Sciences of the United States of America*, 2010, roč. 107. č. 25, s. 11525-11530. ISS 0027-8424.

PERRONE, L. A.; AHMAD, A.; VEGUILLA, V.; LU, X.; SMITH, G.; KATZ, J. M.; PUSHKO, P.; TUMPEY, T. M. Intranasal Vaccination with 1918 Influenza Virus-Like Particles Protects Mice and Ferrets from Lethal 1918 and H5N1 Influenza Virus Challenge. *Journal of Virology*, 2009, roč. 83. č. 11, s. 5726-5734. ISS 0022-538X.

PIELAK, R. M.; SCHNELL, J. R.; CHOU, J. J. Mechanism of drug inhibition and drug resistance of influenza A M2 channel. *Proceedings of the National Academy of Sciences of the United States of America*, 2009, roč. 106. č. 18, s. 7379-7384. ISS 0027-8424.

PINILLA, L. T.; HOLDER, B. P.; ABED, Y.; BOIVIN, G.; BEAUCHEMIN, C. A. A. The H275Y Neuraminidase Mutation of the Pandemic A/H1N1 Influenza Virus Lengthens the Eclipse Phase and Reduces Viral Output of Infected Cells, Potentially Compromising Fitness in Ferrets. *Journal of Virology*, 2012, roč. 86. č. 19, s. 10651-10660. ISS 0022-538X; 1098-5514.

POOVORAWAN, Y.; PYUNGPORN, S.; PRACHAYANGPRECHA, S.; MAKKOCH, J. Global alert to avian influenza virus infection: From H5N1 to H7N9. *Pathogens and Global Health*, 2013, roč. 107. č. 5, s. 217-223. ISS 2047-7724.

PRINCIPI, N.; SCALA, A.; DALENO, C.; ESPOSITO, S. Influenza C virus-associated community-acquired pneumonia in children. *Influenza and Other Respiratory Viruses*, 2013, roč. 7. č. 6, s. 999-1003. ISS 1750-2640.

PUSHKO, P. M.; BRIGHT, R. A.; TUMPEY, T. M.; SMITH, G. E. Engineering Better Influenza Vaccines: Traditional and New Approaches. In: KHUDYAKOV, Y. E., ed. Medicinal Protein Engineering: Crc Press-Taylor & Francis Group, 6000 Broken Sound Parkway Nw, Ste 300, Boca Raton, Fl 33487-2742 USA, 2009.

QIU, J. M. Prognosis of 18 H7N9 Avian Influenza Patients in Shanghai (vol 9, e88728, 2014). *Plos One*, 2014, roč. 9. č. 4, s. ISS 1932-6203.

QURESHI, A.; KANG, W. P.; DAVIDSON, J. L.; GURBUZ, Y. Review on carbon-derived, solid-state, micro and nano sensors for electrochemical sensing applications. *Diamond and Related Materials*, 2009, roč. 18. č. 12, s. 1401-1420. ISS 0925-9635.

RAMADAN, Q.; GIJS, M. A. M. Microfluidic applications of functionalized magnetic particles for environmental analysis: focus on waterborne pathogen detection. *Microfluidics and Nanofluidics*, 2012, roč. 13. č. 4, s. 529-542. ISS 1613-4982.

RAO, S.; NYQUIST, A. C. Respiratory viruses and their impact in healthcare. *Current Opinion in Infectious Diseases*, 2014, roč. 27. č. 4, s. 342-347. ISS 0951-7375.

REBMANN, T.; ZELICOFF, A. Vaccination against influenza: role and limitations in pandemic intervention plans. *Expert Review of Vaccines*, 2012, roč. 11. č. 8, s. 1009-1019. ISS 1476-0584.

REGUERA, J.; CUSACK, S.; KOLAKOFSKY, D. Segmented negative strand RNA virus nucleoprotein structure. *Current Opinion in Virology*, 2014, roč. 5. č., s. 7-15. ISS 1879-6257.

RECHNITZ, G. A. BIOSENSORS INTO THE 1990S. *Electroanalysis*, 1991, roč. 3. č. 2, s. 73-76. ISS 1040-0397.

RITCHEY, M. B.; PALESE, P.; SCHULMAN, J. L. MAPPING OF INFLUENZA-VIRUS GENOME .3. IDENTIFICATION OF GENES CODING FOR NUCLEOPROTEIN, MEMBRANE-PROTEIN, AND NONSTRUCTURAL PROTEIN. *Journal of Virology*, 1976, roč. 20. č. 1, s. 307-313. ISS 0022-538X.

ROSSMAN, J. S.; LAMB, R. A. Influenza virus assembly and budding. *Virology*, 2011, roč. 411. č. 2, s. 229-236. ISS 0042-6822.

RUDENKO, L.; KISELEVA, I.; NAYKHIN, A. N.; EROFEEVA, M.; STUKOVA, M.; DONINA, S.; PETUKHOVA, G.; PISAREVA, M.; KRIVITSKAYA, V.; GRUDININ, M.; BUZITSKAYA, Z.; ISAKOVA-SIVAK, I.; KUZNETSOVA, S.; LARIONOVA, N.; DESHEVA, J.; DUBROVINA, I.; NIKIFOROVA, A.; VICTOR, J. C.; NEUZIL, K.; FLORES, J.; TSVETNITSKY, V.; KISELEV, O. Assessment of Human Immune Responses to H7 Avian Influenza Virus of Pandemic Potential: Results from a Placebo-Controlled, Randomized Double-Blind Phase I Study of Live Attenuated H7N3 Influenza Vaccine. *Plos One*, 2014, roč. 9. č. 2, s. ISS 1932-6203.

RUSSELL, R. J.; KERRY, P. S.; STEVENS, D. J.; STEINHAUER, D. A.; MARTIN, S. R.; GAMBLIN, S. J.; SKEHEL, J. J. Structure of influenza hemagglutinin in complex with an inhibitor of membrane fusion. *Proceedings of the National Academy of Sciences of the United States of America*, 2008, roč. 105. č. 46, s. 17736-17741. ISS 0027-8424.

RYAN, J. R. Natural History of the Influenza Virus. In: RYAN, J. R., ed. Pandemic Influenza: Emergency Planning and Community Preparedness: Crc Press-Taylor & Francis Group, 6000 Broken Sound Parkway Nw, Ste 300, Boca Raton, Fl 33487-2742 USA, 2009.

SADIK, O. A.; ALUOCH, A. O.; ZHOU, A. L. Status of biomolecular recognition using electrochemical techniques. *Biosensors & bioelectronics*, 2009, roč. 24. č. 9, s. 2749-2765. ISS 0956-5663.

SALEZ, N.; MELADE, J.; PASCALIS, H.; AHERFI, S.; DELLAGI, K.; CHARREL, R. N.; CARRAT, F.; DE LAMBALLERIE, X. Influenza C virus high seroprevalence rates observed in 3 different population groups. *The Journal of infection*, 2014, roč. 69. č. 2, s. 182-9. ISS 1532-2742.

SAMSON, M.; PIZZORNO, A.; ABED, Y.; BOIVIN, G. Influenza virus resistance to neuraminidase inhibitors. *Antiviral Research*, 2013, roč. 98. č. 2, s. 174-185. ISS 0166-3542.

SHENG, Z. Z.; RAN, Z. G.; WANG, D.; HOPPE, A.; SIMONSON, R.; CHAKRAVARTY, S.; HAUSE, B. M.; LI, F. Genomic and evolutionary

characterization of a novel influenza-C-like virus from swine. *Archives of Virology*, 2014, roč. 159. č. 2, s. 249-255. ISS 0304-8608.
SHINDO, N.; BRIAND, S. Influenza at the beginning of the 21st century. *Bull. World Health Organ.*, 2012, roč. 90. č., s. 247-247A. ISS
SCHNELL, J. R.; CHOU, J. J. Structure and mechanism of the M2 proton channel of influenza A virus. *Nature*, 2008, roč. 451. č. 7178, s. 591-U12. ISS 0028-0836.
SCHUTTEN, M.; VAN BAALEN, C.; ZOETEWEIJ, P.; FRAAIJ, P. The influenza virus: disease, diagnostics, and treatment. *MLO: medical laboratory observer*, 2013, roč. 45. č. 11, s. 38-40. ISS 0580-7247.
SIN, M. L. Y.; MACH, K. E.; WONG, P. K.; LIAO, J. C. Advances and challenges in biosensor-based diagnosis of infectious diseases. *Expert Review of Molecular Diagnostics*, 2014, roč. 14. č. 2, s. 225-244. ISS 1473-7159.
SINGH, R.; DAS MUKHERJEE, M.; SUMANA, G.; GUPTA, R. K.; SOOD, S.; MALHOTRA, B. D. Biosensors for pathogen detection: A smart approach towards clinical diagnosis. *Sensors and Actuators B-Chemical*, 2014, roč. 197. č., s. 385-404. ISS 0925-4005.
SKALICKOVA, S.; ZITKA, O.; NEJDL, L.; KRIZKOVA, S.; SOCHOR, J.; JANU, L.; RYVOLOVA, M.; HYNEK, D.; ZIDKOVA, J.; ZIDEK, V.; ADAM, V.; KIZEK, R. Study of Interaction between Metallothionein and CdTe Quantum Dots. *Chromatographia*, 2013, roč. 76. č. 7-8, s. 345-353. ISS 0009-5893.
SKEHEL, J. J.; WILEY, D. C. Receptor binding and membrane fusion in virus entry: The influenza hemagglutinin. *Annual Review of Biochemistry*, 2000, roč. 69. č., s. 531-569. ISS 0066-4154.
SMITH, G. L.; LEVIN, J. Z.; PALESE, P.; MOSS, B. SYNTHESIS AND CELLULAR LOCATION OF THE 10 INFLUENZA POLYPEPTIDES INDIVIDUALLY EXPRESSED BY RECOMBINANT VACCINIA VIRUSES. *Virology*, 1987, roč. 160. č. 2, s. 336-345. ISS 0042-6822.
SOUZA, E.; NASCIMENTO, G.; SANTANA, N.; FERREIRA, D.; LIMA, M.; NATIVIDADE, E.; MARTINS, D.; LIMA-FILHO, J. Label-Free Electrochemical Detection of the Specific Oligonucleotide Sequence of Dengue Virus Type 1 on Pencil Graphite Electrodes. *Sensors*, 2011, roč. 11. č. 6, s. 5616-5629. ISS 1424-8220.
STEGEMAN, A.; BOUMA, A.; ELBERS, A. R. W.; DE JONG, M. C. M.; NODELIJK, G.; DE KLERK, F.; KOCH, G.; VAN BOVEN, M. Avian influenza A virus (H7N7) epidemic in the Netherlands in 2003: Course of the epidemic and effectiveness of control measures. *Journal of Infectious Diseases*, 2004, roč. 190. č. 12, s. 2088-2095. ISS 0022-1899.
STEVENS, J.; BLIXT, O.; TUMPEY, T. M.; TAUBENBERGER, J. K.; PAULSON, J. C.; WILSON, I. A. Structure and receptor specificity of the hemagglutinin from an H5N1 influenza virus. *Science*, 2006, roč. 312. č. 5772, s. 404-410. ISS 0036-8075.
STOHR, K. PERSPECTIVE Ill prepared for a pandemic. *Nature*, 2014, roč. 507. č. 7490, s. S20-S21. ISS 0028-0836.
SUN, X. M.; SHI, Y.; LU, X. S.; HE, J. H.; GAO, F.; YAN, J. H.; QI, J. X.; GAO, G. F. Bat-Derived Influenza Hemagglutinin H17 Does Not Bind Canonical Avian or Human Receptors and Most Likely Uses a Unique Entry Mechanism. *Cell Reports*, 2013, roč. 3. č. 3, s. 769-778. ISS 2211-1247.
TAM, P. D.; TUAN, M. A.; VAN HIEU, N.; CHIEN, N. D. Impact parameters on hybridization process in detecting influenza virus (type A) using conductimetric-

based DNA sensor. *Physica E-Low-Dimensional Systems & Nanostructures*, 2009, roč. 41. č. 8, s. 1567-1571. ISS 1386-9477.

TARBET, E. B.; HAMILTON, S.; VOLLMER, A. H.; LUTTICK, A.; NG, W. C.; PRYOR, M.; HURST, B. L.; CRAWFORD, S.; SMEE, D. F.; TUCKER, S. P. A zanamivir dimer with prophylactic and enhanced therapeutic activity against influenza viruses. *The Journal of antimicrobial chemotherapy*, 2014, roč. 69. č. 8, s. 2164-74. ISS 1460-2091.

TISDALE, M. Influenza M2 Ion-Channel and Neuraminidase Inhibitors. In: MAYERS, D. L., ed. Antimicrobial Drug Resistance, Vol 1: Mechanisms of Drug Resistance, 2009.

TONG, S. X.; ZHU, X. Y.; LI, Y.; SHI, M.; ZHANG, J.; BOURGEOIS, M.; YANG, H.; CHEN, X. F.; RECUENCO, S.; GOMEZ, J.; CHEN, L. M.; JOHNSON, A.; TAO, Y.; DREYFUS, C.; YU, W. L.; MCBRIDE, R.; CARNEY, P. J.; GILBERT, A. T.; CHANG, J.; GUO, Z.; DAVIS, C. T.; PAULSON, J. C.; STEVENS, J.; RUPPRECHT, C. E.; HOLMES, E. C.; WILSON, I. A.; DONIS, R. O. New World Bats Harbor Diverse Influenza A Viruses. *Plos Pathogens*, 2013, roč. 9. č. 10, s. ISS 1553-7374.

TONG, S. Y. C.; DAKH, F.; HURT, A. C.; DENG, Y.-M.; FREEMAN, K.; FAGAN, P. K.; BARR, I. G.; GIFFARD, P. M. Rapid Detection of the H275Y Oseltamivir Resistance Mutation in Influenza A/H1N1 2009 by Single Base Pair RT-PCR and High-Resolution Melting. *Plos One*, 2011, roč. 6. č. 6, s. ISS 1932-6203.

TRETYAKOVA, I.; PEARCE, M. B.; FLORESE, R.; TUMPEY, T. M.; PUSHKO, P. Intranasal vaccination with H5, H7 and H9 hemagglutinins co-localized in a virus-like particle protects ferrets from multiple avian influenza viruses. *Virology*, 2013, roč. 442. č. 1, s. 67-73. ISS 0042-6822.

TSANG, J. S.; SCHWARTZBERG, P. L.; KOTLIAROV, Y.; BIANCOTTO, A.; XIE, Z.; GERMAIN, R. N.; WANG, E.; OLNES, M. J.; NARAYANAN, M.; GOLDING, H.; MOIR, S.; DICKLER, H. B.; PERL, S.; CHEUNG, F.; BAYLOR, H. C.; CONSORTIUM, C. H. I. Global Analyses of Human Immune Variation Reveal Baseline Predictors of Postvaccination Responses. *Cell*, 2014, roč. 157. č. 2, s. ISS 0092-8674.

TUMPEY, T. M.; BASLER, C. F.; AGUILAR, P. V.; ZENG, H.; SOLORZANO, A.; SWAYNE, D. E.; COX, N. J.; KATZ, J. M.; TAUBENBERGER, J. K.; PALESE, P.; GARCIA-SASTRE, A. Characterization of the reconstructed 1918 Spanish influenza pandemic virus. *Science*, 2005, roč. 310. č. 5745, s. 77-80. ISS 0036-8075.

VAN BUYNDER, P. G.; KONRAD, S.; VAN BUYNDER, J. L.; BRODKIN, E.; KRAJDEN, M.; RAMLER, G.; BIGHAM, M. The comparative effectiveness of adjuvanted and unadjuvanted trivalent inactivated influenza vaccine (TIV) in the elderly. *Vaccine*, 2013, roč. 31. č. 51, s. 6122-6128. ISS 0264-410X.

VAN DER VRIES, E.; SCHUTTEN, M.; FRAAIJ, P.; BOUCHER, C.; OSTERHAUS, A. Influenza Virus Resistance to Antiviral Therapy. In: DECLERCQ, E., ed. Antiviral Agents. San Diego: Elsevier Academic Press Inc, 2013 (vol 67).

VAN KERKHOVE, M. D. Brief literature review for the WHO global influenza research agenda - highly pathogenic avian influenza H5N1 risk in humans. *Influenza and Other Respiratory Viruses*, 2013, roč. 7. č., s. 26-33. ISS 1750-2640.

VAN REENEN, A.; DE JONG, A. M.; DEN TOONDER, J. M. J.; PRINS, M. W. J. Integrated lab-on-chip biosensing systems based on magnetic particle actuation -

a comprehensive review. *Lab on a Chip*, 2014, roč. 14. č. 12, s. 1966-1986. ISS 1473-0197; 1473-0189.

VARBLE, A.; CHUA, M. A.; PEREZ, J. T.; MANICASSAMY, B.; GARCIA-SASTRE, A.; TENOEVER, B. R. Engineered RNA viral synthesis of microRNAs. *Proceedings of the National Academy of Sciences of the United States of America*, 2010, roč. 107. č. 25, s. 11519-11524. ISS 0027-8424.

VASIN, A. V.; TEMKINA, O. A.; EGOROV, V. V.; KLOTCHENKO, S. A.; PLOTNIKOVA, M. A.; KISELEV, O. I. Molecular mechanisms enhancing the proteome of influenza A viruses: An overview of recently discovered proteins. *Virus Research*, 2014, roč. 185. č., s. 53-63. ISS 0168-1702.

VELASCO-GARCIA, M. N.; MOTTRAM, T. Biosensor technology addressing agricultural problems. *Biosystems Engineering*, 2003, roč. 84. č. 1, s. 1-12. ISS 1537-5110.

VOLZ, E. M.; KOELLE, K.; BEDFORD, T. Viral Phylodynamics. *Plos Computational Biology*, 2013, roč. 9. č. 3, s. ISS 1553-7358.

WANG, R. H.; LI, Y. B. Hydrogel based QCM aptasensor for detection of avian influenza virus. *Biosensors & bioelectronics*, 2013, roč. 42. č., s. 148-155. ISS 0956-5663.

WANG, R. H.; WANG, Y.; LASSITER, K.; LI, Y. B.; HARGIS, B.; TUNG, S.; BERGHMAN, L.; BOTTJE, W. Interdigitated array microelectrode based impedance immunosensor for detection of avian influenza virus H5N1. *Talanta*, 2009, roč. 79. č. 2, s. 159-164. ISS 0039-9140.

WATANABE, T.; WATANABE, S.; KAWAOKA, Y. Cellular Networks Involved in the Influenza Virus Life Cycle. *Cell Host & Microbe*, 2010, roč. 7. č. 6, s. 427-439. ISS 1931-3128.

WEI, H. L.; LENZ, S. D.; THOMPSON, D. H.; POGRANICHNIY, R. M. DNA-Vaccine Platform Development Against H1N1 Subtype of Swine Influenza A Viruses. *Viral Immunology*, 2012, roč. 25. č. 4, s. 297-305. ISS 0882-8245.

WEI, J.; ZHENG, L.; LV, X.; BI, Y.; CHEN, W.; ZHANG, W.; SHI, Y.; ZHAO, L.; SUN, X.; WANG, F.; CHENG, S.; YAN, J.; LIU, W.; JIANG, X.; GAO, G. F.; LI, X. Analysis of Influenza Virus Receptor Specificity Using Glycan-Functionalized Gold Nanoparticles. *Acs Nano*, 2014, roč. 8. č. 5, s. 4600-4607. ISS 1936-0851; 1936-086X.

WICKLEIN, B.; ANGELES MARTIN DEL BURGO, M.; YUSTE, M.; CARREGAL-ROMERO, E.; LLOBERA, A.; DARDER, M.; ARANDA, P.; ORTIN, J.; DEL REAL, G.; FERNANDEZ-SANCHEZ, C.; RUIZ-HITZKY, E. Biomimetic Architectures for the Impedimetric Discrimination of Influenza Virus Phenotypes. *Advanced Functional Materials*, 2013, roč. 23. č. 2, s. 254-262. ISS 1616-301X.

WILLANDER, M.; KHUN, K.; IBUPOTO, Z. H. ZnO Based Potentiometric and Amperometric Nanosensors. *Journal of Nanoscience and Nanotechnology*, 2014, roč. 14. č. 9, s. 6497-6508. ISS 1533-4880; 1533-4899.

WISE, H. M.; FOEGLEIN, A.; SUN, J. C.; DALTON, R. M.; PATEL, S.; HOWARD, W.; ANDERSON, E. C.; BARCLAY, W. S.; DIGARD, P. A Complicated Message: Identification of a Novel PB1-Related Protein Translated from Influenza A Virus Segment 2 mRNA. *Journal of Virology*, 2009, roč. 83. č. 16, s. 8021-8031. ISS 0022-538X.

WISE, H. M.; HUTCHINSON, E. C.; JAGGER, B. W.; STUART, A. D.; KANG, Z. H.; ROBB, N.; SCHWARTZMAN, L. M.; KASH, J. C.; FODOR, E.; FIRTH,

A. E.; GOG, J. R.; TAUBENBERGER, J. K.; DIGARD, P. Identification of a Novel Splice Variant Form of the Influenza A Virus M2 Ion Channel with an Antigenically Distinct Ectodomain. *Plos Pathogens*, 2012, roč. 8. č. 11, s. ISS 1553-7374.

WOLF, Y. I.; VIBOUD, C.; HOLMES, E. C.; KOONIN, E. V.; LIPMAN, D. J. Long intervals of stasis punctuated by bursts of positive selection in the seasonal evolution of influenza A virus. *Biology Direct*, 2006, roč. 1. č., s. ISS 1745-6150.

WONG, C.; SRIDHARA, S.; BARDWELL, J. C. A.; JAKOB, U. Heating greatly speeds Coomassie blue staining and destaining. *Biotechniques*, 2000, roč. 28. č. 3, s. 426-+. ISS 0736-6205.

XIE, Z.; HUANG, J.; LUO, S.; XIE, Z.; XIE, L.; LIU, J.; PANG, Y.; DENG, X.; FAN, Q. Ultrasensitive Electrochemical Immunoassay for Avian Influenza Subtype H5 Using Nanocomposite. *Plos One*, 2014, roč. 9. č. 4, s. ISS 1932-6203.

XU, R.; MCBRIDE, R.; PAULSON, J. C.; BASLER, C. F.; WILSON, I. A. Structure, Receptor Binding, and Antigenicity of Influenza Virus Hemagglutinins from the 1957 H2N2 Pandemic. *Journal of Virology*, 2010, roč. 84. č. 4, s. 1715-1721. ISS 0022-538X.

YASUI, F.; KOHARA, M.; KITABATAKE, M.; NISHIWAKI, T.; FUJII, H.; TATENO, C.; YONEDA, M.; MORITA, K.; MATSUSHIMA, K.; KOYASU, S.; KAI, C. Phagocytic cells contribute to the antibody-mediated elimination of pulmonary-infected SARS coronavirus. *Virology*, 2014, roč. 454. č., s. 157-168. ISS 0042-6822.

YEN, H. L.; MCKIMM-BRESCHKIN, J. L.; CHOY, K. T.; WONG, D. D. Y.; CHEUNG, P. P. H.; ZHOU, J.; NG, I. H.; ZHU, H.; WEBBY, R. J.; GUAN, Y.; WEBSTER, R. G.; PEIRIS, J. S. M. Resistance to Neuraminidase Inhibitors Conferred by an R292K Mutation in a Human Influenza Virus H7N9 Isolate Can Be Masked by a Mixed R/K Viral Population. *Mbio*, 2013, roč. 4. č. 4, s. ISS 2150-7511.

YOSHIKURA, H. Spanish Flu, Asian Flu, Hong Kong Flu, and Seasonal Influenza in Japan under Social and Demographic Influence: Review and Analysis Using the Two-Population Model. *Japanese journal of infectious diseases*, 2014, roč. 67. č. 4, s. 245-57. ISS 1884-2836.

YOSYPCHUK, B.; BAREK, J. Analytical Applications of Solid and Paste Amalgam Electrodes. *Critical Reviews in Analytical Chemistry*, 2009, roč. 39. č. 3, s. 189-203. ISS 1040-8347.

YOSYPCHUK, B.; FOJTA, M.; HAVRAN, L.; HEYROVSKY, M.; PALECEK, E. Voltammetric behavior of osmium-labeled DNA at mercury meniscus-modified solid amalgam electrodes. Detecting DNA hybridization. *Electroanalysis*, 2006, roč. 18. č. 2, s. 186-194. ISS 1040-0397.

YOSYPCHUK, B.; HEYROVSKY, M.; PALECEK, E.; NOVOTNY, L. Use of solid amalgam electrodes in nucleic acid analysis. *Electroanalysis*, 2002, roč. 14. č. 21, s. 1488-1493. ISS 1040-0397.

YOSYPCHUK, B.; NOVOTNY, L. Nontoxic electrodes of solid amalgams. *Critical Reviews in Analytical Chemistry*, 2002, roč. 32. č. 2, s. 141-151. ISS 1040-8347.

YUEN, K. Y.; CHAN, P. K. S.; PEIRIS, M.; TSANG, D. N. C.; QUE, T. L.; SHORTRIDGE, K. F.; CHEUNG, P. T.; TO, W. K.; HO, E. T. F.; SUNG, R.; CHENG, A. F. B.; GRP, H. N. S. Clinical features and rapid viral diagnosis of

human disease associated with avian influenza A H5N1 virus. *Lancet*, 1998, roč. 351. č. 9101, s. 467-471. ISS 0140-6736.

ZHANG, T. R.; WANG, W. D. Existence of traveling wave solutions for influenza model with treatment. *Journal of Mathematical Analysis and Applications*, 2014, roč. 419. č. 1, s. 469-495. ISS 0022-247X.

ZHANG, Z. J.; CHEN, D. M.; CHEN, Y.; WANG, B.; HU, Y.; GAO, J.; SUN, L. Q.; LI, R.; XIONG, C. L. Evaluating the Impact of Environmental Temperature on Global Highly Pathogenic Avian Influenza (HPAI) H5N1 Outbreaks in Domestic Poultry. *International Journal of Environmental Research and Public Health*, 2014, roč. 11. č. 6, s. 6388-6399. ISS 1660-4601.

ZHENG, W.; TAO, Y. J. Structure and assembly of the influenza A virus ribonucleoprotein complex. *Febs Letters*, 2013, roč. 587. č. 8, s. 1206-1214. ISS 0014-5793.

ZHOU, C.-H.; SHU, Y.; HONG, Z.-Y.; PANG, D.-W.; ZHANG, Z.-L. Electrochemical Magnetoimmunosensing Approach for the Sensitive Detection of H9N2 Avian Influenza Virus Particles. *Chemistry-an Asian Journal*, 2013, roč. 8. č. 9, s. 2220-2226. ISS 1861-4728; 1861-471X.

ZHU, X.; WILSON, I. A. 4GDI: A subtype N10 neuraminidase-like protein of A/little yellow-shouldered bat/Guatemala/164/2009. *Worldwide Protein Data Bank*, 2012, roč. č., s. ISS

ZHU, X. Y.; MCBRIDE, R.; NYCHOLAT, C. M.; YU, W. L.; PAULSON, J. C.; WILSON, I. A. Influenza Virus Neuraminidases with Reduced Enzymatic Activity That Avidly Bind Sialic Acid Receptors. *Journal of Virology*, 2012, roč. 86. č. 24, s. 13371-13383. ISS 0022-538X.

ZHU, X. Y.; YU, W. L.; MCBRIDE, R.; LI, Y.; CHEN, L. M.; DONIS, R. O.; TONG, S. X.; PAULSON, J. C.; WILSON, I. A. Hemagglutinin homologue from H17N10 bat influenza virus exhibits divergent receptor-binding and pH-dependent fusion activities. *Proceedings of the National Academy of Sciences of the United States of America*, 2013, roč. 110. č. 4, s. 1458-1463. ISS 0027-8424.

8 SEZNAM OBRÁZKŮ

9 SEZNAM ZKRATEK

AdTS	Adsorptivní přenosová technika
AE	Pomocná elektroda
cDNA	Komplementární DNA
CV	Cyklická voltametrie
DNA	Deoxyribonkleová kyselina
DPV	Diferenční pulzní voltametrie
dsRNA	Dvouřetězcová RNA
EC	Elektrochemická detekce
HA	Hemaglutinin
HB	Hybridizační pufr
HMDE	Vysící kapková rtuťová elektroda
MPA	Merkaptopropionová kyselina
MPs	Magnetické částice
mRNA	Mediátorová RNA
NA	Neuraminidáza
NK	Nukleová kyselina
NP	Nukleoprotein
NPs	Nanočástice
ODN	Oligonukleotid
PB	Fosfátový pufr
PCR	Polymerázová řetězová reakce
PNA	Peptidová nukleová kyselina
QDs	Kvantové tečky
RE	Referenční elektroda
RNA	Ribonukleová kyselina
RNasa	Ribonukleáza
RT-PCR	Polymerázová řetězová reakce s reverzní transkripcí
SDS-PAGE	Elektroforéza v polyakrylamidovém gelu v přítomnosti dodecylsíranu sodného
SEM	Skenovací elektronová mikroskopie
ssRNA	Jednovláknová RNA
SWV	Square wave voltametrie
Tris	Tris(hydroxymethyl)aminomethan
vRNA	Virová (genomová) RNA
WE	Pracovní elektroda